Water flow through tailings dams

Jonathan Paul Welch

Water Flow Through Tailings Dams

by

Jonathan Paul Welch

B.Sc., M.Sc.

**This thesis is submitted to the University of Durham
in candidature for the degree of Doctor of Philosophy**

**School of Engineering and Computer Science
University of Durham**

February 1993

Dedicated to my parents who brought me up,
and Jane who has taken me on.

Declaration

I hereby declare that the work reported in this thesis has not been previously submitted for any degree. All material in this thesis is original except where indicated by reference to other work.

Abstract

Water levels in tailings dams are generally lower than those of standard earth dams. Previously, other authors have shown that embankment geometry and variation in permeability can be responsible for a concave upwards steady state seepage line. These factors are investigated in greater detail using a finite element program to model flow in the saturated portion of the embankment. It is shown that the angle of the upstream slope only has an appreciable effect on the form of the seepage line if the pond is close to the downstream face of the dam. An increasing permeability in the direction of flow and seepage path length are responsible for reducing the height of the seepage line. This effect is demonstrated for both a continuous variation of permeability and a step jump in permeability between the tailings deposit and the dam. Anisotropy of tailings and dam permeability is also investigated.

Transient analyses of saturated flow are performed for tailings dams constructed of dry compacted waste. For this case, the seepage line is straight for a constant pond level, and concave upwards for a rising pond and a low dam permeability. The simple computer model also predicts that for a constantly rising pond level, the seepage line advances at a constant rate dependent on the rate of pond rise, and the material properties of the dam.

A fully automatic finite element program has been written, combining an adaptive mesh regeneration algorithm and a variable mesh technique. The program is shown to provide both an accurate and precise solution of the free surface problem. A method of automatically generating "square" flow nets by post-processing the finite element data is presented for the first time. Flow nets provide a visual proof of the correctness of the computer model and are a useful aid to other workers.

Acknowledgements

I would like to thank my supervisor Professor Peter Attewell for his kind support in this endeavour. Thanks are also due to Dr Alan Craig of the Department of Mathematics for his advice concerning the Finite Element Method, and my colleagues in the Department of Engineering who have given aid, encouragement and above all friendship during my stay in Durham. I am especially grateful to Mark Ainsworth, Norman Powell, Barboros Okan and Steve Lavelle for their help in particular sections of the work. This research was supported in part by a grant from British Coal.

A	area
F	boundary forcing function
d	number of space dimensions considered
e	numerical error
$\mathbf{e}$	error vector
$\mathbf{F}$	boundary condition forcing vector
H	height of upstream pond level.
h_0	seepage line exit height
h_0^*	dimensionless seepage line exit height
h	size of finite element subdivision
$\overline{h}$	recalculated mesh subdivision
h_t	height of tail water
i	hydraulic gradient
I	boundary of finite elements
J	jump in gradient across element boundary
k	degree of nodal basis function + 1
	permeability (hydraulic conductivity)
K	permeability (hydraulic conductivity)
$\mathbf{K}$	conductance matrix
ℓ	effective dam width
ℓ^*	dimensionless effective dam width
L	length of dam upstream/downstream cross-section
	Laplacian operator
m	number of elements
	half of the order of the governing differential equation
n	effective porosity
$\mathbf{n}$	unit outward vector
N	nodal basis function
	number of nodes
$\mathbf{N}$	nodal basis vector
p	pore water pressure
	polynomial degree of nodal basis function
q	seepage discharge (outflow positive)
q^*	dimensionless seepage discharge
r	finite element residual
R	residual function
	rate of tailings lagoon fill

$\mathbf{R}$	residual vector
s	order of derivative
t	time
t^*	simulation time
t_0	extrapolated simulation equivalent start time
u	horizontal velocity component
$\mathbf{u}$	dependent variable of elliptical equation
$\mathbf{u}'$	gradient of $\mathbf{u}$
$\hat{\mathbf{u}}'$	finite element approximated gradient of $\mathbf{u}$
$\mathbf{u}'^*$	recovered gradient of $\mathbf{u}$
v	apparent seepage velocity
	vertical velocity component
	velocity of seepage line base movement
$\mathbf{v}$	apparent velocity vector
$\bar{\mathbf{v}}$	average fluid velocity
W	weighting function
x	horizontal space coordinate
x^*	dimensionless distance travelled
x_0	projected simulation equivalent start distance travelled
y	vertical space coordinate
z	elevation above datum
α	upstream slope angle
β	downstream slope angle
γ	unit weight of water
	seepage discharge / exit height parameter
ξ	finite element mesh refinement parameter
λ	singularity strength
	transient analysis upstream slope factor
η	acceptable error
ϕ	hydraulic head potential
$\bar{\phi}$	finite element approximation of ϕ
θ	downstream slope angle
Δ	length of base below upstream dam slope
Φ	potential function
Γ	finite element domain boundary
Ψ	streamline function

Ω	finite element domain
Ω_i	finite element *i*
[...]	matrix
{...}	vector
det|...|	determinant
||...||	L_2 norm
||...||$_E$	energy norm
O(...)	order of expression

Note

The symbols described above may be accompanied in the text by the use of subscript or superscript modifiers. These additional notations describe the context in which the symbols are used. Where such modifiers are present, their meanings are explained in the adjacent text.

Contents

Contents

Appendices

1: Seepage Line Profiles for a Rectangular Section Dam.

2: Anisotropic and Homogeneous Earth Dams Seepage Lines,
Seepage Exit Heights and Seepage Discharge.

3: Flow Nets for Tailings Dams and Earth Embankments,
Graphs of Seepage Discharge and Seepage Line Exit Height.

4: Advance of Seepage Line Through an Idealized Earth Dam
with Constant Head

5: Seepage Line Advance Through an Idealised Tailings Dam

Figures

Tables

Chapter 1
Introduction

The work of this thesis was instigated by the late Dr Roy Taylor of the Department of Engineering Geology, Durham University. Researchers at the university had been studying the engineering properties of coal mine waste for many years. British Coal (formerly National Coal Board) dispose both coarse solid waste and fine water-suspended waste above ground. Solid waste is dumped on waste tips which are a common feature of the industrial landscape in Britain. Tailings lagoons for the disposal of fine waste are equally important but lesser known structures. No analysis of tailings lagoon safety could be adequate without an assessment of dam seepage which controls in a large part the stability of the structure. Dr Taylor wished to extend research at Durham to include a consideration of the water flow through tailings embankments. It was well known that water levels within tailings dams were lower than those found in typical earth dams. Research concerning seepage in tailings dams had been carried out previously (particularly in the United States); however, research was concentrated on tailings structure designs which were significantly different from those used in Britain. British Coal wanted an explanation of what factors influenced the level of water in their dam structures. They were particularly interested in a transient analysis of seepage conditions to provide a possible explanation of the concave upwards seepage line within low permeability tailings dams. Mr Andrew Bacon, Head of Civil Engineering Services at British Coal Corporation Technical Services & Research Executive, Burton, was instrumental in obtaining a grant from British Coal to support the author in this research. Dr Taylor died unexpectedly soon after the commencement of this work but an effort has been made to keep as close as possible to the original intentions of the project.

The second chapter deals with the background to the study of seepage through tailings structures. Topics dealt with include tailings dam design and construction techniques, causes of tailings dam failure, methods of controlling dam seepage and modelling techniques applied to tailings dam analysis.

Finite element techniques are discussed in Chapter 3. Special consideration is given to the methods used by the computer program which was developed specifically for this thesis. These methods include a brief description of automatic finite element mesh

generation and adaptive techniques which may be used to obtain highly accurate solutions with minimal interference by the user.

Chapter 4 describes the finite element program used for the flow analysis work. The chapter is designed to take the place of a user manual. There is an explanation of the program's design and objectives. A detailed description of how to use the program is included together with examples which are used to verify the results obtained.

Several steady state and transient flow problems are analysed in Chapter 5. These problems are designed to investigate the influence of the geometry, permeability and transient flow development on the water level within the dam or embankment. Each case includes a description, results section, analysis and conclusion. Both earth dams and tailings embankments are considered. Results are compared with analytical and/or empirical results obtained from the literature.

Chapter 6 contains a summary of the most important results obtained in the thesis. Evidence is drawn from the analyses of the previous chapter with which to assess the significance of each of the factors considered on the position of the seepage line within the tailings dam. Recommendations are made for future work.

Chapter 2
Tailings Lagoons and Embankments

The aim of this chapter is to introduce the design, construction and use of tailings embankments and lagoons with special reference to the importance of seepage flow within the structure. The discussion moves from the purpose and significance of tailings structures to their design requirements and methods of construction. This is followed by a description of the common modes and agents of failure, including seepage flows, which are important in determining the safety of tailings structures. There is a discussion of the factors which control the seepage line within the tailings embankment and lagoon. Finally, there is a brief introduction to the methods by which seepage in a tailings dam has been studied for the purpose of stability analyses.

2.1. Introduction

"Tailings" or "tails" is the name given to fine-grained industrial wastes commonly, though not exclusively, produced as a waste product from mining and quarrying activities. The particles range from sand to clay-size fraction. The term "slimes" is frequently used to describe fine tailings suspended in water, that is to say, composed mainly of particles less than 0.074 mm in diameter. The particle size distribution of the tailings depends on the nature of the material involved, the method of production and handling, and the method of tailings deposition. Green (1980) differentiates between two types of industrial tailings:

(i) Fine waste makes up only part of the total; this is the case in most coal mining activities, where the waste is made up of run-of-the-mine discard and fine tailings from the washery or flotation plant.

(ii) All waste is fine; this is true of the salt industries of Cheshire, leather processing and some dredging activities.

Green lists six main types of industry involved in the production of tailings; coal, metal mines, phosphate mines, aluminium processing plants, sand and gravel pits, and china clay workings. The processes involved in the production of this waste (e.g. milling in metalliferous mines) normally result in the production of a slurry having a very high moisture content. For convenience and economy, the tailings are usually transported to the disposal site in slurry form (ICOLD, 1982). The tailings range from 5 to 50%

solids by weight. It is the function of the tailings impoundment to retain the slurry during the process of sedimentation, in which the tailings fall out of suspension and are deposited at the bottom of the pond or lagoon. Before the use of tailings impoundments, fine grained waste from the milling plant was typically disposed of in the local water course.

Tailings impoundments may be sited in existing ground depressions, but more commonly they form part of a tailings embankment which rises above the natural ground level. This necessitates the building of a dam to retain the impounded water and unconsolidated slimes. The types of site which may be developed for the storage of tailings can be classified into five broad categories, as follows (ICOLD, 1989):

I Cross Valley Impoundments.

The dam is on a single side of the impoundment. It must carry the load of partly liquid tailings deposited upstream. A major disadvantage of this type of impoundment is that it has to cope with normal streamflow and exceptional floods. However, with improved fundamental knowledge and design technique such problems have largely been solved, and this type of arrangement is now commonly used (Down & Stocks, 1977).

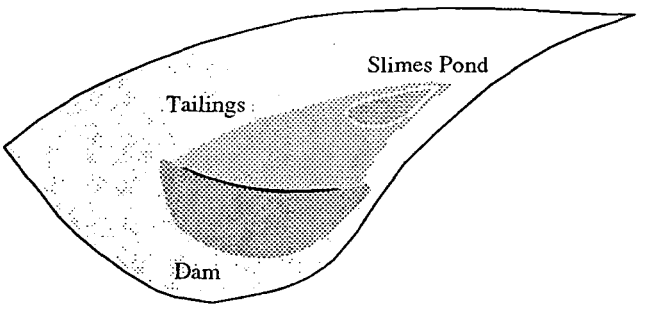

Figure 2.1 Cross-Valley Impoundment

II Dyked Impoundment.

The impoundment is surrounded by a single dyke. This case applies to structures on flat ground. An important consideration is the volume of material required for the dam.

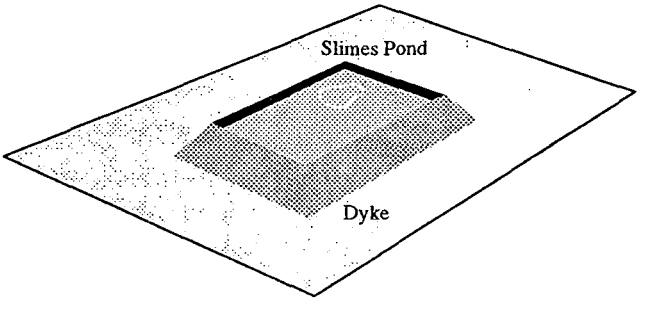

Figure 2.2 Dyked Impoundment

III Hillside Impoundment.

The embankment is on three sides of the impoundment and carries the load of the impounded tailings.

IV Incised Impoundment.

The impoundment is partly buried, and the dam affects only part of the periphery. This type applies on generally flat ground.

V Combination Impoundment.

An example of this type of dam might be the cross-valley impoundment with two embankment dams. The downstream embankment is required to carry the load of the tailings.

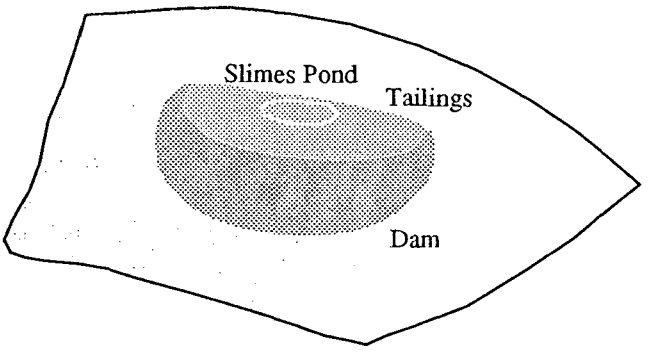

Figure 2.3 Hillside Impoundment

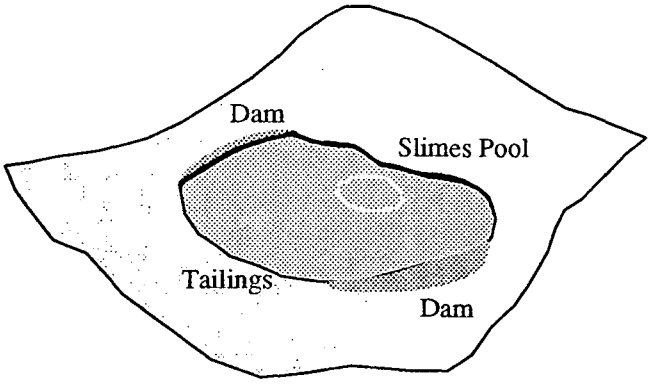

Figure 2.4 Incised Impoundment

The range in tailings embankment size is enormous; from small scale lagoons measured in a few metres, to the largest artificial structures on earth. There are tailings dams currently under construction which will have ultimate heights of 200 metres (ICOLD, 1989). Morgenstern et al (1985) reported that the Phalaborwa embankment in South Africa has a volume of 162×10^6 m^3 of tailings. The World Register of Mine and Industrial Tailings Dams has data on 28 countries, listing six impoundments which have a surface area greater than 100 km^2 (ICOLD, 1982). In 1985, World Mining Equipment (1985) put the number of tailings dams at 200,000.

In an evaluation of 93 technological hazards conducted by Christoph Hohenser at the Hazard Assessment Group at Clark University, dam failure rated 18th in front of private and commercial aviation crashes, fires from smoking, and the toxic effects of asbestos insulation (World Mining Equipment, 1985). Failures of tailings dams occur more often than other types of dam; this is because they are viewed as temporary structures (not requiring as stringent controls as apply to water retaining dams). Small scale failures killing only a few miners, or doing only environmental damage, have been relatively common, but have usually been dismissed simply as an occupational hazard (ICOLD, 1982). The well publicised failure of several large waste disposal structures in recent years has channelled both professional and public interest to the question of tailings dam safety.

The loss of life caused by the Aberfan waste dump disaster of 1966, and the El Cobre tailings dam failures in Chile (1965), created a new consciousness of the need for a high standard of design for large engineering structures (Brawner & Campbell, 1973). In 1972 a coal refuse embankment at the head of the Buffalo Creek, West Virginia (USA) failed, sending 11 million cubic metres of water and sludge onto sleeping residents of Logan County, leaving over 100 fatalities, 1100 injuries, 1500 houses demolished, and 4000 homeless people (Kealy & Busch, 1979). Study of the failure revealed that the refuse embankment was constructed with total disregard for engineering design and expertise. A more recent failure at Stava in Italy on the 19th July 1985 indicates that tailings dam safety is still a matter for concern. A failure of the top dam at the Prealpi Mineria site swept away a lower dam and much of the tourist resort of Stava, 1311 metres below. The flood of water and tailings claimed the lives of 250 people (World Mining Equipment, 1985).

Public concern is not only restricted to this type of catastrophic failure; an increasing worry concerns the environmental affects on the groundwater (Klohn, 1979). Tailings impoundments have the potential to modify the groundwater regime of an area in two general ways (Parsons, 1980):

(i) Disturbance of the groundwater flow system, brought about by either dewatering and drainage or groundwater mounding. The effects of such disturbances may manifest themselves as changes in water levels in neighbouring wells, seepages, or in certain areas, even flooding.

(ii) Alteration of groundwater quality due to infiltration of contaminants derived from tailings water and leachate. The effects of water quality alterations may be manifested as degradation of existing and future water supplies, both in the ground and on the surface.

Deju (1974, p. 44) lists some of the waste characteristics of common extractive industries. Many of these chemicals may find their way into tailings impoundments. Vick (1983, p. 301) notes that not all mill effluent contains toxic material, and for mill effluent that does, it is not necessarily the case that seepage of this effluent will result in pervasive groundwater contamination. Geochemical processes may retard or inhibit movement of some constituents, and these processes are often most effective in reducing mobility of the most troublesome metallic ions associated with low-pH effluents. The general trend in waste disposal is now for "closed systems", in which the maximum water is recirculated back to the mill (Klohn, 1972). This diminishes both the use of fresh water and the quantity of pollutant released.

Industry	*Waste Characteristics*
Salt mining	high in suspended solids, high salts, corrosive
Coal mining	fine suspended coal, high total dissolved solids, acid mine drainage, trace metals
Integrated iron & steel industries	high total dissolved solids, high iron, high acidity, high concentration of many metallic salts, pickle liquor, mill scale, phenols, alcohols, cyanides, tars, oils, heated water
Smelters	high sulphur dioxide, high cyanides, phenols, and finely-divided suspended matter
Electroplating	high in salts of copper, zinc, chromium, and nickel, high in cyanides
Oil refineries	high in organics, acids, alkalies, phenols, and some trace metals, high in oil-coated solids
Flotation plants	high in mercaptans, cyanides, arsenic, and many toxic metals

Table 2.1 Waste Characteristics of Some Extractive Industries

(after Deju [1974; pp. 44])

Down & Stocks (1977) foresaw a trend towards a decreasing grade of ore dictated by both economics and resource availability. The consequence of a decreasing ore grade is an increasing proportion of waste to valuable mineral. This trend is accelerated by technological advancements in ore retrieval such as chemical processing and finer grinding at the mill. Longhurst (1983) reported an increasing proportion of waste to coal in the United Kingdom and North America due to modern mining practice and the exploitation of thinner, dirtier seams. The Department of the Environment (1988) found that the general increase of spoil production is coupled with a steady increase in the proportion of fines in the spoil.

Several alternatives to tailings impoundments are sometimes employed when the opportunity arises. These include marine, in-pit and underground disposal of tailings (Green, 1980). Pettibone & Kealy (1971) proposed the use of tailings for the construction of road embankments and earth dams. In the United States, it is quite common for the coarse and fine waste of coal mines to be combined before they are dumped together (Almes, 1978). However, the general view, expressed by Vick

(1983), is that dams, embankments and related types of structures are likely to remain the most common disposal methods of tailings disposal.

2.2. Tailings Dam Design

As a rule, the storage of waste material generates no profit, although exceptions do exist:

- The waste may be reprocessed with a finer grind, e.g. a precious metalliferous ore such as gold or platinum.
- A component of the waste material may become newly profitable to exploit, e.g. barite is now "won" from lead mine waste tips in Northern England.
- The "waste" may itself be valuable. Tailings impoundments are frequently used to store coal-rich slurries while they settle and consolidate (NCB, 1970).

As a consequence of this, the waste must be disposed of in the most economic, acceptable way (Morgenstern et al, 1985). One usual aim of tailings embankment design is to spread the cost of disposal over the life of the dam. Vick (1983) made the point that keeping the initial costs to a minimum, and building the dam to keep pace with waste production, may decide the viability of the entire mining operation.

The tailings disposal facilities are required to provide adequate space to impound the slimes at their rate of production throughout the life of the operation. The dam must always be higher than the stored waste, and so the slowest acceptable rate of dam construction is controlled by the influx of tailings (Galpin, 1971). The tailings dam is built of coarse waste wherever possible; this provides a useful dump for the coarse waste as well as minimizing the use of borrow material. This is done to reduce the cost associated with the import of material from off-site and the unnecessary on-site movement of earth. In the coal mining industry, both coarse and fine waste (or discard) is disposed of above ground. The normal practice is to use the coarse discard to build a confining embankment in order to impound the fine discard (NCB, 1971). In other types of mining operation there may be no secondary source of coarse waste material. In this case it may be possible to use the tailings themselves as material for dam construction.

This is commonly performed in one of three ways:

(i) Reclamation of spigotted slimes. A common practice in many dams is to deliver the tailings into the impoundment from a peripheral discharge system of spigots sited on the crest of the dam. The tailings flow down a beach against the interior of the embankment and into the pond. The coarser particles are deposited on the upper reaches of the beach, and the slimes flow into the pond. After a period of drying out and consolidation, the tailings harden into a surface crust. Scrapers may be used to "harvest" the beach tailings for material to use in dam construction. This is the oldest method of raising the tailings embankment. Klohn (1972) explained the apparent success of this method in the case of the upstream method of construction (see following section) in arid regions.

(ii) Cyclones (hydrocyclones) in which the coarse and fine tailings are separated centrifugally. The coarse underflow of medium to fine sand is used for embankment construction, and the finest particles (slimes) flow into the lagoon. If a coarser gradation is required then double cycloning will further reduce the proportion of fines. Klohn (1972) gave a detailed description of the use of cyclones from his experience in British Columbia.

(iii) Hydraulic cell method, in which the tailings are fed into partitions on the crest of the embankment. The coarse tailings are allowed to settle and the waste water is bled away, carrying the fines into the lagoon. Morgenstern & Kupper (1988) advocated the wider use of hydraulic fill techniques.

The availability of this coarse material is an important consideration in the design of the embankment. The section dealing with dam construction shows how different methods vary in their requirement for coarse embankment material as the embankment is raised. The tailings structure design should have an in-built flexibility in order to cope with changes in operational demands.

The control of mine process water is a secondary function of the tailings structure. The climate, tailings water toxicity and the engineering properties of the tailings themselves are the primary factors in determining the water control regime adopted. Good practice is to recirculate water from the lagoon, back to the mill (ICOLD, 1982). The water balance for the milling operation should be determined at the design stage. If water management is aimed at minimizing the loss of water (closed system), then this has consequences for the consolidation and safe storage of the tailings. Rubinchic (1960) criticised the use of water retaining dams for tailings impoundment in the Soviet Union for this reason; they are over-designed for waste disposal and, by stopping free

drainage, they prevent consolidation of the slimes. Where the toxicity of the tailings is of primary concern (e.g. uranium tailings), seepage out of the lagoon is prevented by the use of seepage barriers such as cutoff trenches, slurry walls, grout curtains, and natural or artificial liners of extremely low hydraulic conductivity (Vick, 1983, pp. 300-321).

The tailings structure is required to provide adequate safety with respect to the risks posed to life and property. ICOLD (1989) divides the question of safety into two basic considerations. The first item is the structural stability of the embankment against failure mechanisms such as sliding, slumping, over-topping, piping, and so on. Modes of embankment failure are discussed in a later section. The second item relates to the safe containment of any toxic materials that might be stored in the pond. While the embankment might be structurally sound, this does not preclude the possibility that toxic material might contaminate the groundwater or downstream water courses. The environmental safety of the embankment depends not only on the imperviousness of the pond and dam, but also on the physical properties of the tailings and re-agents used in the milling process (ICOLD, 1989). Assessing the environmental safety of a given tailings facility requires a knowledge of physiochemical and chemical reactions as well as seepage flows and groundwater movements. In addition, there are wider environmental considerations which must also be taken into account: spontaneous combustion, dust, impact on the landscape, and land take. The environmental impact of a tailings structure continues after waste production has ceased. Reclamation of the tailings site has been a common design consideration for a number of years (Brawner & Campbell, 1973). Down & Stocks (1976) stated that the reclamation should be designed to leave the widest possible choice for future land use.

The plan for tailings disposal must take into account the following design considerations:

- Choice of site
- Preparation of foundations
- Construction materials
- Dam zoning
- Slope angles
- Embankment construction methods
- Tailings delivery and deposition
- Drainage measures.

The method of construction has a profound influence on the seepage through the dam. The next section describes the most common methods of embankment construction.

2.3. Tailings Dam Construction

The types of tailings dams are usually divided into three camps: conventional earth dams, upstream construction tailings dams, and downstream construction tailings dams. The three groups are described here. These methods of construction have been developed largely by trial and error, and there is no reason why new innovative techniques should not emerge. The analysis of later chapters of the thesis is directed to a variety of the downstream construction method used by British Coal in the United Kingdom. The important aspects of British Coal practice with respect to seepage through the embankment dam are also discussed in this section.

2.3.1. Conventional Dam Construction

Figure 2.5 shows a typical conventional earth dam construction. Conventional dams may be used to impound any kind of tailings using any of the common discharge methods. Water retaining type dam technology is more expensive than that for raised embankments, and is often described as over-engineered for the purpose of ordinary tailings disposal. There are certain circumstances in which a conventional dam may be advantageous. An example of such a case might be where the dam must retain ponded water against its upstream slope. This eventuality is most likely if there is a risk of flooding and the dam must provide freeboard to prevent over-topping and failure. The upstream slope may be steeper than is required for water-retaining dams because they are not subject to rapid drawdown (Vick, 1983, p. 70).

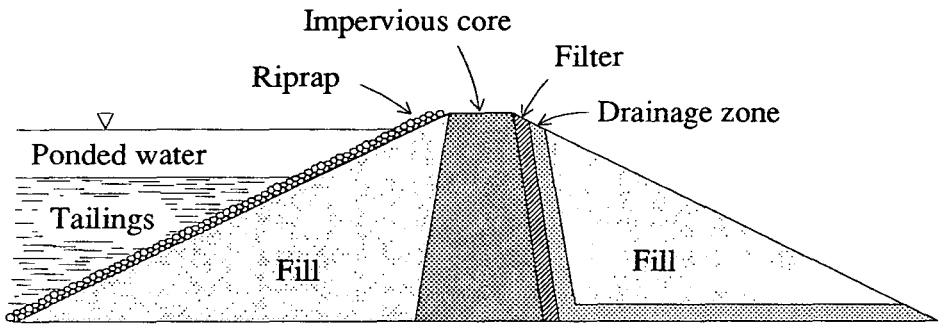

Figure 2.5 Conventional Earth Dam

Conventional earth dams are usually completed before the waste is impounded. (Minns (1988) gives examples of "conventional type" dams which are designed to be raised during the life of the operation.) The expense of dam construction must be born at the beginning of the operation. The dam requires a variety of borrow material which may have to be imported. Conventional earth dams have a good resistance to seismic shocks (Vick, 1983, pp. 80).

2.3.2. Upstream Construction Method

In the past, practically all tailings dams were constructed by some variation of the upstream method of construction (ICOLD, 1989). This was because the upstream method is more economical and simple to use (Kealy & Busch, 1979). The original upstream method normally involved the construction of a low earth "starter" dyke, 3 to 6 metres in height. This starter dyke was usually constructed from locally available borrow material and was seldom subject to engineering design (Klohn, 1972). The tailings were discharged by spigotting off the top of the starter dyke. When the initial pond was nearly filled, the dyke was raised by borrowing material from the dried surface of the previously deposited tailings, and the cycle was repeated. As the height of the dam increases, each successive dyke moves further upstream and is underlain by the soft, previously deposited tailings. Casagrande & McIver (1971) presented a remarkable photograph of one such structure built entirely by hand to the height of approximately 100 metres and a slope of 60 degrees. Figure 2.6 shows the upstream construction method without drainage measures. The starter dam should be permeable so that it might act as a toe drain. It is not unknown for an impervious starter dam to be used (Kealy & Busch, 1979).

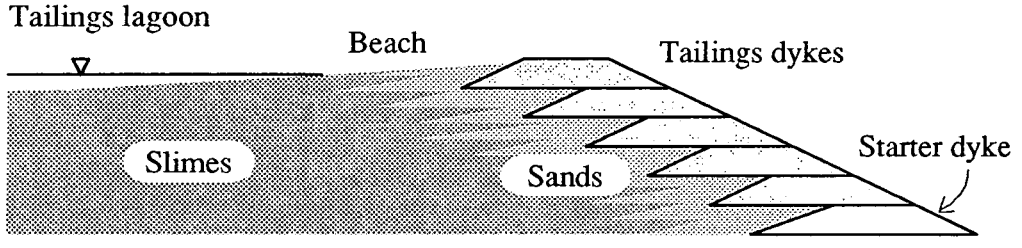

Figure 2.6 Upstream Construction Method

Upstream methods of construction have been used successfully in dry, arid climates where evaporation losses are high and a minimum of water is stored in the pond (ICOLD, 1989). Under these conditions the phreatic line through the tailings dam is

low. Upstream construction methods have also been used successfully where spigotting, combined with good underdrainage, has been utilized (ICOLD, 1982).

Upstream construction is efficient in its use of material suitable for dam construction. Only minimal volumes of mechanically placed fill are necessary for the construction of the perimeter dykes, and large embankment heights can be attained at very low cost (Vick, 1983). The basic structures, the starter dam and the decant works are the fastest built and are therefore the fastest in operation. That is why they are always preferred if the necessary conditions for their adoption are present (ICOLD, 1982).

The major disadvantage with the upstream method is that the most critical failure circle (potential failure surface) may cut through the unconsolidated slimes which are traversed by the beach. As the height of the dam increases, the potential failure surface is located at an increasingly greater distance from the downstream face and through the slimes. As a result, the outside shell contributes less to stability as the height increases. This may in itself cause the dam to fail. Thus the stability of this type of embankment is inversely proportional to the height. This results in a limiting height for this type of dam. The properties and characteristics of the beach determine at what point the slimes underlying the embankment affect the factor of safety. It is essential that the tailings form a reasonably competent beach for support of the perimeter dykes. As a general rule, the tailings should not be less than 40-60% sand (Vick, 1983). Cyclones are now frequently used as an alternative to spigotting (ICOLD, 1989). This should provide a greater concentration of sand for construction.

Location of the phreatic surface is a critical element in determining the embankment stability (Vick, 1983). For upstream embankments constructed by spigotting, there are few structural measures which can be taken for the control of the phreatic surface within the embankment. Upstream embankments are poorly suited to water retention, and so near-total diversion of runoff and flood inflow is essential for this method (Vick, 1983).

The upstream method is susceptible to the build-up of excess pore pressures in the consolidating slimes (Vick, 1983). For this reason the upstream method is not suitable for fast rates of construction, particularly if the foundation is impervious (Mittal & Morgenstern, 1977). Slimes may be in a sufficiently loose condition for failure by liquefaction to occur if they are subjected to seismic shock (ICOLD, 1982). Consequently, the upstream method may be unsuitable in regions of appreciable seismicity.

2.3.3. Downstream Construction

The downstream method of tailings dam construction evolved from a blending of the engineering knowledge and experience available in the field of water storage dams and the knowledge of the mining operators responsible for the construction and operation of the tailings dams (ICOLD, 1989). The downstream method of tailings dam construction involves extending the dam in a downstream direction from the initial starter dam. Such a dam should be impervious to minimize seepage through the structure (Brawner & Campbell, 1973). This requires that the starter dam will usually be constructed of compacted borrow material which contains significant silt and clay size fractions. Subsequent raises are constructed by placing fill on the downstream slope of the previous raise (Vick, 1983). Figure 2.7 shows the basic upstream method.

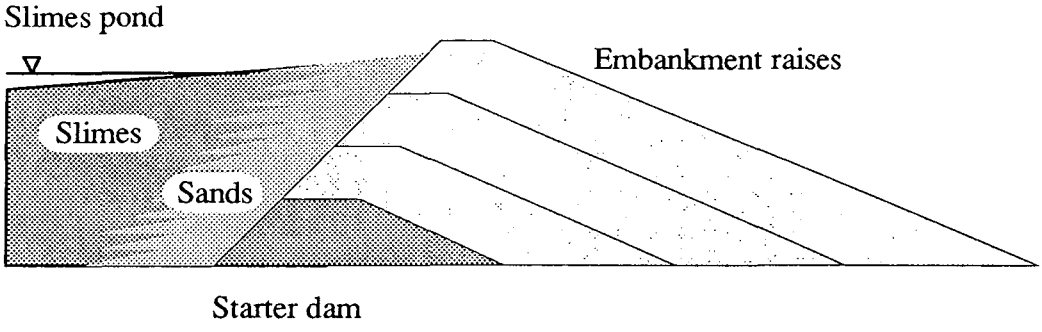

Figure 2.7 Downstream Construction Technique

Compaction to improve the shear strength properties of the embankment and installation of internal drains to control the phreatic surface can be included in the design to obtain the required degree of safety under both static and dynamic loading (Brawner & Campbell, 1973). This method is also amenable to the incorporation of other structural measures more commonly associated with water-retention dams, such as a clay core in order to control seepage (Vick, 1983).

Most downstream methods of construction involve the use of cyclones to separate the sand sizes from the slimes (ICOLD, 1989). The sands are then used in dam construction and the slimes are deposited in the tailings pond. In areas of high seismicity, and where the tailings are too fine to produce sufficient quantities of sand suitable for dam construction, suitable borrow materials should be used to construct the tailings dam. Downstream raising methods require careful forward planning because the dam must advance from the toe as its height increases (Vick, 1983). The height of the dam may be limited by the vast amount of sand needed for each incremental

increase (ICOLD, 1982). The method is more costly than the upstream technique because of the mechanical equipment needed to make the low-angled downstream slope. According to the International Commission on Large Dams (ICOLD, 1982), the downstream method is awkward and not one of the better operating systems.

Performance records of earth dams that have been subjected to earthquake forces reveal that well-compacted unsaturated fills do not liquefy and do not tend to suffer appreciable damage during earthquakes (Brawner & Campbell, 1973). Even uncompacted hydraulically placed fills may be sufficiently strong for regions of low seismicity (Mittal & Morgenstern, 1977). In areas of high seismic risk, where failure of the tailings dam poses a threat to life and property, current good engineering practice is to use downstream methods of tailings dam construction (ICOLD, 1989).

The centreline method of tailings dam construction may be considered to be a variant of downstream construction. The crest of the dam is maintained at the same horizontal position as the height of the dam is increased (Brawner & Campbell, 1973), so giving rise to the name. Initially, a starter dyke is constructed and the tailings are spigotted from the periphery of the dyke crest to form a beach (Vick, 1983). The dam is then raised by spreading and compacting additional coarse tailings on the top, on the downstream shoulder and on the downstream slope (Brawner & Campbell, 1973). Figure 2.8 shows the geometry of the centreline construction method.

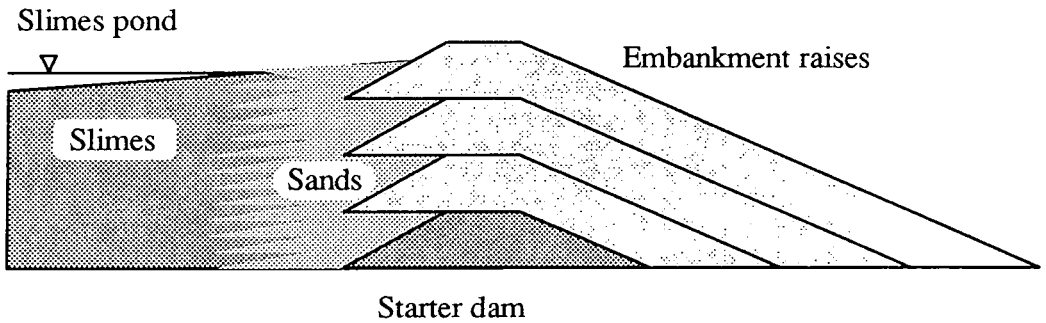

Figure 2.8 Centreline Construction Method

The centreline method requires much less cyclone underflow than does the downstream method (ICOLD, 1982). It can use finer grind than the upstream method. The centreline method has generally good seismic resistance however, in the event of tailings liquefaction, a portion of the upstream fill placed upon the beach may fail. Unlike the downstream construction method, the centreline method cannot be used for permanent storage of large depths of water (Vick, 1983).

2.3.4. British Coal Construction Techniques

Several dam designs for use with different constructions materials and techniques are detailed in *Spoil Heaps and Lagoons*, a technical handbook produced by British Coal (NCB, 1970). The dam designs are a guide to the variety of measure which might be considered in order to deal with the variability of site conditions and of grading and permeability of the materials between one colliery and another. All the designs are based on the downstream or conventional earth dam techniques mentioned above. The handbook describes designs for both permeable and impermeable type dams, and covers a wide variety of methods for seepage control including dam zoning, drainage blankets and strip drains. Many of these techniques owe more to water retention type dam technology than the usual tailings disposal techniques. In the case of a low, permeable embankment (less than 6 metres) with a low downstream slope angle (1 in 4), or an "impermeable" embankment (with a permeability less than 10^{-8} ms^{-1}), the requirement for internal drainage may be relaxed, and a simple non-zoned dam used. This thesis is primarily concerned with the flow of water through this simple type of embankment in order to investigate the "natural" flow development in a general way. Some of the operating procedures used by British Coal are mentioned here because they affect the choice of parameters used in the numerical model tested in a later chapter.

British Coal produce two types of fine tailings which may make up to 20% of the total spoil production (Department of the Environment, 1988):

- fine tailings from the froth flotation plant consisting predominantly of shale,
- coal rich slurry from the washery.

The fine discard has a nominal maximum particle size of 0.5mm, although a large proportion can be of much smaller size, being less than 10 microns. The slurry is usually a coarser grained material than tailings, so the rate of sedimentation and consolidation will be more rapid and the permeability of the deposit will usually be greater (NCB, 1970). However, certain preparation plants may produce slurries having gradings as fine as those usually associated with tailings. With some tailings, the high clay content or the low specific gravity may cause the amount of consolidation to be relatively small. Initially the tailings from the flotation plant are very dilute and so they are treated with a flocculent which causes the particles to settle in a thickener, allowing the water to be recycled (Department of the Environment, 1988). At this stage the thickened tailings resemble a sludge having a moisture content of between 60 and 70%.

The dam is constructed with the coarse discard, run-of-the-mine dirt or burnt shale. The material is placed mechanically (not hydraulically), and at as low a moisture content as is practicable. The typical moisture content of fresh coarse discard is 10% (Department of the Environment, 1988). Construction is staged in a series of lifts which are compacted by earth moving equipment. The surface of each lift is scarified before the embankment is raised in order to prevent the development of impervious layers. Because the construction material is not saturated, the seepage line must travel through the dam before reaching the downstream face. The permeability of the dam is likely to be different from that of the tailings in the impoundment.

The fine discard or slurry is spigotted into the impoundment. The coarser particles settle more quickly than the finer particles, and so particle size decreases away from the point of discharge. The recommended practice is to move the discharge point periodically around the lagoon (NCB, 1970) in order to produce a sequence of fine and coarse lenses which enhances the consolidation characteristics of the deposit. This practice is also beneficial for slurry impoundments because it creates a more uniform, saleable product (the dried slurry can be mixed with low grade coal for industrial uses). The resulting lagoon deposits may be considered homogeneous (if these layers are sufficiently thin) but anisotropic.

Several impoundments are used at the same site in order to allow continuity of waste disposal. Three lagoons are required so that one may be built, one filled and a third allowed to dry out (Department of the Environment, 1988).

2.4. Tailings Dam Failure

Kealy & Busch (1971) found that water is the factor that precipitated most structural failures of tailings embankment in the United States. Table 2.2 indicates the causes cited by World Mining Equipment (1985) as those most frequently leading to earth and rockfill dam failure.

Cause of Failure	Frequency
Piping & seepage	38%
Over-topping	35%
Foundation	21%
Other	6%

Table 2.2 Causes of Earth and Rockfill Dam Failure

(World Mining Equipment, 1985)

The most common types of failure are listed below.

Slips

The embankment may fail by a rotational or translational slope failure mechanism. This may be a result of earthquake, an increase in pore water pressure, an increase in the load (due to a raising of the embankment or heavy vehicles and equipment), or a decrease in the restraining forces (by a steepening of the slope by excavation or surface erosion) (NCB, 1970).

Flowslides

Flowslides are caused by a liquefaction of the tailings and/or the embankment. Flowslides are initiated by a seismic event, embankment settlement or other shock. Liquefaction occurs in loosely packed frictional soils of relatively poor permeability (Klohn, 1980).

Surface Erosion

Surface erosion may be a result of overtopping, freeze-thaw action, wind, rain or runoff (Mantei, 1985). Tailings are commonly cohesionless and very susceptible to the erosive action of runoff and seepage (ICOLD, 1982).

Internal Erosion

Excessive uncontrolled seepage exit gradients are responsible for making the soil particles buoyant. The fine particles are transported in the flow and the permeability increases. The result may be a piping failure caused by the development of a flow channel from the downstream slope back into the embankment.

Differential Settlement

Changes in the engineering properties of the embankment material or an uneven foundation can result in an abrupt change in the amount of settlement. This may cause the fracture of water conduits or failure of the seepage control measures (NCB, 1970).

Foundation Heave

Excessive pore pressures in the foundation below the embankment (created by the emplacement of embankment material) may cause heave in the foundations in front of the downstream slope (Mantei, 1985).

Desiccation

The clay core and other "impermeable" zones may be prone to desiccation if they are left uncovered. This may cause the dam to fail when the tailings water is impounded (Mantei, 1985).

Excessive Seepage

When the level of seepage is too great for the local water courses (in terms of quantity or polluting content), or the water losses are too great for the milling operation to sustain, then the embankment may be considered to have "failed".

2.5. Seepage Control in Tailings Dams

It has been shown that the pore pressures, and by implication the location of the water level within the dam, exert a fundamental influence on its behaviour. Control of the phreatic surface is of primary importance in embankment design. In particular, the emergence of seepage on the downstream slope and saturation of the dam toe should be avoided because it may lead to instability (NCB, 1970). The causes of excess pore pressures and seepage gradients are discussed in this section, together with the most common methods of improving embankment seepage characteristics.

2.5.1. Sources of Seepage Water

The sources of seepage water in the tailings structure are as follows (Klohn, 1979):

(i) free water in the tailings pond

(ii) construction water from the cyclone underflow or hydraulic fill

(iii) water from spigotting operation to form the tailings beach

(iv) consolidation water squeezed out of the tailings

(v) precipitation falling onto tailings dam.

The pond water originates from the mill, washery or flotation plant, and hydrological runoff. The level of precipitation cannot be changed, but the runoff can be controlled indirectly by the choice of site (e.g. flat land will have no runoff). In a cross-valley tailings structure, the runoff may be considerable; the usual practice is to use diversion works and spillways to pass the water around or over the structure, or use a water retaining type dam. The amount of water contributed by the consolidation of the tailings will be small compared to the free water obtained in the initial settlement (NCB, 1970). Mittal & Morgenstern (1976) used the predicted consolidation water to modify the theoretical seepage pattern for tailings dams having a high rate of

construction (5 to 10 metres per year). The other factors are controlled by the on-site operational procedures that are followed. Windolph (1973) reported a rise in the phreatic surface (measured down wells in the embankment) due to flow from the saturated embankment. Nyren et al (1978) found that seepage from the hydraulic cell method of construction can be more critical than the position of the pond in determining the position of the phreatic surface. In a permeable embankment built by on-dam cycloning, the water levels may correlate exactly with the cycles of construction (Stauffer & Obermeyer, 1988). The cyclone underflow is saturated when discharged and must have time to drain in order to keep the phreatic surface low enough for stability (ICOLD, 1982). However, these reports of the influence of construction water may be exceptional. Nelson et al (1977) suggested that the effects of beach infiltration from spigots are relatively minor, producing a rise in the water level of only 2-4%. Field observations by Abadjiev (1976) found that the increase in seepage line elevation due to beach infiltration was only a few percent.

2.5.2. Seepage Losses

Water is removed directly from the pond for recycling. The three most common methods are:

- decant tower and water conduits
- barge pumps
- siphons.

Historically, decants have been the most popular method, however barge pumps are becoming more popular wherever the terrain permits (ICOLD, 1982). In addition to the use of these methods, it is usual to make use of emergency spillways or overflow pipes if the dam freeboard is not adequate in the event of flooding.

Seepage losses from the tailings structure are as follows:

(i) seepage through the foundation into the groundwater

(ii) seepage through the dam to the seepage surface

(iii) evaporation (and transpiration).

The quantity of water lost by evaporation may be controlled by managing the size of the pond (Swaisgood & Toland, 1973). A small pond will reduce evaporation, while a large pond will increase evaporation (obviously this is only applicable in hot climates). If evaporation rates are still too high, it is possible to cut water loss further by placing a thin layer of chemicals on top of the water. Seepage losses may be controlled by the

use of pond control, compaction, material zoning, drains or drainage barriers. These are discussed in the following sections.

2.6. Pond Control

The tailings pond does not have the same geometrical relationship with the dam found in classic water retaining dams. Kealy & Williams (1971b) found that the near horizontal interface between the ponded water and the confining tailings had a profound effect on the position of the seepage line in their finite element model. The bottom of the pond forms an equipotential (surface of equal head potential), and so the flow lines in the tailings dam are nearly vertical (instead of nearly horizontal, as is the case in water retaining dams). Kealy & Williams ascribed much of the concave shape of the seepage line to this difference in boundary conditions. Abadjiev (1976) found that for the particular case where the distance from pond to dam toe was 5 times the embankment height, the effect of the low water/dam interface angle caused a lowering of the equivalent water retaining dam's phreatic surface by 3 to 4% of the dam height.

The distance of the pond to the dam controls the seepage length path, and hence the hydraulic gradient. Vick (1983) concurred with Abadjiev (1976) in saying that the location of the ponded water with respect to the embankment crest (or the width of the exposed tailings beach) is often the most important factor influencing phreatic surface location.

2.7. Compaction

Compaction of the dam structure and beach are used to improve the shear strength of the tailings or earth dam, reduce the permeability, reduce the air void and potential for spontaneous combustion, and to decrease the land take or the tailings structure (NCB, 1970). Increasing the relative density of fine-grained sand tailings is extremely effective in preventing the possibility of liquefaction, but care should be taken not to build up excess pore pressures in deposits which are not free draining.

2.8. Tailings Embankment Zoning

A general principle of phreatic surface control is that the permeability should increase in the direction of seepage. As permeability increases, the phreatic surface is progressively lowered, and ideally the most permeable material should be located at or beneath the embankment face. It is the relative permeability that is of primary importance in the context of steady state seepage. The arrangements and types of embankment zoning are also governed by filter requirements to prevent the migration of soil or tailings into adjacent coarse fill (Vick, 1983). Problems related to piping and

improper filter zones are most often encountered where coarse mine waste is used as a construction material directly in contact with the tailings, especially when the coal waste has been end-dumped (Vick, 1983).

2.8.1. Control of Seepage in the Tailings

The cyclone and hydraulic fill methods for embankment construction and spigotting of tailings to provide a wide beach have already been discussed. The tailings are coarser at the embankment crest than at the slimes pond. Tailings are well known to fit Hazen's rule which states that permeability decreases with particle size. Kealy & Busch (1971) used a finite element program to model the fall of the seepage as it moves downstream through increasingly more permeable deposits. Their conclusion was that a lateral variation in permeability was by far the most significant factor in determining the location of the phreatic surface. The ratio of downstream sand to pond slime permeability may be as high as 100 or even 1000 (ICOLD, 1982). On the basis of theory and material testing, Abadjiev (1976) analysed the effect on the phreatic surface of an exponential variation in permeability from the pond to the embankment crest. Using a simple analytical technique based on Dupuit's solution (and confirmed by finite element results), he showed that for any intermediate beach width, the variation in permeability can critically affect the elevation of the phreatic surface within the tailings structure. For a tailings dam having a distance from pond to downstream toe 5 times its height, Abadjiev predicted that a ratio of toe to pond slime permeability of 5 would be enough to produce a concave phreatic surface. A permeability ratio of 100 (sand to slimes) with even a small beach may be enough to produce an acceptable phreatic surface (Vick, 1983). Care should be taken when using this classic zoned model of transition from high permeability sands to low permeability slimes (Vick, 1983). This degree of particle size separation requires that there be an appreciably wide range of particle sizes present in the mill discharge and a low tailings pulp density, and that the spigots be sufficiently closely spaced to minimize deposition of slime on the beach.

The degree of tailings consolidation increases with depth because the tailings are under a greater overburden pressure and have had longer to consolidate. This creates a fall in void ratio and hence permeability as the depth of tailings increases. If the pond is maintained at a constant distance from the embankment crest, then the tailings will also decrease in size downwards in the upstream method (and increase in size in the downstream method). This transgressional effect may also have an influence on the vertical permeability. Kealy et al (1974) found that the consolidated slimes at the base of the impoundment prevented high rates of flow out of the bottom of the impoundment. Vick (1983) suggested that the decrease in permeability could be a

factor of 5 or even 10. Abadjiev (1976) estimated that in the case of a moderate degree of consolidation, the decrease in permeability would be a factor of 2 or 5. In Abadjiev's estimation, this would lead to a raise in the seepage surface of about 5% of the embankment height, or a safe limit of 10% in practice.

Most authors agree that the foundation permeability exerts a greater influence on the seepage flow pattern than does tailings consolidation. Donaldson (1959) ignored permeability variation in the tailings, but by the use of flow nets was able to determine the effect on the phreatic surface of a permeable base. He found that for a saturated base the influence of base permeability was not as significant as that for an unsaturated base. In the case of an unsaturated and highly permeable base, the elevation of the seepage line is considerably reduced. This may be very significant in the explanation of the apparent success of the upstream method in some regions (Klohn, 1972). Stauffer & Obermeyer (1988) measured pore pressures in a number of cycloned sand tailings dams, and found that the measured pore pressure distribution was lower than hydrostatic. This is what might be expected because the foundations of these dams were relatively permeable and unsaturated. Stauffer & Obermeyer calculated that the factor of safety was 20% higher for the measured pore pressure distribution compared to an estimate based on hydrostatic assumptions. Kealy & Busch (1971) found (from their finite element analyses) that if the permeability of the base is less than that of the embankment, the common assumption of an impervious base is valid.

The biggest potential influence on tailings permeability comes from the day to day operation of the tailings discharge system. Swaisgood & Toland (1973) discuss the problem that may arise if horizontal layers of slimes which are deposited on the beach area interfere with the vertical seepage of water through the structure at a later date. This situation may give rise to a perched water table within the embankment. The same effect may occur in the case of a compacted waste dam if a hard surface is allowed to develop between successive lifts.

Anisotropy of permeability is a less significant but more commonplace phenomenon found in spigotted tailings or compacted sand embankments. This effect arises from interlayering of sand and slimes at a finer level in the case of spigotting, and a particle shape effect due to the elongated and ribbed nature of common tailings (Abadjiev, 1976). When the layering is of a centimetre scale or less, then the material can be considered to be anisotropic rather than vertically inhomogeneous. Klohn (1979) suggests that for stratified soil deposits the ratio of horizontal to vertical permeability may be more than 10. Even for compacted embankments, where great care has been taken to minimize horizontal stratification, the horizontal permeability is likely to be 4

to 9 times the vertical permeability. For embankments of tailings sands placed in horizontal lifts, 4-10 might be reasonable. In the case of hydraulically placed sand, the ratio of horizontal to vertical permeability may be unity. For spigotted tailings beaches Klohn suggested that a ratio of 9 appears to fit the observed piezometric water pressures. Abadjiev (1976) suggested that the anisotropy ratio may be as high as 15, and is likely to increase as the technological deviations become more harsh. Vick (1977) measured an anisotropy ratio (horizontal to vertical permeability) in gypsum tailings of 20 to 80, but in his model he also used a "more realistic" value of 5. The tailings anisotropy has the effect of lowering the phreatic surface near the pond (due to the greater vertical component of flow), and raising the phreatic surface in the downstream portion of upstream dams (due to the greater horizontal flow component) (ICOLD, 1982). Abadjiev (1976) estimated that the total rise in phreatic surface due to the tailings anisotropy is typically between 5 and 10%. However, the hydrodynamic pressure is reduced (the equipotential lines are inclined), and the influence on the stability of the slope is equivalent to some decrease of the seepage surface of about 3 to 5% or more of the embankment height. In cases where the phreatic surface is close to a shallowly inclined embankment face, a small change in the phreatic surface could cause a significant rise in the seepage exit point. Kealy & Busch (1971) found that an 8 degree inclination of the tailings sand stratification has little influence on the location of the phreatic surface. ICOLD (1982) state that it is only the anisotropy of the downstream portion of the tailings dam which is effective in altering the position of the phreatic surface exit point.

The combination of the somewhat compensating action of the tailings anisotropy and non-homogeneity, entry condition of the pond flow, and infiltration from the beach results in a phreatic surface which is between 20% and 50% lower than that in a conventional earth dam (ICOLD, 1982).

2.8.2. Control of Seepage in the Dam

The starter dam is the most obvious control of dam seepage in tailings embankment construction methods. In the upstream method, the starter dam lies on the downstream side and acts as a drainage toe. For this reason, the upstream method starter dam should be permeable to keep the seepage line low in the downstream portion of the dam. Nelson et al (1977) suggested that a permeable starter dam is more significant in reducing the phreatic surface than even a drainage blanket underneath the embankment. In the downstream method, the starter dam is on the base of the upstream dam slope. The use of an impermeable starter dam reduces seepage in these circumstances and

lowers the level of the seepage line within the dam (because the permeability increases downstream).

In the case of downstream (and centreline) techniques, it is possible to use an inclined impermeable core on the upstream side of the dam (Vick, 1983) or in the centre of the dam, as for a conventional earth dam (see Figure 2.5). Once again, care should be taken to see that the proper filter requirements are adhered to in order to prevent the migration of fines into the more permeable zone. The use of internal cores is not possible in the case of the upstream construction method.

Brawner & Campbell (1973) advocated the use of slimes deposited on the upstream face of tailings dams built using the downstream construction technique. These slimes are used in conjunction with an impervious membrane. Any seepage through the dam will be easily handled by the relatively permeable embankment. The use of an impervious seal on the upstream face of the dam may be a requirement if a significant depth of water is likely to be ponded against the dam (Mittal & Morgenstern, 1976). Kealy et al (1974) suggested that the use of slimes alone will not necessarily provide an efficient seal because the upper 5 to 6 metres will remain unconsolidated.

If the material for the starter dam is not sufficiently permeable, then a drainage toe may be used to prevent the development of a seepage line high up in the dam. The National Coal Board (NCB, 1970) suggested extending the toe back into the dam to increase dam drainage. Abadjiev (International Water Power Dam Construction, 1985) proposed a tongue shaped component to the lower part of the starter dam to extend its influence on drainage further upstream. Where a seepage surface does develop in the downstream slope, a permeable berm (of the correct filter requirements) can be placed against the downstream slope (NCB, 1970). This keeps the seepage line away from the downstream slope and prevents the saturation of the toe of the dam.

2.9. Drainage Measures

Drains have the effect of increasing the quantity of seepage and so it is particularly important for drains to have the requisite filter characteristics to prevent particle transport. Graded filter zones may be necessary to prevent internal erosion. Drains play a role in controlling the seepage and reducing the water level and pore pressures in the dam.

Internal drains may be used to control the seepage flow in downstream construction dams, but they are less effective for upstream construction dams because they are too close to the downstream face of the dam (Vick, 1983). Blanket drains (for high seepage), strip drains and pipe drains (low seepage) are laid before the placement of the

dam embankment. The location of strip drains is dependent on the ground topology. The National Coal Board (NCB, 1970) suggested that strip drains should be closely spaced in order to reduce the seepage that each drain must sustain. The drainage system connects to a drainage outlet at the base of the downstream slope. If the foundations are subject to artesian pressures, then the drains should be capable of preventing the development of excess pore pressures in the foundations. The horizontal drains may be linked to a vertical or inclined chimney drain in downstream (and centreline) dams in order to intercept lateral seepage (Vick, 1983). Chimney drains can be used in conjunction with a low permeability core (see Figure 2.5).

Collector ditches dug downstream of the dam may be cheap and highly effective for shallow permeable foundations (Brawner & Campbell, 1973). Collector wells incorporate the same principles as do collector ditches. An impervious lower layer is desirable but not essential if the wells penetrate deep enough (Vick, 1983). Collector systems have the advantage that they may be used in upstream, downstream and centreline dams. In addition, they can be added to a tailings structure as a remedial measure to control seepage as problems develop.

Drains may also be used to improve the rate of tailings consolidation. This has the effect of increasing their shear strength and reducing their volume (increasing disposal capacity). Drainage may be essential for the upstream method in the absence of a permeable foundation.

2.10. Drainage Barriers

The use of grout curtains, slurry walls and cutoff trenches is popular for shallow permeable foundations, but these measures are expensive and by no means always successful (Brawner & Campbell, 1973). Drainage barriers may prevent excessive seepage losses and the pollution of the groundwater and downstream water courses. Unfortunately, they also slow down consolidation of the tailings and increase the volume required for waste storage. The amount of seepage through the foundations can also be reduced by placing an impervious blanket upstream of the dam (Brawner & Campbell, 1973). This may consist of slimes, fine grained overburden (e.g. a clay liner) or a synthetic liner. The latter two techniques are common for uranium tailings (ICOLD, 1982). Impermeable liners cannot be guaranteed and so they are often used in conjunction with a drainage system in order to reduce the hydraulic gradient.

2.11. Seepage Analysis of Tailings Dams

The primary purpose of seepage evaluation is to assess pore pressures for input to stability analyses (Vick, 1983). Seepage in tailings embankments is commonly

assumed to occur under gravity flow and, for the purposes of pore pressures evaluation, is usually determined for steady state. These assumptions are useful in the context of stability analyses because they yield conservative estimates of pore pressures. Seepage evaluation for the purpose of determining impoundment seepage loss, on the other hand, is quite another matter. Here it may be necessary to assess unsaturated flow that occurs under capillary rather than gravity gradients (Vick, 1983).

The limiting factor to the usefulness of saturated flow analysis appears to be the difficulty in obtaining reliable values of permeability. For unsaturated flow analysis the problem is even more severe. The permeability and pore pressure are functions of the moisture content of the soil. These relationships also depend on whether the soil is in a wetting cycle or a drying cycle. For a combined saturated/unsaturated problem (the unconfined aquifer), the relative permeability of two soils of different particle size but the same moisture content will be dependent on their degree of saturation. McWhorter (1985) reviews these and other difficulties of modelling unsaturated flow. Unsaturated soil properties are difficult and time consuming to obtain, and probably as subject to gross error as is the measurement of saturated permeability. The transient unsaturated flow model also requires starting values of moisture content at every point in the soil at the beginning of the analysis. The analysis of the phreatic surface in the saturated case is either independent of the soil permeability, or dependent only on the relative permeability of the soils. As a consequence, the results for one analysis is applicable for soils having the same geometry and, in the case of multiple soil types, having the same relative permeabilities. The soil specific nature of unsaturated analysis would seem to preclude its usefulness for the general case.

2.11.1. Theory of Groundwater Flow

Slope stability analyses using limit equilibrium methods are restricted to the consideration of 2-dimensional cross sections. In order to keep the discussion simple, only two dimensions are considered here.

The fundamental equation for laminar groundwater flow in one dimension is known as Darcy's law:

$$v = ki \qquad \text{Eq. 2.1}$$

where v is the seepage velocity, k is the hydraulic conductivity, and i is the hydraulic gradient. The seepage velocity refers to the average velocity of the water, not the actual speed and direction taken by the water between the soil particles. The hydraulic

gradient i is the ratio of the difference in head potential (energy) and distance between two points. The head (or water) potential for flow in saturated porous media is approximated by an equation (derived from the steady state Benoulli equation) summing the elevation head (z) and the pore water fluid pressure (p) to unit weight of water (γ) ratio:

$$\phi = z + \frac{p}{\gamma} \quad . \qquad \text{Eq. 2.2}$$

Hydraulic conductivity is a term which is used synonymously with permeability in hydrogeology. It refers to the measured constant which relates the seepage velocity to the hydraulic gradient for a particular soil section. This concept has been extended to two dimensions (and also three) by considering the seepage velocity at a point $v(x,y)$:

$$\begin{Bmatrix} v_x \\ v_y \end{Bmatrix} = \begin{bmatrix} k_{xx} & k_{xy} \\ k_{yx} & k_{yy} \end{bmatrix} \begin{Bmatrix} \partial\phi/\partial x \\ \partial\phi/\partial y \end{Bmatrix} \qquad \text{Eq. 2.3}$$

where $\{v_x,v_y\}$ is the seepage velocity vector in x,y coordinates, $[\{k_{xx},k_{xy}\},\{k_{yx},k_{yy}\}]$ is the permeability tensor, and ϕ is the water potential.

The steady state condition is where the quantity of water flowing into a representative volume of soil equals the quantity of water flowing out. In an unconfined aquifer the compressibility of the soil and of the water is usually ignored because it is unimportant compared to displacements of the free surface which affect the flow pattern. The principle of conservation of mass determines that unconfined saturated flow may be modelled by Richard's equation for anisotropic and inhomogeneous media, or by Laplace's equation if the permeability is a constant:

Richard's equation $$\frac{\partial}{\partial x}\left(k(x)\frac{\partial\phi}{\partial x}\right) + \frac{\partial}{\partial y}\left(k(y)\frac{\partial\phi}{\partial y}\right) = 0 \qquad \text{Eq. 2.4}$$

Laplace's equation $$\frac{\partial\phi^2}{\partial x^2} + \frac{\partial\phi^2}{\partial y^2} = 0 \qquad \text{Eq 2.5}$$

These equations may also be used for unsteady (transient) saturated flow. The position of the free surface may be obtained for a series of time intervals by calculating the distance travelled by water in a direction normal to the free surface in the corresponding time interval. This calculation depends on the effective porosity n; that is the fraction of the soil void space which is free to fill or drain in gravity flow. It is assumed that the effective porosity is non-hysteretic and isotropic. The velocity $\bar{\mathbf{v}}$ of the free surface may be written:

$$\bar{\mathbf{v}} = \frac{\mathbf{n} \cdot \mathbf{v}}{n} \qquad \text{Eq. 2.6}$$

where **n** is the unit outward normal vector to the free surface, and **v** is the Darcian seepage velocity vector.

2.11.2. Graphical Solution to the Flow Through Tailings Dams

The graphical solution to the problem of saturated flow is known in the literature as a flow net. The beauty of flow net construction is that it represents a dimensionless solution to the problem. The same flow net may be homogeneously scaled to fit a geometrically congruent problem with the same ratio of permeabilities. Cedergren (1977) presented flow nets for a variety of different problems. Flow nets are constructed from two families of curves with special properties:

I. Equipotentials are the loci of points of equal head potential.

II. Streamlines join points along the flow path.

These curves are the contours of the two orthogonal functions $\Phi(x,y)$ and $\Psi(x,y)$ respectively (see Figure 2.9). The velocity components u,w may be expressed as:

$$u = -\frac{\partial \Phi}{\partial x}$$
$$w = -\frac{\partial \Phi}{\partial y} \qquad \text{Eq. 2.7}$$

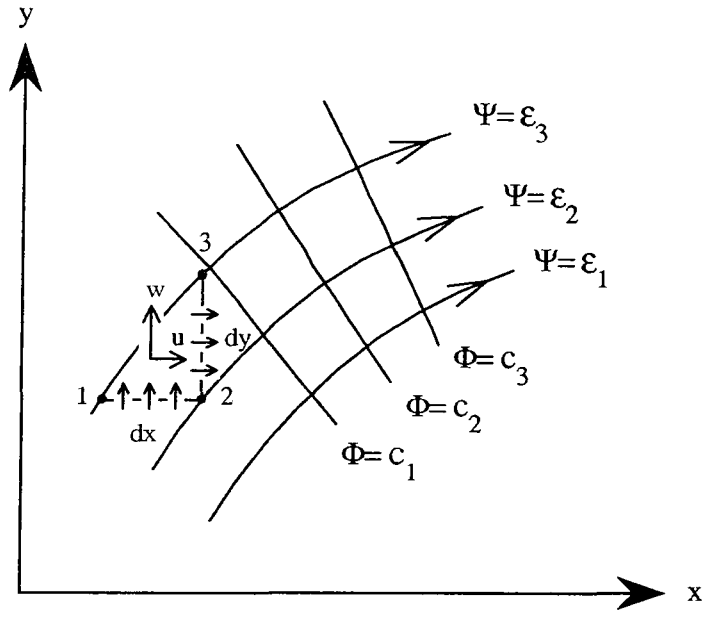

Figure 2.9 Streamlines and Equipotential Lines

Continuity requires that the flow rates passing through section 1-2 and 2-3 of Figure 2.9 are equal. If second order terms are neglected, then we have:

$$w\,dx - u\,dy = 0 \quad . \qquad \text{Eq. 2.8}$$

Both the velocity potential and streamline functions are governed by Laplace's equation. For homogeneous and isotropic media, a set of these curves is drawn so that they intersect at 90 degrees and form a patchwork of curvilinear squares. The Cauchy-Riemann equations give the mathematical relationship between the gradient of the potential and streamline functions:

$$\frac{\partial \Phi}{\partial x} = \frac{\partial \Psi}{\partial y} \qquad \frac{\partial \Phi}{\partial y} = -\frac{\partial \Psi}{\partial x} \qquad \text{Eq. 2.9}$$

Harr (1962) showed how the method may be extended to certain anisotropic and inhomogeneous sections by means of a geometrical transformation. The steady state

free surface is a streamline, but its position is not known and must be found by trial and error. The ratio of the gaps between the streamlines and the drops in equipotential is unique for each problem studied.

Flow nets were used by Donaldson (1959, 1960) to investigate the influence of a permeable base (with high and low water table) on the position of the free surface in tailings dams. Klohn (1979) uses flow nets to show the influence of various seepage control measures within a tailings dam and embankment. The popularity of flow nets has dwindled with the introduction of numerical methods. Mantei (1985) reported that flow nets were seldom used at the Bureau of Reclamation, U.S. Department of the Interior, because of their inflexibility in handling the complexities of flow.

There is still interest being shown in the use of flow nets as a method of presenting numerical results (Fan et al, 1992; Aziz et al, 1992). A computer produced flow net offers self justification for the solution since it can be judged good or bad by the same criteria as a hand drawn net. The computer produced flow net can also be used as a guide to drawing others and a dimensionless solution for similar problems.

2.11.3. Analytical Solutions

Much has been written concerning the analytical solution of groundwater flow equations (e.g. Polubarinova-Kochina, 1962; Harr, 1962; De Wiest, 1965) which is beyond the scope of this thesis. One method of solution is, however, worth describing because it has been used in the study of tailings dam flow and it is mentioned in a later section. Dupuit's solution for the flow of water in an earth dam is described in all the textbooks mentioned above. Under the assumptions that flow was predominantly horizontal and the water table was nearly flat, Dupuit suggested that the flow in any vertical column could be considered horizontal and exactly equal to the gradient of the free surface. For a rectangular cross section dam (see Figure 2.10), the equation corresponding to these conditions is as follows:

$$\frac{q}{k} = \frac{\left(H^2 - h_t^2\right)}{2L} \qquad \text{Eq. 2.10}$$

where q is the seepage discharge per unit width (m^3s^{-1}/m), k is the permeability (ms^{-1}), H is the height of the water in the upstream reservoir (m), h_t is the depth of the tailwater, and L is the length of the dam.

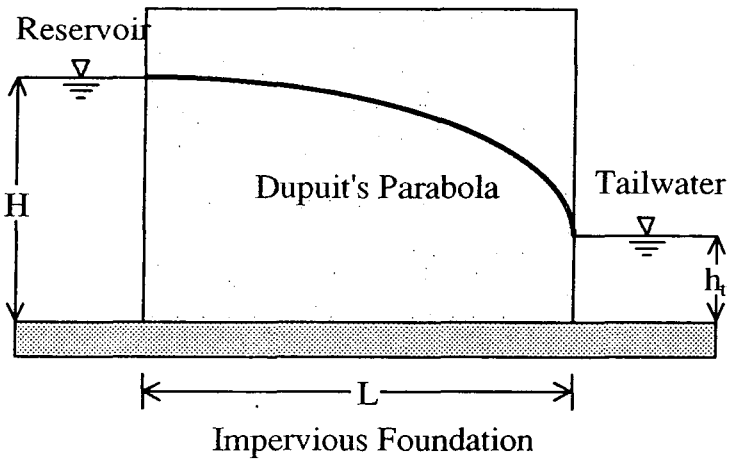

Figure 2.10 Dupuit's Parabola for an Earth Dam

The position of the free surface in Figure 2.10 is obviously incorrect because the velocity at the seepage exit point would be infinite without the development of a seepage surface. However, the quantity of discharge predicted by Equation 2.10 is known to be exact for this problem.

Pavlovsky (Polubarinova-Kochina, 1962), Schaffernak and van Iterson (Harr, 1962) extended Dupuit's solution to the flow through earth dams with inclined slopes and a seepage surface by approximating the flow equation in the upstream and downstream portions of the dam. Casagrande (Harr, 1962) obtained a solution for the dam problem by approximating the horizontal gradient by the sine of the angle the free surface makes with the horizontal. These methods are covered in more detail in a later chapter.

Pavlovsky's method of slices (Polubarinova-Kochina, 1962) is a development from Equation 2.10. The problem under consideration is split into standard form slices along approximate equipotentials. Charts are available which give the shape factor for the relative dimensions of each standard form. Equations based on Dupuit's approximation are combined with these shape factors and used to calculate the flow within each slice. Continuity requirements for the flow allow the solution of quite complex geometries.

Mittal & Morgenstern (1976) used Dupuit's equation to obtain the position of the seepage line within part of a tailings dam (and consolidation induced pore pressures in an adjacent section of the structure). Abadjiev (1976) also used Dupuit's equation, in this case on a transformed section of a tailings embankment to take into account the horizontal variation in permeability. The results are in good agreement with a finite element solution (results not given). Stello (1987) gave a charted solution to the

method of slices in earth dams with or without a core. However, these methods have also been superseded by the use of numerical methods.

2.11.4. Physical Models and Analogues

Bear (1988, pp. 665-725) listed several types of models and analogues which may be used to study groundwater problems. He defined a model as being of a different scale to the prototype problem, but with every element faithfully reproduced. An analogue uses a different physical phenomenon but with characteristic equations of the same form.

Sand box models are scaled down reproductions of the problem in question. According to Cargill et al (1983), the capillary effects which cannot be scaled make the sand box model invalid for modelling earth dam flow. Cargill used a centrifugal model in which the artificially high "gravity" is able to counteract the capillary effects. However, the evidence of this paper seems to suggest that this type of model does not yet provide very reliable results.

Types of analogues include the Hele-Shaw viscous flow analogue, the electric analogue, ion motion analogue and the elastic membrane analogue. Mantei (1985) reported that the Bureau of Reclamation, U.S. Department of the Interior, has successfully used an electrolytic tank (a version of the electric analogue) for many years. They found that it was still useful for the process of screening the results of numerical solutions for gross errors.

2.11.5. Numerical Methods

Numerical methods have been used in the study of flow through tailings dams since the early work of Kealy & Williams (1971a),(1971b) and Kealy & Busch (1971). Kealy used a finite element program developed by R.L.Taylor at the University of California at Berkeley. Taylor's program uses the method of Taylor & Brown (1967) to obtain the position of the free surface. The same program has also been used by Vick (1977) and Nelson et al (1977). Mantei (1985) reported that the U.S. Bureau of Reclamation also used 3-dimensional finite element models to study both saturated and unsaturated flow. However, they do not view the unsaturated model as a general purpose tool because of the extra computational effort required and the need for more exotic data gathering. Mantei also reported an interest in the development of the boundary integral element method for saturated flow analysis. Finite element methods are discussed in another chapter in this thesis.

Finite difference methods have been used to analyse vertical (saturated/unsaturated) seepage below tailings embankment (e.g. Davis, 1980) and 3-dimensional seepage below ponded water (e.g. Fipps & Skaggs, 1990).

Chapter 3
The Finite Element Method

Analytical methods such as Dupuit's solution may be used to solve the governing equations exactly over a simple problem domain. Extension of the analytical solution to more complex domains (e.g. by the method of fragments) requires simplifying assumptions to be made concerning the problem geometry, material properties and/or boundary conditions. The *finite element* (FE) method is an alternative technique in which the partial differential equations are solved approximately for more realistic problem descriptions. A properly formulated finite element result actually converges to the exact solution as the size of the element decreases (Strang & Fix, 1973, p. 47). A description of the finite element method can be found in many textbooks, such as, for example, Zienkiewicz & Taylor (1989), Strang & Fix (1973), Connor & Brebbia (1976) and Desai & Abel (1972). This chapter does not attempt to give a full description of the FE method, but rather it is an introduction to the concepts and techniques used in the computer program developed for this thesis. Hence the description is restricted to a specific implementation of linear triangular elements.

The finite element method is just one of a complementary set of numerical techniques that have been employed to solve partial differential equations. The *finite difference method* and the *boundary integral element method* are also commonly used to solve problems involving groundwater flow. A comparison of these methods is beyond the scope of this thesis. Each of these techniques has advantages in certain particular cases, an individual's or team's previous experience usually being the deciding factor in making a choice.

3.1. The Finite Element Concept

Clough (1960) described how the finite element method developed in the field of structural engineering. The first step in its evolution was the approximation of the mechanical relationships of the discrete components (bars) of a structural assemblage. For each bar there is a set of equations which relate the forces and displacements (direct stiffness method) or the flexibilities at the interconnections. Attempts were made to apply these matrix methods to continuous structures. In the first instance, the continuum was replaced by an equivalent assemblage of trusses in a lattice system. The

elastic properties of a portion of the continuum may be modelled by a suitable choice of the areas which make up the corresponding lattice structure. The important leap follows immediately from the lattice element technique; the continuum is partitioned into an assemblage of "finite" elements which are interconnected at the corners (and at mid-side nodes for higher order elements). Clough (1960) not only used the term "finite element" for the first time, but he also described the basis for most of the techniques used in this thesis:

- The principal effect of the finite element discretization is to relax continuity requirements between elements, except at nodal points.
- The dependent variable is assumed to vary linearly over the surface of the element.
- The elements are constrained to maintain the continuity of the dependent variable.
- The error of the solution may be reduced to any required degree by increasing the degrees of freedom.

The finite element method gained mathematical respectability when it was recognised as a special case of the Ritz approximation (Strang & Fix, 1973, p. ix). A proof of convergence for the method followed from a rigorous mathematical treatment.

3.2. A Finite Element Solution to Laplace's Equation

The finite element approach described here is the *method of weighted residuals*. This method of approximation is more flexible (e.g. in the study of nonlinear problems) than the variational method which requires a variational formulation of the problem. The disadvantage of the method is that it is considered less rigorous. This is not a problem in the case of the algorithm used for this thesis because the resulting finite element equations are identical.

The 2-dimensional steady state equation for unconfined groundwater flow through an incompressible saturated porous medium is written as:

$$\frac{\partial}{\partial x}\left(K_x \frac{\partial \phi}{\partial x}\right)+\frac{\partial}{\partial y}\left(K_y \frac{\partial \phi}{\partial y}\right)=0 \qquad \text{Eq. 3.1}$$

where ϕ is the head potential (a function of the space coordinates x,y), and K_x and K_y are the permeabilities (hydraulic conductivities) in the x and y directions. It is assumed that the permeability tensor is in alignment with the coordinate system.

The differential equation to be solved is of the form:

$$L(\phi(x,y)) - F(x,y) = 0 \qquad \text{Eq. 3.2}$$

where L is a differential operator, and F is a known function to force the prescribed boundary conditions. The function ϕ is replaced by the finite element approximation $\hat{\phi}$:

$$\hat{\phi}(x,y) = \sum_{i=1}^{m} N_i(x,y)\phi_i \qquad \text{Eq. 3.3}$$

where N_i is an interpolating function to obtain $\hat{\phi}$ from discrete values at the nodes, and m is the number of nodes. When Equation 3.3 is substituted into Equation 3.2 a residual term must be included to take into account the approximation:

$$L\left(\hat{\phi}(x,y)\right) - F(x,y) = R(x,y) \neq 0 \qquad \text{Eq. 3.4}$$

The *method of weighted residuals* minimizes the difference between the true head potential and the finite element approximation by forcing the weighted sum of the residual term to zero. The summation is carried out over the finite element domain Ω:

$$\int_{\Omega} W(x,y)R(x,y)\, d\Omega = 0 \qquad \text{Eq. 3.5}$$

Substituting Equation 3.4 into Equation 3.5 for a 2-dimensional domain Ω produces:

$$\iint_{\Omega} W(x,y)\left[L\left(\hat{\phi}(x,y)\right) - F(x,y)\right] d\Omega = 0 \qquad \text{Eq. 3.6}$$

The equation as it appears in 3.6 suggests that the head potential at one point affects the head potential at every other point in the domain. The crucial step in the finite element method is the choice of polynomial approximating functions for $W(x,y)$ and $N_i(x,y)$ which are defined in a piecewise fashion over a set of partitions or elements of the domain. These elements have continuity enforced between neighbours at the element

nodes. Nodes may be at element vertices or, in higher order polynomial approximations, on the element edges (e.g. the mid-sides). The nodal basis functions $N_i(x,y)$ interpolate the values of the head potential across the element. They have a value of unity at the node for which they are defined, and a value identically zero at every other node. Figure 3.1 shows a linear nodal basis function for a triangular element in a 2-dimensional domain. A linear nodal basis function has a constant slope over the elements containing node *i*.

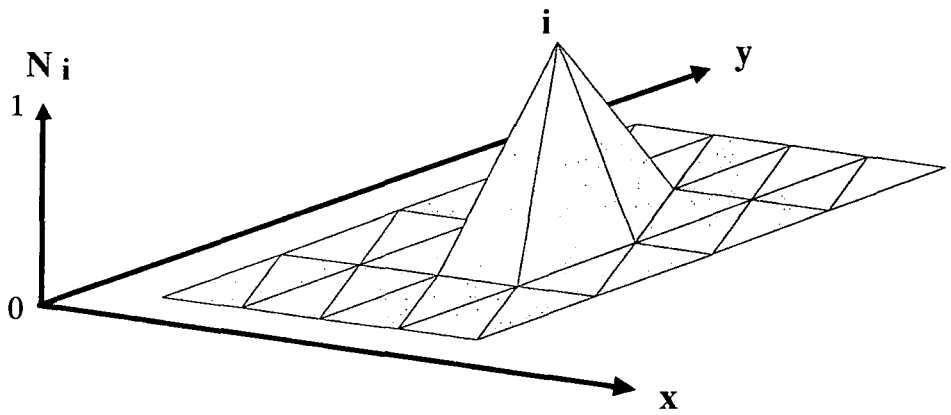

Figure 3.1 Linear Nodal Basis for a Triangular Element

Except locally (i.e. for functions at nodes which have elements in common), the nodal basis functions are orthogonal. Clearly these functions satisfy Equation 3.3.

For a particular element (*e*) (see Figure 3.2), the values of $\hat{\phi}(x,y)$ may be obtained at any point $P(x,y)$ within the element by multiplying the value of ϕ at each of the nodes by the node's basis function evaluated at $P(x,y)$:

$$\hat{\phi}_n^e(x,y) = N_i\phi_i + N_j\phi_j + N_k\phi_k \qquad \text{Eq. 3.7}$$

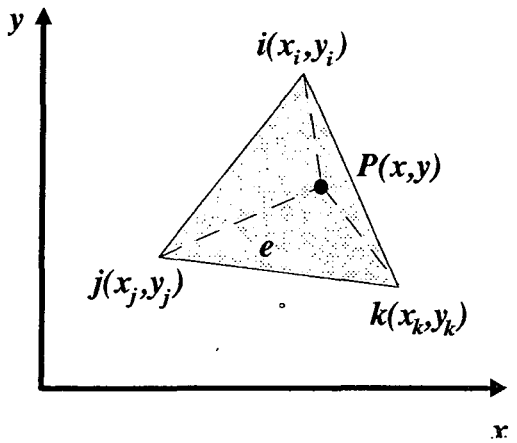

Figure 3.2 Interpolation Within a Linear Triangular Element

In the *Galerkin method* the interpolation functions and weighting functions are identical. The contribution to the residual of node i of element e with area A and boundary Γ can be written:

$$R_i^{(e)} = -\iint_{A^{(e)}} N_i^{(e)} \left[K_x^{(e)} \frac{\partial^2 \hat{\phi}^{(e)}}{\partial x^2} + K_y^{(e)} \frac{\partial^2 \hat{\phi}^{(e)}}{\partial y^2} \right] dxdy \qquad \text{Eq. 3.8}$$

In this form the equation contains second derivatives which are required to have finite energy in the approximation (Strang & Fix, 1973). Integration by parts is used to reduce the order of the equation and allow the use of linear elements (which only have first derivatives of finite energy):

$$R_i^{(e)} = -\iint_{A^{(e)}} \left[K_x^{(e)} \frac{\partial N_i^{(e)}}{\partial x} \frac{\partial \hat{\phi}^{(e)}}{\partial x} + K_y^{(e)} \frac{\partial N_i^{(e)}}{\partial y} \frac{\partial \hat{\phi}^{(e)}}{\partial y} \right] dxdy + \oint_{\Gamma} N_i^{(e)} K_x^{(e)} \frac{\partial \hat{\phi}^{(e)}}{\partial x} + N_i^{(e)} K_y^{(e)} \frac{\partial \hat{\phi}^{(e)}}{\partial y} \, d\Gamma \qquad \text{Eq. 3.9}$$

The line integral for interior elements (those not lying on the boundary) will be zero because the incoming and outgoing flows cancel one another. For boundary elements this term represents the specified rates of groundwater flow (Neumann boundary conditions).

Matrix algebra is the usual form of representing the set of linear equation to be solved. The surface integral is collected in a square $m \times m$ matrix (where m is the number of nodes) called the *global conductance matrix* $[\mathbf{K}]$ (or stiffness matrix). The line integral is collected into a forcing vector $\{\mathbf{F}\}$. The residual terms make up the *global residual vector* $\{\mathbf{R}\}$:

$$\{\mathbf{R}\} = [\mathbf{K}]\{\hat{\phi}\} - \{\mathbf{F}\} = \{0\} \qquad \text{Eq. 3.10}$$

For the element e of Figure 3.2, the contribution to the global conductance matrix (element conductance matrix) may be written:

$$\left[\mathbf{K}^{(e)}\right] = \iint_{A^{(e)}} \begin{bmatrix} \frac{\partial N_i^{(e)}}{\partial x} & \frac{\partial N_i^{(e)}}{\partial y} \\ \frac{\partial N_j^{(e)}}{\partial x} & \frac{\partial N_j^{(e)}}{\partial y} \\ \frac{\partial N_k^{(e)}}{\partial x} & \frac{\partial N_k^{(e)}}{\partial y} \end{bmatrix} \begin{bmatrix} K_x^{(e)} & 0 \\ 0 & K_y^{(e)} \end{bmatrix} \begin{bmatrix} \frac{\partial N_i^{(e)}}{\partial x} & \frac{\partial N_j^{(e)}}{\partial x} & \frac{\partial N_k^{(e)}}{\partial x} \\ \frac{\partial N_i^{(e)}}{\partial y} & \frac{\partial N_j^{(e)}}{\partial y} & \frac{\partial N_k^{(e)}}{\partial y} \end{bmatrix} dxdy \qquad \text{Eq. 3.11}$$

If q represents the specified nodal flow rate normal to the element edge (for *natural* or Neumann boundary conditions), then the integrated specified flow rate for node i of element e may be written:

$$F_i^{(e)} = \oint_{\Gamma^{(e)}} N_i^{(e)} K_x^{(e)} \frac{\partial \hat{\phi}^{(e)}}{\partial x} + N_i^{(e)} K_y^{(e)} \frac{\partial \hat{\phi}^{(e)}}{\partial y} \, d\Gamma = \int_{\Gamma} N_i^{(e)} q \, d\Gamma \qquad \text{Eq. 3.12}$$

It is assumed that the *essential* (Dirichlet) boundary conditions are to be satisfied exactly in the solution process.

The evaluation of these integrals for each node in element e gives the components of the element specified flow matrix ($\{\mathbf{F}^{(e)}\}$) for element e:

$$\left\{\mathbf{F}^{(e)}\right\} = \begin{Bmatrix} F_i^{(e)} \\ F_j^{(e)} \\ F_k^{(e)} \end{Bmatrix} \qquad \text{Eq. 3.13}$$

Combining Equations 3.11 and 3.13:

$$\begin{Bmatrix} R_i^{(e)} \\ R_j^{(e)} \\ R_k^{(e)} \end{Bmatrix} = \left[\mathbf{K}^{(e)}\right] \begin{Bmatrix} \phi_i \\ \phi_j \\ \phi_k \end{Bmatrix} - \begin{Bmatrix} F_i^{(e)} \\ F_j^{(e)} \\ F_k^{(e)} \end{Bmatrix} \qquad \text{Eq. 3.14}$$

The global system of equations is obtained by summing the contributions from all the elements, and Equation 3.10 becomes the finite element equation:

$$[\mathbf{K}]\{\phi\} = \{\mathbf{F}\} \qquad \text{Eq. 3.15}$$

The remaining problem is to calculate the derivatives of the nodal basis functions and integrate them over the elements. The choice of linear triangular elements simplifies this problem considerably. The nodal basis functions used here are based on triangular coordinates (Zienkiewicz et al, 1970, pp. 383-432). This element is a trivial example of an isoparametric element; that is to say one whose coordinates may also be interpolated using the nodal basis functions. The functions used to interpolate coordinates are commonly called shape functions. The element *e* with nodes *i,j,k* pictured in Figure 3.2 is given linear shape functions $N_i^{(e)}$, $N_j^{(e)}$, and $N_k^{(e)}$. The sum of the shape functions must be unity so that their value at the nodes is unity for the corresponding shape function, and zero for the others.

The interpolation equations (both nodal basis functions and shape functions) are as follows:

$$\begin{aligned} 1 &= N_i^{(e)} + N_j^{(e)} + N_k^{(e)} \\ x &= N_i^{(e)} x_i + N_j^{(e)} x_j + N_k^{(e)} x_k \\ y &= N_i^{(e)} y_i + N_j^{(e)} y_j + N_k^{(e)} y_k \\ \hat{\phi} &= N_i^{(e)} \phi_i + N_j^{(e)} \phi_j + N_k^{(e)} \phi_k \end{aligned} \qquad \text{Eq. 3.16 a,b,c,d}$$

Equations 3.16 a, b and c may be inverted to obtain equations for the shape functions:

$$\begin{aligned} N_i^{(e)}(x,y) &= \frac{1}{2A^{(e)}}(a_i + b_i x + c_i y) \\ N_j^{(e)}(x,y) &= \frac{1}{2A^{(e)}}(a_j + b_j x + c_j y) \\ N_k^{(e)}(x,y) &= \frac{1}{2A^{(e)}}(a_k + b_k x + c_k y) \end{aligned}$$

$$
\begin{aligned}
a_i &= x_j^{(e)} y_k^{(e)} - x_k^{(e)} y_j^{(e)} \quad & a_j &= x_k^{(e)} y_i^{(e)} - x_i^{(e)} y_k^{(e)} \quad & a_k &= x_i^{(e)} y_j^{(e)} - x_j^{(e)} y_i^{(e)} \\
b_i &= y_j^{(e)} - y_k^{(e)} & b_j &= y_k^{(e)} - y_i^{(e)} & b_k &= y_i^{(e)} - y_j^{(e)} \\
c_i &= x_k^{(e)} - x_j^{(e)} & c_j &= x_i^{(e)} - x_k^{(e)} & c_k &= x_j^{(e)} - x_i^{(e)}
\end{aligned}
$$

$$
2A^{(e)} = \det \begin{vmatrix} x_i^{(e)} & y_i^{(e)} & 1 \\ x_j^{(e)} & y_j^{(e)} & 1 \\ x_k^{(e)} & y_k^{(e)} & 1 \end{vmatrix}
$$

Eq. 3.17

The derivatives of the shape functions are as follows:

$$
\begin{aligned}
\frac{\partial N_i^{(e)}}{\partial x} &= \frac{b_i}{2A^{(e)}} \quad & \frac{\partial N_j^{(e)}}{\partial x} &= \frac{b_j}{2A^{(e)}} \quad & \frac{\partial N_k^{(e)}}{\partial x} &= \frac{b_k}{2A^{(e)}} \\
\frac{\partial N_i^{(e)}}{\partial y} &= \frac{c_i}{2A^{(e)}} \quad & \frac{\partial N_j^{(e)}}{\partial y} &= \frac{c_j}{2A^{(e)}} \quad & \frac{\partial N_k^{(e)}}{\partial y} &= \frac{c_k}{2A^{(e)}}
\end{aligned}
$$

Eq. 3.18

Rather than use numerical integration, the nodal basis functions may be integrated directly. Noting that $\iint_{A^{(e)}} dxdy = A^{(e)}$ the element conductance matrix (Equation 3.11) is given by:

$$
\left[K^{(e)}\right] = \frac{K_x^{(e)}}{4A^{(e)}} \begin{bmatrix} b_i^2 & b_i b_j & b_i b_k \\ b_j b_i & b_j^2 & b_j b_k \\ b_k b_i & b_k b_j & b_k^2 \end{bmatrix} + \frac{K_y^{(e)}}{4A^{(e)}} \begin{bmatrix} c_i^2 & c_i c_j & c_i c_k \\ c_j c_i & c_j^2 & c_j c_k \\ c_k c_i & c_k c_j & c_k^2 \end{bmatrix}
$$

Eq. 3.19

Note that these matrices are symmetrical.

The essential boundary conditions are commonly forced on the matrices by altering rows containing the nodes at which the potential is known. This may be done by multiplying the appropriate diagonal of the global conductivity matrix by an arbitrarily large number, and setting the corresponding right hand side of the equation to the product of the known potential and the new diagonal value (Payne-Irons method). This method weights the resulting calculated head potential heavily towards the prescribed

value. An alternative method is to change all the coefficients on the appropriate row to obtain an "exact" solution for the prescribed potential.

The resulting system of simultaneous equations may be solved using a direct method such as *Gauss elimination*, or an iterative method such as *successive over relaxation* (SOR) (e.g. Norrie & de Vries, 1978, pp. 223-225, 238-239).

3.3. Mesh Generation

The discussion of mesh generation has been restricted to 2-dimensional finite element schemes. However, many of the principles are pertinent to 3-dimensional mesh generators. The Finite Element domain is partitioned into a patchwork (mesh) of compatible (or consistent) elements without openings, overlaps or geometric discontinuities. This process takes up a disproportionate length of time in the FE analysis cycle. In the early stages of finite element development, the finite element mesh was calculated by hand and passed as data to the computer program. The advance of finite element techniques including higher order elements (with greater number of nodes), mesh refinement (in order to increase solution accuracy), together with the increasing capacity of the computing facilities (in terms of increased memory and computational speed), has necessitated the development of automatic mesh generation techniques. This trend has been further accelerated by the development of error estimation and adaptive meshing techniques (see later).

3.3.1. Finite Element Mesh Requirements

General

The FE mesh is required to be a reasonable fit to the geometrical boundaries of the domain to be modelled. This may include both exterior boundaries and interior boundaries describing distinct regions or holes in the domain. The location of the boundary may be part of the finite element solution and not known *a priori*. Triangles are a more flexible geometry than quadrilaterals because a single element can fill a triangular hole and a pair may fill any quadrilateral element. They may also be varied in size smoothly across a mesh faster than quadrilateral elements. It is common to have a transitional zone of triangular elements in a predominantly quadrilateral mesh to change the nodal density across the mesh (see Figure 3.3). Quadrilateral elements are often preferred because they are slightly less stiff than their triangular equivalents of the same polynomial degree.

Boundaries may be made up of straight line segments or curves. If the problems to be considered has curved boundaries, then advantages may accrue by having elements with curved boundaries such as quadratic (or higher degree) isoparametric elements (Zienkiewicz et al, 1970).

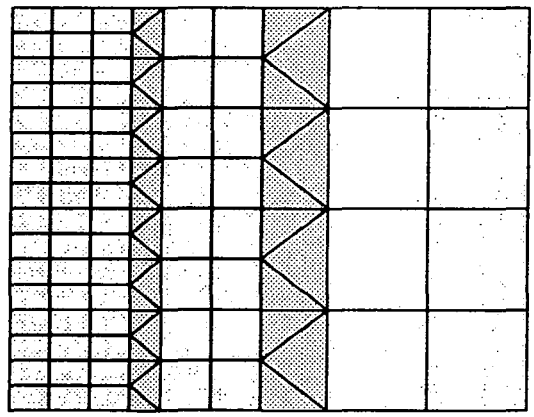

Figure 3.3 Triangular Mesh Transition Zone

The semi-bandwidth of the resulting mesh (the greatest node number difference in any element plus one) should be kept to a minimum in order to reduce the computational cost and memory requirement of the solution technique.

Nodes

According to Desai & Abel (1972, pp. 156-159) the nodes of the FE mesh are required to have sufficient densities at:

- Concentrated loads
- Abrupt changes in distributed loads
- Abrupt changes in material properties
- Geometrical boundary complexities.

The nodal density may be decided by the program user or, in the case of modern adaptive meshing algorithms, by the program itself. In an *a priori* technique the mesh spacing is calculated before the first mesh generation using the theoretical convergence rate for the solution. *A posteriori* methods are used after an initial FE solution in order to calculate a more accurate mesh. The *a priori* techniques tend to be too pessimistic because they are based on the worst possible case (Craig et al, 1989). Methods for

calculating an optimal mesh using an *a posteriori* technique are discussed in a later section.

Elements

There are requirements for the properties of the elements themselves which may conflict with the optimum nodal densities:

- The elements are required to have good aspect ratios. For triangular elements this means that no angle should be too close to 180° (Babuska & Aziz, 1976).
- Elements should vary in size smoothly across the mesh (Thacker, 1980).
- Triangular elements should be as nearly equilateral (or right in the case of quadrilaterals) as possible (Cavendish, 1974).
- For the purposes of gradient recovery in the case of triangular partitions (see later section), it is also beneficial if each (internal) node is connected to six edges (Levine, 1985).

3.3.2. Automatic Mesh Generation

The object of automatic mesh generation is to relieve the user from the tedious and error prone job of constructing the finite element mesh by hand. Zienkiewicz & Phillips (1971) and Cavendish (1974) suggested that the job of a mesh generator should be to minimize the quantity of data required by the finite element program consistent with:

(1) Adequate boundary description

(2) Different material properties

(3) Graded mesh

(4) Good aspect ratio

(5) Numbering scheme to reduce bandwidth

(6) Economy in computer time and user effort.

Cavendish et al (1985) divided automatic mesh generators into *interpolation* and *triangulation* algorithms.

Interpolation Methods

Interpolation algorithms use some technique such as mapping (e.g. Zienkiewicz & Phillips, 1971) to transfer a standard pattern of nodes to a more complex geometry. This is usually preceded by a division of the original geometry into a set of simpler sub-

regions. The data specifies, albeit in some general way, a predetermined pattern of nodes and elements. The job of the meshing algorithm is to calculate and store the interpolated coordinates and element topologies. These types of algorithm produce highly structured meshes which are pleasing to the eye. Unfortunately they are rather inflexible and not suited to adaptive techniques (see later section).

Triangulation methods

Triangulation algorithms (e.g. Cavendish, 1974; Yerry & Shephard, 1983; Cavendish et al, 1985) construct a set of nodes and an element topology appropriate for the geometry (and the required nodal spacing) using some criteria for the requisite element shape and size. For irregular geometries it would be difficult to predict the final mesh coordinates and topology without simulating the algorithm itself. This type of algorithm usually requires post-processing to obtain a smooth mesh. One favoured method is Laplacian smoothing in which internal nodes are centred within the area surrounded by adjacent connected nodes (e.g. Cavendish, 1974).

The *advancing front method* of Peraire et al (1987) which was used for this thesis is an example of a triangulation algorithm. The biggest difference between this method (described more fully in a later chapter) and the other methods cited is that the nodes are calculated at the same time as the element topologies. This process occurs from the domain boundaries into the interior (hence giving rise to the name).

3.4. Error and Convergence for the Finite Element Method

This section is intended to provide a brief explanation of the theory concerning the measurement of error and adaptive techniques utilized in this thesis. For a more complete analysis the reader is directed to the primary sources used by the author:

- Strang & Fix (1973) for a mathematical treatment of the finite element method.
- Krizek & Neittaanmaki (1987) for a brief survey and bibliography of superconvergence in the solution of differential and integral equations.
- Levine (1985) for an analysis of the superconvergent recovery of the gradient from linear triangular meshes.
- Zhu, Zienkiewicz & Craig (1987) for a description of the h-adaptive strategy using a local and global error estimator.
- Istok, J. (1989) for an in-depth description of the assembly of the finite element equation for groundwater flow.

The logical order of explanation is to consider the convergence and error estimates for the FE method, followed by the mesh generation techniques which take advantage of the convergence properties. Unfortunately the convergence of the FE method also depends on the mesh generation scheme employed. This means that "adaptive" methods of mesh generation are mentioned before they are defined. The reader is referred ahead to Page 54 for the definitions of adaptive techniques and terminology.

3.4.1. The Source of Error in the Finite Element Method

Ramstad (1970) divided the errors in approximation into two groups:

Rounding errors.

These are errors introduced into the solution due to the computational nature of the solution process. Digital computers hold a binary representation of the calculated values of all floating point variables to only a fixed number of digits. Mathematical operations (particular the subtraction of similar numbers) lead to a degradation of the accuracy of the number stored because the least significant digits are commonly lost. This process is slowed down if the numbers are calculated at a higher accuracy and then rounded to the required number of places. A complete truncation of the variables leads to a sharp fall in the accuracy. In extreme cases this may lead to a failure for the solution to converge.

The magnitude of the rounding errors depends most strongly on the size of the mesh spacing h, and the order of the partial differential equation to be approximated. Rounding error may be decreased by using a higher degree basis function and a larger mesh spacing. The effects of rounding error may be diminished by using a higher data precision (i.e. double precision).

The solution of the mass matrix system is the largest potential source of rounding error. The choice of solution method (e.g. to remove steps in which similar numbers are subtracted one from another) plays an important role in managing the rounding error. The residual error from the solution process may be reduced by replacing the original right hand side by the residual vector, and solving for the approximate errors (e.g. Norrie & de Vries, 1978, pp. 232).

Discretization errors

The discretization error depends on the details of the numerical procedure employed. For conforming elements, the discretization error for the element $\|e\|_E \Rightarrow 0$ as $h \Rightarrow 0$. The rate at which the error decreases with respect to the discretization is known as the *rate of convergence*. Convergence properties are discussed in the next section.

Discretization error occurs both in the interior of the finite element domain and on the boundary. In the program presented here, the curved seepage line is represented by a series of linear segments. Mitchell (1973) concluded that such an approximation is both natural and justified if linear trial functions are used (as in this case). However, with higher degree basis functions the solution cannot be expected to retain the same accuracy. In these circumstances the use of isoparametric elements (e.g. France et al, 1971) is to be recommended. Strang & Fix (1973; p. 51) showed that the linear interpolation of Neumann boundary conditions is of a lower order error than the mesh discretization error (for the linear triangular element).

3.4.2. Error Convergence

An understanding of the convergence properties of the finite element solution is fundamental to the adaptive technique. For the following analysis it is assumed that the rounding error is negligible compared to the discretization error. Strang (1972) and Strang & Fix (1973; pp 166-167) proved that for a problem with smooth coefficients of strain energy (and satisfying the ellipticity condition), the finite element approximation $\hat{\mathbf{u}}$ differs from the true solution by:

$$\begin{aligned} \|\mathbf{u}-\hat{\mathbf{u}}\|_s &\le Ch^{k-s}\|\mathbf{u}\|_k \qquad \text{if } s \ge 2m-k \\ \|\mathbf{u}-\hat{\mathbf{u}}\|_s &\le Ch^{2(k-m)}\|\mathbf{u}\|_k \qquad \text{if } s \le 2m-k \end{aligned} \qquad \text{Eq. 3.20}$$

where $\mathbf{u}$ is used here as a matter of convention to symbolise the dependent variable (in Laplace's equation it is equivalent to the potential function ϕ), k-1 is the degree of the nodal basis function, $2m$ is the order of the differential equation, s is the order of the derivative in question, and C is a positive constant independent of h. Strang and Fix stated that these exponents are optimal; therefore the order of the error never exceeds $2(k\text{-}m)$ in any norm and in all realistic cases the order is $k\text{-}s$.

The finite element method is known to optimize the error in the energy norm, that is when s=m. The global rate of convergence in the energy norm for a finite element solution of Laplace's equation (a second order differential equation; m=1) for a particular problem using uniform mesh refinement may be written (Zhu et al, 1987):

$$\|e\|_E \le Ch^{\min(p,\lambda)} \qquad \text{Eq. 3.21}$$

where $\|e\|_E$ is a measure of the error in the energy norm, p is the polynomial degree of the basis function, λ is a constant which is related to the regularity of the true solution **u**, and C is a positive constant which does not depend on h. That is to say, the convergence rate of a finite element solution for a smooth problem using linear basis functions is of order h or $O(h)$. For a problem involving a singularity (such as a re-entrant corner) λ is normally taken as equal to 0.5 for the purposes of adaptive meshing (Zhu et al, 1987). Strang & Fix (1973, p. 155) stated that for an optimal h-adaptive (alteration of mesh spacing) scheme the same order of accuracy may be achieved for a singular as for a regular solution. This is the basis for the adaptive scheme utilized in this thesis.

For a 2-dimensional domain the number of nodes N is roughly equal to the square of the reciprocal of the mesh spacing h. The *a priori* estimate of the error becomes:

$$\|e\|_E \leq CN^{-0.5\min(p,\lambda)} \qquad \text{Eq. 3.22}$$

For p refinement on a fixed mesh the error can be bounded by (e.g. Craig et al, 1989):

$$\|e\|_E \leq CN^{-\beta} \qquad \text{Eq. 3.23}$$

where β is a positive constant that depends on the regularity of the true solution. In the presence of a singularity $\beta=\lambda$, the global convergence rate of the p-adaptive technique is obviously better than uniform refinement. However, it should be noted that low order elements adjacent to a singularity may prove beneficial by bounding the error away from the rest of the domain. The h- and p-adaptive methods can be combined to provide an exponential convergence rate (Craig et al, 1989):

$$\|e\|_E \leq Ce^{-\alpha N^{\theta}} \qquad \text{Eq. 3.24}$$

where α and θ are positive constants that depend on the smoothness of the true solution and the regularity of the mesh.

3.4.3. Error Estimation

The *a priori* discretization error estimates of the previous section are not suited to the design of the mesh because they are overly pessimistic. An algorithm based on interpolation using the *a priori* estimates may be suitable and easy to use as an *error*

indicator (Zhu & Zienkiewicz, 1990). Fortunately the finite element approximation itself may be used to provide a more realistic measure of the error to facilitate mesh refinement or regeneration to provide an optimal mesh.

A posteriori error estimators come in two main groups known as residual types and postprocessing types of estimators. Zhu & Zienkiewicz (1990) proved that these two methods are in fact closely related; it seems that the residual type of estimator may be derived from a postprocessing scheme.

Residual type estimators

Babuska & Rheinboldt (1978) developed a residual type error estimator based on an integral of the finite element residual and the inter-element jump in gradient:

$$\|e\|_E^2 = C_1 \int_{\Omega} r^2 \, d\Omega + C_2 \int_{I} J^2 \, dI \qquad \text{Eq. 3.25}$$

where C_1 and C_2 are positive constants for the particular problem, r is the FE residual, Ω is the finite element domain, J is the jump in gradient on the element interfaces, and I is the boundary of the elements. Zhu & Zienkiewicz (1990) showed that this estimator is equivalent to one built on the superconvergence principles developed in the next section. For low order elements the gradient jumps dominate the expression. This provides a theoretical basis for the common practice of using the gradient jumps to characterize the finite element error (Zienkiewicz & Taylor, 1989, p. 422). For higher order elements the line integral becomes cumbersome to evaluate.

Postprocessing error estimators

Gradient recovery methods provide a more direct way of obtaining an error estimate by postprocessing the finite element solution. The error in the energy norm $\|e\|_E$ is written:

$$\|e\|_E^2 = \int_{\Omega} (\mathbf{u}' - \hat{\mathbf{u}}')^2 \, d\Omega \qquad \text{Eq 3.26}$$

where $\hat{\mathbf{u}}'$ is the finite element approximation to the true gradient $\mathbf{u}'$, and Ω is the finite element domain. Hence in the postprocessing type of error estimator it is the gradient $\mathbf{u}'$ which is of interest. Postprocessing error estimators are based on recovering a gradient of $\mathbf{u}$ ($\mathbf{u}'^*$) which is a better approximation to the true gradient $\mathbf{u}'$ than the finite element approximation $\hat{\mathbf{u}}'$.

Zienkiewicz & Taylor (1989, pp. 417-421) gave a graphical interpretation to the process of obtaining a more accurate solution by smoothing or projection. Consider the gradient function **u'** for a fictitious one-dimensional problem pictured in Figure 3.4.

The FEM approximation to **u** using piecewise linear elements provides a piecewise constant approximation for the gradient **u'**. A better approximation to the gradient may be obtained by some reasonable method of smoothing. Hinton & Campbell (1974) achieved this by a least squares method to minimize the difference between the FEM gradient at the Gauss points and a piecewise linear approximation. The process may be performed globally by summing the contribution for each element to obtain a unique value of the gradient at each node, or locally for each element. This local gradient recovery method is in fact a simple interpolation of the gradient from the Gauss points to the nodes. Every node is given an approximate gradient from each element of which it is a part. These contributions are averaged at the nodes to provide a unique value. The local method proved to be as accurate as the global method but considerably cheaper to calculate.

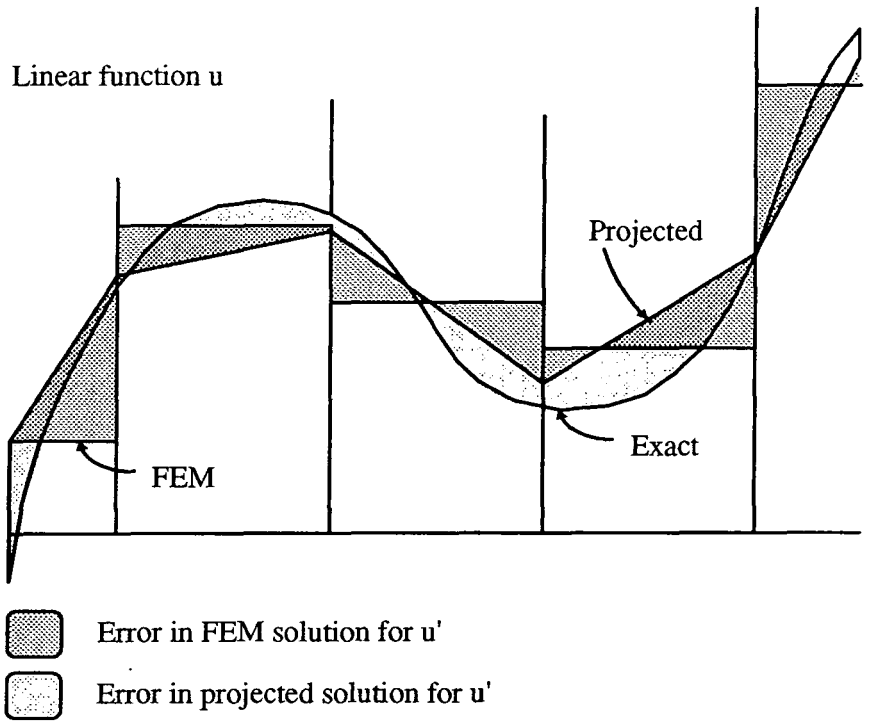

Figure 3.4 One Dimensional Gradient Smoothing

(adapted from Zienkiewicz & Taylor, 1989, p. 421)

Averaging is in fact the simplest method of smoothing the FEM solution. For example, for Figure 3.4 a smoothed approximation could be obtained by a linear fit through the averaged gradients obtained from adjacent elements.

Zienkiewicz & Zhu (1987) used a projection technique based on Galerkin's weighted residual method to calculate a C_0 continuous approximation to the gradient (continuous gradient but discontinuous second derivative):

$$\mathbf{u}'^{*} = \sum_{i=1}^{m} \mathbf{N}_i \hat{\mathbf{u}}' \qquad \text{Eq. 3.27}$$

where $\mathbf{u}'^{*}$ is the recovered gradient, $\hat{\mathbf{u}}'$ is the finite element approximation to the gradient, and $\mathbf{N}_i$ is the finite element nodal basis function over the m nodes.

An alternative approach used in this thesis involves a more direct method. Equation 3.20 indicates that there may be certain points at which the convergence rate for $\mathbf{u}'$ is an $O(h)$ higher than is globally achievable. Such points are known in the literature as *stress points* (Strang & Fix, 1973, p. 151). Although the nodes are good points to sample $\mathbf{u}$, they are as a general rule very poor places at which to sample the derivatives (an exception is the mid-side nodes of a quadratic triangle). Strang & Fix (1973, pp. 168-169) explain that the discretization error must vary in sign rapidly within the element because the derivatives are in error by $O(h^{k-1})$ at "typical" points, and h^k on average. The key to the usefulness of *stress points* is that the position of this sign change is known *a priori*. This phenomenon of enhanced accuracy is known as *superconvergence*; a brief survey of such methods may be found in Krizek & Neittaanmaki (1987). The simple method of obtaining the recovered gradient utilized in this thesis relies on knowing the superconvergent scheme for linear triangular elements. Strang & Fix (1973, p. 107) surmised that linear triangles have superconvergent tangential gradients at their mid-sides, but not the normal derivative. Levine (1985) proved that under certain restricted conditions the full superconvergent gradient could be obtained globally by averaging the finite element gradient (a piecewise constant) between adjacent elements. These conditions may be summarised as follows: the mesh should consist of a smooth transformation of a square grid of identical triangles arranged so that 6 elements surround each internal node (see Figure 3.5). The consequence of these conditions is that adjacent pairs of elements form parallelograms in which the error terms cancel out at the middle of the diagonal (being of opposite sign).

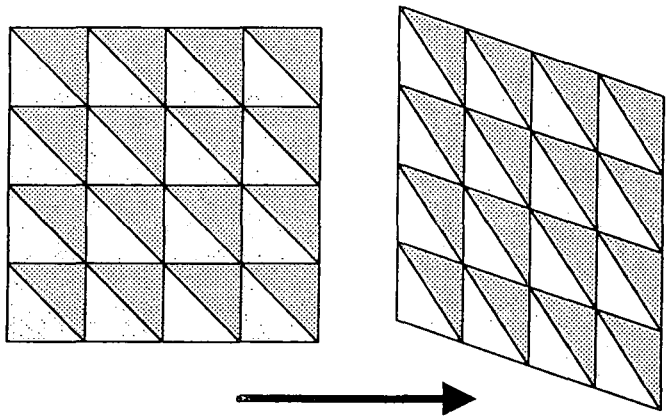

Figure 3.5 Superconvergent Mesh of Linear Triangles

This rather restrictive scheme may be relaxed by dividing the mesh into bands separated by chevron style interfaces. Down the interface a special scheme is employed to obtain the superconvergent gradient (see Figure 3.6).

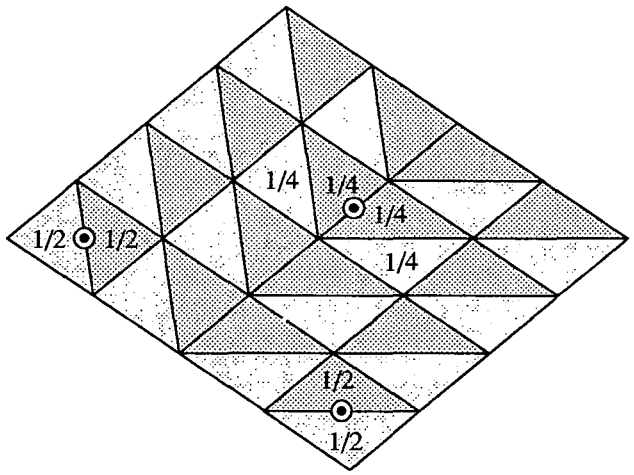

Figure 3.6 Weighting Scheme for Superconvergent Gradient over Linear Triangular Elements

The elements on the boundary provide a further problem for the implementation of this scheme. There is no simple and general method of obtaining a superconvergent solution for boundary sides. Levine also made two important observations which will make the general scheme viable for an unstructured mesh. Although irregularities in the mesh (and particularly the boundary) may degrade the global superconvergence, local superconvergence occurs in regions bounded away from the non-superconvergent parts of the mesh. Furthermore, even with an irregular mesh, the averaging scheme

produces an increased rate of convergence over the finite element solution. Levine proved that an average of the superconvergent gradients at the mid-sides gives a superconvergent estimate for the gradient at the centroid of the element. Whiteman & Goodsell (1987) stated that a superconvergent estimate of the gradient can be recovered at the nodes of a linear triangular element by calculating the average of the gradients obtained by a linear interpolation of the mid-side (averaged) gradients from all the surrounding elements.

MacKinnon & Carey (1990) showed that stress points may be found using a Taylor series expansion to calculate the error terms. For bilinear and higher order elements it is found that the Gauss-Legendre integration points have gradient superconvergence. Zhu & Zienkiewicz (1990) used this property to develop a projection method involving both a term to interpolate the gradient from the Gauss points, and a term to interpolate the difference between the superconvergent solution and the Gauss point interpolant. This method has obvious attractions; however it is not applicable in the case of linear triangular elements because they do not have points at which the full gradient is superconvergent.

3.5. Adaptive Techniques

The object of finite element mesh generation is to facilitate a solution of an acceptable global accuracy and tolerable maximum local error with the minimum of effort. As a suitable mesh cannot in general be obtained using *a priori* error estimates, the common practice is to use the initial finite element solution to obtain a better mesh design. This method of mesh generation is called an adaptive technique. The three most common adaptive techniques involve increasing the degrees of freedom of the nodal basis functions (not to be confused with the degrees of freedom relating to the physical problem, e.g. displacement in three directions):

(1) *h-adaption* involves an increase in the number of elements of the same degree. The method typically utilizes the simpler low degree nodal basis functions at the expense of a more complicated finite element mesh. The convergence rate is the lowest of the three methods (see Equation 3.22). h-adaption is suited to problems involving strong irregularities because the polynomial basis functions need only be satisfied over a small region.

(2) *p-adaption* uses the same mesh spacing, but increases the degree of the nodal basis functions (and by implication the number of nodes). The convergence rate is better than that for h-adaption (see Equation 3.23), and so fewer degrees of freedom are required to obtain the same accuracy. However, it is more expensive to compute the

nodal basis functions and perform the numerical integration for higher degree polynomials. Higher order basis functions also have in general a greater connectivity leading to a wider bandwidth. The method may use mixed elements of different basis functions, or a uniform p-refinement. An overview of the method and extensive bibliography is presented in Babuska & Shri (1990).

(3) *h-p adaption* utilizes both the previous schemes to obtain an exponential convergence rate (see Equation 3.24). In practice the two adaptive schemes are performed individually in different iterations of the same refinement (Craig et al, 1989). Babuska & Shri (1990) also discussed h-p adaptive techniques.

As an alternative to increasing the number of degrees of freedom, the *r-adaptive* technique uses a redistribution of the nodes to create an optimal mesh (e.g. Chung & Kikuchi, 1987).

The discussion will now turn to the h-adaptive technique which has been used in this thesis. The other techniques will not be discussed in any further detail.

3.6. h-Adaptive Mesh Generation

Once an estimate of the local and global error has been obtained, the convergence rate may be used to predict a mesh spacing. The usual requirement is for the error to be equally distributed between all the mesh elements. Such a mesh is known as *optimal.* The acceptable accuracy η defines the ratio of the acceptable error in the energy norm $\|e\|_E$ and the total solution energy $\|\mathbf{u}'\|_E$:

$$\eta = \frac{\|e\|_E}{\|\mathbf{u}'\|_E} \approx \frac{\|e\|_E}{\sqrt{\|\hat{\mathbf{u}}'\|_E^2 + \|e\|_E^2}} \qquad \text{Eq. 3.28}$$

In practice the solution energy is obtained approximately from the finite element solution for the energy $\|\hat{\mathbf{u}}'\|_E$ and the error estimate. For engineering problems the acceptable value of η usually lies between 5 and 10%. The global error is to be distributed equally through all the m elements.

The required error for each element $\|e\|_{E_{ri}}$ is:

$$\|e\|_{E_{ri}} = \sqrt{\frac{\|e\|_E^2}{m}} \qquad \text{Eq. 3.29}$$

The ratio between the estimated element error $\|e\|_{E_i}$ and the required element error can now be written as the local refinement parameter ξ:

$$\xi = \frac{\|e\|_{E_i}}{\|e\|_{E_{ri}}}$$

If ξ=1 then the element is optimal, if ξ<1 then the element is over-refined, and if ξ>1 then the element needs further refinement. The refinement parameter ξ can be used to drive a simple mesh refinement scheme using a successive subdivision of elements. The disadvantage with this method is that the mesh may require many such iterations to obtain a globally acceptable error. However, the nested grids obtained by this method are suitable for multigrid techniques to accelerate the finite element solution (e.g. Rivara, 1986).

The more sophisticated approach developed by Zienkiewicz & Zhu (1987) utilized the convergence rate for h-adaption to calculate the required size of element directly. Zienkiewicz & Zhu assumed that the global convergence rate from Equation 3.22 could be used to obtain directly the new element size $\bar{h}_i$:

$$\bar{h}_i = \frac{h_i}{\xi^{1/p}} \qquad \text{Eq. 3.30}$$

where p is the degree of the polynomial basis function. Onate & Castro (1991) objected to this refinement parameter because the convergence rate for an individual element is not the same as the global convergence rate. The global convergence rate (Equation 3.22) is based on a changed mesh spacing h and a constant size of domain Ω. In the case of the element, both the spacing h_i and the size of the element Ω_i are varied. The consequence of ignoring the local convergence rate is an oscillation between successive

over-refinement and under-refinement of the mesh. The refinement parameter should be required to take into account the effect of this change in element size on its contribution to the total error. Remembering that the square of the error is to be shared between the elements, they wrote the element convergence rate as:

$$\|e\|_{E_i} \approx \mathrm{O}\left(h_i^p\right)\Omega_i^{1/2} \approx \mathrm{O}\left(h_i^{p+d/2}\right) \qquad \text{Eq. 3.31}$$

where d is the number of space dimensions for the domain. Onate & Castro split the Zienkiewicz-Zhu refinement parameter into a local and a global constituent:

Local

$$\bar{\xi}_i = \frac{\|e\|_{E_i}}{\|e\|_E m^{-1/2}} \qquad \text{Eq. 3.32}$$

Global

$$\xi_g = \frac{\|e\|_E}{\eta\|\mathbf{u}\|_E} \qquad \text{Eq. 3.33}$$

The product of $\bar{\xi}_i$ and ξ_g is equal to the Zienkiewicz-Zhu refinement parameter, but now the different convergence rates of Equation 3.22 and 3.31 are combined with Equations 3.32 and 3.33 to calculate the new mesh spacing:

$$\bar{h}_i = \frac{h_i}{\xi_c} \qquad \text{Eq. 3.34}$$

with $\quad \xi_c = \bar{\xi}_i^{2/(2p+d)} \xi_g^{1/p}$

3.7. Calculation of the Free Surface

The position of the seepage line for the steady state dam problems is unknown at the commencement of the analysis. In the finite element literature such a case is called a free-surface problem. Fortunately the problem is not indeterminate; the boundary conditions of head and flux are well known to be sufficient to provide a unique solution (see Figure 3.7).

The discussion briefly reviews some of the common methods which are used to obtain the seepage line position in the case of saturated flow in an earth embankment or dam. Particular attention is given to the methods of Taylor & Brown (1967) and the less common method of France et al (1971) which were both used to solve flow problems in this work. The seepage line divides the saturated flow domain from the unsaturated zone. For this analysis it is assumed that the flow in the unsaturated region is negligible.

Finite element algorithms to solve the free surface problem can be split into two groups: variable domain and fixed domain techniques.

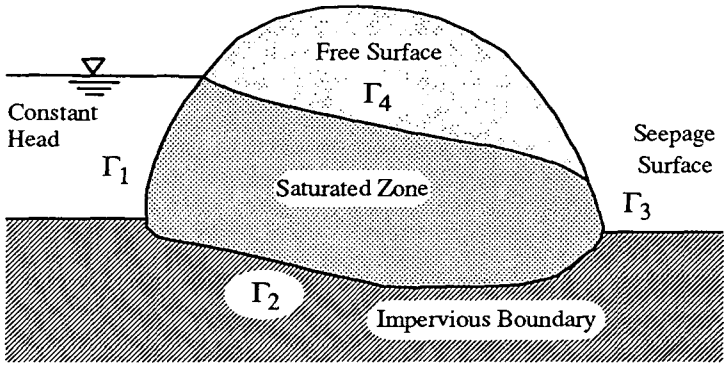

$$\phi = H_1 \quad \text{on } \Gamma_1$$
$$\frac{\partial \phi}{\partial \mathbf{n}} = 0 \quad \text{on } \Gamma_2$$
$$\phi = y \quad \text{on } \Gamma_3$$
$$\left.\begin{array}{l} \dfrac{\partial \phi}{\partial \mathbf{n}} = 0 \\ \phi = y \end{array}\right\} \quad \text{on } \Gamma_4$$

where $\mathbf{n}$ is the outward normal to the boundary
y is the height above the datum
H_1 is the height of the dam water
ϕ is the head potential

Figure 3.7 Dam Problem Boundary Conditions

3.7.1. Variable Domain Techniques

The variable domain techniques are the oldest variety. In these methods the FE mesh covers only the saturated portion of the flow domain. An initial starting position is chosen (this may affect the convergence of the solution), and the FE solution is used to predict a closer approximation to the position of the free-surface. Either of the two

boundary conditions may be imposed on the solution to obtain values for the other. The two methods are split into those which impose the flow condition (Neumann boundary), and those which impose the head condition (Dirichlet boundary). Isaacs (1980) reviewed several alternative variable domain techniques and concludes that the method of adjustment makes no significant difference to the results obtained. The choice depends on the methods' suitability for the particular application and its ease of application.

Constrained Flow Seepage Line Movement

Taylor & Brown (1967) and Finn (1967) independently arrived at similar methods of moving the seepage line between iterations. The finite element solution is calculated with the assumption that the flow across the seepage line is zero (not actually correct before the ultimate position of the seepage line has been obtained). The solution of the FE equations produces a new value of head potential for the nodes of the seepage line. The second boundary condition is now applied and the seepage line is adjusted so that the head is equal to the elevation. Finn's method required a manual reorganisation of the mesh, while the more favoured Taylor-Brown method constrains the mesh nodes along predetermined lines (vertically in the original paper) allowing easy automation. The iterative process is stopped when the movement of the seepage line is below some prescribed value. The determination of the seepage line exit point is an awkward problem for all variable mesh algorithms because of an ambiguity in the boundary conditions. The node at the downstream end of the seepage line divides a boundary with zero flow along the seepage line on one side, and flow out of the domain across the seepage surface on the other. Taylor & Brown suggested that the mesh spacing should be reduced at the exit point to minimize this difficulty. Some authors have reported that this ambiguity at the seepage line exit point causes a failure of the algorithm to converge to the correct solution (Neuman & Witherspoon, 1970; and more recently Cividini & Gioda, 1989). These claims were hotly disputed by Griffiths (1990) who has solved the same problems under consideration without any convergence problems. The Taylor-Brown method has been used successfully in this thesis for all problems except those in which the seepage line descends at a very steep angle (but for other reasons).

Neuman & Witherspoon (1970) used a two stage approach to try to remove the seepage line exit point ambiguity. Each seepage line movement iteration is performed in two steps. First, the flow at the seepage line exit point is obtained by solving the finite element solution with a fixed head condition on the seepage line and the seepage exit point. A value of the flux is obtained at the seepage exit point from this stage. Then

the problem is resolved using a zero flow condition on the boundary, and a fixed flow condition on the seepage line exit point (using half the result obtained in the first iteration). Neumann & Witherspoon allowed the seepage line nodes to move along user defined directions rather than just vertical lines. Where the seepage line is vertical, they converted excessive vertical movement of the nodes (which do not deviate far from the seepage line) into lateral movement. They accelerated movement of the free surface with the use of a relaxation factor. Neuman & Witherspoon (1971) extended the scheme to solve transient flow problems using an implicit Crank-Nicholson difference method. The time stepping routine was unconditionally stable, although the accuracy depends on the length of the time step (which may be big). The mesh was divided into fixed and variable mesh zones in order to reduce computation required for each new iteration. The model included the ability to simulate the influence of the unsaturated zone using a concept of delayed yield from storage.

The difficulty of constructing a suitable mesh has proved to be a serious limitation to the variable mesh approach. In most of the published examples the successive FE meshes have been produced by deforming the previous mesh (typically the seepage line nodes move vertically and the elements deform to accommodate this). If the seepage line movement is excessive then it is also common for further rows of elements to be added or subtracted. More recently Chung & Kikuchi (1987) solved steady state flow problems using an *r-adaptive* technique to allow the mesh to deform between iterations. The technique involves the minimization of some error measure using the same element topology but different node locations. They conclude that unreasonable oscillations in the seepage line are a consequence of drastic changes in the velocity field and that adaptive techniques may be necessary to avoid free surface oscillations and obtain the best possible computed results.

Constrained Head Seepage Line Movement

For this method the head along the free surface is fixed to equal the nodal elevation. Unlike the constrained flow method, this condition is justifiable on purely physical grounds. The head gradient across the free surface is calculated from the finite element result. Unfortunately the gradients are less accurate than the seepage heads and so this technique is less convenient that the constrained flow method (Chung & Kikuchi, 1987). The seepage velocity is calculated using Darcy's law, and the result is divided by the effective porosity to obtain the velocity of nodes on the free surface (see previous chapter). The distance travelled in each iteration is the product of the nodal velocities and the length of the time step. France et al (1971) used this method to obtain both transient and steady state solutions. Their time stepping algorithm

employed an explicit (Euler) forward difference method. The resulting position of the free surface is smoothed by fitting a polynomial least squares regression curve to the data. This measure circumvents the problem of calculating the velocity of the seepage exit point. The true time taken is not required for steady state problems, and so the effective porosity and the time step may be combined into a relaxation parameter (which need not be identical for all nodes). Steady state convergence is assumed when the velocity normal to the seepage surface is below some acceptable tolerance. This method is found to converge much slower than the constrained flow method unless the time steps are optimal. Isaacs (1980) reported that the slow convergence and the restriction on seepage line shape make this method less suitable for steady state problems.

3.7.2. Fixed Domain Techniques

The fixed domain technique employs a finite element grid over the whole of the physical domain considered, including a portion which is unsaturated. The solution is usually obtained iteratively using the same mesh in each successive approximation. More recently the h-adaptive technique has been used. In this case the solution domain remains the same, but the FE mesh is varied between iterations.

The problem of the fixed domain techniques is to force the unsaturated zone to have a negligible contribution to the flow below the seepage line (where the head potential is equal to the elevation).

The obvious method of solving an unconfined problem in a fixed domain is to include the analysis of flow in the unsaturated zone. Unsaturated flow may be modelled using Darcy's equation if the hydraulic conductivity is made a function of the potential head. Neuman (1973) used such a method to solve the position of the seepage line in a steady state and transient analysis. Unfortunately the permeability characteristics of the unsaturated zone are complex and need to be measured for each individual material. The method is very powerful for particular problems, but is less useful for the general case.

Baiocchi et al (1973) used a transformation to map the variables onto a space in which the problem could be solved for the unknown "permeabilities". The problem becomes one of solving a variational inequality. The method is highly mathematical in nature and does not provide a general method of solution for irregular dam shapes and complex inhomogeneous and anisotropic permeabilities. Burkley & Bruch (1991) have used the Baiocchi transformation with h-adaption to solve a problem involving a rectangular dam with a blanket drain.

Desai (1976) used a fixed domain method to solve a general problem involving unconfined saturated flow. The finite element solution is found for the entire structure, and the approximate seepage line obtained by finding where the potential head is equal to the elevation. A residual flow vector is constructed from the quantities of flow across the seepage line. The change in nodal potentials required to remove this residual is found by using the finite element method a second time (the conductivity matrix remains the same, but the right hand side is replaced by the residual flow matrix). The algorithm is repeated with the new head distribution until a converged solution is obtained. This method has been extended by Desai (1983) for unsteady flow problems.

An alternative approach used by Bathe & Khoshgoftaar (1979) is to use an artificial relationship between the hydraulic head and the potential head. In this method the hydraulic conductivity of the unsaturated zone is given an arbitrarily low value to maintain stability (1/1000 of saturated permeability). Rank & Werner (1986) combined the method of Bathe & Khoshgoftaar with an h-adaptive technique. They observed severe oscillations in the iterative process in an inhomogeneous problem with a steeply inclined free surface. This instability was abated by adding a ramp section to the hydraulic conductivity function so that the value of permeability varied smoothly between head values just above and below the elevation.

Chapter 4
Program DFLOW

4.1. Introduction

4.1.1. Description

Program DFLOW was designed to investigate the flow of water in shallow confined or unconfined aquifers. The user is able to determine the head potential distribution and flux values within the area of concern, together with the flow across external or internal sections. Additionally, the equipotentials and flow lines may be plotted as a traditional "flow net". In the case of an unconfined aquifer, the position of the seepage line may be determined. Permeability may be varied both in direction (anisotropic) and space (heterogeneous). In the case of transient problems, the porosity may also be defined in a piecewise fashion over the area of interest.

DFLOW uses the Finite Element (FE) method to solve Laplace's equation over a 2-dimensional domain subject to prescribed boundary conditions. DFLOW automatically determines the position of the seepage surface for steady state unconfined problems. This process is carried out iteratively by fixing one of the two boundary conditions (known head, or known flux), and moving the seepage line in accordance with the calculated value of the other. In the case of transient problems, the seepage line moves in a stepwise fashion by calculating the distance travelled by the free surface in the previous time period.

4.1.2. Objectives

The design of a new FE program would seem wholly unnecessary unless some new objectives are sought which cannot be provided by an already existing package. Commercial finite element programs are available at Durham University, but these proved to be quite inflexible when dealing with free surface problems (ones in which the geometry of the problem is not known *a priori*).

The code for DFLOW was programmed over several years. At the beginning of the project there was no fixed design philosophy, rather the program evolved as a response to the difficulties encountered. The program was rewritten periodically to improve its functionality. Various ideas for program structure and design became established

within this framework. The following list of objectives indicates some of the factors considered while developing the program.

Ease of data input

Input data should be simple and concise so that errors may be easily spotted and corrected. This is achieved by splitting data into self contained blocks, each of which has a separate and discrete purpose. These blocks start with a unique header label which identifies to the program what data is to follow, e.g. the label "GEOMETRY" indicates that the following data describe the coordinates and nodal properties of the problem domain.

These main blocks are in many cases divided into several sub-blocks, each with its own sub-heading. Sub-headings start with a period followed directly by the text; e.g. heading GEOMETRY may include subheadings:

.NODES	(mandatory)	node coordinates and flags
.SEGMENTS	(mandatory)	boundary properties between nodes
.LOOPS	(optional)	node ordering
.MOVES	(optional)	specify pre-defined nodal movements.

The same subheading names are sometimes used in more than one block to describe similar types of data, e.g. .NODES appears in GEOMETRY, GRID, PERMEABILITIES and POROSITY blocks to define nodal coordinates (and associated flags or values). A block or sub-block is ended at the first line which cannot be interpreted in its current context. For example, block "GEOMETRY" may be terminated by any other main header.

Data blocks may be in any order within the input file. The data must be terminated by a "STOP" heading, which may be followed by further lines which are ignored. The headings and subheadings may be in upper, lower or a mixture of cases, but must not be shortened. Comments may be added at the end of headings or sub-headings. All lines starting with an underscore character are also ignored as comments. Comments may be placed between headings, subheadings or even lines of data. One exception is the title, which must be placed directly after the "TITLE" heading. Data blocks may not be repeated even if they only contain sub-blocks which have not previously been defined.

Minimization of data

One common problem with FE programs is the sheer quantity of information which must be included in the program input. Large data files increase the time required for data preparation to solve a new problem, and increase the probability of typing errors

and logical errors in the data. DFLOW requires very little data compared with a "conventional" finite element program.

The meshing algorithm itself reduces much of the work needed in an FE program. DFLOW designs its own mesh from boundary points dense enough to describe only the geometry and boundary conditions. As a consequence there is no need to define a mass of nodal coordinates or element topologies.

In addition, the program employs two techniques to cut down the quantity of data required:

data interpolation

Mesh properties such as nodal spacing, permeability and porosity are defined at three or more points either in or outside the problem domain. The user supplies an element topology (much the same as the FE topology used in the numerical analysis) describing triangles over which the corresponding values at these points are interpolated. Figure 4.1 provides an example of interpolation over the FE domain Ω.

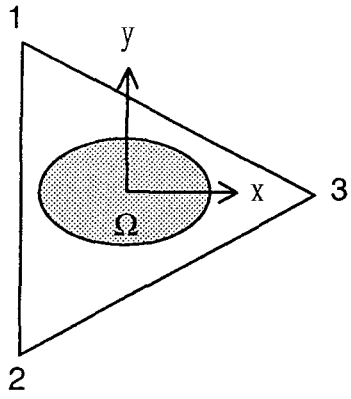

Figure 4.1 Interpolation of Mesh Values

Values of mesh grading (inter-nodal distances) are to be defined for the FE meshing of Ω. If the mesh grading is 2 units for the entire mesh, then the following code is suitable:

```
GRID
.NODES
3
1    -1000.0    1000.0     2.0
2    -1000.0   -1000.0     2.0
3     1000.0       0.0     2.0
.ELEMENTS
1
1    1    2    3
```

The header GRID instructs the program to expect mesh grid spacing data. The sub-heading .NODES holds the number of points (3) and point numbers, coordinates and mesh spacing for nodes 1, 2 & 3. The nodes are linked together by triads of points describing triangular elements analogous to the Turner triangles used in the FE analysis. The sub-heading .ELEMENTS is followed by the number of elements and then, for each element, the sequence number and the corresponding node numbers (from the .NODES section, numbered counter clockwise). In this case, as long as the points form a triangle of a reasonable magnitude (to avoid truncation errors), the actual position of the points does not matter. If the FE mesh nodal point for which the interpolated value is required lies outside all the defined elements, then the value used is taken from the interpolated value at the closest point in the closest element. This is to protect the interpolation routine from extrapolating a value which would not make physical sense (e.g. a negative nodal spacing).

use of default values

Much of the data which are used in the analysis have some default value (if it is not explicitly declared). One example of this concerns the entry of the mesh spacing data. If no GRID header is included then a default value of 1 unit is used. Other instances of the use of default values are invisible to the user. In the preceding data concerning the mesh spacing, the choice of nodal coordinates was arbitrary. Rather than using the .NODES and .ELEMENTS sub-headings, the user may use a .CONSTANT sub-heading, e.g.

```
GRID
.CONSTANT
2.0
```

The .CONSTANT sub-heading actually triggers the program into defining its own large interpolation triangle with nodes, mesh spacings and element topology. The default values (if any) are defined in the section dealing with data format.

Automation of solution processes

The finite element routine should take responsibility for the design of the FE mesh. The normal cycle for FE problem solution involves several mesh design and redesign stages to obtain a required accuracy. Starting from a simple mesh, the user identifies the areas in which the mesh fails to describe the hydraulic head adequately. The mesh in these areas may be refined (h-adaption), the nodes may be relocated (r-adaption), the polynomial degree of the basis function increased (p-adaption), or there may be a

combination of these methods. This process is slow and requires the user to have some degree of expertise in numerical modelling.

DFLOW obtains a greater accuracy in the mesh by automatically increasing the number of nodes in areas where the estimated error is high (h-adaption). The user has only to enter the required accuracy (as percentage relative error) and a description of the geometry, boundary conditions, initial mesh density, material properties and so on. The program performs the mesh generation automatically using an iterative scheme. Cycles of mesh refinement (and de-refinement) are performed by the program to provide an optimal mesh (one in which the error is spread evenly over the elements). The process requires at most 3 iterations for a well posed steady state analysis.

Flexibility in Problem Formulation

The program should be flexible enough to solve the problem in question by an alteration of the program data and not require a rewriting of the computer code. It is common for academic computer programs to consist of a library of subroutines. These are linked together with a specially written main program on a one-off basis to solve a particular problem. Although this allows the maximum flexibility, it also restricts use of the program to the "expert".

General programs fall into a different trap. To ensure accuracy and stability, they restrict the user to proven algorithms. The user may be allowed to solve only a subset of the possible problems. Cases involving free surfaces, where the geometry of the domain is not known before the solution procedure starts, are particularly difficult to solve.

DFLOW attempts to solve this problem by allowing the user some control over the detailed workings of the algorithm from within the data. The difference between this technique and the specially written program is that the core of the program is already written; the user need only concentrate on the data required to change the default data.

One example of this concerns the procedure to determine the seepage line exit point (see below).

DFLOW is a very specialised program despite the generality of most of the techniques employed. Whereas a general finite element program may be used to perform calculations involving stress, fluid flow, magnetics and so on, this program deals only with a subset of groundwater hydrology problems.

Control of output data

The computer output should be easy to interpret and present all the requisite information. A common problem with finite element programs is the massive quantity of information produced. Too much output data is nearly as much a handicap as too little.

As DFLOW generates its own FE mesh automatically, the element topology (and in many cases the nodal coordinates) is unlikely to be of interest to the user. A possible exception to this rule might be if nodal values are to be interpolated over the mesh by the user in a separate analysis. Because DFLOW has specific graphical methods of presenting hydrological data, this aspect of post-processing was ignored.

The most important output data are:

- head potential and fluxes at the boundary nodes
- seepage discharge through portions of the boundary (and occasionally through internal sections)
- position of the seepage line for unconfined problems.

For values in the interior of the problem domain, the most efficient method of presenting nodal values is graphically by the use of contour plots. Occasionally it may be necessary to provide head potentials and coordinates for internal points (e.g. for the calculation of seepage uplift pressures beneath a structure).

In DFLOW all data output must be requested explicitly. To make this convenient and simple, a marker is placed against nodes or segments defining the geometry and boundary conditions. The values of these markers are propagated to the appropriate mesh nodes and element segments. The header DISCHARGE defines the segment markers, and the header HEADS defines the node markers which are activated for output. The marker 0 (zero) is given to all internal nodes and so the values at these nodes may also be included in the output.

Raw numbers are a very inefficient method of presenting data. Thus, in addition to data values, files may also be produced holding the information necessary for the plotting of flow nets, finite element meshes and nodal spacing contours using UNIRAS (a commercial graphics package).

Data Consistency Checking

An FE program should check the input data and report the presence and location of errors. Types of error occurring can be grouped in 5 classes:

I. **Syntactical**. These are errors which make the data "incomprehensible" to the program. Possibilities are the misspelling of a text command or an incorrect data type (floating point number instead of an integer). Syntactical error is frequently caused by one of the other error types such as missing data.

II. **Logical inconsistency**. Data frequently contains a certain amount of duplicated information. The program should draw inferences from the data and cross-check these inferences against the remaining input file. Where incompatibilities occur there must be a logical inconsistency in the data. An example of this might be the definition of a boundary condition for a node which does not exist, or definition of seepage exit node bounds when the problem has no seepage line.

III. **Inappropriate data**. This covers the case where a value is outside the acceptable range for the data. A negative number, a very small or very large number may all be suspect in a particular context. It would not make sense to define a negative number of boundary nodes to define the geometry.

IV. **Missing data**. Although much of the data may have a default value, certain parts of the data cannot be omitted. For example, a problem cannot be defined without a specific geometry.

V. **Duplicated or redefined data.** In many programs it is acceptable to repeat a segment of the data with the same or different values; usually it is the last defined data value which is used. However, it may be more sensible to prevent duplication in order to facilitate debugging.

In addition an error may be caused by the lack of a proper data termination command.

DFLOW satisfies most of these criteria. Criteria II is the most difficult to follow, and has not been implemented in the current version of the program. Criteria III has to a large extent been implemented, but it is still possible to trip the program up by feeding it bad data.

4.1.3. Limitations

DFLOW has been designed to solve a particular set of problems involving the flow of water through simple earth dams and tailings embankments. The program has application for other problems (such as flow below sheet pile walls), but there are limitations to the program and these should be understood before an attempt is made to solve a different type of problem. The major limitations are listed below:

- DFLOW is restricted to problems showing a strong 2-dimensional predisposition (axisymmetric conditions not yet incorporated).
- Fluid and porous media are assumed to be incompressible.
- Flow is single phase (saturated conditions without density variation).
- Permeability tensor must be orthogonal to the space coordinates used (so the space coordinates must be chosen carefully - they need not be vertical and horizontal).
- Only Dirichlet (constrained head potential) and Neumann (constrained flux) boundary conditions may be modelled.
- No support for point sources or sinks.
- No accretion on seepage surface (percolating water).
- No support for breaks in spline continuity along the seepage line for abrupt changes in permeability.

Many of these limitations could be removed in the future with only a relatively small amount of programming effort.

4.1.4. Acknowledgements

It is opportune at this stage to state the external contribution to the formulation of this finite element program:

- Cubic B-spline routine was modified from a subroutine provided by M.B. Okan (Senior Research Assistant, Durham University, 1988-).
- Mesh generation algorithm is based on the paper of Peraire, J., M. Vahdati, K. Morgan, and O. C. Zienkiewicz, "Adaptive remeshing for compressible flow computations", *J. Comp. Phys.*, **72**, 449-66, 1987.
- Mesh smoothing routine after Cavendish J. C., *Int. J. Num. Meth. Eng.*, **8**, 679-696, 1974.

- Node renumbering scheme taken from Cuthill E. and J. McKee, "Reducing the Bandwidth of Sparse Symmetrical matrices", *Proc. ACM Nat. Conf., 24th,* Barndon Systems Press, NJ, 157-172, 1969.
- Gaussian solver for symmetric banded matrices by Smith I.S. and D.V. Griffiths "Programming the Finite element method", Second edition, John Wiley and Sons, London, 1988.
- Basis for error estimator, M. Ainsworth (Research Student, Durham University, 1986-1989).
- Routine for the calculation of flow nets for the graphical output was developed jointly with N. J. Powell (Research Student, Durham University, 1988-).
- Known head seepage line algorithm, France P. W., J. Parekh, J. C. Peters, C. Taylor, "Numerical Analysis of Free Surface Seepage Problems", *J. Irrig. Drain. Div.*, ASCE, **97**, 165-179, 1971.
- Known flux seepage line algorithm, Taylor R. L. and C. B. Brown, "Darcy Flow Solutions With a Free Surface", *J. Hydr. div.*, ASCE, **93**, 20-33, March 1967.

4.2. Program Design

The program DFLOW is written in FORTRAN 77. It consists of approximately 8000 lines of code (excluding comments) in 174 sub-programs. These routines perform six major tasks:

- Program-user interface
- Mesh generation
- Numerical solution
- Error estimation
- Seepage line movement
- Data output.

Figure 4.2 is a simplified schematic view of the program. A brief description of the workings of the program is given in this section.

4.2.1. Program Interface

The input data for the program are read from a single plain text file. The data are divided into blocks, and these blocks may be divided further into sub-blocks (see Page 64). The input sub-program reads sequentially through the file, ignoring blank

lines and comments (lines beginning with an underscore). Each line is stripped of its leading blank spaces, converted into uppercase and matched with a dictionary of text strings. Each time a match is made, control is given to another sub-program to interpret the following lines. In the case of a data block which is divided into sub-blocks, this process is repeated once more.

If the program encounters a block or sub-block for the second time, an error message is sent to the standard output device to that effect, and the program is terminated.

Once all heading levels have been dealt with, the following data are read into the appropriate variable(s). If an error is encountered while reading in the data (e.g. insufficient data, or data of the wrong type), then an error message is sent to the standard output device, and the program is terminated. The program suggests what the error might be and where it occurs in the data.

When an unidentified command is met, the sub-program checks if all the necessary data are complete for the current block or sub-block. If some of the data required for the block or sub-block are missing, then if a default for the data exists, a sub-program is called to complete the missing data. If the data do not have a default value, then a suitable error message is sent to the standard output device, and the program is terminated.

The unrecognised command is then interpreted by the sub-program in the next level up and the process repeated. If the main input sub-program cannot identify the command, an error message is sent to the standard output device together with the offending line and the program is terminated.

The input data are terminated by a STOP command. When this command is reached the program checks to see if the mandatory information has been successfully read in. If data are missing then the program sends an error message to the standard output device and terminates. If optional data are missing, then the program calls the appropriate sub-programs to fill in the default values.

Finally, a formatted and reorganised version of the data is sent out to a second file. This file is useful for debugging, comparing and presenting the original data.

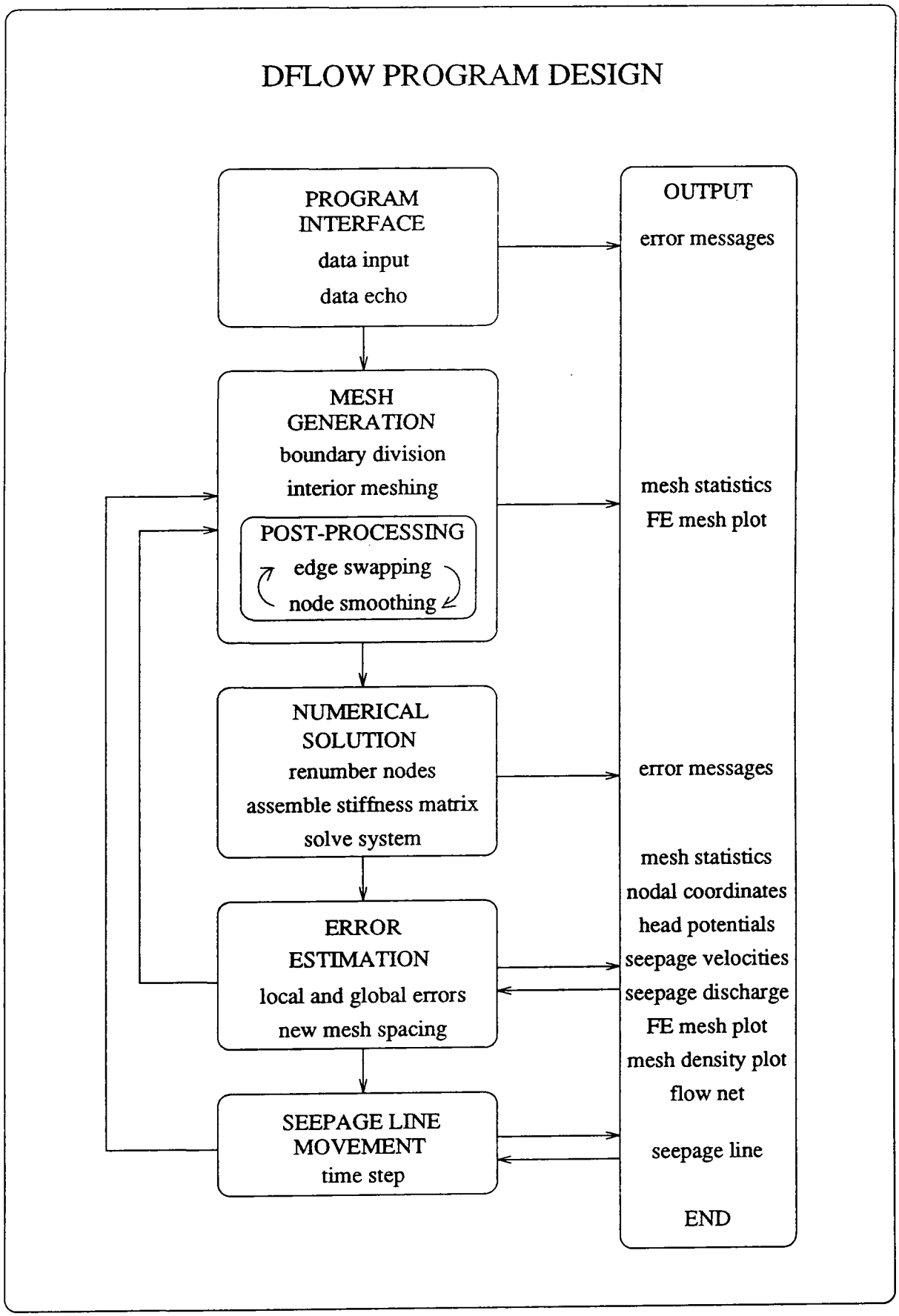

Figure 4.2 DFLOW Program Design

4.2.2. Mesh Generation

DFLOW generates a finite element mesh of three-noded triangular partitions for use with a linear basis function. The program builds an unstructured mesh using the advancing front method (Peraire et al, 1987). The density of the finite element mesh is defined by a similarly defined "background" mesh which defines the required nodal spacing over a set of linear triangular partitions. This background mesh is obtained in the first instance from the input data or from the default mesh. After the first numerical solution is obtained, a better background mesh is calculated. This mesh gives an estimate for the element sizes required for the production of a new optimal finite element mesh (one with the error spread equally over all elements).

Several program routines interpolate values for some variable (i.e. optimal mesh size, permeability and porosity) from a triangular background mesh. This mesh is analogous to a typical finite element mesh of linear triangular elements. The program stores the triangle's nodal coordinates, the topology (list of node numbers for each element), an element map (list of elements adjacent to each element), and the value to be interpolated. When a value of the variable is required for a particular point, a search is made for the element closest to the point, and then a value is obtained using a linear interpolation involving triangular coordinates.

The search routine is as follows:

(I) The search is started using the final element chosen for the previous search (or element 1 for the very first search in the relevant background mesh).

(II) If this element contains the point sought then the search is terminated.

(III) If the point is no closer to any of the element's neighbours, a new search element is obtained by finding the closest background node to the point. An element is found which incorporates the background node, and the search is terminated.

(IV) Otherwise, the search is restarted from (II) using the neighbouring element which is closest to the point.

Generation of the finite element mesh is completed in three stages: division of the boundary, internal meshing and mesh post-processing.

Boundary Division

The first stage of the mesh generation is to divide the boundary of the domain (and internal regional boundaries) into segments in accordance with the required nodal density from the background mesh.

The mesh boundary is divided using the following algorithm (starting with the first boundary segment, and the node with highest nodal density):

(I) The required mesh spacing at the current node is obtained from the background mesh.

(II) A point is marked off along the segment using the spacing for the current node.

(III) The required nodal spacing is obtained at the half way point between the current node and the marked position from (II).

(IV) A point is marked off along the boundary from the current node using the nodal spacing obtained at the approximate mid-point at (III). This point is the position for the new node.

The process is repeated along each boundary segment in turn until the segments have no room for another node (see Figure 4.3).

The process is identical for curved sections of the boundary. The cubic B-spline algorithm converts distances along a curved boundary to x,y coordinates for the mesh nodes.

Interior Meshing

Once the boundary nodes have been calculated, the interior of the mesh is triangulated. This algorithm takes each segment of the incomplete interior boundary (or front) and constructs a new element using the nodal spacing parameter obtained at the mid-side of the element. The incomplete sides of this new element are included in the advancing front, while the original segment is lost. The new element may use a new node at its third vertex (case a) or an old node (cases b, c & d)(see Figure 4.4).

To chose a vertex for a new element the program considers several criteria:

- The sides of the element must not cross the advancing front.
- The element must lie in the empty region to be meshed.
- The element must be as nearly equilateral as possible.

The vertex chosen is the one that fits all the criteria from the list of nodes on the advancing front, and the prospective new node obtained by forming an equilateral triangle subtended from the segment.

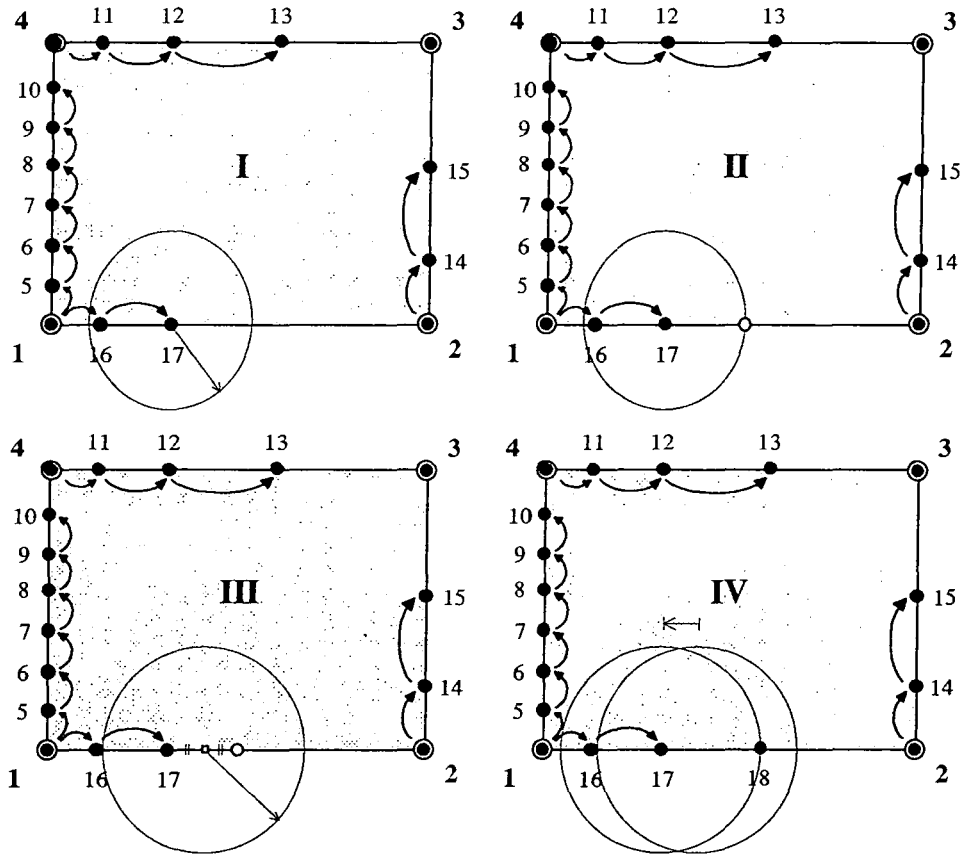

Figure 4.3 Division of Boundary Segments

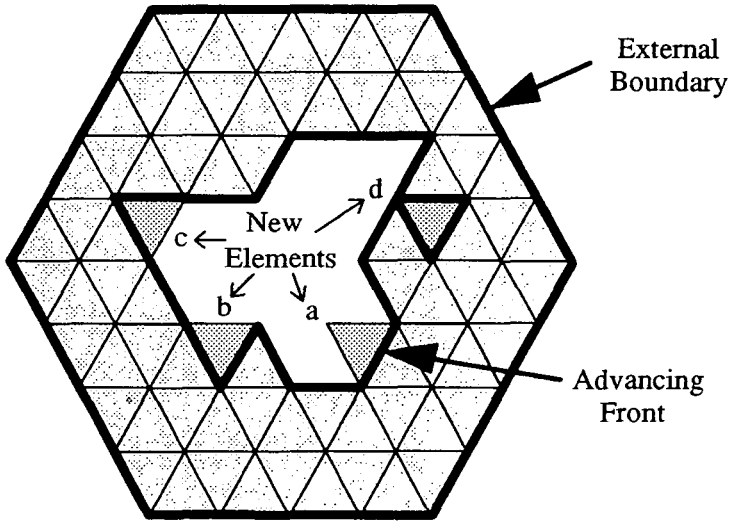

Figure 4.4 Construction of Interior Mesh

Mesh Post-Processing

The preceding meshing algorithm does not produce a good finite element mesh alone. The advancing front method attempts to obtain a graded mesh of nearly equilateral triangles. At the closure of the advancing front, the elements are typically badly misshapen. The meshing algorithm makes no effort to achieve a six-sided property (each interior node having 6 sides). Both of these properties are necessary for an error estimator based on Levine's superconvergent gradient recovery techniques (see previous chapter).

Two program routines are used to improve the mesh characteristics:

- Nodal smoothing (improvement of grading characteristics). The interior nodes are moved to the centre of the surrounding elements in an iterative procedure. This process is repeated four times for each node (by default unless otherwise specified).
- Edge swapping (to obtain 6-sided property). The number of nodal connections (connectivity) at each mesh node is counted. For interior nodes the optimum connectivity is 6, while for boundary nodes it depends on the internal angle of the boundary. The difference between the actual number of connections and the optimum number is calculated for each node. The edge between adjacent elements is switched to join up the opposite vertices of the elements if this will reduce the total difference between the actual and optimum connectivity for the mesh (see Figure 4.5). Side swapping is prevented in circumstances where negative triangle areas are produced (with nodes numbered counter clockwise).

After a side redistribution and node smoothing cycle has been completed, the area of each element is checked. On rare occasions the smoothing routine may move a segment side across the exterior boundary. If this situation occurs, the mesh processing is repeated with the offending segment back in an acceptable position. If the smoothing routine again moves the segment across the external boundary, then the mesh post-processing is terminated after the side redistribution routine.

4.2.3. Numerical Solution

Mesh Renumbering

The mesh generation algorithm does not produce a mesh with adjacent elements having similar node numbers. As a consequence, the stiffness matrix will have an extremely large bandwidth; that is to say, the non-zero values in the matrix rows will not all be close to the matrix top-left to bottom-right diagonal, and so substantially more computer memory and time will be required to solve the stiffness matrix. A mesh

renumbering scheme is employed to reduce the matrix bandwidth and decrease the computational effort required.

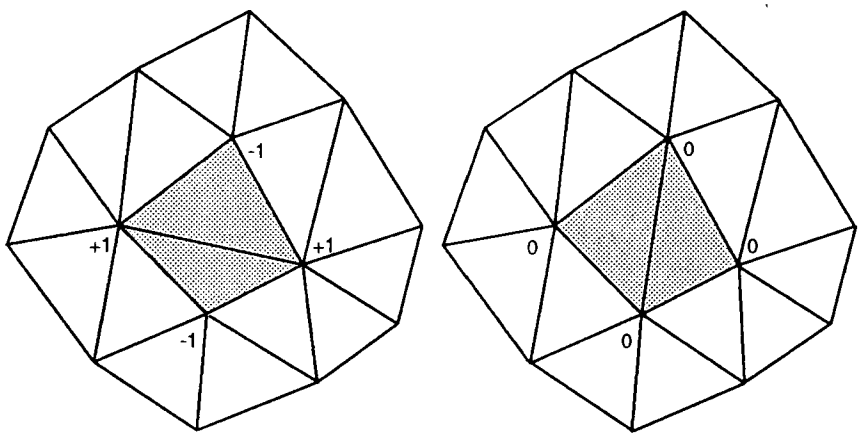

Figure 4.5 Mesh Post-Processing: Improving the Connectivity

The Reverse Cuthill-McKee renumbering scheme is a variation on the original method of Cuthill & McKee (1969). It consists of two sweeps using the same algorithm. The first sweep cannot be guaranteed to produce a good numbering scheme because the starting point is arbitrary. The second sweep uses the final node of the first iteration as the starting point for the second renumbering iteration, and usually produces a superior result.

The renumbering scheme is essentially a recursive routine which is difficult to program elegantly in FORTRAN. The least well-connected node should be chosen as a starting point. The routine follows two rules:

- Nodes with fewer connecting edges between themselves and the starting node (along the shortest path in terms of total number of edges) are numbered before other nodes.
- Nodes with fewer connected (adjacent) nodes are numbered before other nodes.

The sequence of operations for the first few nodes is as follows (see Figure 4.6). The starting node is numbered first (1). The nodes connected to the starting node are then numbered; the node with fewest connecting nodes is numbered first (2), followed by the other nodes in increasing order of connectivity (3,4...). The numbering routine is then restarted using each successive node (2,3,4...) as the base for the renumbering (moving to the next node when all the connected nodes have already been renumbered).

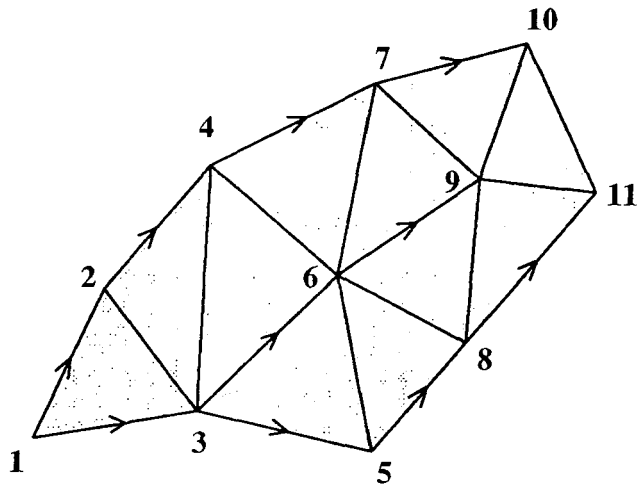

Figure 4.6 Cuthill-McKee Node Renumbering Scheme

Assembly of Stiffness Matrix

DFLOW assembles a stiffness matrix from linear triangular elements (variously called Turner or Courant triangles) using a triangular coordinate system. Dirichlet boundary conditions are forced using the Payne-Irons method (the "big spring").

Solution of Stiffness Matrix

The problems for which DFLOW is designed involve the solution of sparse, positive definite and symmetrical matrices. During the initial development stage, a commercial Cholesky decomposition subroutine for symmetrical matrices was used to solve the stiffness matrix. Unfortunately this routine was unable to solve all the matrices posed and so a backup routine was incorporated into the program. This routine is based on a Gaussian elimination technique for banded, symmetrical matrices. Although this routine was marginally slower than the commercial Cholesky method, in all the cases studied there was no difficulty in solving the stiffness matrix by this method. It proved quicker to use the Gauss method alone than to use the Cholesky method and repeat failed solutions with the Gauss method.

4.2.4. Error Estimation

The error estimation algorithm is the key to the adaptive finite element method. DFLOW employs a very simple technique which uses the recovered gradient (the hydraulic gradient in x and y directions in this context) from a smoothed solution based on the finite element solution. For an ideal mesh (one in which every pair of elements forms a parallelogram), the recovered gradient is equivalent to the gradient obtained from a quadratic element solution (superconvergent solution). The distance (L_2 norm) between

the recovered gradient and the finite element gradient is used as a measure of the error. A new mesh spacing is obtained by sharing the total error equally between all the elements. The convergence rate for the element error is used to calculate the new mesh spacing for each element. The values of new mesh spacing are then averaged to obtain values at the mesh nodes. This old finite element mesh with the new optimum values of mesh spacing is used as a background mesh for the next iteration.

Local Error Estimation

The finite element gradient (hydraulic gradient in x and y directions) is obtained for each linear element. The gradient is then averaged between adjacent pairs of elements to obtain the gradient at the middle of the element edges. The tangential gradient component is known to be superconvergent at this point, but the normal component is not. The gradient at a boundary edge is obtained by an extrapolation of the gradients in the interior.

The gradient is known at the mid-side of each element, and so values of gradient can be interpolated in each element to obtain values at the element node. For a typical node surrounded by 6 elements, there will be 6 different estimates for the gradient. These values are averaged to obtain the recovered gradient. The recovered gradient is not truly superconvergent except in the case of a perfect mesh geometry (where each pair of elements forms a parallelogram). Figure 4.7 shows the patch of elements involved in the calculation of the recovered gradient. The recovered gradient for the boundary nodes is obtained by an extrapolation of the best available local information. The best sources of accurate data are the mid-side averaged gradients of adjacent elements, followed by the recovered gradients at other nodes and least of all, the finite element gradients.

The largest component of error (squared) in each element (excluding elements with singularities) is equal to the squared difference between the FE gradient and the recovered gradient integrated over the element's area. This value is the local error estimator used. The *effectivity* of this estimator, that is the ratio of the estimated error to the true error, is typically only about 80%. The advantage of this method is its speed and simplicity.

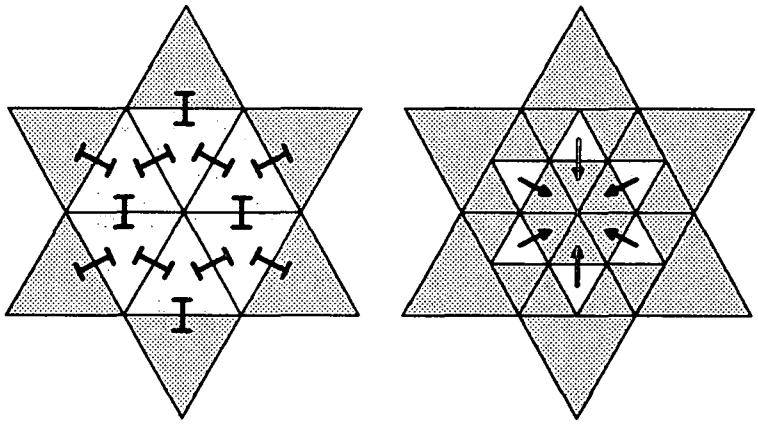

Averaging scheme for mid-sides Recovery of gradient at nodes

Figure 4.7 Gradient Recovery at the Nodes

Global Energy

In order to calculate the relative significance of the error, some term which measures the amount of global energy in the problem under consideration is needed. The most convenient measure is simply the square root of the integral of the squared gradient over the FE domain. This squared gradient is integrated over each element in turn, and then summed to provide the global measure.

Global Error Estimation

The global error estimator is simply the square root of the sum of the squared local error estimates. In order to interpret the magnitude of the global error another term, the relative error (also frequently called the accuracy), is calculated. The relative error is the global error divided by the global energy, and is often expressed as a percentage.

Calculation of New Mesh Spacing

The criterion used for an optimal mesh spacing is that the error in each element should be the same. The relationship, or rate of convergence, between the size of the element (h) and the error is used to calculate what element size is required for an optimal spacing. Zienkiewicz & Zhu (1987) used the global convergence rate for the solution. This method proved unstable and the mesh generator oscillated between under- and over-refinement of the mesh. This oscillation was successfully damped down by using the square root of the ratio between old and new element sizes. The success of this method has been explained by Oñate & Castro (1991) who also found the Zhu-Zienkiewicz method unstable. Their element convergence rate is equal to the measure used in this program. When the global error is satisfied, the convergence rate of Oñate

and Castro is identical to the convergence rate used here. This is always true for a transient analysis where the FE mesh changes by only a small amount from one iteration to the next. For a steady state analysis, the mesh generator already over-achieves the required global accuracy in two iterations. The Zienkiewicz-Zhu method was unable to obtain the required accuracy in a single iteration, and so the intermediate Oñate and Castro method is not in this case an advantage.

4.2.5. Seepage Line Movement

Two different methods for obtaining the steady state position of the seepage line are incorporated into the program. The Taylor-Brown method (Taylor & Brown, 1967) constrains the seepage line boundary with a zero flow boundary condition. Points on the seepage line are moved vertically to satisfy the calculated head and achieve the head-equals-elevation condition. The France method (France et al, 1971) fixes the head potential at the seepage line nodes to equal the elevation, and the seepage line is moved in accordance with the flow calculated normal to the seepage line. The France method is also used for the solution of transient flow problems.

The Taylor-Brown and France methods do not always converge to the same solution. The unmodified Taylor-Brown method is not suitable for problems in which the seepage line is inverted or vertical because points on the seepage line cannot be moved horizontally. Neuman & Witherspoon (1970) have adapted the method to cope with this problem. For steeply inclined seepage lines, fine meshes do not always converge to the correct solution. The problem is solved by first using a very coarse mesh (high relative error) and obtaining an approximate answer, and then using the seepage line obtained as the starting point for a more accurate solution.

The France method usually converges at a much slower rate than the Taylor-Brown method. Its advantage is that with a suitable choice of time step the solution usually converges, whatever the starting position. Unfortunately, oscillations in the position of points along a steeply inclined (or inverted) seepage line may prevent an accurate solution to the steady state position being achieved.

4.2.6. Data Output

The program uses several different routes for output data:

- The input data, as interpreted by the program and reformatted, is sent to file "DATA".
- Information concerning mesh statistics and seepage discharges is sent to the standard output device (FORTRAN unit 6), which is normally the computer monitor.
- Calculated potential heads and seepage discharges are sent to the file "OUTPUT".
- Seepage line coordinates are sent to file "FREE".
- FE mesh plots, flow nets and nodal density plots are sent to file "unipict.upi". These may be viewed, edited and printed using the UNIRAS suite of programs.

The flow nets are calculated and plotted directly from the FE data. The equipotentials (that is contours of equal head) are calculated from the linear head distribution in the elements. Each element is examined in turn. When an equipotential value to be plotted lies between the values of head at the element nodes, the two intersections where the element's sides have the same head value as the equipotential are joined. It is assumed here that the space coordinates (x,y) and permeability tensor K are aligned. The flow lines are obtained by integrating the streamline×permeability gradient from node to node across the mesh. The streamline gradient is orthogonal to the fluid velocity, and can therefore be obtained at each mid-side by rotating the fluid velocity counter clockwise through 90 degrees (the fluid velocity is calculated from the permeability and the recovered gradient at the mid-side, or directly from the boundary conditions). The process begins with the selection of a starting node (i) at which the streamline× permeability function is given the arbitrary value of zero. Ideally the starting node should be chosen so that error in the integration procedure is not propagated through any singular points.

The streamline×permeability function is now calculated at adjacent nodes (j) by summing the function value at the first node and the product of the streamline× permeability gradient at the mid-side and the space displacement vector:

$$\Psi_j = \Psi_i + \left(K_y \frac{\partial \Psi}{\partial x} \right)_{ij} (x_j - x_i) + \left(K_x \frac{\partial \Psi}{\partial y} \right)_{ij} (y_j - y_i) \qquad \text{Eq. 4.1}$$

where *ij* refers to the value at the mid-side between nodes *i* and *j*, and Ψ is the streamline function (note that the permeability directions coincide with the velocity function from which the streamline function is derived). This process is repeated for all the nodes using the renumbered node ordering to ensure that the node being considered is joined to one for which the streamline×permeability function is known. Where a node is joined to more than one node for which the streamline×permeability function is known, then the node whose value was calculated earliest is used. Where a singularity has been declared for the problem, the node and connected nodes are only chosen as bases for the integration in the last resort. A relaxation method by which the streamline ×permeability function is calculated from all the surrounding nodes is being considered. The flow lines are plotted by contouring the streamline×permeability function using the equipotential plotting routine. The flow line contour interval is the same as that used for the equipotentials. Thus the permeability must be scaled to unity in order to produce a flow net with "square" divisions of the net. Although this method is simple, it has not been found in the literature. The reason for this is probably that an extremely accurate finite element solution is required for well-formed flow lines. The usual method requires the solution of the system matrix a second time to calculate the streamlines using streamline boundary conditions.

4.3. Data Input

4.3.1. Miscellaneous Output Controls

This section describes the set of commands which are used to control the quantity of data output produced by the program. Some of the commands use the same modifiers. These modifiers influence the frequency at which the command is obeyed:

- .LAST output only for the last iteration
- .STAGE output only for end of stage (when acceptable accuracy is achieved)
- .ALL output for every iteration.

4.3.1.1. TITLE

As the name suggests, TITLE defines the literal string (sequence of ascii characters) to be printed in the output. The literal string follows on the next line after the heading. TITLE is unique in not allowing any comments immediately after the heading (a line starting with an underscore will become the title itself). There is a restriction of 50 characters on the length of the title.

The format for TITLE is:

```
TITLE
This is the title in less than 50 characters
_the title is in the line above
```

4.3.1.2. NOBLURB

This heading takes no parameters. The data read into the program is echoed back into a file in a predetermined order and with all the data formatted for presentation. Comments are inserted in the data to describe the function of each part of the data (the original comments are removed). The heading NOBLURB prevents the output of these comments. This shortens the echoed file and makes it more readable for the experienced user.

The format is simply:

```
NOBLURB
```

4.3.1.3. HEADS

The HEADS command controls the output of nodal data (coordinates, head and seepage fluxes). Each mesh node has a marker defined in the GEOMETRY data block. The HEADS block lists the markers for which nodal data is required. The number of markers used follows the heading, and then the markers are listed. A marker of 0 (zero) specifies all interior nodes, together with boundary nodes with zero markers.

The frequency of output is controlled by the OUTPUT heading.

For Figure 4.10 the requisite data to obtain the output for the heads along the sheet pile wall is:

```
HEADS
_number of markers
_(integer)
2
_list of nodes
_(integers)
1  3
```

4.3.1.4. DISCHARGE

Each node boundary segment has a marker for use by the DISCHARGE block. The DISCHARGE heading defines the markers which will be used in calculation of the seepage discharge across boundary segments, and the recording of the resultant values. The DISCHARGE heading is followed by the number of markers used (from the GEOMETRY block data) and a list of the markers. The discharge into and out of the domain for Figure 4.10 can be specified by:

```
DISCHARGE
_number of discharge markers used
_(integer)
2
_list of discharge markers
_(integers)
1  2
```

4.3.1.5. OUTPUT

The OUTPUT command controls the frequency of data output defined by HEADS and DISCHARGE. The command is modified by .LAST, .STAGE or .ALL. The default value is .ALL (output for every iteration). For example, to output calculated data values at every mesh generation:

```
OUTPUT
_output data at every iteration
.ALL
```

4.3.1.6. POTENTIALS

The POTENTIALS heading is a request for the production of flow nets. The default for the number of equipotentials drawn is 19 (that is, the equipotentials drawn for a problem with boundary conditions of 0 and 20 head are contoured values of 1.0, 2.0,3.0...19.0). The frequency of output is modified using .ALL, .STAGE and .LAST. The basic command is:

```
POTENTIALS
_plot equipotentials for every iteration
.ALL
```

The equipotentials plotted may be changed by the use of .NUMBER or .VALUES (but not both):

- .NUMBER, followed on the next line by the number of equipotential required. e.g.

```
POTENTIALS
.LAST
.NUMBER
_specifies 9 equipotentials to plot for the final solution
_(integer)
9
```

- .VALUES, followed on the next line by the value of the first equipotential, the last equipotential and the interval required, e.g.

```
POTENTIALS
.STAGE
_specify the equipotentials to plot for each time step
.VALUES
_start from finish at   interval
_(float)    (float)     (float)
0.5         19.5        1.0
```

4.3.1.7. SPACING

The SPACING block controls the output of a mesh density plot. The format for SPACING is exactly the same as that for POTENTIALS. The plots themselves are drawn with a logarithmic scale for fixed numbers of spacing values. This may be overridden by using the .VALUES command to specify an evenly spaced set of values. An example of the use of this command is as follows:

```
SPACING
.STAGE   (specify output for every time step)
.NUMBER
_specifies 10 spacing contour values
_(integer)
10
```

4.3.1.8. MESHES

The MESHES heading controls the output of the finite element meshes. The command is modified by .ALL, .STAGE, and .LAST. The format is the same as that for POTENTIALS except that there are no definitions for contour spacings (.NUMBER or .VALUES), e.g.

```
MESHES
.STAGE
```

Miscellaneous Output Commands			
Block	Status	Description	Default
TITLE	optional	defines title written on output data	"NO TITLE"
NOBLURB	optional	removes comments from output data	include comments
HEADS	optional	controls output of nodal values of head etc.	no output
DISCHARGE	optional	controls output of seepage discharges	no output
OUTPUT	optional	controls frequency of HEADS and DISCHARGE	no output
POTENTIALS	optional	output of flow nets	no output
SPACING	optional	output of contours of nodal spacing (mesh density)	no output
MESHES	optional	output of finite element meshes	no output
.ALL	modifier	specifies output for all iterations	none
.STAGE	modifier	specifies output for each time step	none
.LAST	modifier	specifies output for just last iteration	none
.NUMBER	modifier	defines the number of contours	19
.VALUES	modifier	defines the bounds and interval for contours	see above

Table 4.1 DFLOW: Miscellaneous Commands

4.3.2. Miscellaneous Program Flow Control Instructions

This section is a round-up of program instructions which do not describe the problem directly but affect the way in which the program algorithm operates.

4.3.2.1. ACCURACY

The ACCURACY block describes the relative error to be obtained for each time step (steady state) problem. The data consists of 2 numbers:

- Target accuracy (relative error as a percentage).
- Acceptable accuracy (as above).

For almost all cases, the generated finite element mesh out-performs the requested accuracy. In some particularly difficult problems it may be necessary to accept a higher error than that requested.

The format for ACCURACY is as follows:

```
ACCURACY
_target      acceptable relative error (%)
_(float)     (float)
9.0          10.0
```

This is in fact the default for ACCURACY. All problems in the thesis are solved to at least 5% unless otherwise stated. The mesh is regenerated for each iteration until the maximum number of iterations (see ITERATIONS) or the acceptable accuracy is achieved.

4.3.2.2. TIMES

In most cases the real time units will not be used. The program does not scale input data and so it is best if the permeabilities are scaled in order to avoid truncation errors. To transfer from real time to simulation time, multiply the real time by the permeability (each with the same time units). For an unconfined steady state analysis in which the head is fixed and the flow is calculated (see FREE SURFACES), the real time is meaningless; the time step is just a method of obtaining a quick convergence.

The TIMES block first defines the time at the start of the simulation. This is useful when a transient problem is stopped and restarted part way through. The time steps for a transient (or pseudo time for an unconfined steady state problem) analysis do not have to be of the same length. The time period for the simulation is divided into smaller time segments. The number of time steps is defined in the data. Then for each time step, the segment sequence number and the time step for the segment is required, together with the time at which the segment will be terminated (measured from zero).

The following section of data gives an example:

```
TIMES
_time at start of iteration
_(float)
0.0
_number of time segments
_(integer)
3
_n time step            time at end of segment
_(integer)  (float)     (float)
1  0.01        0.2
2  0.2        10.0
3  0.4      1000.0
```

The simulation stops when the highest segment time or the maximum number of stages (see STAGES) is exceeded. The default time start is 0.0 with a time step of 1.0 with a segment end time of 1×10^6 units.

4.3.2.3. ITERATIONS

The ITERATIONS block defines the maximum number of iterations allowed in the mesh generation loop. If the problem is ill-posed then the mesh generator will not be able to achieve the required accuracy. The format for the command is as follows:

```
ITERATIONS
_maximum number of iterations
_(integer)
4
```

This is in fact the default for the maximum number of iterations.

4.3.2.4. STAGES

The STAGES block defines the maximum number of time steps (or stages) allowed in the simulation. The format is as follows:

```
STAGES
_maximum number of time steps
_(integer)
100
```

The default number of stages is 1.

4.3.2.5. NOSOLV

The heading NOSOLV stops the program after mesh generation, and before assembly of the stiffness matrix. This allows the user to examine the initial finite element mesh generated without solving the problem. There are no parameters or modifiers, e.g.

```
NOSOLV
```

4.3.2.6. NOSWAP

The heading NOSWAP prevents the mesh post-processor in the program from changing the diagonals of the mesh to try and obtain the 6-side property (each node having six sides). There are no parameters or modifiers, e.g.

```
NOSWAP
```

4.3.2.7. NOSMOOTH

The heading NOSMOOTH prevents the mesh post-processor from moving the original nodes produced in the meshing. There are no parameters or modifiers, e.g.

```
NOSMOOTH
```

4.3.2.8. SMOOTH

The SMOOTH block redefines the number of smoothing loops performed in the mesh post-processor algorithm. The default number of smoothing loops is 3. To set the algorithm to do just 1 smoothing cycle:

```
SMOOTH
_number of smoothing cycles
_(integer)
1
```

4.3.2.9. STOP

The STOP heading is the only heading which must be in order. It informs the program that the end of the data has been reached. Anything written after the STOP is ignored, e.g.

```
STOP
this line is ignored.
```

4.3.3. GEOMETRY

The GEOMETRY block has three functions:

- Describes the external and internal region boundaries of the problem domain; that is, coordinates and node ordering.
- Cross-references the boundary conditions; defines which of the boundary conditions defined elsewhere refer to which node.
- Marks the nodes and boundary segments required for output. The actual commands to print the data are defined in HEADS, DISCHARGE and OUTPUT.

The block GEOMETRY is composed of up to 4 sub-blocks:

.NODES
.SEGMENTS
.LOOPS
.MOVES

Program Flow Control Commands			
Block	Status	Description	Default
ACCURACY	optional	defines target and acceptable relative errors (%)	9% & 10%
TIMES	optional	defines time at start, time interval and time end	0.0, 1.0, 1×10^6
ITERATIONS	optional	defines maximum number of iteration per FE meshing	4
STAGES	optional	defines maximum number of time steps	1
NOSOLV	optional	prevents assembly of stiffness matrix	none
NOSWAP	optional	prevents swap of calculated mesh sides	none
NOSMOOTH	optional	prevents the movement of the calculated mesh nodes	none
SMOOTH	optional	specifies the number of nodal smoothing cycles	none
STOP	mandatory	terminates data	none

Table 4.2 DFLOW: Flow Control Commands

4.3.3.1. .NODES

The .NODES sub-heading defines the number of points defined around the boundary and along internal subdivisions or holes, together with their nodal numbers, coordinates, boundary condition markers and output markers. For Figure 4.8, the following data would describe the nodal data:

```
GEOMETRY
.NODES
_number of boundary nodes (lines starting "_" are comments)
_(integer)
4
_n x          y           bc          p
_(integer)   (float)     (float)     (integer)    (integer)
1   1.0       3.0         3           0
2   6.0       2.0         2           0
3   5.0       4.0         -1          1
4   2.0       6.0         2           1
```

The total number of nodes follows the .NODES sub-heading, followed by the nodal data. The numbering of the nodes (n) and coordinates (x,y) is quite straightforward. The nodes may be in any order, but all the nodes must be defined, and only once.

The fourth column (bc) indicates the boundary conditions at the nodes. The number itself is just a cross-reference to the same number in the CONSTRAINTS block. The sign of the number is significant; if the number is negative, then it belongs to a free surface defined in block FREE SURFACES. A free surface in this context may be a seepage line or a boundary section, the points of which define a cubic B-spline curve (if there are 5 points or more). One point to note is that the first free surface marker must be numbered -1, and markers for further free surfaces -2, -3...-9. The modulus of the markers for free surfaces refer to the boundary conditions defined in the CONSTRAINTS block. For Figure 4.8, the constraints at nodes 1 and 2 are defined by boundary condition 2 and 3 respectively, and those at nodes 3 and 4 are defined by boundary condition 1. Nodes 3 and 4 also lie at the ends of free surface 1.

The marker 0 (zero) is a special case; it does not refer to a specific reference in the CONSTRAINTS block. A zero boundary condition marker defines the natural boundary condition for the FE method; i.e. it is a no-flow boundary for exterior boundary nodes, and a regular interior node for inter-regional boundaries.

The fifth column holds the print reference marker. Printing of the calculated nodal values is controlled by heading HEAD. The HEAD block lists the markers for which

the output of data is required. In this case both nodes 3 and 4 will be printed if marker 1 is selected. Any integer number may be used as a marker.

4.3.3.2. .SEGMENTS

The .SEGMENTS sub-heading defines the boundary conditions on all points lying between pairs of adjacent nodes, and the printing markers which are cross-references to the discharge calculation and output routines. For Figure 4.8 the following data are appropriate:

```
GEOMETRY
.SEGMENTS
_number  of segments
_(integer)
4
_ns          n1          n2          bc          p
_(integer)   (integer)   (integer)   (integer)   (integer)
1  1         2           0           0
2  2         3           2           3
3  3         4           -1          2
4  4         1           3           1
```

The number of the segment follows the .SEGMENTS sub-heading. This is followed by the segment numbers (ns) and their node numbers (n1,n2), boundary condition markers (bc) and print markers (p).

Each connected pair of nodes around the boundary and along region boundaries within the domain must be specified just once in the list of segments. The order of the segments and their nodes is not important.

The boundary conditions along edges of the problem domain are included after the specification of the end nodes. The boundary conditions are cross references to the same markers held in the CONSTRAINTS block. The rules for boundary condition markers are the same as those for nodal boundary conditions (see above). The nodes generated along the boundary of the FE domain have the same boundary condition as the segment of which they are a subdivision.

The print markers (p) are references used by the heading OUTPUT to specify what seepage discharges to calculate and write to file. In this case the markers refer to the left, top and right boundaries of the domain. The use of markers allows the user to specify the total seepage discharge over more than one segment of the boundary by marking them with the same number. Any integer number may be used as a marker.

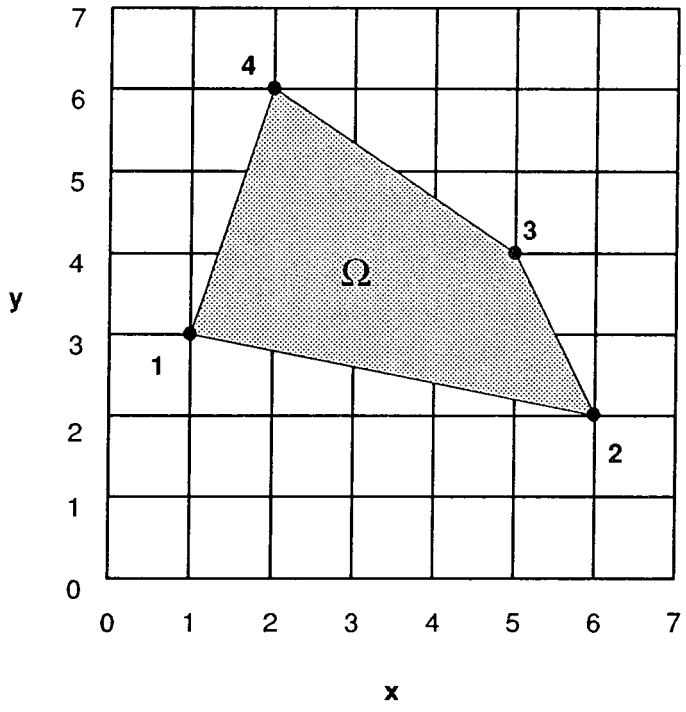

Figure 4.8 Boundary Node Geometry

4.3.3.3. .LOOPS

The .LOOPS subheading defines the ordering of the exterior boundary nodes and internal nodes in region boundaries and holes. For Figure 4.8 the .LOOPS data is as follows:

```
GEOMETRY
.LOOPS
_number of regions
_(integer)
1
_number of bounding nodes (repeating first)
_(integer)
5
_ordered list of bounding nodes
_(integers)
1   2   3   4   1
```

The .LOOPS sub-block defines the subdivision of the FE domain into regions and specifies the node ordering around these regions. The first value following the .LOOPS sub-heading is the number of domain subdivisions or regions. Figure 4.8 consists of just one region. The node ordering around each region follows next. First the number of nodes is specified. This figure includes an allowance for the repetition of the first

node at the end of the list. The reason for this will become obvious when the definition of holes in a region is discussed. The list of nodes is numbered counter-clockwise for exterior region boundaries, and clockwise for holes in the region.

Figure 4.9 shows a complex domain consisting of two regions (I & II) with a hole in region II. For this domain the .LOOP sub-block data is as follows:

```
GEOMETRY
.LOOPS
_number of regions
_(integer)
2
_number of nodes around first region
_(integer)
5
_(integers)
_list of nodes (ordered counter clockwise)
1     3     4     2     1
_number of nodes in second region
_(integer)
10
_list of nodes (exterior clockwise, hole counter clockwise)
_(integers)
1     9     10     3     1     5     6     8     7     5
```

The nodes defining holes in a region are simply included in the list of nodes describing the region's exterior nodes. The first node listed for the hole is also repeated. The repeated nodes allow the inclusion of holes simply and efficiently.

A further use of regions is discussed in connection with the definition of material properties, e.g. permeability.

N.B. Regions I and II could have been combined into one. However, there is a possibility that the elements formed adjacent to the interior angle at 3 could become badly distorted, or even cross outside the FE domain. Regions are meshed separately, and so mesh generation is also quicker if the domain is split into several parts. In the case of an internal flow barrier having a negligible thickness, it is essential that regional boundaries are used to prevent connections between one side of the flow barrier and the other.

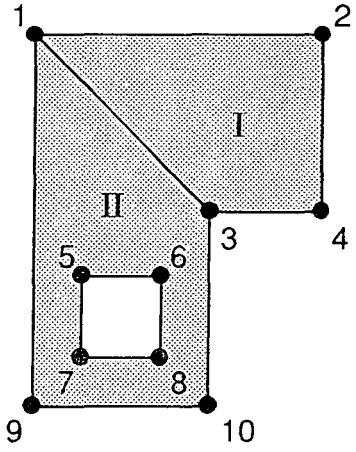

Figure 4.9 Complex Boundary Loop Definition

4.3.3.4. .MOVES

The .MOVES sub-heading describes the movement of nodes for transient problems. The data includes the number of nodes for which movement is defined, the simulation time at the beginning and end of movement, and the amount of movement in x and y coordinates (positive for up and from left to right) for each simulation time unit. An example of the use of .MOVES might be the seepage line entry point of the upstream slope of a dam. The use of .MOVES is demonstrated below:

```
GEOMETRY
.MOVES
_number of moving nodes
_(integer)
1
_node        time start  time stop   x-step       y-step
_(integer)   (float)     (float)     (float)      (float)
2  10.0      20.0        0.0         1.0
```

This data informs the program that there is one moving node. Node 2 from the .NODES sub-block starts moving at 10.0 simulation time, and stops at a time of 20.0. In each of the 10 intervening time units node 2 moves vertically up at 1 space unit per time unit.

GEOMETRY			
Block	Status	Description	Default
GEOMETRY	mandatory	describes the problem geometry	none
.NODES	mandatory	specifies the boundary nodes, the boundary condition references and head potential output markers	none
.SEGMENTS	optional	specifies the boundary segments, their nodes, boundary conditions and seepage discharge calculations	adjacent nodes (and first/last) paired with zero markers.
.LOOPS	optional	specifies node ordering for boundary nodes and holes.	simply connected region in order of nodal definitions,
.MOVES	optional	defines node movement for transient simulation	no moving points

Table 4.3 DFLOW: Geometry Definition

4.3.4. CONSTRAINTS

The CONSTRAINTS block describes the boundary conditions used in the FE simulations. Two types of boundary condition can be modelled:

- Constant head or Dirichlet boundary.
- Constant flow or Neuman boundary.

The seepage surface in a transient analysis may be specified as a constant head or constant flow boundary depending on which method is used (see FREE SURFACES section).

The FE boundary nodes are not known *a priori* and so the program must be instructed how to calculate the boundary condition for nodes formed by a subdivision of the boundary. Three different sub-blocks are used to specify whether nodes should be fixed at a particular value of head or flow (.FIXED), or the nodes may have the same head as a reference node which is defined in the .NODES section (.RELATIVE), or nodes may have a head equal to their elevation (.ELEVATION). Descriptions of these different sub-blocks follow.

4.3.4.1. .FIXED

The .FIXED sub-block defines boundary conditions of constant flow and constant head which are known before the simulation commences. Figure 4.10 shows a problem concerning the flow of water beneath a sheet pile wall. There are two fixed head conditions which could be defined using a .FIXED sub-block:

```
CONSTRAINTS
.FIXED
_number of defined conditions
_(integer)
2
_n +/- marker            value
_(integer)   (integer)    (integer)
1  1         16.0
2  2         10.0
```

The .FIXED sub-heading is followed by the number of fixed conditions (head and/or flow). Each condition is numbered in sequence and followed by the marker or cross-reference to the nodal and segment definitions. The marker has a positive sign for fixed head and a negative sign for fixed flow. Note that values 1 and -1 actually refer to the same marker, and so cannot both be used. The fixed value of head or flow follows after the marker.

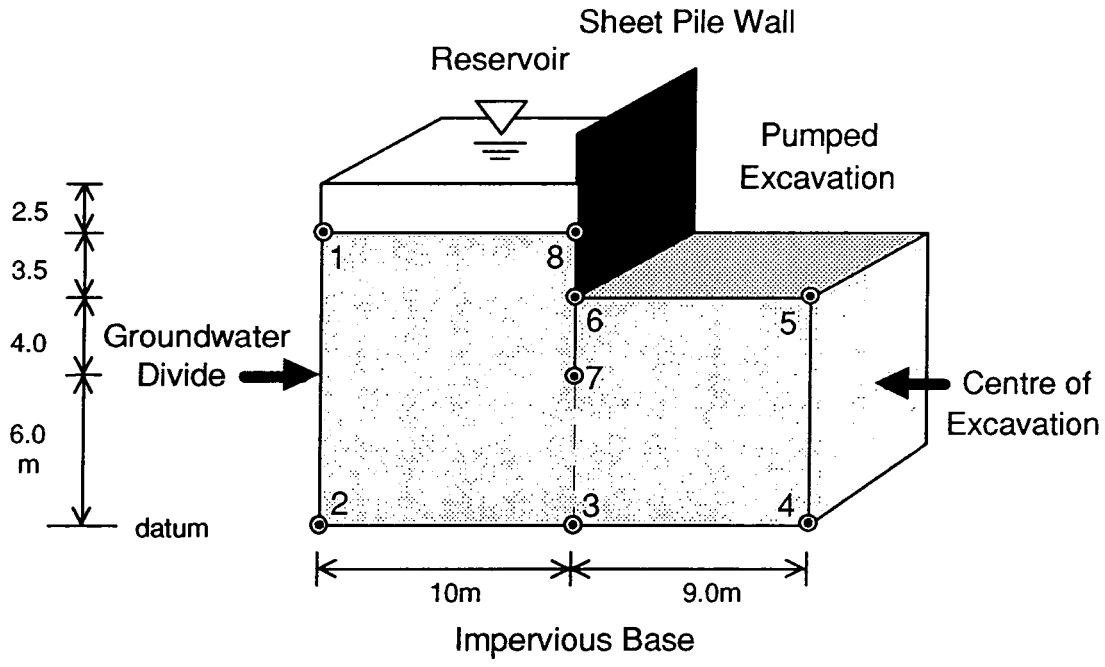

Figure 4.10 Constraints for Flow Below a Sheet Pile Wall Excavation

The markers (Page 99) show how the boundary conditions tie in with the geometry data. Nodes 1 and 8 and segment 5 which lie under the ponded water are labelled with marker 1, while nodes 5 and 6 and segment 8 which lie in the excavation are labelled with marker 2. The CONSTRAINTS block fixes the head of nodes with marker 1 (including all nodes dividing segment 5) to equal 16 metres, and nodes with marker 2 to equal 10 metres.

```
GEOMETRY
.NODES
9
1   13.5        0.0          1              0
2    0.0        0.0          0              0
3   10.0        0.0          0              0
4   19.0        0.0          0              0
5   19.0       10.0          2              0
6   10.0       10.0          2              0
7   10.0        6.0          0              1
8   10.0       13.5          1              0
.SEGMENTS
9
1   1          2              0              0
2   2          3              0              0
3   3          7              0              0
4   7          8              0              3
5   8          1              1              1
6   3          4              0              0
7   4          5              0              0
8   5          6              2              2
9   6          7              0              3
.LOOPS
2
6
1       2       3       7       8       1
6
3       4       5       6       7       3
```

Note that the "no-flow" boundaries (to the left, right and bottom) and internal boundaries (down from the tip of the sheet pile wall) do not need boundary condition markers. However, a fixed flow of zero could have been defined for the flow boundaries thus:

```
CONSTRAINTS
.FIXED
_number of fixed constraints
_(integer)
3
_n +/-marker            value
_(integer)   (integer)    (integer)
1  1         16.0
2  2         10.0
3  -3        0.0
_where the negative marker indicates fixed flow
```

4.3.4.2. .ELEVATION

The .RELATIVE sub-heading defines heads at marked nodes to equal the elevation of the node. This is very useful in defining the heads on a seepage face, or in some cases the seepage line itself (if we are using a "known head" method of moving the seepage line in a transient solution: see FREE SURFACES). All the markers are given positive values in the .ELEVATION sub-block. An example of this syntax is as follows:

```
CONSTRAINTS
.ELEVATION
_number of markers defining head = elevation
_(integer)
1
_n +marker
_(integer)   (integer)
1  2
```

It is recommended that if an elevation marker is used for the seepage line, then a second and different marker is used for other elevation = head boundary conditions.

For the sheet pile wall problem (Page 99), the fixed head constraint for marker 2 could be replaced by this elevation constraint.

4.3.4.3. .RELATIVE

The .RELATIVE sub-heading defines the head at one node (or nodes lying on a boundary segment) to be equal to the head of one of the original boundary nodes. The .RELATIVE sub-heading is followed by the number of relative markers, and a row for each marker containing the row sequence number, the marker (always positive) and the node number for the reference boundary node. This is particularly useful in defining the potential head for a submerged slope. The seepage line entry point has a marker to fix the head to the elevation, while the slope below uses a marker to fix the head equal to that of the first node. In the case of a steady state problem, the head in the reservoir

is known before the simulation. However, in the simulation of a changing reservoir height, the .MOVES sub-block of the GEOMETRY block is used to alter the position of the seepage line entry node during the simulation. The head at the seepage line point changes as its elevation changes. The heads on the upstream slope defined with .RELATIVE markers are automatically updated as the simulation progresses. The CONSTRAINTS block for Figure 4.8 can be written as follows:

```
CONSTRANTS
.ELEVATION
2
1  1
2  2
.RELATIVE
_number of relative markers
_(integer)
1
_n +marker  node number
_(integer)   (integer)    (integer)
1  3         4
```

The .RELATIVE block cannot be used to fix fluxes.

CONSTRAINTS			
Block	Status	Description	Default
CONSTRAINTS	mandatory (for solution to matrix)	defines boundary conditions	none
.FIXED	optional	specifies fixed values of head or flow	none
.ELEVATION	optional	fixes the head to equal the nodal elevation	none
.RELATIVE	optional	sets the nodal heads to equal the head at a defined node	none

Table 4.4 DFLOW: Constraints

4.3.5. SINGULARITIES

The SINGULARITIES block speeds up the convergence of the adaptive mesh algorithm in the vicinity of a sudden change in flow direction due to the particular geometry or change in boundary condition. In practice this block is rarely needed because the mesh generation algorithm almost invariably achieves the set accuracy

without any special provisions. One exception to this occurs when the size of the problem to be solved is close to the program limits. The use of the SINGULARITIES block cuts down the total number of elements required by forcing the program to concentrate mesh refinement at the singularity.

The SINGULARITY heading is followed by the number of singularities. The following rows list the sequence number, the node number at the singularity and the singularity strength. The strength of a singularities lies between 0.5 and 1.0, but there is little harm in using 0.5 (the maximum strength) for every case. In the sheet pile dam example, (Figure 4.10) node 7 is sited at a singularity (in the numerical model the water changes instantly from vertical downward through to vertical upward motion when rounding the base of the sheet pile wall). The following data describes this singularity to the program:

```
SINGULARITIES
_number of singularities
_(integer)
1
_n node      strength
_(integer)   (integer)    (float)
1  7         0.5
```

SINGULARITIES			
Block	Status	Description	Default
SINGULARITIES	optional	specifies convergence rate for singularities	none

Table 4.5 DFLOW: Singularities

4.3.6. GRID

The GRID block specifies the starting nodal density for the FE mesh. In most FE programs this would have a crucial significance because it would directly control the accuracy of the program. In DFLOW, the program estimates the error using the original mesh and then re-designs a better optimal mesh automatically. Although a good initial mesh may speed up this process, the time taken to produce a better initial mesh will be several orders of magnitude higher than the time required by the program to carry out just one extra iteration. The only instance when a starting mesh is important occurs when a coarse mesh fails to pick up changes in material properties which occur over a short distance.

All the problems solved for this thesis used a constant mesh density over the starting mesh. Thus:

```
GRID
.CONSTANT
_value of spacing
_(float)
5.0
```

is sufficient to produce an FE mesh with a node spacing of 5 units. In the absence of a GRID block, the default value for the FE mesh spacing is 1.

If a more complex mesh is required, then sub-headings .NODES and .ELEMENTS are required.

4.3.6.1. .NODES

The .NODES sub-heading defines the spacing at each of a minimum of three nodes. The number of spacing nodes follows immediately after the sub-heading. In subsequent lines there are the node numbers, the (x,y) nodal coordinates and the nodal spacing. The values of mesh spacing at the nodes are interpolated between the nodes in accordance with the .ELEMENTS sub-block. The following data for the nodal values at the vertices of a triangle would provide a 1 by 1 square with a bottom-left corner at the origin with a mesh spacing of 1 at the left hand side, and 2 at the right hand side:

```
GRID
.NODES
_number of nodes
_(integer)
3
_n x          y            spacing
_(integer)   (float)       (float)      (float)
1   0.0        10.0         1.0
2   0.0       -10.0         1.0
3   10.0        0.0        10.0
```

The values outside the defined region are equal to the interpolated value at the nearest point of the nearest element.

4.3.6.2. .ELEMENTS

The .ELEMENTS sub-heading defines the triangles over which the linear interpolations of the nodal values will be carried out. The elements should define one multiply-connected region, preferably corresponding with the problem area. The sub-heading is followed by the number of elements defined, and for each element a sequence number,

together with the 3 nodal coordinates ordered in a **counter-clockwise** direction. For the previous example there is only one element and so the requisite data is as follows:

```
GRID
.ELEMENTS
_number of element
_(integer)
1
_n n1        n2           n3
_(integer)   (integer)    (integer)    (integer)
1  1         2            3
```

GRID			
Block	Status	Description	Default
GRID	optional	specifies nodal density of starting grid	1 unit spacing
.CONSTANT	optional	define a constant mesh spacing	none
.NODES	optional	define spacings over a set of points for interpolation	none
.ELEMENTS	together	define triangular spaces over which to interpolate	none

Table 4.6 DFLOW: Grid Spacing

4.3.7. POROSITY

The POROSITY sub-heading defines the effective porosity for the porous medium. Steady state analyses are independent of the porosity. If this heading is missing then a default value of 1 is used. In the transient case where the porosity does not vary over the area of interest, it is more useful to incorporate the value of porosity into the permeability value (both parameters are scalar functions in the calculation of seepage line movement). The rules for POROSITY are the same as those for GRID (see above). For example:

```
POROSITY
.NODES
_number of nodes
_(integer)
3
_n x         y           porosity
_(integer)   (float)     (float)      (float)
1   0.0       10.0       0.3
2   0.0      -10.0       0.3
3   10.0       0.0       1.0
```

```
.ELEMENTS
_number of element
_(integer)
1
_n n1        n2          n3
_(integer)   (integer)   (integer)    (integer)
1  1         2           3
```

defines the porosity over a unit square to be 0.3 on the left hand side and 0.4 on the right hand side.

POROSITY			
Block	Status	Description	Default
POROSITY	optional	specifies effective porosity	1
.CONSTANT	optional	define a constant porosity	none
.NODES	optional	define spacings over a set of points for interpolation	none
.ELEMENTS	together	define triangular spaces over which to interpolate	none

Table 4.7 DFLOW: Porosity Definition

4.3.8. PERMEABILITIES

The PERMEABILITIES heading defines the permeabilities in the x and y directions. For a confined problem, the space coordinates may be rotated to ensure that they are orthogonal to the permeability tensor. Unfortunately, the boundary conditions will not be correct for seepage lines and seepage surfaces.

The program does not scale input values in order to reduce the possibility of numerical error. Permeabilities should be scaled by the user so that they are close to 1.0 units. Flow nets will have a square mesh for an isotropic permeability of 1.0.

The format for the PERMEABILITIES block is similar to that for GRID (see above). The only difference is that the single value for spacing is replaced by the x and y permeabilities.

In problems involving big changes in permeability, the mesh generator may become unstable. In different mesh generations, portions of the domain in the vicinity of the interface will be part of an element which crosses the interface, or lie in an element

wholly on one side or the other. The error estimator is a poor measure for elements which cross the interface, and therefore the estimated error for the area in question will oscillate between iterations. When the error is low, the element will increase in size and cross the permeability interface. The estimated error will then be high, and the element will shrink again. This problem is usually cured by dividing the problem domain into separate regions at the break in permeability continuity. This forces the mesh generator to keep a line of nodes along the interface and stabilise the solution.

Figure 4.11 shows a problem concerning a step jump in the permeability across the centre of the problem domain (isotropic problem). The material properties are interpolated linearly over the background properties mesh. The solution to this problem is to use a thin layer of elements straddling the boundary between the different permeability zones. The following data correspond to the permeability conditions for Figure 4.11:

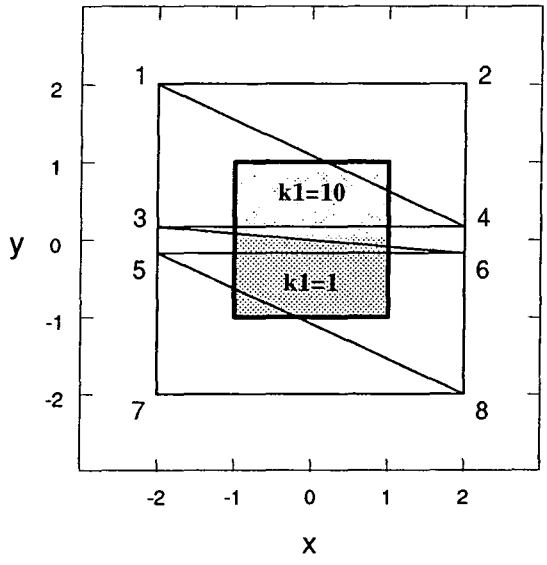

Figure 4.11 Approximation of Step Jump in Isotropic Permeability

```
PERMEABILITIES
.NODES
_number of nodes
_(integer)
8
_n x-coord  y_coord     kx          ky
_(integer)  (float)     (float)     (float)     (float)
1  -2.0      2.0       10.0        10.0
2   2.0      2.0       10.0        10.0
3  -2.0      0.1       10.0        10.0
4   2.0      0.1       10.0        10.0
5  -2.0     -0.1        1.0         1.0
6   2.0     -0.1        1.0         1.0
7  -2.0     -2.0        1.0         1.0
8   2.0     -2.0        1.0         1.0

.ELEMENTS
_number of elements
_(integer)
6
_n n1       n2          n3
_(integer)  (integer)   (integer)   (integer)
1  1        4           2
2  1        3           4
3  3        6           4
4  3        5           6
5  5        8           6
6  5        7           8
_etc
```

PERMEABILITY			
Block	Status	Description	Default
PERMEABILITY	optional	specifies effective permeability	kx=ky=1.0
.CONSTANT	optional	define a constant permeability	none
.NODES	optional	define spacings over a set of points for interpolation	none
.ELEMENTS	together	define triangular spaces over which to interpolate	none

Table 4.8 DFLOW: Permeability Definition

4.3.9. FREE SURFACES

The FREE SURFACES heading describes the shape of curved sections of the FE boundary. The block is principally designed for seepage line definition and some of the mandatory sub-blocks will not make sense in the context of some other boundary type. Dummy values should be used to satisfy the program input routines. The dummy values will not be used unless movement is specified for the boundary and/or its ends.

Up to 9 free surfaces may be defined at one time. If the curved boundary section crosses an interface between two widely different permeabilities, then the free surface may be split into two. The internal node may be constrained to move (in the case of a seepage line) along the permeability interface.

The FREE SURFACE heading is followed by a value specifying the number of free surfaces.

The FREE SURFACES block is divided into a number of different sub-blocks, all of which must be included if FREE SURFACES is declared:

- .POINTS defines the free surface coordinates
- .ENDS specifies the free surface end node numbers and points to the appropriate movement vectors (see below)
- .VECTORS defines the paths constraining movement of the end nodes, and the bounds to the seepage line itself.

In addition to these sub-blocks, there are two commands:

- .FLOW specifies that the seepage line is moved with respect to the calculated flow
- .HEAD specifies that the seepage line is move with reference to the calculated head.

The sub-blocks are now described in more detail.

4.3.9.1. .POINTS

Sub-block .POINTS lists the coordinates of a set of points along the free surface. The points must be ordered along the length of the free surface. The end points must correspond to the equivalent nodal coordinates specified for the boundary. There must be at least 2 points. If there are fewer than 5 points then the mesh nodes will lie on the straight line segment between the free surface end nodes. For 5 points or more, the mesh nodes will fall on a cubic B-spline passing through the free surface points.

Following the .POINTS sub-heading is the sequence number of the free surface (this number is the modulus of the marker used in specifying the boundary conditions; see

GEOMETRY) and the number of points in the free surface list. For each free surface point there is a data row giving the sequence number of the point and the coordinates; e.g. for Figure 4.8 we have:

```
FREE SURFACES
_number of free surfaces
_(integer)
1
.POINTS
_+marker    number of points
_(integer)  (integer)
1  2
_n x-coord  y_coord
_(integer)  (float)      (float)
1  2.0      6.0
2  5.0      4.0
```

If the program is stopped part way through a transient simulation, then the simulation may be restarted by copying the coordinates from the last simulation iteration output into the .POINTS data. The simulation "time clock" will also need resetting to reflect the time already passed (see TIMES). In addition, the boundary nodes in the GEOMETRY block definition will need to be updated.

4.3.9.2. .ENDS

The .ENDS sub-block is required to inform the program information concerning:

- Which boundary nodes correspond with the free surface ends.
- Whether the free surface and its ends are fixed or moving.
- Which paths the free surface ends follow (or which paths constrain the free surface).

The sub-block contains 3 data lines for each free surface. The first line contains the free surface marker in question. The marker is negative for a moving free surface (seepage line), and positive for a fixed boundary. In the second line, the boundary node number for the first free surface point is followed by a marker pointing to a constraining path held in .VECTORS (see below). The markers are numbered in sequence up from 1 (i.e. for two free surface the markers are 1 and 2). The second line contains the boundary node number of the last free surface point (negative if movement is allowed), followed by its geometrical constraint path marker. The data for Figure 4.8 are below:

```
FREE SURFACES
.ENDS
_free surface marker (negative for moving surface)
_(integer)
-1
_node        vector marker (negative for moving)
_(integer)   (integer)
4    1
3   -2
```

4.3.9.3. .VECTORS

Sub-block .VECTORS specifies the paths of moving nodes and a constraint for the free surface. If in a transient solution the seepage line moves outside the space bordered by the vectors defined, then the seepage line is truncated at the intersection. The new position for the seepage path end is located at the point of intersection (in the case of a moving end point; see above in .ENDS definition). If the seepage line end "undershoots" the constraining vector, then the rules in block INTERPOLATION are used to calculate a new seepage line exit position (the default is a straight line extrapolation using the last two internal points). If the intersection of the seepage line and the constraining vector (interpolated or extrapolated) lies outside the line defined by the vector, then the simulation is stopped. In the case of transient flow within an earth embankment (where the seepage line is moving along the base of the dam), the vector is defined so that this point occurs when the seepage line reaches the downstream toe.

Following the sub-heading there is the number of vector bounds (minimum of two). For each vector there is a row containing the vector marker (see .ENDS above), and the *x,y* coordinates of the first vector end, and then the x,y coordinates of the other end of the vector.

For Figure 4.8 the .VECTORS sub-block could be defined as follows:

```
FREE SURFACES
.VECTORS
_number of vector bounds
_(integer)
2
_marker      x1          y1          x2          y2
_(integer)   (float)     (float)     (float)     (float)
1   1.0      3.0         2.0         6.0
2   6.0      2.0         4.0         6.0
```

FREE SURFACES			
Block	Status	Description	Default
FREE SURFACES	optional	defines curved boundaries (moving and stationary)	none
.HEAD	optional	seepage line moved in accordance with calculated head	.FLOW
.FLOW	but not both	seepage line moved in accordance with calculated flow	.FLOW
.POINTS	mandatory	curved boundary point coordinates	none
.ENDS	mandatory	free surface properties	none
.VECTORS	mandatory	free surface geometrical constraints	none

Table 4.9 DFLOW: Free Surface Definition

4.3.10. INTERPOLATION

The INTERPOLATION block controls the method of interpolating a seepage line locus to the seepage surface on the boundary of the flow domain. The default method of calculating the seepage line exit point involves a linear extrapolation from the last two points on the seepage line. If the seepage exit point obtained by this method oscillates wildly, then changing the interpolation function used is the last thing to consider! The usual cause is too big a time step, or a badly posed problem.

If every other avenue has been tried, then the INTERPOLATION block may be used to smooth the numerical oscillations. The program uses the data to obtain a best fit polynomial equation through a set number of points along the seepage line (interior to the problem domain). The seepage line points may be weighted so that points close to the seepage face have a greater or lesser significance in the calculation. Once a polynomial equation has been obtained, the seepage line points used for its calculation are moved towards the equation line. The proportion of the distance moved is controlled by the data and may take the value 0 (fixed), 1 (full movement), or any intermediate value.

Following the INTERPOLATION heading is the number of seepage line points involved in the calculation and the polynomial degree of the equation. There must be at least 2 interpolation points, and the total number must be less than the total number of

seepage line points produced by the mesh generator. The polynomial degree must be at least one less than the number of points included in the calculation. It is best to keep the polynomial degree low in order to avoid excessive wandering, and probably a cubic will suffice. The following lines contain the weight and then the movement factors for each interpolation point. These are ordered along the seepage line, starting from the seepage exit point. The following data would define a linear extrapolation ignoring the point closest to the seepage exit point:

```
INTERPOLATION
_number of points and polynomial degree (linear)
_(integer)  (integer)
3  1
_interpolation point weight
_(floats)
0.0          1.0          1.0
_movement factors (only exit point moved here)
_(floats)
1.0          0.0          0.0
```

A more complicated example might smooth the end section of the seepage line using a higher degree of polynomial and more seepage line points:

```
INTERPOLATION
_number of points and polynomial degree (cubic)
8  3
_weights
1.0          1.0          1.0          0.9          0.8
0.6          0.4          0.2
_movement vectors
1.0          1.0          1.0          0..6         0.4
0.2          0.0          0.0
```

INTERPOLATION			
Block	Status	Description	Default
INTERPOLATION	optional	specifies method of fixing location of seepage exit point	linear fit through last pair of points

Table 4.10 DFLOW: Seepage Line Interpolation

4.4. Examples

4.4.1. Flow Under a Concrete Dam with Cutoff

This example has been selected to demonstrate the ease of use and quality of results obtained from the DFLOW program for an unconfined problem. The solution can be readily judged by the accuracy of the flow net which fits all of the criteria for a perfect flow net construction.

Geometry

This example has been taken from Berry and Reid (1987). The problem is concerned with the geometry pictured in Figure 4.12. The water flows from the upstream reservoir, below the concrete dam and beneath the cutoff wall, and finally to the tailwater reservoir.

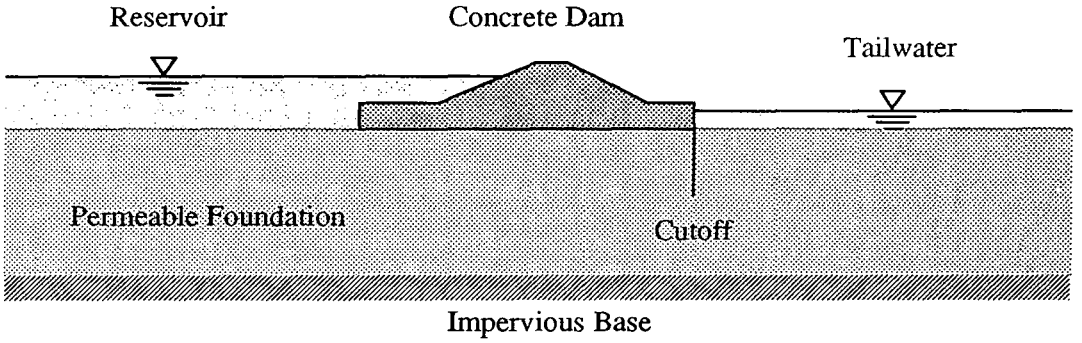

Figure 4.12 Geometry for Flow under a Concrete Dam with Cutoff

Data

```
TITLE
Concrete Dam (Berry and Reid 3.2)

ACCURACY
_    target        acceptable
       .4000E+01     .5000E+01

TIMES
_time periods, time steps and termination time
_time at simulation startup
_number of time periods
  .0
      1
_   No.         time step      end
      1       .1000E+01      .1000E+07

POTENTIALS
.ALL        plot every iteration
.NUMBER
_number of interior contours
     17
```

```
SPACING
.ALL        plot every iteration

MESHES
.ALL        plot every iteration

OUTPUT
.STAGES     plot final iteration in each stage


GEOMETRY
_mesh information for problem geometry
_tokens  control boundary conditions
_markers control data output

.NODES
_number of nodes
    10
_  No.    x-coordinate  y-coordinate   token    marker
     1      .0000E+00     .1400E+02        1    0
     2      .0000E+00     .0000E+00        0    0
     3      .6000E+02     .0000E+00        0    0
     4      .1100E+03     .0000E+00        0    0
     5      .1100E+03     .1400E+02        2    0
     6      .6000E+02     .1400E+02        2    0
     7      .6000E+02     .7000E+01        0    3
     8      .6000E+02     .1200E+02        0    0
     9      .5000E+02     .1200E+02        0    0
    10      .5000E+02     .1400E+02        1    0
.SEGMENTS
_number of segments
    11
_  No.     node pair    token    marker
     1       1    2         0    0
     2       2    3         0    0
     3       3    4         0    0
     4       4    5         0    0
     5       5    6         2    2
     6       6    7         0    0
     7       7    8         0    0
     8       8    9         0    0
     9       9   10         0    0
    10      10    1         1    1
    11       7    3         0    0
```

```
.LOOPS
_number of regions
     2
_number of nodes for region boundary
     8
_closed list of region nodes
     1    2    3    7    8    9   10    1
_number of nodes for region boundary
     6
_closed list of region nodes
     3    4    5    6    7    3

GRID
.CONSTANT
_single value over background mesh
    .3000E+01

SINGULARITIES
_position and strength of singularities
_number of singular nodes
     2
_  No.    node    strength
     1       7     .5000E+00
     2       9     .7500E+00

CONSTRAINTS
.FIXED
_constant head and flux boundaries
_token is +ve for fixed head and -ve for fixed flux
_number of fixed condition tokens
     2
_  No.   token    value
     1       1     .2400E+02
     2       2     .1500E+02

ITERATIONS
_maximum number of accuracy iterations
     8

HEADS
_output required of nodal data for following markers
_number of markers
     1
_list of markers
     3

DISCHARGE
_output required of discharge for following markers
_number of markers
     2
_list of markers
     1    2
STOP
```

Screen Output

```
perlis [hp-pa] 55% DFLOW < berry.dat
 Concrete Dam (Berry and Reid 3.2)

 MESH VITAL STATISTICS
 TIME         .0000E+00
 STAGE             1
 ITERATION         1

 *************************
 NODES              329
 SEGMENTS           895
 BANDWIDTH           13
 ELEMENTS           567
 ACCURACY %        21.7
 MEMORY USAGE       1.8
 *************************

 Concrete Dam (Berry and Reid 3.2)

 MESH VITAL STATISTICS
 TIME         .0000E+00
 STAGE             1
 ITERATION         2

 *************************
 NODES             1288
 SEGMENTS          3712
 BANDWIDTH           54
 ELEMENTS          2425
 ACCURACY %         6.4
 MEMORY USAGE      13.7
 *************************

 Concrete Dam (Berry and Reid 3.2)

 MESH VITAL STATISTICS
 TIME         .0000E+00
 STAGE             1
 ITERATION         3

 *************************
 NODES             2704
 SEGMENTS          7876
 BANDWIDTH           98
 ELEMENTS          5173
 ACCURACY %         3.4
 MEMORY USAGE      43.6
 *************************
 DISCHARGE/FLUX              -.3460E+01      .3460E+01
 DISCHARGE/FLUX               .3414E+01      .3414E+01
perlis [hp-pa] 56%
```

Head Potentials and Discharge Output

```
*****************************************************************
Concrete Dam (Berry and Reid 3.2)
TIME         .000000E+00
STAGE      1
ITERATION  3
*****************************************************************

 NODES             1666
 SEGMENTS          4805
 BANDWIDTH           79
 ELEMENTS          3140
 ACCURACY %         4.4
 MEMORY USAGE      22.9

*
*    NODAL VALUES
*

 MARKER    3

 NODE                7
 XCOORD      .6000E+02
 YCOORD      .7000E+01
 XVEL        .6486E+01
 YVEL       -.2594E+00
 HEAD        .1834E+02

*
*    CALCULATED DISCHARGES
*

 MARKER    1

 NO.        NODES        LENGTH         VELOCITY       DISCHARGE
   1       10    167      .8022E+00     -.4474E+00     -.3589E+00
   2      167    168      .5694E+00     -.4474E+00     -.2547E+00
   3      168    169      .5261E+00     -.3968E+00     -.2088E+00
   4      169    170      .5443E+00     -.3561E+00     -.1938E+00
   5      170    171      .5810E+00     -.3204E+00     -.1862E+00
   6      171    172      .6269E+00     -.2874E+00     -.1802E+00
   7      172    173      .6816E+00     -.2568E+00     -.1751E+00
   8      173    174      .7437E+00     -.2287E+00     -.1701E+00
   9      174    175      .8127E+00     -.2030E+00     -.1650E+00
  10      175    176      .8884E+00     -.1793E+00     -.1593E+00
  11      176    177      .9716E+00     -.1576E+00     -.1531E+00
  12      177    178      .1063E+01     -.1376E+00     -.1463E+00
  13      178    179      .1164E+01     -.1195E+00     -.1392E+00
  14      179    180      .1276E+01     -.1028E+00     -.1312E+00
  15      180    181      .1402E+01     -.8737E-01     -.1225E+00
  16      181    182      .1546E+01     -.7319E-01     -.1131E+00
  17      182    183      .1712E+01     -.6042E-01     -.1035E+00
  18      183    184      .1918E+01     -.4921E-01     -.9437E-01
```

19	184	185	.2169E+01	-.3936E-01	-.8538E-01
20	185	186	.2499E+01	-.3022E-01	-.7550E-01
21	186	187	.2945E+01	-.2227E-01	-.6559E-01
22	187	188	.3550E+01	-.1534E-01	-.5445E-01
23	188	189	.4551E+01	-.9920E-02	-.4515E-01
24	189	190	.6008E+01	-.5789E-02	-.3478E-01
25	190	1	.1045E+02	-.2796E-02	-.2921E-01

DISCHARGE PER UNIT WIDTH IS -.3445E+01

FLUX PER UNIT WIDTH IS .3445E+01

MARKER 2

NO.	NODES		LENGTH	VELOCITY	DISCHARGE
1	5	82	.5209E+01	.2950E-02	.1537E-01
2	82	81	.6828E+01	.4801E-02	.3278E-01
3	81	80	.4984E+01	.8155E-02	.4064E-01
4	80	79	.3866E+01	.1297E-01	.5014E-01
5	79	78	.3147E+01	.1917E-01	.6032E-01
6	78	77	.2655E+01	.2645E-01	.7023E-01
7	77	76	.2305E+01	.3482E-01	.8027E-01
8	76	75	.2032E+01	.4432E-01	.9005E-01
9	75	74	.1806E+01	.5492E-01	.9920E-01
10	74	73	.1627E+01	.6660E-01	.1083E+00
11	73	72	.1503E+01	.7936E-01	.1192E+00
12	72	71	.1395E+01	.9323E-01	.1301E+00
13	71	70	.1300E+01	.1082E+00	.1406E+00
14	70	69	.1216E+01	.1243E+00	.1511E+00
15	69	68	.1148E+01	.1413E+00	.1623E+00
16	68	67	.1092E+01	.1593E+00	.1740E+00
17	67	66	.1049E+01	.1781E+00	.1869E+00
18	66	65	.1024E+01	.1976E+00	.2025E+00
19	65	64	.1013E+01	.2177E+00	.2206E+00
20	64	63	.1025E+01	.2375E+00	.2435E+00
21	63	62	.1072E+01	.2571E+00	.2757E+00
22	62	61	.1192E+01	.2740E+00	.3265E+00
23	61	6	.1512E+01	.2864E+00	.4331E+00

DISCHARGE PER UNIT WIDTH IS .3413E+01

FLUX PER UNIT WIDTH IS .3413E+01

Graphical Output

The graphical output of finite element meshes, flow nets and nodal spacing plots have been combined in Figure 4.13.

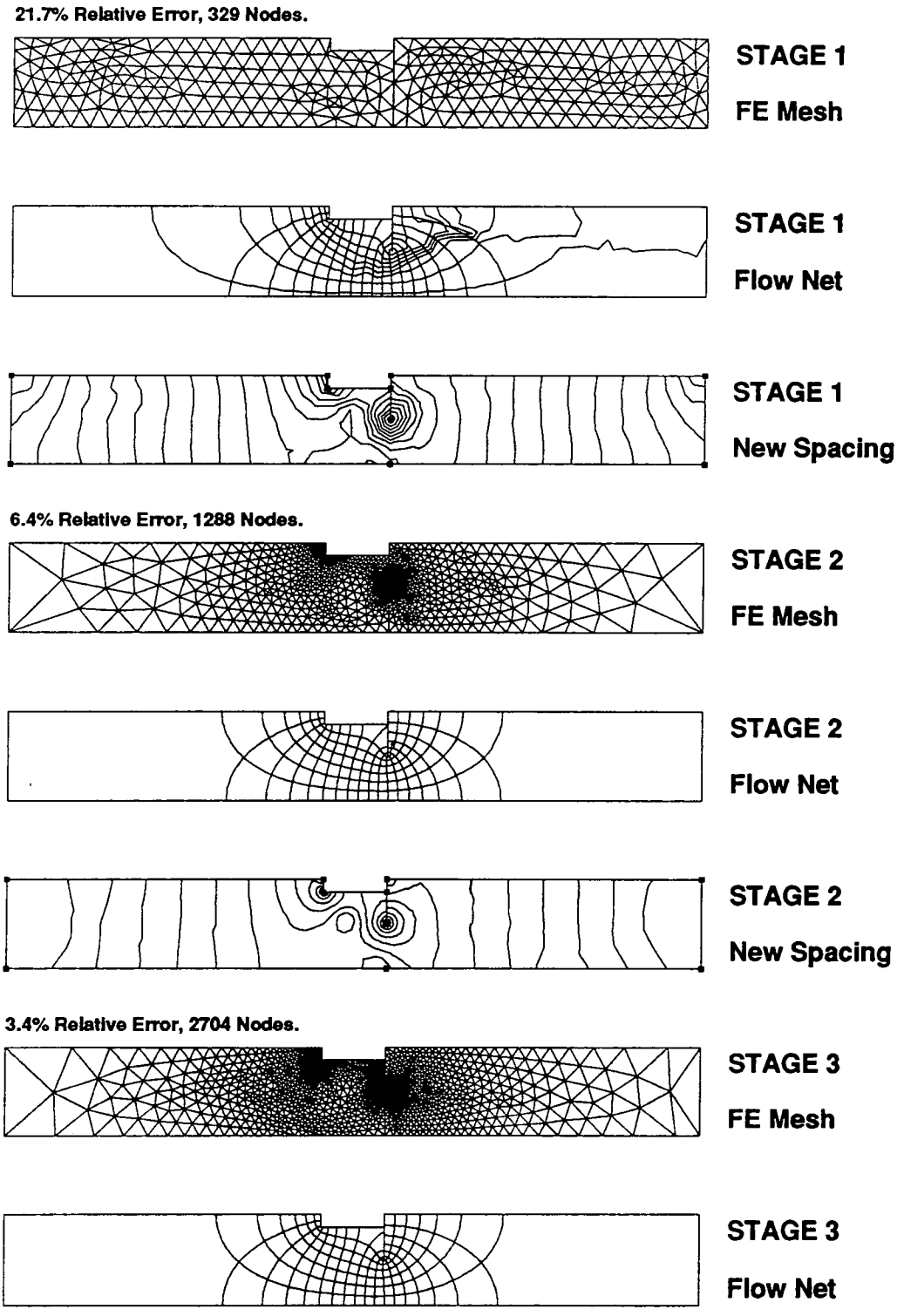

Figure 4.13 FE Solution for Flow Beneath a Concrete Dam and Cutoff

4.4.2. Free Surface Problem with Known Solution

This example demonstrates the use of DFLOW to solve a problem governed by Laplace's equation with a free surface. The problem, taken from Rank & Werner (1986), is not a standard groundwater hydrology problem. In order to check the accuracy of the error estimator, the left hand boundary condition has been fixed so that the exact solution is known (see Figure 4.14).

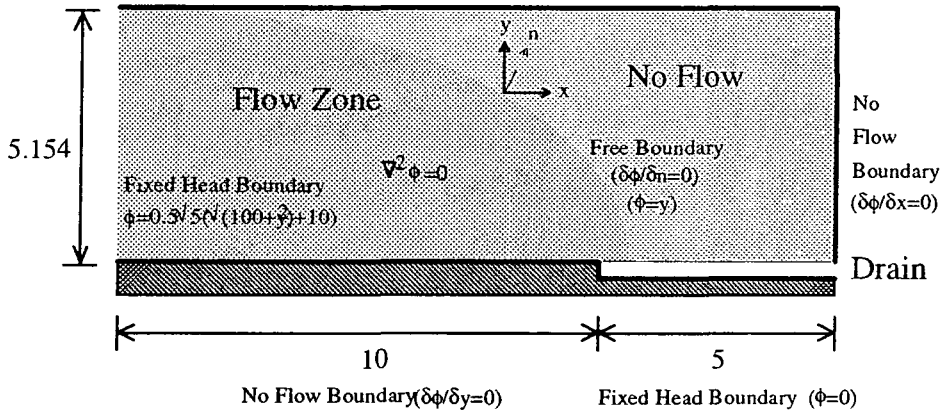

Figure 4.14 Free Surface Problem

(After Rank & Werner, 1986)

For this problem the solution for the potential function is:

$$\phi(x,y)=0.5\sqrt{5\left(\sqrt{x^2+y^2}-x\right)} \qquad \text{Eq. 4.2}$$

And the position for the free surface is given by:

$$y=\sqrt{1.25(1.25-2x)} \qquad \text{Eq. 4.3}$$

Minor adaptations to the program were made so that the left hand side boundary condition could be applied, and a close approximation of the true error obtained. The "true" error was calculated by integrating the squared differences between the FE solution for element gradients, and the true solution calculated at the nodes. The "true" error could not be obtained for all elements because first derivatives of the function cannot always be obtained (e.g. at the singularity). The error was ignored for these elements. The integration scheme is exact for quadratic functions. The measure of effectivity for the error estimator was calculated as the ratio of the estimated error and the "true" error.

The problem was first solved roughly using a coarse mesh (15% relative error) and the Taylor-Brown seepage line iteration scheme to ensure quick convergence. The

accuracy required was increased to 4% relative error to obtain a good solution. The problem was then solved with a fixed seepage line at different accuracies for both uniform (constant) and adaptive mesh spacings.

The plots obtained for these solutions are presented in Figures 4.15 and 4.16. The relative error is the estimated value using the recovered gradient. The "true" error may be obtained by dividing the quoted relative error by the effectivity. The adaptive meshes clearly show the advantage of concentrating elements close to the singularity (at the edge of the drain). The adaptive mesh using 71 nodes has almost the same accuracy as a uniform mesh of 930 nodes. An accuracy of 5% would be impossible to achieve with this program using a uniform mesh. Figure 4.17 shows the convergence rate for the global solution. The convergence rates for the uniform meshing (-0.28) and adaptive meshing (-0.44) are a reasonable match to the theoretical values (-0.25 and -0.5 respectively).

Uniform Meshing of a Free-Surface Problem with Singularity

(problem taken from Rank and Werner, 1986)

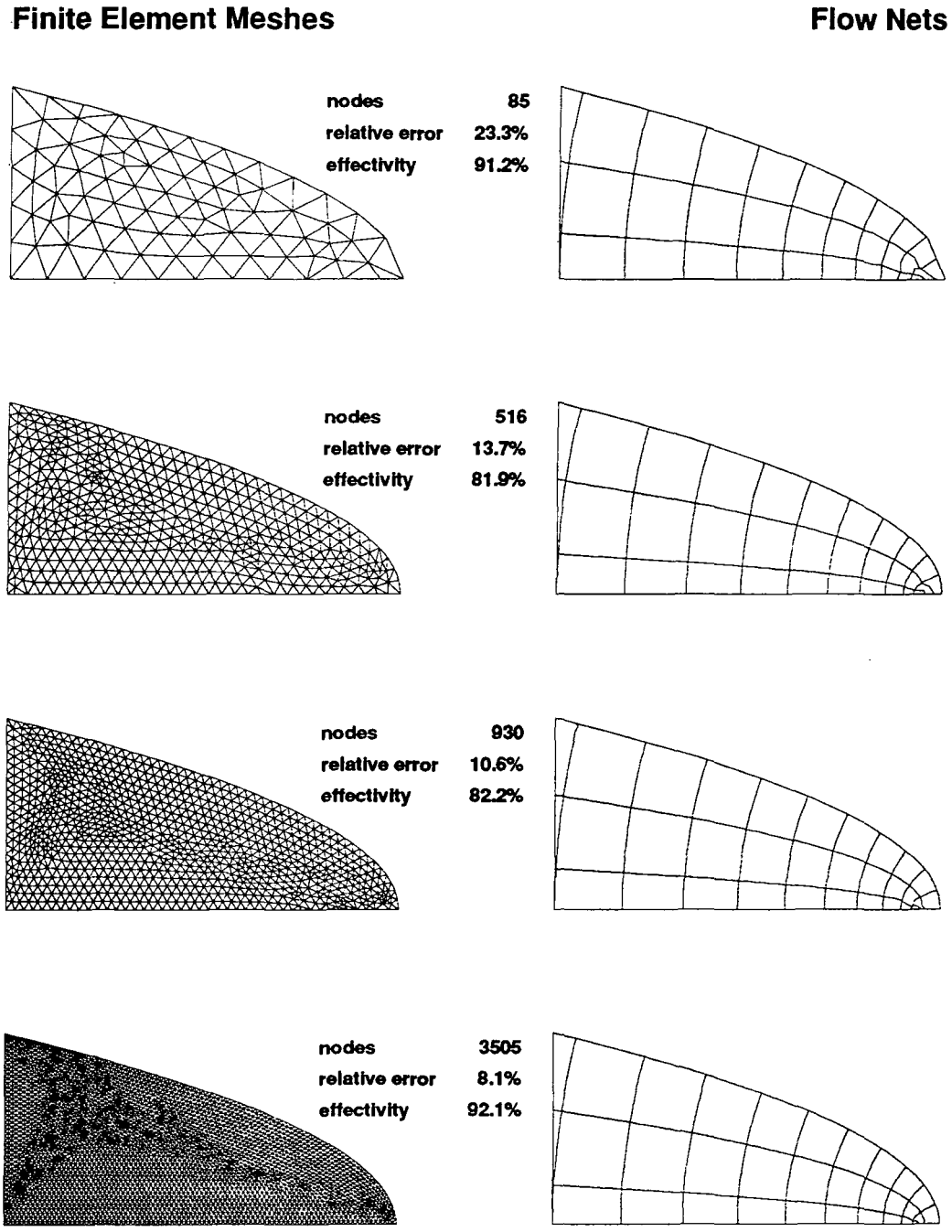

Figure 4.15 Uniform Meshing of a Free-Surface Problem with a Singularity

Adaptive Meshing of a Free-Surface Problem with Singularity

(problem taken from Rank and Werner, 1986)

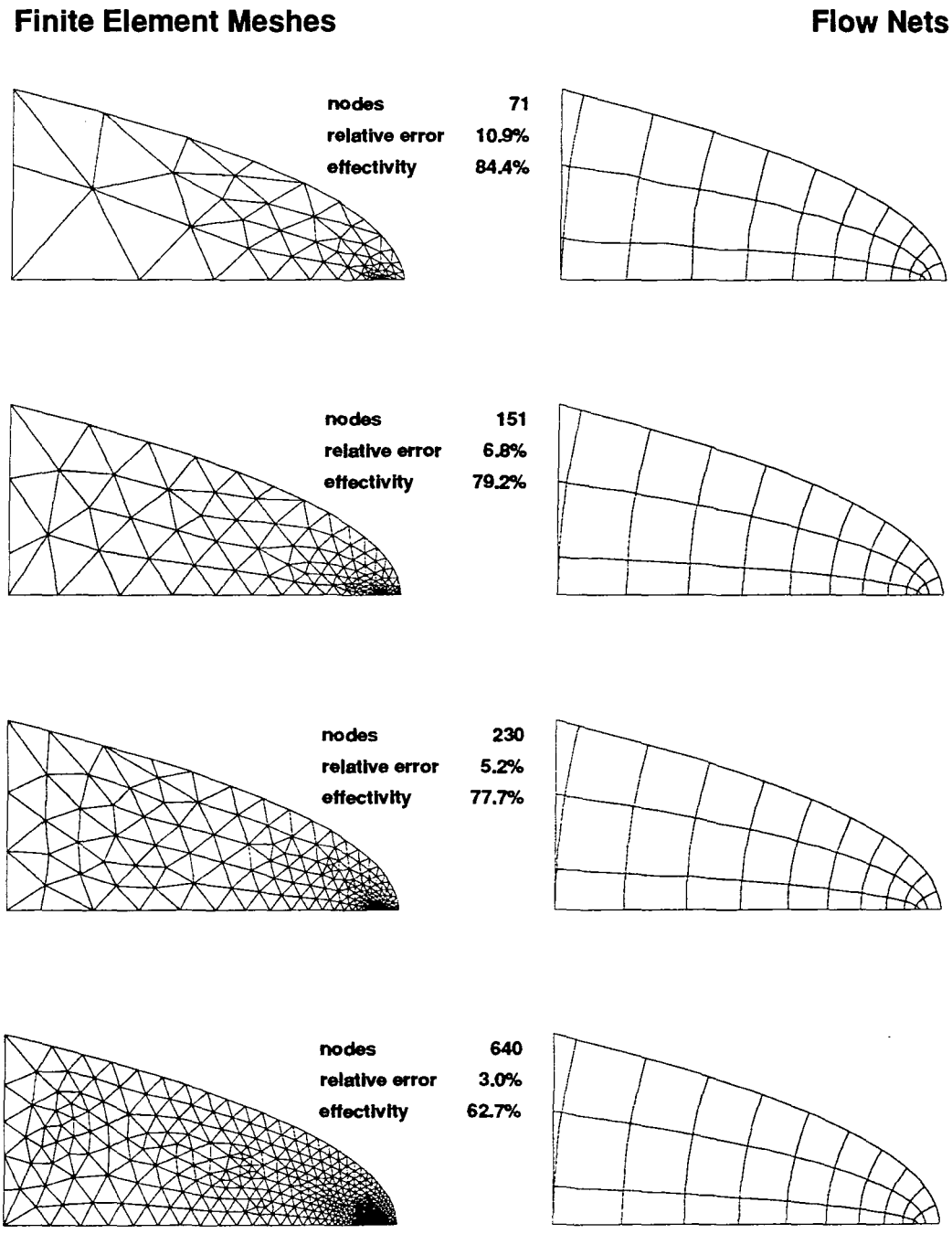

Figure 4.16 Adaptive Meshing of a Free-Surface Problem with a Singularity

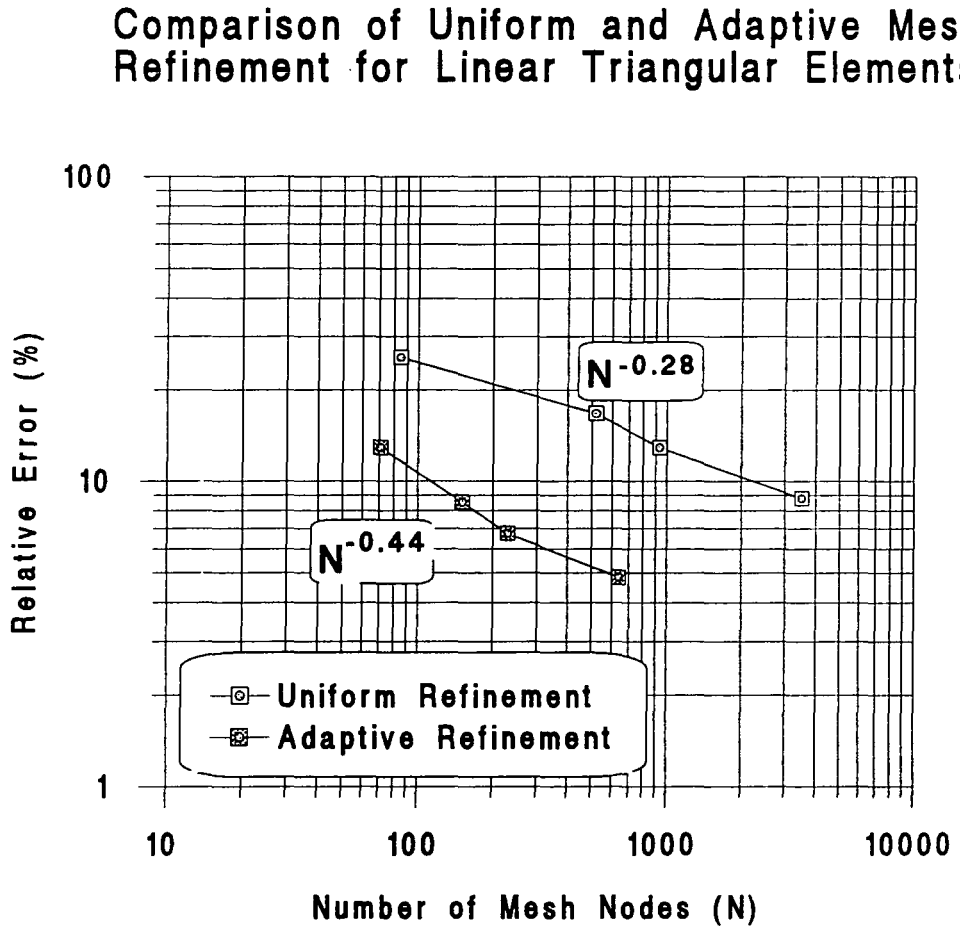

Figure 4.17 Comparison of Uniform and Adaptive Meshing

4.4.3. Transient Flow

Description of Problem

An example of transient flow conditions with a free surface is presented together with solutions from an analogue, finite difference method and another finite element program. The problem is taken from France et al (1971), and concerns the movement of the seepage line after the rapid drawdown of water in a field drain. Only half the problem need be solved because of the symmetry due to the presence of a second, parallel drain (see Figure 4.18).

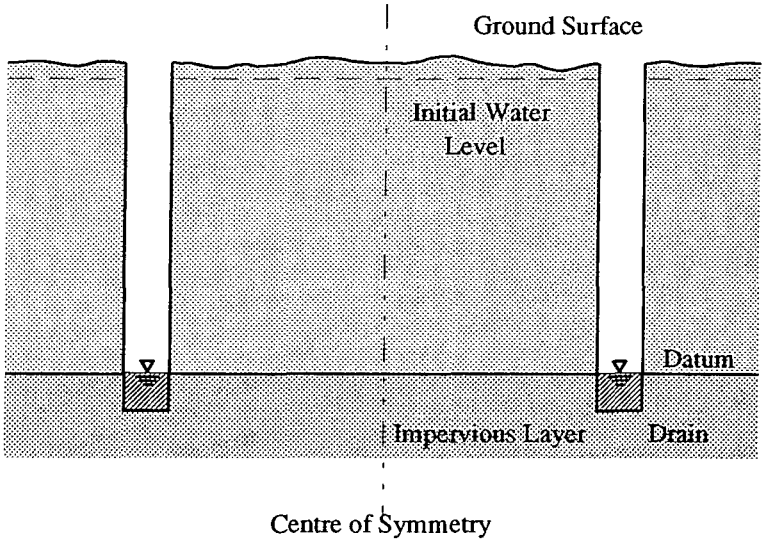

Figure 4.18 Rapid Drawdown Between Drains

(after France et al, 1971)

Data

```
TITLE
Sudden Drawdown (France '71)

ACCURACY
_   target        acceptable
      .4000E+01     .5000E+01
TIMES
_time periods, time steps and termination time
_time at simulation startup
_number of time periods
 .0
     4
_  No.        time step      end
     1      .2000E+01      .4000E+00
     2      .2000E+01      .2000E+01
     3      .2000E+01      .1000E+02
     4      .2000E+01      .1000E+05
```

```
POTENTIALS
.STAGES    plot final iteration in each stage
.NUMBER
_number of interior contours
    20

MESHES
.STAGES    plot final iteration in each stage

OUTPUT
.STAGES    plot final iteration in each stage

GEOMETRY
_mesh information for problem geometry
_tokens  control boundary conditions
_markers control data output

.NODES
_number of nodes
     4
_  No.   x-coordinate  y-coordinate   token    marker
     1     .0000E+00     .0000E+00       0    0
     2     .1328E+02     .0000E+00       2    0
     3     .1328E+02     .1970E+02      -1    0
     4     .0000E+00     .1970E+02      -1    0

.SEGMENTS
_number of segments
     4
_  No.     node pair    token    marker
     1       1    2        0    0
     2       2    3        2    2
     3       3    4       -1    3
     4       4    1        0    1

.LOOPS
_number of regions
     1
_number of nodes for region boundary
     5
_closed list of region nodes
     1    2    3    4    1

GRID
.CONSTANT
_single value over background mesh
    .2000E+01

POROSITY
.CONSTANT
_single value over background mesh
    .1315E+02

CONSTRAINTS
```

```
.ELEVATION
_head equal to node elevation
_number of elevation tokens
     2
_  No.    token
     1        1
     2        2

STAGES
_maximum number of movement stages
     180

ITERATIONS
_maximum number of accuracy iterations
     4

DISCHARGE
_output required of discharge for following markers
_number of markers
     3
_list of markers
     1    2    3

FREE SURFACES
_control meshing to a set of ordered points
_mesh nodes are interpolated between list points
_number of free surfaces
     1

.FLOW
_set next y-coordinates according to flow velocities
.POINTS
_define points along free surfaces
_number of surface, number of points
     1                   2
_  No.        x-coordinate  y-coordinate
     1          .1328E+02     .1970E+02
     2          .0000E+00     .1970E+02

.ENDS
_define properties of free surface ends
_number of free surface (-ve sign allows movement)
    -1
_  node  token  /first node (counter-clockwise)
     3      -1
_  node  token  /last  node
     4      -2

.VECTORS
_define bounding vectors confining end point movement
_number of vectors
     2
_  No.          x1             y1           x2           y2
     1       .1328E+02    .2000E+02    .1328E+02    .0000E+00
     2       .0000E+00    .2000E+02    .0000E+00    .0000E+00
```

```
INTERPOLATION
_free surface movement prescribed by interpolation through
_points using a weighted least squares best fit polynomial
_movements of the free surface end points are smoothed using
adjustment factors
_no. points  polynomial order (1=linear)
     3                  1
_weights ordered from seepage point
    .0000  1.0000  1.0000
_adjustments for points above
   1.0000   .0000   .0000
STOP
```

Solution

The flow nets obtained from DFLOW are reproduced in Figure 4.19. A rough sketch of the seepage line positions has been superimposed on the solutions given in France et al (1971) in Figure 4.20. The Szabo & McCaig solution was calculated using a finite difference program. The exact character of the analogue solution was not specified, but it would appear to be from a physical flow model.

The results from DFLOW are certainly close to those of all the other methods. In the upstream portion the predicted seepage line position is closest to the analogue model. In the downstream portion DFLOW gives results closest to France's finite element solution.

4.5. Recommendations for Future Development

Some of the simpler modifications considered, but not implemented, are listed here:

- Allow lateral movement of seepage line using Taylor-Brown adjustment.
- Allow breaks in cubic B-spline derivatives at permeability interfaces to allow the development of sharp changes in seepage line gradient.
- Specification of seepage exit condition (tangential or normal).
- Variation in requested accuracy between stages.
- Extension to axisymmetric problems.
- Accretion on free surface.
- Check input data for compatibility.
- Partial mesh adjustment between iterations to cut down cost of regenerating mesh.
- Graphical interface to improve productivity.

Rapid Drawdown Between Symmetrical Drains Problem

(Example taken from France et al, 1971)

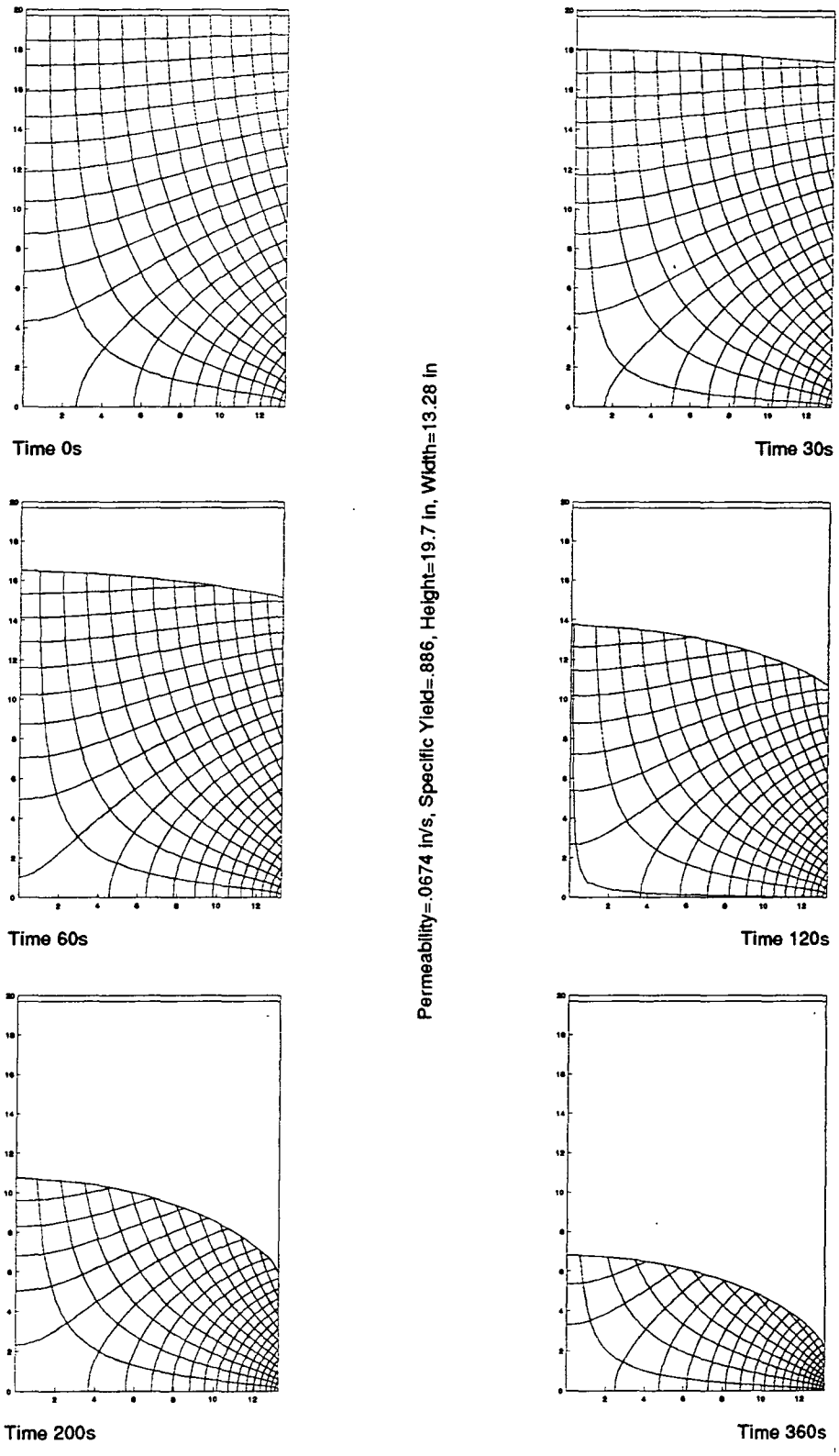

Figure 4.19 DFLOW Rapid Drawdown Between Symmetrical Drains

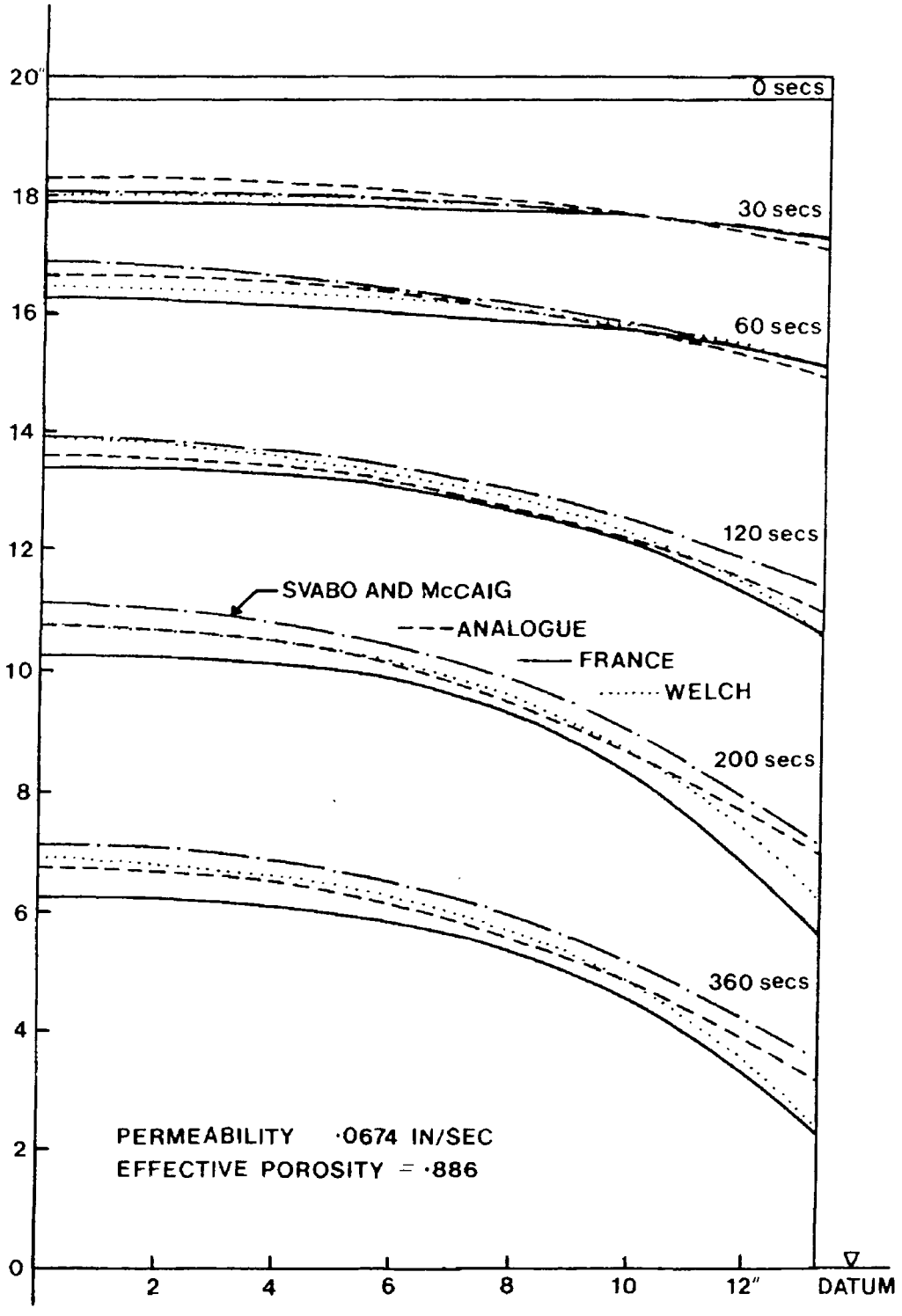

Figure 4.20 France Rapid Drawdown Between Symmetrical Drains (taken from France et al, 1971)

Chapter 5
Results and Analysis

An object of this project is to ascertain which factors are responsible for the low phreatic surface within a tailings dam. Three factors are considered:

- Permeability
- Dam geometry
- Transient flow development

Naturally these factors cannot be considered in isolation, but by varying just one or two at a time, general conclusions are obtained as to the relative importance of each factor. The FE analyses are broken down into more or less self-contained sections which deal with a separate well-defined problem:

A) Steady state analysis of flow through a rectangular cross-section earth dam. Both the height/length ratio and the influence of varying permeability are examined.

B) Steady state analysis of a homogeneous and isotropic earth dam. The influence of upstream and downstream slope angles and crest width is investigated.

C) Steady state analysis of an idealized tailings dam geometry. Conditions of inhomogeneous and anisotropic permeability are considered.

D) Miscellaneous steady state examples concerning foundation permeability and depth of foundation, together with results for a tailings dam with toe drain.

E) Transient water flow in a dam upon a sudden filling of the pond or reservoir. The analysis considers upstream slope angle (including tailings dam geometry), permeability, effective porosity, and dam height.

F) Transient flow in a tailings dam with an increasing depth of tailings. Again, the analysis considers permeability, effective porosity and dam height.

The FE results are checked for self consistency and against alternative analytical solutions (where appropriate). This provides a check on the FE program and enables the verification or otherwise of the simplifying assumptions used in the analytical methods.

5.1. Analysis of Flow in a Rectangular Dam of Variable Permeability

Water flow in a dam of rectangular cross-section is a much studied problem because it is amenable to an analytical solution. Analytical solutions for the problem are available in any good textbook such as Harr (1962; pp. 40-42) and De Wiest (1965; pp. 233-237). Classically, the problem considered is an isotropic and homogeneous dam based on an impervious foundation. Also considered here is a dam in which the permeability is isotropic but varies in the direction of flow. Solutions for flow through a tailings dam frequently involve such an arrangement (Kealy & Busch, 1971).

5.1.1. Analytical Solution of a Homogeneous Rectangular Dam

The well-known method of solving this problem is Dupuit's solution, in this case without tailwater. Consider the rectangular dam of Figure 5.1.

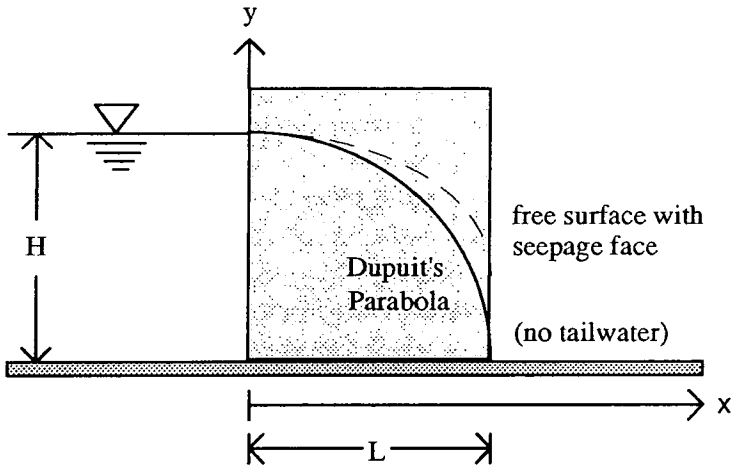

Figure 5.1

The Dupuit-Forchheimer assumptions state that if the seepage line is nearly horizontal, then it can be assumed that there will be no flow of water in the vertical direction. The consequences of this assumption are that the potential gradient must be constant in any vertical column. The potential gradient on the seepage (zero pressure) line is equal to the slope, and so combining these assumptions with Darcy's Equation:

$$q = ky\frac{\delta y}{\delta x} \qquad \text{Eq. 5.1}$$

where q is the discharge through a vertical cross-section of the dam in m^3s^{-1} per metre width, and k is the permeability in ms^{-1}. Assuming that permeability is constant, Equation 5.1 may be integrated between the limits $0 \le x \le L$ and $0 \le y \le H$:

$$q = \frac{kH^2}{2L} \qquad \text{Eq. 5.2}$$

where H and L are the dimensions in metres of the height of water in the dam and the length of dam, respectively (see Figure 5.1). Equation 5.2 gives the discharge through a rectangular dam without tailwater and with constant permeability. It is well known that Dupuit's equation is an exact solution for the discharge in this problem (De Wiest, 1965).

Unfortunately, the equation does not predict the height of the seepage exit point on the downstream seepage face; in fact the form of the free surface "Dupuit's Parabola" exits at $y=0$ with no seepage face at all. Polubarinova-Kochina (1962, p. 292) presented a chart of seepage exit point height for different dam height (H) to length (L) ratios and different depths (h) of tailwater (see Figure 5.2). This chart was based on an approximate analytical solution of the differential equations and was claimed by Polubarinova-Kochina to be very accurate for the case without tailwater.

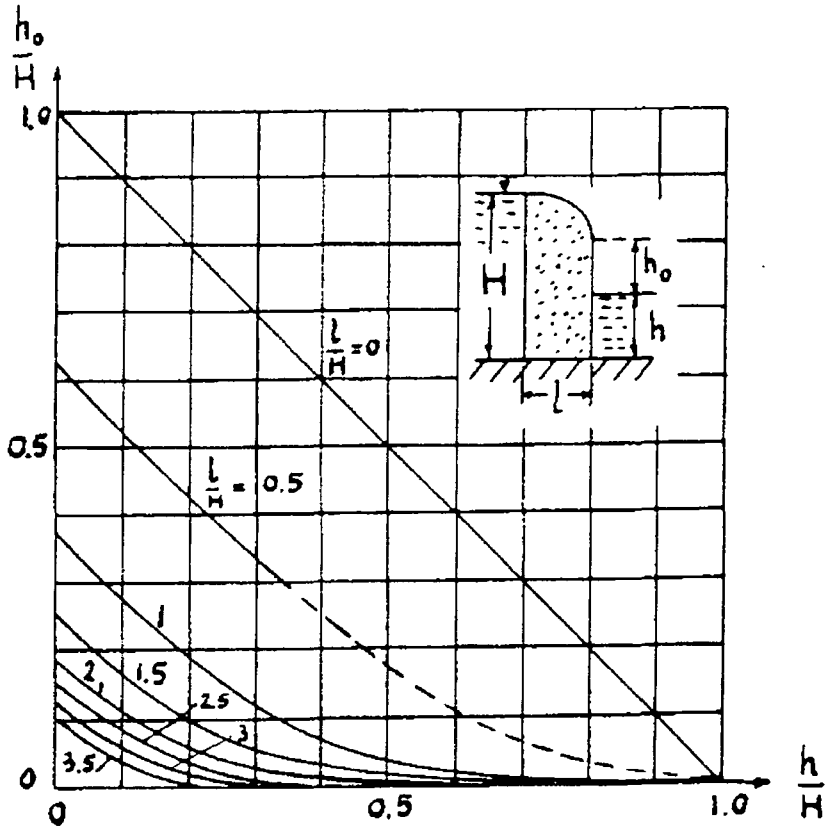

Figure 5.2 Chart of Exit Point Height for a Rectangular Dam
(after Polubarinova-Kochina, 1962)

5.1.2. Analytical Solution for a Horizontally Inhomogeneous Rectangular Dam

In a tailings dam, the permeability may vary by as much as 2 orders of magnitude in the horizontal direction (Abadjiev, 1976) (see Chapter 2). Abadjiev used the Dupuit solution to study flow through a tailings dam with exponentially changing values of permeability:

$$k(x) = k_0 e^{-ax} \qquad \text{Eq. 5.3}$$

where $k(x)$ is the permeability function, k_0 is the permeability at the top of the beach, and a is a variable dependent on the material properties of the tailings. Although the choice of an exponential function fits in with sedimentary theory for deposition on a beach, the use of such a function adversely affects the generality of the solution. It is common in groundwater hydrology for only the relative permeability to be important in determining the steady state position of the seepage line. Problems may be solved for a particular ratio of permeabilities and the solution is general; a simple scalar multiplication by the actual permeability transforms the quantity of discharge to the problem in question. Equation 5.3 depends on the measured properties of the tailings dam. If a particular embankment is being investigated, it makes sense to use the permeability distribution as measured. In view of the lack of precision in both the measurement and the true variation of tailings permeability, it is reasonable to model the permeability as a linear function of distance for the general case. This is easier to program and interpret, and is certainly no worse than making the common assumption that the dam may be split into a few zones in which the permeability is constant.

If it is assumed that the permeability is a linear function of x, then the variation in permeability is:

$$k(x) = k_1 + \frac{x}{L}(k_2 - k_1) \qquad \text{Eq. 5.4}$$

where k_1 and k_2 are the permeabilities in ms^{-1} on the upstream and downstream sides of the dam respectively.

Combining Equations 5.1 and 5.4:

$$\frac{q}{k_1 + x(k_2 - k_1)/L}\,\delta x = y\,\delta y \qquad \text{Eq. 5.5}$$

Integrating between the limits $0 \le x \le L$ and $0 \le y \le H$:

$$q = \frac{H^2}{2L}\,\frac{(k_2 - k_1)}{\ln k_2 - \ln k_1} \qquad \text{Eq. 5.6}$$

5.1.3. Numerical Results

Results are listed in Tables 5.1 and 5.2 for the FE solution of the flow through a rectangular dam with four different height/length ratios, and eleven different permeability ratios. All the FE solutions are calculated to a high level of numerical accuracy (less than 5% relative error). The iterative scheme to calculate the position of the seepage line used an artificial time stepping method similar to that of France et al (1971).

The position of the seepage exit point is independent of the actual permeability involved. To obtain the height of the seepage exit point, one should multiply the value obtained from the graph by the real height of the pond (H). The seepage depends on both the real height of the dam and the permeability. The values of L used in the FE analysis have been scaled by dividing the length of the dam (l_x) by the height (l_y). To obtain a value for the seepage discharge one should multiply the value from the graph by both the real height of the dam and the **permeability of the upstream face of the dam**. This is because k_1 has been set to 1 ms^{-1} in the FE data (the ratio of k_2/k_1 is in fact k_2).

The seepage line graphs for each simulation are plotted separately for each dam geometry to allow easy comparison (Appendix 1). These are followed by graphs for the seepage discharge and seepage exit height. Permeability is plotted on a $\log_{10}$ scale in both cases to linearize the data and obtain "well behaved" graphs. The seepage line graphs show that the steady state seepage line plunges more when the permeability is increasing in the direction of flow. The head loss within the dam is greatest per unit length in the relatively low permeability upstream zone. The slope of the seepage line is roughly equal to the hydraulic gradient (Dupuit's assumption), and so the slope of the

seepage line is higher in the upstream zone and lower in the downstream zone compared with the homogeneous case.

Values of seepage discharge and exit height calculated by the FE program are plotted in Table 5.1 and 5.2

Rectangular Dam - Variable Hydraulic conductivity Seepage discharge per unit width/($K_{x1}l_y$)				
K_{x2}/K_{x1}	Ratio of Length to Height l_x/l_y			
	0.5	1.0	2.0	4.0
0.02	-0.248	-0.125	-0.062	-0.031
0.05	-0.316	-0.158	-0.079	-0.040
0.1	-0.390	-0.195	-0.097	-0.049
0.2	-0.497	-0.249	-0.124	-0.062
0.5	-0.721	-0.361	-0.180	-0.090
1.0	-1.00	-0.500	-0.250	-0.125
2.0	-1.44	-0.720	-0.360	-0.179
5.0	-2.48	-1.24	-0.621	-0.311
10.0	-3.91	-1.95	-0.983	-0.487
20.0	-6.33	-3.19	-1.59	-0.798
50.0	-12.5	-6.21	-3.11	-1.56

Table 5.1 Seepage Discharge for a Horizontally Inhomogeneous Rectangular Dam

Rectangular Dam - Variable Hydraulic conductivity Seepage Exit Point				
K_{x2}/K_{x1}	Ratio of Length to Height l_x/l_y			
	0.5	1.0	2.0	4.0
0.02	0.882	0.782	0.656	0.516
0.05	0.849	0.720	0.560	0.396
0.1	0.816	0.658	0.472	0.300
0.2	0.772	0.582	0.375	0.214
0.5	0.699	0.462	0.256	0.131
1.0	0.632	0.368	0.185	0.092
2.0	0.557	0.283	0.136	0.067
5.0	0.452	0.199	0.094	0.047
10.0	0.377	0.155	0.075	0.036
20.0	0.310	0.126	0.060	0.030
50.0	0.239	0.098	0.047	0.024

Table 5.2 Seepage Exit Height for a Horizontally Inhomogeneous Rectangular Dam

The following trends are evident in the FE results:

I. Longer dams have lower seepage exit points (shorter seepage faces).

II. Increasing downstream permeability depresses the seepage line.

III. Decreasing downstream permeability raises the seepage line.

IV. Seepage lines are convex upwards when $k_1 \geq k_2$.

V. Seepage lines are concave upwards when k_2/k_1 lies above some critical value which is dependent on the dam height to length ratio.

In the shortest dam, all the seepage lines are convex upwards, but the trend suggests that there is some ratio of permeability $k_2 >> k_1$ where the seepage line will be concave. As the dam height to length ratio decreases, the tendency for the seepage line to become concave upwards increases when $k_2 > k_1$.

5.1.4. Comparison of Analytical and Numerical Results

The values of seepage discharge for the homogeneous dams in Table 5.1 exactly match those predicted by Equation 5.2. The seepage line exit heights for homogeneous rectangular dams are in close agreement with those predicted by the analytical solution of Figure 5.2.

The remaining 40 values of seepage discharge ($k_1 \neq k_2$) are compared with the analytical solution using a regression technique. It is assumed that Equation 5.5 is inexact and two parameters a and b are sought which minimize the sum of least-squares of the difference between this new equation and the data:

$$q = a\left[\frac{H^2}{2L}\frac{(k_2 - k_1)}{\ln k_2}\right] + b \qquad \text{Eq. 5.7}$$

The regression analysis was performed using NONLIN1.2, a shareware program used to perform nonlinear least squares regression analysis (Sherrod, 1992). For a total of 40 points, the coefficient of multiple determination is 0.999988 for a=0.997258 and b=0.000970338.

Figure 5.3 and 5.4 show the relationship between the seepage exit height and the discharge/permeability ratio (for homogeneous and inhomogeneous dams). For low ratios of discharge/permeability (less than 1.0) Figure 5.4 shows a fairly linear relationship. However, for the dams with a high discharge/permeability ratio, the data diverge. The regression statistics for a straight line fit are given in Table 5.3. In the

first case all the data points are included, for the second only data with a ratio of discharge to permeability equal to or lower than 1.0 are included.

Regression Statistics for the Rectangular Earth Dam
Seepage Discharge/Permeability and Seepage Exit Height Relationship

$$\frac{q}{k_{x2}} = aH$$

Number of Points	a	Standard Error	Average Deviation	Maximum Deviation	r^2
44	1.09	0.25	0.18	0.88	0.9877
25*	1.28	0.035	0.026	0.11	0.9994

*** points with q/k> 1.0 omitted.**

Table 5.3 Regression Statistics for a Rectangular Earth Dam

Both regression models have very high coefficients of multiple determination, despite the obvious discrepancy in the visual match. The lower the dam's length and upstream to downstream permeability ratio, the greater the deviation away from the general trend. The seepage exit heights are discussed in a later section where they are compared with data from other analyses.

5.1.5. Conclusions

The FE program gives the exact solution (to a reasonable level of accuracy) for the analysis of flow through a rectangular dam with permeability varying in the direction of flow. The results of this analysis imply that steady state solutions using this program can be very reliable.

As predicted by Kealy & Busch (1971) and Abadjiev (1976), an increasing permeability in the direction of flow may be responsible for the concave seepage line found in tailings dams. Long seepage lines are influenced more than short seepage lines for the same permeability ratio. This suggests an added benefit for the maintenance of a long tailings beach.

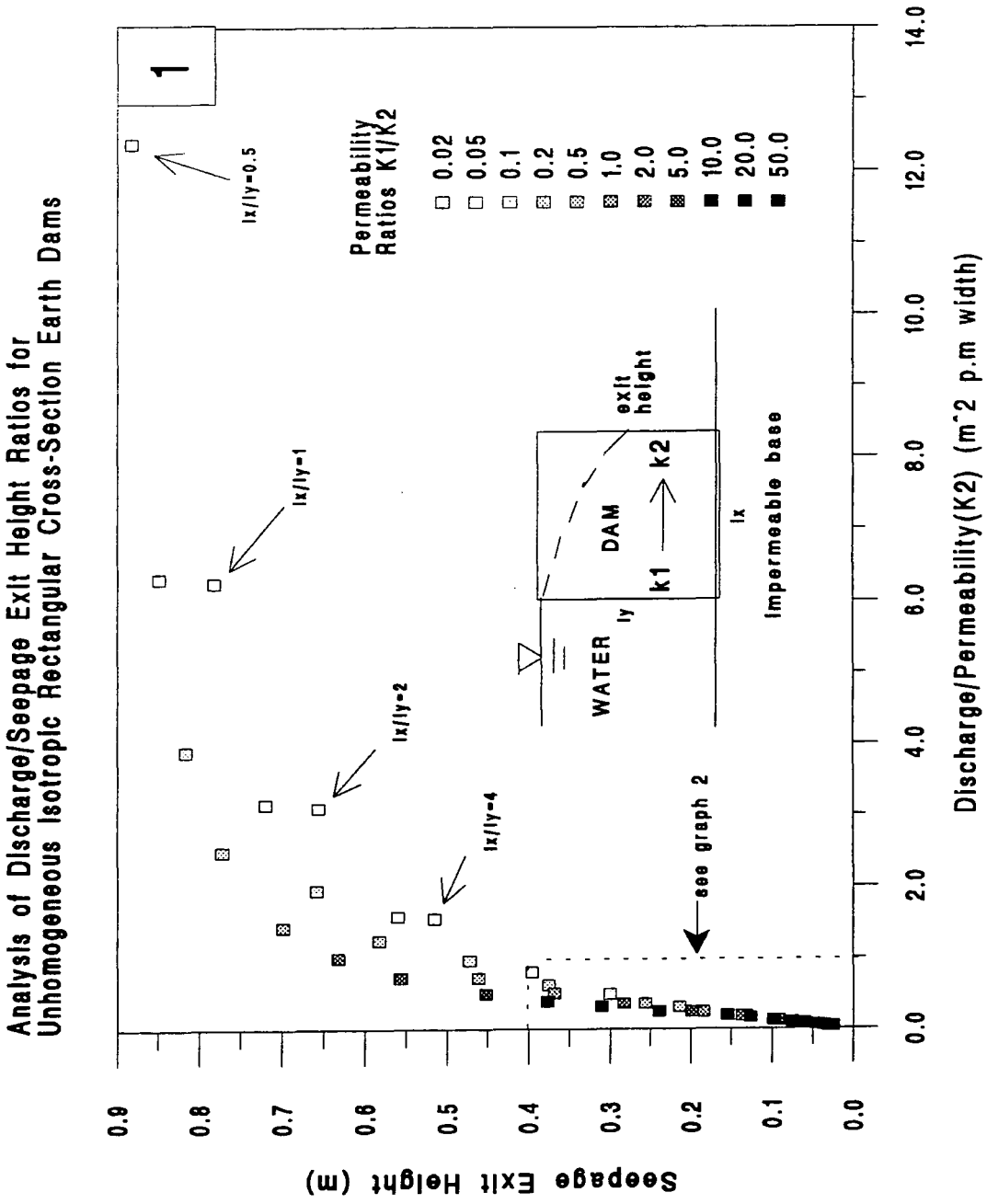

Figure 5.3 Analysis of Discharge/Seepage Height for a Rectangular Dam (1)

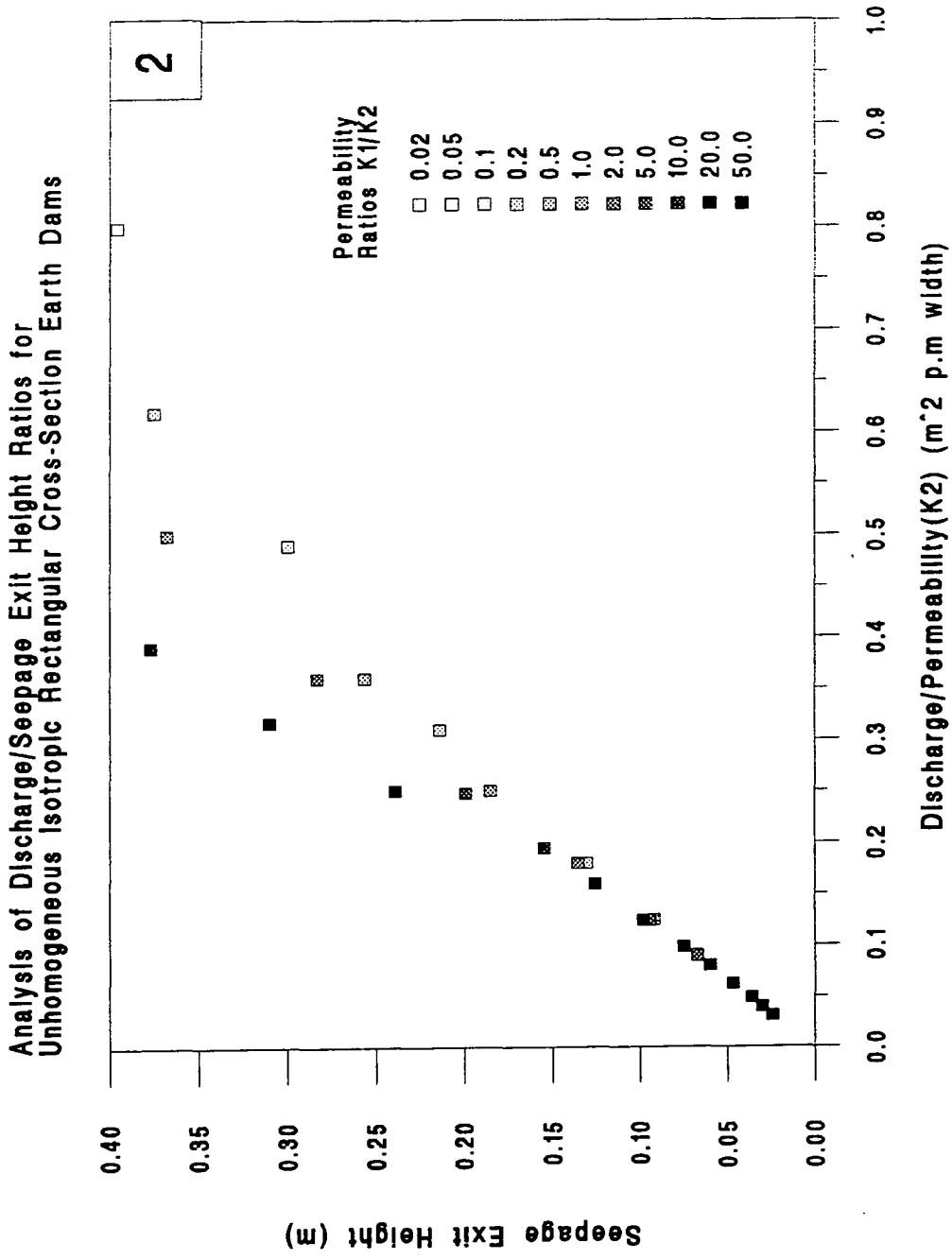

Figure 5.4 Analysis of Discharge/Seepage Height for a Rectangular Dam (2)

5.2. Steady State Flow Through a Homogeneous and Isotropic Earth Dam

The preceding analysis of the rectangular earth dam took no account of the influence of either the upstream or downstream slope angle on the position of the seepage line. The object of this section is to investigate a series of different dam geometries to take these factors into account. The dam to be considered is homogeneous and isotropic, and once again the foundation is considered impervious to flow (see Figure 5.5).

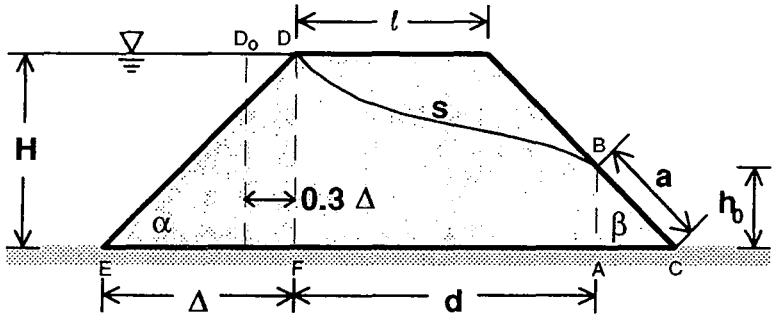

Figure 5.5 Cross-section Through an Idealized Earth Dam

5.2.1. Analytical Solution

Three analytical solutions to the problem posed in Figure 5.5 are common in the literature (Harr, 1962; De Wiest, 1965; Polubarinova-Kochina, 1962; Raudkivi & Callender, 1976):

(a) Schaffernak (and independently, van Iterson)

(b) Casagrande

(c) Pavlovsky.

These solutions are constructed by dividing the dam into two or more sections in which simplifying assumptions are used to approximate the flow conditions. The flow between sections is matched (conservation of mass), and an equation obtained for the seepage discharge and seepage line exit point.

The methods used by Schaffernak and Pavlosky are based on Dupuit's assumptions that

(i) vertical flow may be neglected, and

(ii) the hydraulic gradient is equal to the slope $\delta y/\delta x$ of the seepage line.

For the saturated toe of the dam (see Figure 5.5),

$$q = ky\frac{\delta y}{\delta x} = kh_0 \tan\beta \qquad \text{Eq. 5.8}$$

where q is the seepage discharge (in m^3s^{-1} per unit width) and k is the permeability (in ms^{-1}). Equation 5.8 is obviously deficient for steep downstream slope angles because $\tan(\alpha)$ becomes very large.

Taking exception to Dupuit's second assumption, Casagrande set the hydraulic gradient equal to $\delta y/\delta s$, where s is measured along the seepage line. Hence for seepage in the toe,

$$q = ky\frac{\delta y}{\delta s} = kh_0 \sin\beta \qquad \text{Eq. 5.9}$$

Casagrande used an *ad hoc* method of extending the length of the section of the dam considered (***d***) in order to take account of the upstream dam slope. His solution is to add 3/10ths of the base below the slope (0.3Δ; see Figure 5.5) to the value of ***d*** used in the equation. Of course this approximation can also be applied to Schaffernak's method. Schaffernak and Casagrande complete their methods by integrating Equations 5.8 and 5.9 respectively, between appropriate limits (where S is the distance measured between B and D_0).

Schaffernak's solution

$$a = \frac{d'}{\cos\beta} - \sqrt{\frac{d'^2}{\cos^2\beta} - \frac{H^2}{\sin^2\beta}}$$

$$d' = d + 0.3\Delta \qquad \text{Eq. 5.10}$$

$$q = ka \sin\beta \tan\beta$$

$$a = S - \sqrt{S^2 - \frac{H^2}{\sin^2 \beta}}$$

Casagrande's solution Eq. 5.11

$$q = ka \sin^2 \beta$$

Pavlovsky chose to convert the curvilinear streamlines (*a-b*) of the upstream section (EFD) into equivalent horizontal flow tubes (*c-b*) (see Figure 5.6). The dividing boundary section between the upstream and central portion of the dam is arbitrarily taken to be the perpendicular dropped from the actual dam crest to the base (DF). Pavlovsky used the Dupuit solution for the central portion of the dam (ABDF) and Equation 5.8 for the dam toe (ACB). The equations for the three sections are combined to obtain the solution. The Pavlovsky method cannot readily be compared with the numerical results (or indeed Schaffernak's or Casagrande's method) because of the arbitrary choice of position for DF.

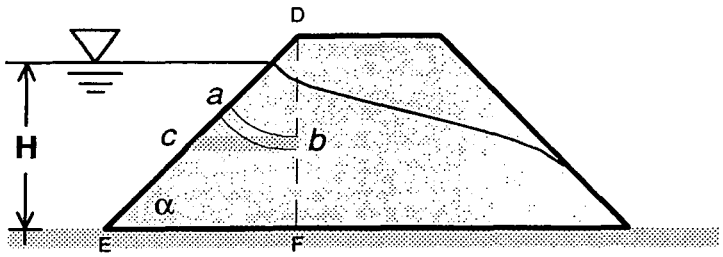

Figure 5.6 Pavlovsky's Solution for the Flow Through an Earth Dam
(adapted from Harr, 1962)

The method by which these three solutions take into account the upstream slope make them inappropriate for low values of α. Raudkivi & Callender (1976) also recognised the inability of the methods to cope with a high angle for the downstream slope β. The numerical method has little trouble dealing with such geometrical difficulties.

5.2.2. Numerical Solution

The problem considered in the FE solution is identical to that described for the analytical solutions, but the range of slope angles is less restricted. Each dam is scaled with respect to the height of the saturated portion of dam (h_0) and permeability (k). The results of the FE program are presented in Table 5.4. The data have been scaled by a factor of 1000 in order to make the table more readable. Plots of seepage discharge and seepage line exit height for each of the geometries considered are also presented in Appendix 2 for easy comparison. Values chosen for the upstream slope angle α are 0, 15, 30, 45, 60, 75 and 90 degrees. An angle α of zero degrees represents an idealized tailings dam with a horizontal pond-dam interface. In this case, the upstream boundary stretches 5 times the height of the dam. This arbitrary choice of a distance for the "far" boundary was justified on the basis of the flow net results. The values chosen for the downstream slope β are 15, 30, 45, 60, 75 and 90 degrees. For each value of α and β, different crest lengths ℓ are considered. In this context ℓ is measured horizontally from the seepage entry point (D) to the downstream slope (see Figure 5.5). The FE analyses were all solved with a relative error of less than 5% or better. In order to obtain the appropriate values of seepage discharge and seepage exit height from the tabulated values, the following transformations should be used:

$$h_e = h_0 H$$
$$q_d = qkH \qquad \text{Eq. 5.12}$$

where h_e is the seepage line exit height (in metres), h_0 is the exit height read from the table, H is the height of the earth dam (in m), q_d is the seepage discharge (m^3s^{-1} per metre width), q is the seepage discharge from the table and k is the permeability (in ms^{-1}).

Plots of the seepage lines are in Appendix 2. The slope angle and crest length have a direct influence on the position of the seepage line. The seepage line enters the dam at an angle perpendicular to the upstream slope (for slope angles between 0 and 90 degrees). For a low upstream slope angle, the seepage line is directed at a steep downwards angle, whereas for a high upstream angle the seepage line is nearly horizontal. This result is well known (e.g. Casagrande, 1940) but is still significant because it confirms the program's ability to model the flow in the upstream portion of the dam. According to Kealy & Busch (1971), the upstream slope angle is particularly important in the case of the tailings dam geometry.

Finite Element Seepage Line Exit Height and Seepage Discharge

Exit Height*1000/Dam Height
0.5 Crest/Dam Height Ratio

β \ α	90	75	60	45	30	15	0
90	630	557	497	447	409	377	354
75	608	539	481	441	408	383	360
60	600	540	485	451	423	400	381
45	607	551	509	476	452	432	415
30	623	580	547	522	496	485	468
15	681	644	616	595	572	561	543

Exit Height*1000/Dam Height
1.0 Crest/Dam Height Ratio

β \ α	90	75	60	45	30	15	0
90	360	330	295	276	261	254	242
75	367	336	312	294	277	266	255
60	387	363	336	320	309	298	287
45	413	389	367	349	337	322	316
30	463	440	423	410	399	394	382
15	548	532	515	489	478	471	453

Exit Height*1000/Dam Height
2.0 Crest/Dam Height Ratio

β \ α	90	75	60	45	30	15	0
90	181	173	164	155	151	144	141
75	204	188	186	180	172	168	160
60	225	222	216	204	198	195	190
45	261	251	242	236	238	232	227
30	317	305	302	297	287	284	279
15	415	405	393	392	388	387	384

Exit Height*1000/Dam Height
4.0 Crest/Dam Height Ratio

β \ α	90	75	60	45	30	15	0
90	086						
75	105						
60	124						
45	154						
30	192						
15	292						

Seepage Discharge per unit width
(*1000/Permeability/Dam Height)
0.5 Crest/Dam Height Ratio

β \ α	90	75	60	45	30	15	0
90	1000	778	661	586	533	493	457
75	708	588	518	469	435	408	383
60	530	459	415	384	360	341	323
45	398	355	328	308	292	280	268
30	282	259	243	232	222	215	208
15	163	153	147	142	138	134	131

Seepage Discharge per unit width
(*1000/Permeability/Dam Height)
1.0 Crest/Dam Height Ratio

β \ α	90	75	60	45	30	15	0
90	500	443	400	375	355	337	323
75	405	367	340	319	304	292	280
60	336	309	289	274	263	253	244
45	273	255	240	230	222	214	208
30	209	198	189	183	177	173	168
15	132	127	123	119	116	114	111

Seepage Discharge per unit width
(*1000/Permeability/Dam Height)
2.0 Crest/Dam Height Ratio

β \ α	90	75	60	45	30	15	0
90	254	235	225	214	210	202	197
75	222	210	202	195	190	184	178
60	198	189	182	176	171	166	162
45	173	165	160	155	153	150	147
30	142	138	134	130	128	125	124
15	101	097	095	093	092	091	090

Seepage Discharge per unit width
(*1000/Permeability/Dam Height)
4.0 Crest/Dam Height Ratio

β \ α	90	75	60	45	30	15	0
90	124						
75	117						
60	109						
45	101						
30	089						
15	069						

Table 5.4 FE Solutions for an Isotropic and Homogenous Earth Dam

The influence of this initial orientation depends on the length of the dam. A narrow dam has the greatest range of seepage line position; in this case the seepage line for a low upstream slope angle is predominantly concave, although the exit point is still higher than that for a dam with the same slope angles but with a wider crest. A wide dam has a low range of seepage line positions. All the seepage lines are predominantly convex upward.

The downstream slope angle affects the seepage line exit height. This effect is masked by the increase in the overall length of the dam when the crest is of the same length and the downstream slope angle is decreased. Even so, it is evident that as the downstream slope angle is decreased, the height of the seepage exit point increases. This is due to the relative shortening of the higher streamlines relative to the lower ones. There is an increase in the quantity of water flowing higher up in the dam and a consequent rise in the seepage line exit point.

5.2.3. Regression Analysis of the Flow Through an Earth Dam

Correlation between seepage discharge and seepage line exit height

As the methods of Schaffernak and Casagrande make different assumptions for the hydraulic gradient (Equations 5.8 and 5.9), it is a natural step to investigate which method best matches the FE results. A graph of seepage exit height against seepage discharge/permeability is plotted in Figure 5.7. Least squares best fit lines are drawn through the origin for each series of points having the same downstream angle (see Table 5.5).

β	Standard error	Maximum deviation	Coeff. of multiple determination	Regression slope ($1/m$)
90	0.02330	0.0880	0.9749	0.7179
75	0.00998	0.0376	0.9944	0.9118
60	0.00344	0.0175	0.9984	1.1654
45	0.00384	0.0065	0.9990	1.5338
30	0.00409	0.0089	0.9987	2.2408
15	0.00505	0.0099	0.9975	4.1705

Table 5.5 Regression Analysis of FE Exit Height-Discharge/Permeability Graphs

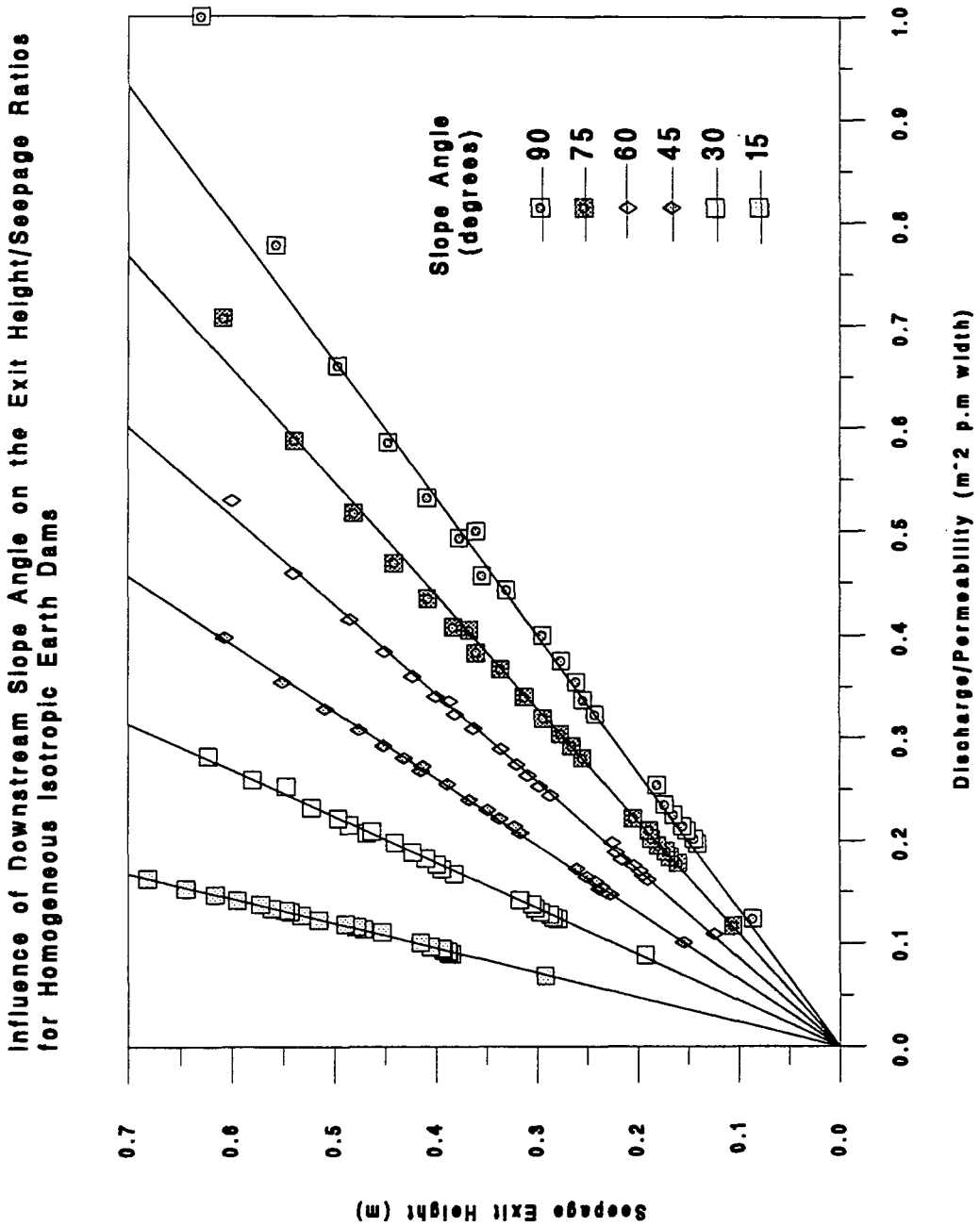

Figure 5.7 Influence of Slope Angle on Exit Height

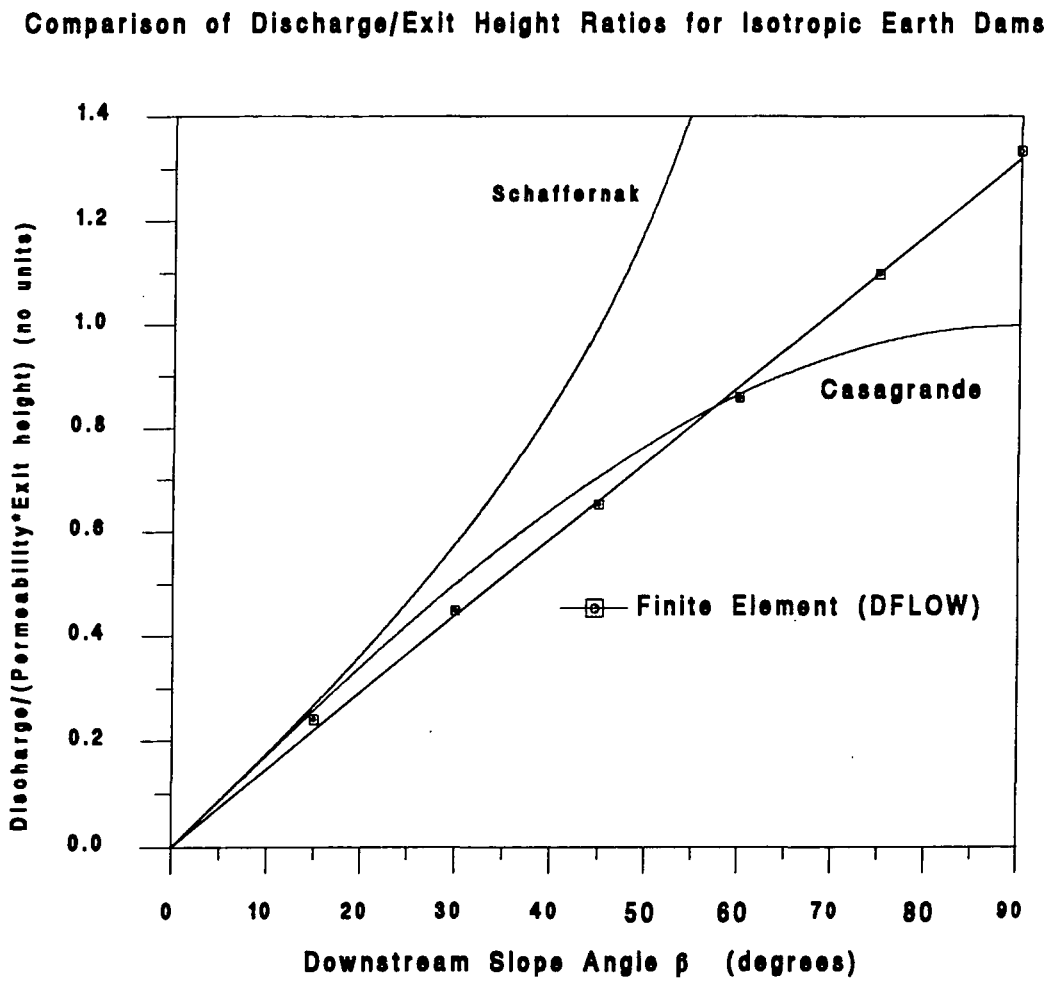

Figure 5.8 Comparison of Exit Height Ratios

The regression statistics show an extremely good match between the points for each downstream angle (better than 97% for 21 degrees of freedom). The fit for narrow dams with a near vertical downstream slope is less good than the average. The reciprocals of the regression slopes as calculated (m) are plotted against the downstream slope angle, together with the equivalent curves for Schaffernak's and Casagrande's method (see Figure 5.8). A second least squares best fit line has been constructed through the origin.

The relationship between the seepage discharge and the exit height is given by the following equation:

$$q = kh_0\gamma\beta \qquad \text{Eq. 5.13}$$

where q is the seepage discharge in m^3s^{-1} per unit width, k is the permeability in ms^{-1}, h_0 is the exit height m, γ is a constant, and β is the downstream slope angle in degrees. The data was re-analysed using NONLIN to obtain the value of γ:

$$\gamma = 0.0148745 \qquad \text{Eq. 5.14}$$

The coefficient of multiple determination (r^2) for this equation is 0.9879 with a standard error of 0.0168. The high degree of correlation between the data and the equation shows that the FE data are self consistent. Bearing in mind the accuracy indicated in the section dealing with the analysis of a rectangular dam, the most reasonable explanation is that Equation 5.13 is not an artefact of the FE analysis. The relationship assumed by Casagrande (Equation 5.9) is very close to Equation 5.13 for downstream angles below 60 degrees. This matches the expected deficiency of Casagrande's method for high angles (Raudkivi & Callender, 1976).

Subsequent to obtaining this formula, the author found the same result in Polubarinova-Kochina (1962; pp 306-307). Polubarinova-Kochina presented a solution by S.V. Falkovich which was derived analytically from the governing differential equations. Figure 5.9 is a reproduction of the graph with Q being the seepage discharge (m^3s^{-1} per metre width of dam), k being the permeability (m^3s^{-1}), l_0 being the length of the seepage surface, and with θ as the downstream slope angle. The vertical scale for each graph is written against each of the four curves. The gradient of the straight-line section of Falkovich's solution (downstream slope angle θ of between 0 and 80 degrees) had a value of 0.0143 which is in very close agreement with the result for γ obtained here.

Polubarinova-Kochina (1962; pp 295) also presented a separate solution for an earth dam with a vertical downstream slope; for this case the value of γ is 0.015. The significance of these results has been ignored in the Western literature.

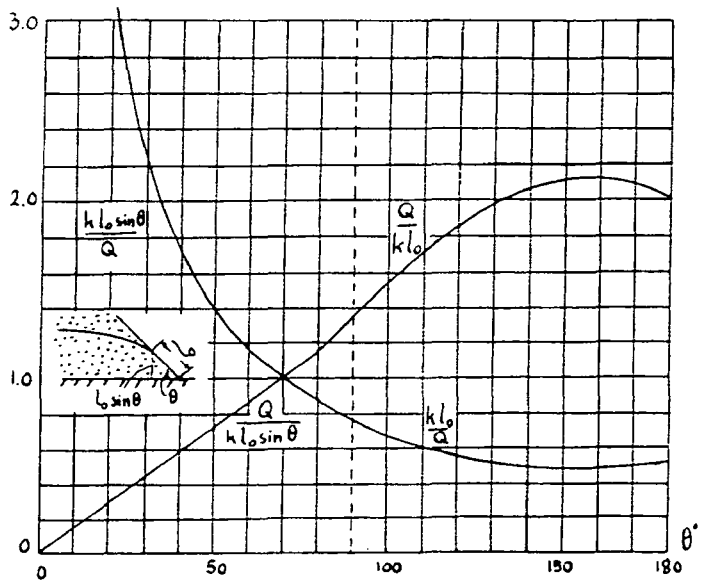

Figure 5.9 Analytical Solution for Seepage Exit Height

(after Polubarinova-Kochina [1962])

Determination of seepage discharge and seepage line exit height.

Following Pavlovsky's lead, Dupuit's solution seems the obvious starting point from which to construct a new equation to model the seepage through an earth dam. Rather than model upstream and downstream slope portions separately, the requirement is to obtain influence factors from a regression analysis to take into account the variation in geometry (see Equation 5.15).

In the conventional analysis, the dam length, as considered, is shortened to exclude the portion of the downstream slope below the seepage surface. The seepage discharge for this shorter dam is an overestimate, so the final equation includes a term to reduce the flow. The regression model that was chosen takes into account the whole of the downstream toe, and a factor to increase the seepage discharge is added for sub-vertical downstream slopes.

The influence of the upstream slope is modelled by increasing the effective length of the dam, as was done by Casagrande. The difference is that while Casagrande adds a factor of 0.3 times the length of dam below the downstream dam (see Equation 5.1),

here a trigonometric function involving the downstream dam angle is used. The cosine function is employed for both the upstream and downstream slope factors because:

- the factor disappears for vertical angles to give Dupuit's solution,
- changes in high angles are more important than changes in low angles.

Thus the factors introduced into the regression model have an obvious physical meaning. The regression parameters were obtained using NONLIN. The equation which gave the best fit is:

$$q^* = \frac{\left(1 + A h_0^{*2} \cos\beta\right)}{2\left(\ell^* + B\cos\alpha + \cot\beta\right)}$$

where $A = 0.84$ Eq. 5.15

$B = 0.518$,

and where q^* is the seepage discharge/(permeability×dam height) per unit width, h_0^* is the seepage exit height/dam height, ℓ^* is the crest length/dam height, and α and β are the upstream and downstream slope angles, respectively. The results of the regression analysis are tabulated below (Table 5.6).

Number of observations	Coefficient of multiple determination	Standard error	Average deviation	Maximum deviation
132	0.9989	0.005042	0.003107	0.03422

Table 5.6 Statistics for Regression Model of Flow

Polubarinova-Kochina (1962, p 307) reported semi-empirical work carried out by G.K. Mikhailov concerning the influence of the upstream slope on the flow regime. Mikhailov suggested that the triangle of the upstream face may be replaced by an equivalent rectangle of $0.5H\cos(\alpha)$ in length for an upstream slope angle of greater than 53 degrees, and $H/(2+\tan(\alpha))$ for angles greater than 53. In both cases the values are remarkably similar to the value of $B\cos(\alpha)H$ obtained by the regression analysis.

5.2.4. Computer Program for Quick Solution of Flow Through an Earth Dam

Equations 5.13, 5.14 and 5.15 can be solved iteratively or exactly to obtain an FE extrapolation of the solution for seepage discharge and seepage line exit point. In view of the accuracy shown by the FE program, it is likely that the predicted seepage discharge and exit height will be more accurate than current approximate solutions.

In order to demonstrate the effectiveness of the regression model, a computer program was written to compute values of seepage discharge and seepage exit height from the regression equation, Schaffernak's and Casagrande's solution. The results of the program are in Tables 5.7-5.9. The tables are shaded to show the divergence of the program results from the FE data. The program uses an iterative scheme starting from values obtained using Dupuit's solution and the corresponding seepage exit height/seepage discharge relationships. The same results were obtained using an arbitrary starting value. Roughly half of the results for Schaffernak's and Casagrande's methods could not be calculated because the equations have no real roots for the geometry concerned. This was not a problem for the regression models. Graphs of the predicted values of seepage discharge and seepage line exit height against the FE data are also presented (Figures 5.11 and 5.14). Again it is noted that the original FE data is not a suitable check for the absolute validity of the method. However, the goodness of fit does show that the regression analysis has satisfactorily modelled the FE data (particularly in the case of seepage discharge). Table 5.9 tabulates the regression statistics for the comparisons between the computer program results and the original data.

The Schaffernak and Casagrande methods do not correlate well with the FE data. The tables show that good results are obtained for these methods when both slope angles are close to 45 degrees and the crest length is at least twice the height of the dam. The graphs suggest that the Schaffernak method seriously underestimates the seepage exit height, while that of Casagrande may be an overestimate or underestimate. Casagrande underestimates the seepage discharge for most cases, while Schaffernak performs far better for discharge predictions.

Schaffernak Seepage Line Exit Height and Seepage Discharge

Exit Height*1000/Dam Height
0.5 Crest/Dam Height Ratio

β \ α	90	75	60	45	30	15	0
90							
75	194	172	152	132	108	072	
60	391	332	289	248	203	139	
45				437	327	218	
30						357	
15							

Exit Height*1000/Dam Height
1.0 Crest/Dam Height Ratio

β \ α	90	75	60	45	30	15	0
90							
75	110	103	096	087	076	057	
60	206	194	181	167	147	111	
45	333	309	287	262	230	175	
30				499		276	
15							

Exit Height*1000/Dam Height
2.0 Crest/Dam Height Ratio

β \ α	90	75	60	45	30	15	0
90							
75	060	058	055	053	048	040	
60	117	113	109	104	096	080	
45	184	178	172	164	152	127	
30	291	281	270	258	238	200	
15						409	

Exit Height*1000/Dam Height
4.0 Crest/Dam Height Ratio

β \ α	90	75	60	45	30	15	0
90							
75	031	031	030	029	028	025	
60	064	063	061	060	057	051	
45	103	102	100	097	093	083	
30	163	161	158	154	148	133	
15	312	306	300	292	279	251	

Seepage Discharge per unit width
(*1000/Permeability/Dam Height)
0.5 Crest/Dam Height Ratio

β \ α	90	75	60	45	30	15	0
90							
75	725	642	568	493	402	269	
60	677	574	500	430	352	241	
45				437	327	218	
30						206	
15							

Seepage Discharge per unit width
(*1000/Permeability/Dam Height)
1.0 Crest/Dam Height Ratio

β \ α	90	75	60	45	30	15	0
90							
75	409	383	356	326	285	211	
60	358	336	314	289	254	192	
45	333	309	287	262	230	175	
30				288	222	160	
15							

Seepage Discharge per unit width
(*1000/Permeability/Dam Height)
2.0 Crest/Dam Height Ratio

β \ α	90	75	60	45	30	15	0
90							
75	223	215	207	196	181	148	
60	202	195	188	179	166	138	
45	184	178	172	164	152	127	
30	168	162	156	149	138	115	
15						110	

Seepage Discharge per unit width
(*1000/Permeability/Dam Height)
4.0 Crest/Dam Height Ratio

β \ α	90	75	60	45	30	15	0
90							
75	118	115	113	110	105	093	
60	111	109	106	104	099	088	
45	103	102	100	097	093	083	
30	094	093	091	089	085	077	
15	084	082	080	078	075	067	

123 — Data within 10% of FE result
345 — No FE data calculated for this data

456 — Data outside 10% of FE result
(blank) — Method failed for this geometry

Table 5.7 Schaffernak's Seepage Discharge Prediction for an Earth Dam

Casagrande Seepage Line Exit Height and Seepage Discharge

Exit Height*1000/Dam Height
0.5 Crest/Dam Height Ratio

β \ α	90	75	60	45	30	15	0
90							
75					550	288	
60					581	292	
45						328	
30						473	
15							

Exit Height*1000/Dam Height
1.0 Crest/Dam Height Ratio

β \ α	90	75	60	45	30	15	0
90							
75		481	420	367	308	221	
60		485	421	368	311	227	
45			530	427	351	254	
30						332	
15							

Exit Height*1000/Dam Height
2.0 Crest/Dam Height Ratio

β \ α	90	75	60	45	30	15	0
90							
75	269	225	216	205	188	154	
60	333	230	221	210	194	160	
45		259	249	237	218	182	
30		338	324	307	282	234	
15						440	

Exit Height*1000/Dam Height
4.0 Crest/Dam Height Ratio

β \ α	90	75	60	45	30	15	0
90							
75	130	130	119	117	113	108	096
60	147	147	126	123	120	115	102
45	188	188	144	141	138	132	118
30	311	311	187	183	179	171	154
15			320	313	305	291	261

Seepage Discharge per unit width
(*1000/Permeability/Dam Height)
0.5 Crest/Dam Height Ratio

β \ α	90	75	60	45	30	15	0
90							
75					531	278	
60					503	253	
45						232	
30						237	
15							

Seepage Discharge per unit width
(*1000/Permeability/Dam Height)
1.0 Crest/Dam Height Ratio

β \ α	90	75	60	45	30	15	0
90							
75		465	406	355	298	214	
60		420	364	319	269	196	
45			375	302	248	180	
30						166	
15							

Seepage Discharge per unit width
(*1000/Permeability/Dam Height)
2.0 Crest/Dam Height Ratio

β \ α	90	75	60	45	30	15	0
90							
75	260	218	209	198	181	148	
60	288	200	192	182	168	139	
45		183	176	167	154	128	
30		169	162	153	141	117	
15						114	

Seepage Discharge per unit width
(*1000/Permeability/Dam Height)
4.0 Crest/Dam Height Ratio

β \ α	90	75	60	45	30	15	0
90							
75	125	115	113	110	105	093	
60	128	109	107	104	099	089	
45	133	102	100	097	093	084	
30	155	093	092	089	086	077	
15		083	081	079	075	067	

123 — Data within 10% of FE result
345 — No FE data calculated for this data

456 — Data outside 10% of FE result
Method failed for this geometry

Table 5.8 Casagrande's Seepage Discharge Prediction for an Earth Dam

Regression Model Seepage Line Exit Height and Seepage Discharge

Exit Height*1000/Dam Height
0.5 Crest/Dam Height Ratio

β \ α	90	75	60	45	30	15	0
90	747	589	492	431	394	374	367
75	635	527	456	410	380	364	358
60	598	514	456	417	391	376	372
45	607	535	484	448	425	411	407
30	663	596	548	514	492	479	474
15	816	744	695	660	636	623	618

Exit Height*1000/Dam Height
1.0 Crest/Dam Height Ratio

β \ α	90	75	60	45	30	15	0
90	374	329	297	274	258	249	246
75	364	327	299	279	265	257	255
60	376	344	318	299	286	279	276
45	411	380	356	337	324	317	314
30	479	448	424	405	392	384	381
15	623	591	566	546	532	524	521

Exit Height*1000/Dam Height
2.0 Crest/Dam Height Ratio

β \ α	90	75	60	45	30	15	0
90	187	175	165	158	153	149	148
75	199	188	179	171	166	163	162
60	222	211	201	193	188	185	184
45	259	247	237	229	223	220	218
30	323	310	299	290	284	280	279
15	458	443	430	420	413	408	407

Exit Height*1000/Dam Height
4.0 Crest/Dam Height Ratio

β \ α	90	75	60	45	30	15	0
90	093	090	088	086	084	083	083
75	105	102	099	097	095	094	094
60	123	120	117	114	112	111	111
45	152	147	144	141	139	137	137
30	201	196	192	189	186	184	184
15	313	307	301	297	293	291	290

Seepage Discharge per unit width
(*1000/Permeability/Dam Height)
0.5 Crest/Dam Height Ratio

β \ α	90	75	60	45	30	15	0
90	1000	789	659	577	527	500	491
75	708	588	509	457	424	406	400
60	534	459	407	372	349	336	332
45	406	358	324	300	284	275	272
30	296	266	245	230	219	214	212
15	182	166	155	147	142	139	138

Seepage Discharge per unit width
(*1000/Permeability/Dam Height)
1.0 Crest/Dam Height Ratio

β \ α	90	75	60	45	30	15	0
90	500	441	397	366	345	333	329
75	406	365	334	311	296	287	284
60	336	307	284	267	255	249	246
45	275	254	238	226	217	212	210
30	214	200	189	181	175	171	170
15	139	132	126	122	119	117	116

Seepage Discharge per unit width
(*1000/Permeability/Dam Height)
2.0 Crest/Dam Height Ratio

β \ α	90	75	60	45	30	15	0
90	250	234	221	211	204	200	199
75	222	210	199	191	185	182	181
60	198	188	179	173	168	165	164
45	173	165	159	153	149	147	146
30	144	138	133	130	127	125	124
15	102	099	096	094	092	091	091

Seepage Discharge per unit width
(*1000/Permeability/Dam Height)
4.0 Crest/Dam Height Ratio

β \ α	90	75	60	45	30	15	0
90	125	121	117	115	112	111	111
75	117	114	111	108	106	105	105
60	110	107	104	102	100	099	099
45	101	099	096	094	093	092	092
30	090	088	086	084	083	082	082
15	070	068	067	066	065	065	065

123 — Data within 10% of FE result
345 — No FE data calculated for this data

456 — Data outside 10% of FE result
Method failed for this geometry

Table 5.9 Regression Model Prediction for a Homogenous Earth Dam

5.2.5. Comparison of Regression Model and Chart Solution

Stello (1987) used the method of fragments to calculate the flow through homogeneous and zoned embankments. The results were combined with flow net analyses for steep sided dams (for which the method did not converge). Tables of correction factors were provided for crest width, pool freeboard and the permeability ratio of dam and core. Stello compared his results with published flow net results. This section compares the Stello solution, the finite element solution and the regression model.

Figure 5.10 shows the flow net calculated by DFLOW for a dam problem posed by Stello as an example. Stello provided a flow net for this problem, but it is clearly inferior to the one presented here.

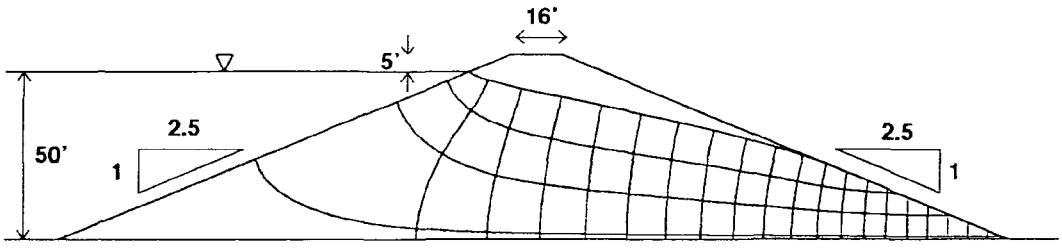

Figure 5.10 Flow Net for a Homogeneous Embankment
(for problem posed by Stello [1987])

The variables and dimensions for this problem are as follows:

effective dam height	H	50 feet	15.24 metres
effective crest width	ℓ	41 feet	12.5 metres
upstream slope angle	α	21.8 degrees	
downstream slope angle	β	21.8 degrees	
seepage discharge	q	(in m^3s^{-1} per metre width of dam)	
permeability	k	(in ms^{-1})	

Stello obtained values for $q/(kH)$ = 0.16 by chart and = 0.15 from his flow net (an error of +7%), and h_0/H = 0.45 by chart and 0.51 from his flow net (an error of -12%). The finite element program DFLOW gave results of $q/(kH)$ = 0.155 and h_0/H = 0.466. These figures are much closer to those of Stello's chart method than his flow net. A recalculation of the errors (using Stello's results with one more significant figure than quoted in the final results of the original paper) obtained an error in $q/(kH)$ of 0.6% and an error in h_0/H of -3.6%.

The solution using the method based on the regression method is as follows:

I. First an approximate solution is obtained for either $q/(kH)$ or h_0/H. If a value for the exit height is guessed, then the solution procedure skips to Part III. In this instance it is convenient to use Dupuit's solution:

$$q/kH = \frac{H}{2L}$$

where L is the cross-sectional length of an "equivalent" rectangular dam. The chosen approximation for the equivalent width is the sum of the crest width ($\ell = 12.5$) and half of each of the dam slope bases (0.5*(38.1+38.1) metres). The solution for the seepage term is therefore:

$$q/kH = \frac{15.24}{2 \times 50.6} = 0.151$$

The error in this approximate solution is -2.6% and so in this case the solution would be accurate enough without further refinement.

II. The approximation for the seepage line exit height uses Equations 5.13 and 5.14:

$$\begin{aligned} h_0/H &= \frac{1}{\lambda\beta}\frac{q}{kH} \\ &= \frac{1}{0.0149 \times 21.8}\frac{q}{kH} \\ &= 3.08\frac{q}{kH} \\ &= 3.08 \times 0.151 = 0.465 \end{aligned}$$

This approximate solution has an error of -0.2%; a degree of accuracy which may be regarded as fortuitous. The solution is refined further until convergence occurs.

III. The seepage discharge is calculated using Equation 5.15:

$$\frac{q}{kH} = \frac{\left(1 + \mathrm{A}\cos\beta h_0^{*2}\right)}{2\left(\ell^* + \mathrm{B}\cos\alpha + \cot\beta\right)}$$

where $h_0^* = h_0/H$

$\ell^* = \ell/H$

$$\frac{q}{kH} = \frac{\left(1 + 0.84 \times 0.9285 \times h_0^{*2}\right)}{2(0.82 + 0.518 \times 0.9285 + 2.5)}$$

$$= \frac{\left(1 + 0.78 h_0^{*2}\right)}{7.6}$$

$$= \frac{\left(1 + 0.78 \times 0.465^2\right)}{7.6} = 0.154$$

The error is now reduced from -2.6% to -0.6%.

The cycle from II to III may now be repeated until the results fails to change. Once the constants of the equations have been obtained (as above) the calculation becomes trivial. In this case the converged values of $q/(kH)$ and h_0/H are 0.155 and 0.477 with errors of 0% and 2.4%, respectively. These values are slightly more accurate than the values obtained by Stello. The seepage exit height errs on the conservative (high side), while that of Stello slightly underestimates the seepage line exit height.

5.2.6. Conclusions

The study of flow through an earth dam with upstream and downstream slopes less than 90 degrees is far more complex than that for a simple rectangular dam. The analytical methods do not provide as good a solution as that of Dupuit for the simpler case. A regression analysis of the FE results allows the problem to be linearized, and the development of a simple and accurate solution developed from Dupuit's solution. The dam slopes may be taken into account by means of regression parameters obtained from the FE data. The value of the upstream slope factor is found to be similar to that suggested by G.K. Mikhailov (in Polubarinova-Kochina, 1962, p 307).

The study confirms the linear relationship first calculated by S.V. Falkovich (in Polubarinova, 1962, pp 306-307) between the angle of the downstream slope, the seepage line exit point and the seepage discharge/permeability ratio for dams having a downstream slope angle between 0 and 90 degrees. The exception to this rule is the narrow rectangular dam (height/length>1).

Upstream and downstream slope angles, together with overall dam length, have a direct influence on the height of the seepage line exit point and on the form of the seepage line. A short dam with a low upstream slope angle may develop a steady-state seepage line which is concave upwards. In the case of a long dam, the upstream slope angle has little effect on the position of the seepage line (except in the vicinity of the upstream slope).

Schaffernak and FE Seepage Exit height

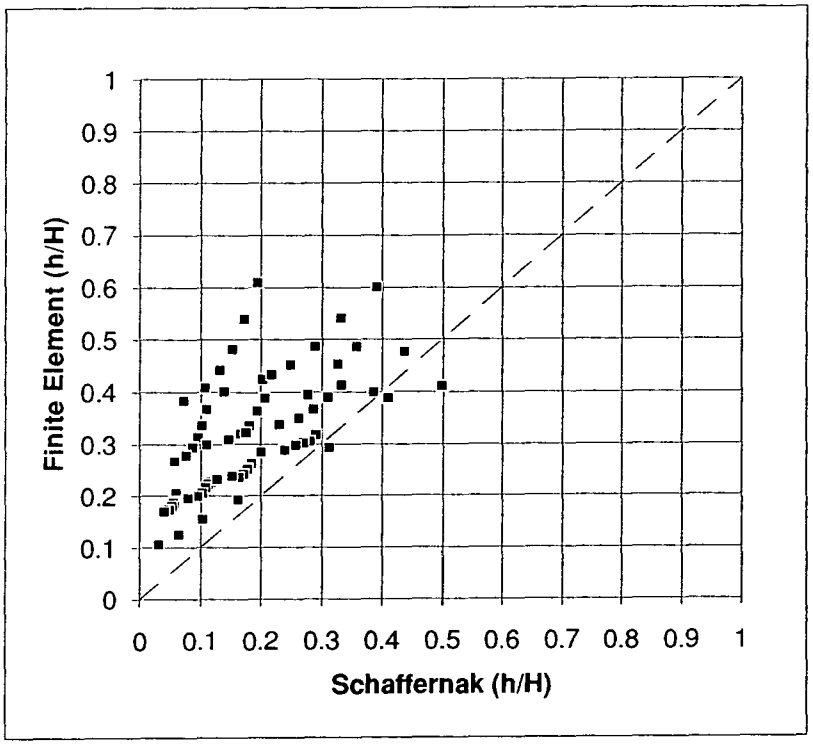

Schaffernak and FE Seepage Discharge

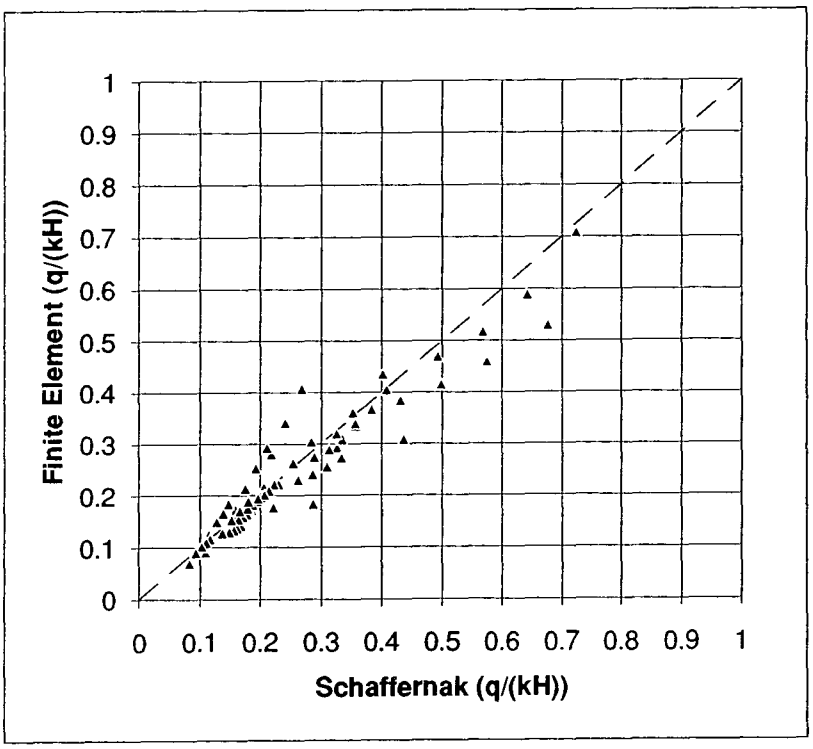

Figure 5.11 Graphs of Schaffernak against FE Solution

Casagrande and FE Seepage Exit Height

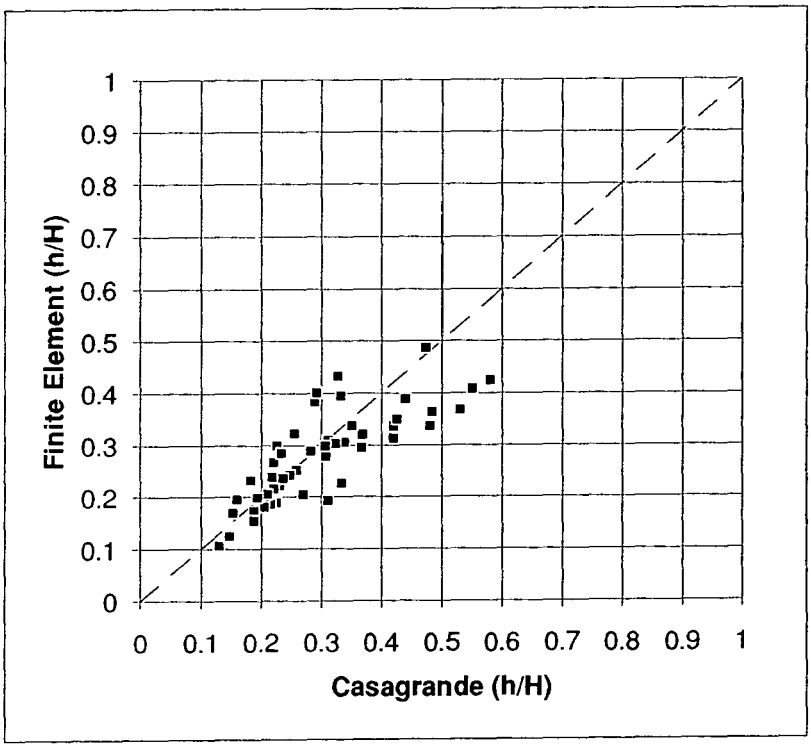

Casagrande and FE Seepage Discharge

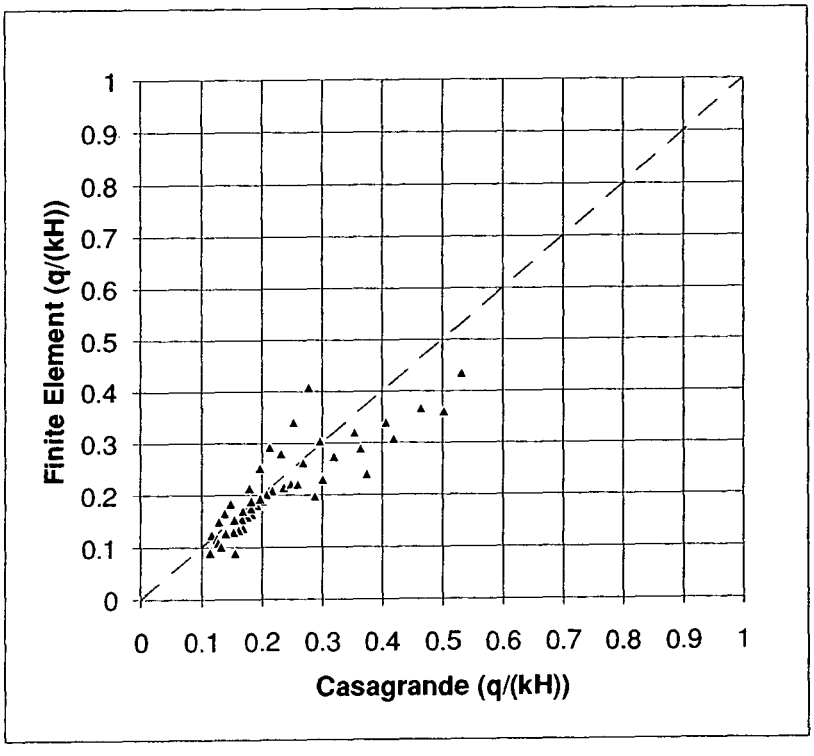

Figure 5.12 Graphs of Casagrande against FE Solution

Regression Model and FE Seepage Exit Height

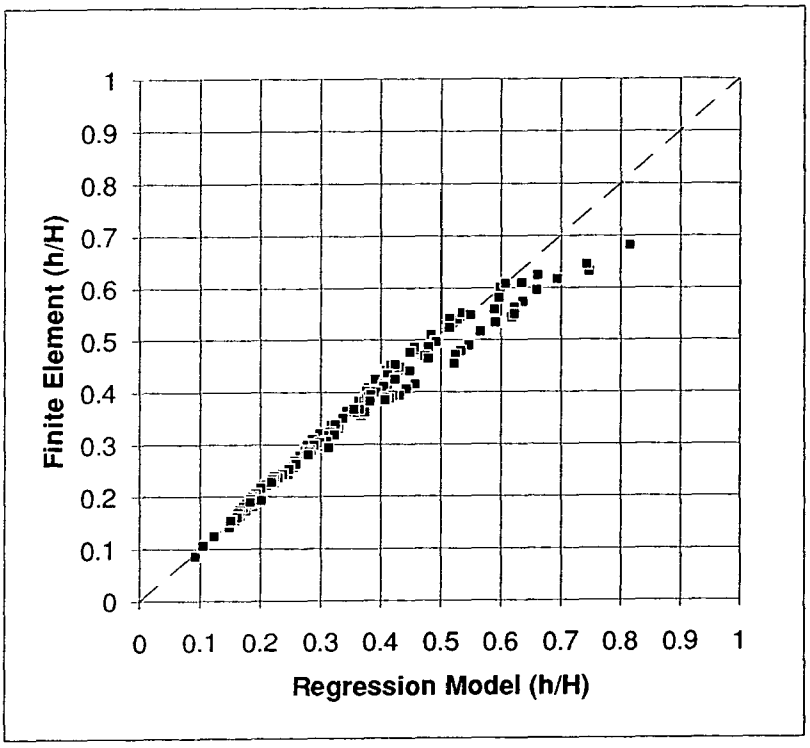

Regression Model and FE Seepage discharge

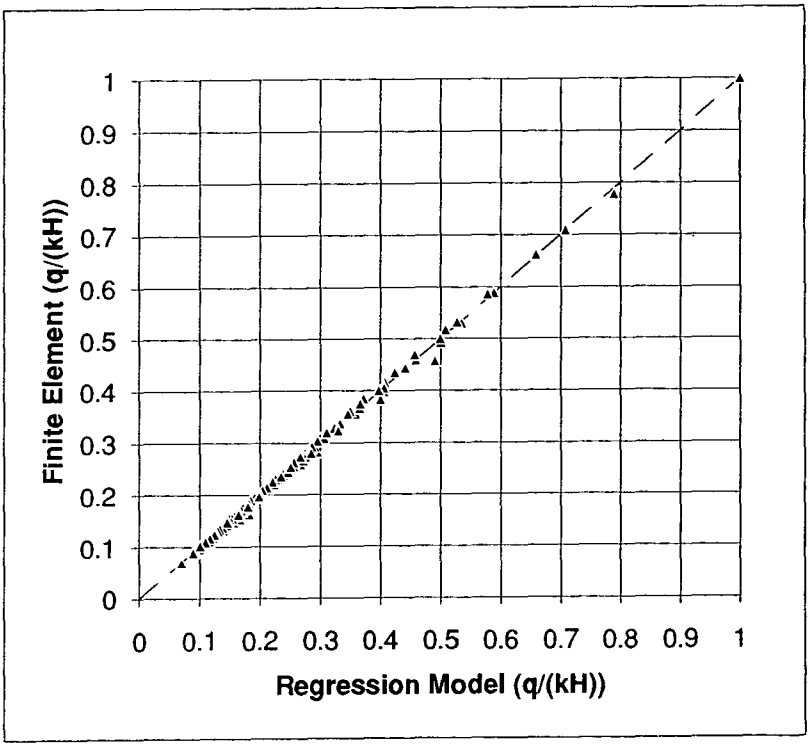

Figure 5.13 Graphs of Regression against FE Solution

Schaffernak and Casagrande Exit Height

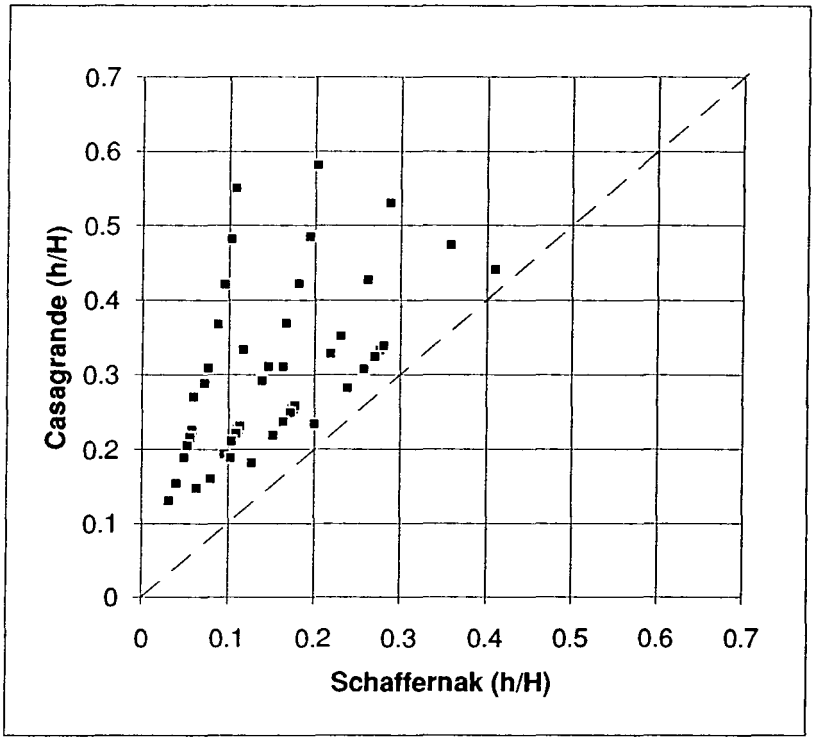

Schaffernak and Casagrande Seepage Discharge

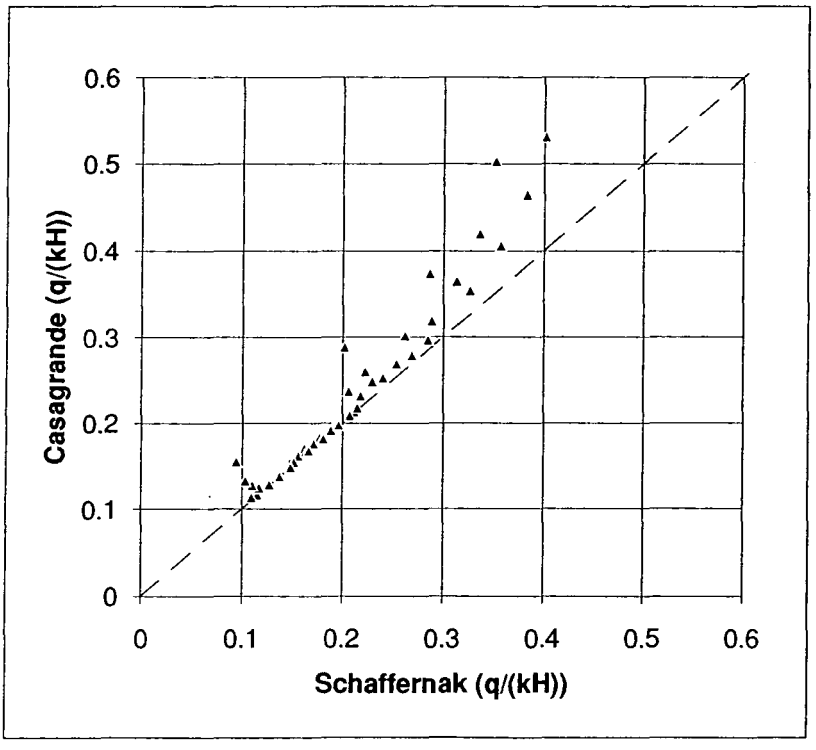

Figure 5.14 Graphs of Schaffernak against Casagrande Solution

5.3. Steady State Analysis of an Idealised Tailings Dam Geometry

Studies of water flow through tailings dams in the literature have been almost exclusively aimed at the upstream construction geometry (see Chapter 2). This is, no doubt, because tailings dams are most commonly built using the downstream method (ICOLD, 1989), and it is these types of dams which are most prone to failure due to high seepage pressures (Vick, 1983). British Coal use the downstream tailings technique to construct all dams (NCB, 1970). This will be the principal type of dam investigated.

Each subset of the analyses is coded in the text, titles and on the figures to allow a quick identification of the data sets, e.g. TD0 is a tailings dam of downstream construction type with a zero beach length (ponded water lying directly against the dam) (see Table 5.10). Appendix 3 contains the following information for each simulation (each marked with an identification code):

- diagrammatic cross-sections
- tables of seepage discharge and seepage line exit height
- graphs of seepage discharge and seepage line exit height
- flow nets.

5.3.1. Assumptions of the Analysis

The previous section dealing with earth dams has investigated the effect of the geometry (crest length, upstream slope and downstream slope) on the flow through a homogeneous and isotropic earth dam. This section relaxes these last two assumptions, and looks at the effect on the steady state seepage line of commonly found tailings dam properties. The dam geometry was kept identical for each case so that the effect of changing dam properties can be studied in isolation. The choice of dam geometry to be studied is essentially arbitrary, but in view of the special interest in British Coal tailings dams, dimensions from "Spoil Heaps and Lagoons" (NCB, 1970) were chosen.

The handbook stated that a regular dam should not exceed 18m in height, have a crest width no narrower than 5m, have an upstream slope of no more than 1:1.5, have a downstream slope no more than 1:2, and have a freeboard of at least 1m. The preceding limits together form, what is considered here, the limiting geometry for British Coal dams. This was the geometry chosen for all the various tailings dam analyses (see Figure 5.15).

Code	Description
TD0	Tailings dam with downstream geometry, zero beach length, isotropic, horizontally inhomogeneous, discontinuous permeability.
TD10	Tailings dam with downstream geometry, 10m beach length, isotropic, horizontally inhomogeneous, discontinuous permeability.
TD20	Tailings dam with downstream geometry, 20m beach length, isotropic, horizontally inhomogeneous, discontinuous permeability.
TD30	Tailings dam with downstream geometry, 30m beach length, isotropic, horizontally inhomogeneous, discontinuous permeability.
TDDIHIC	Tailings dam with downstream geometry, 20m beach length, isotropic, horizontally inhomogeneous, continuous permeability.
TDDIVID	Tailings dam with downstream geometry, 20m beach length, isotropic, vertically inhomogeneous, discontinuous permeability.
TDUAOHC	Tailings dam with upstream geometry, 20m beach length, anisotropic, homogeneous, continuous permeability.
TDDAOID	Tailings dam with downstream geometry, 20m beach length, anisotropic, inhomogeneous, discontinuous permeability.

Table 5.10 Identification Codes for Tailings Dam Analyses

The base of the tailings and lagoon was considered to be impervious to flow; this is the most conservative assumption with respect to embankment safety (ignoring the possibility of artesian pressures). The tailings dam model had no internal drainage because the study was concerned with the worst case scenario.

Two types of dam and two different material properties were investigated:

- "Downstream tailings dam type" with a break in permeability properties between the dam and the embankment.
- "Upstream tailings dam type" with tailings and embankment having the same (or at least continuous) permeability properties.
- Inhomogeneity of permeability, i.e. value of permeability dependent on position.
- Anisotropic permeability, i.e. value of permeability dependent on direction of flow.

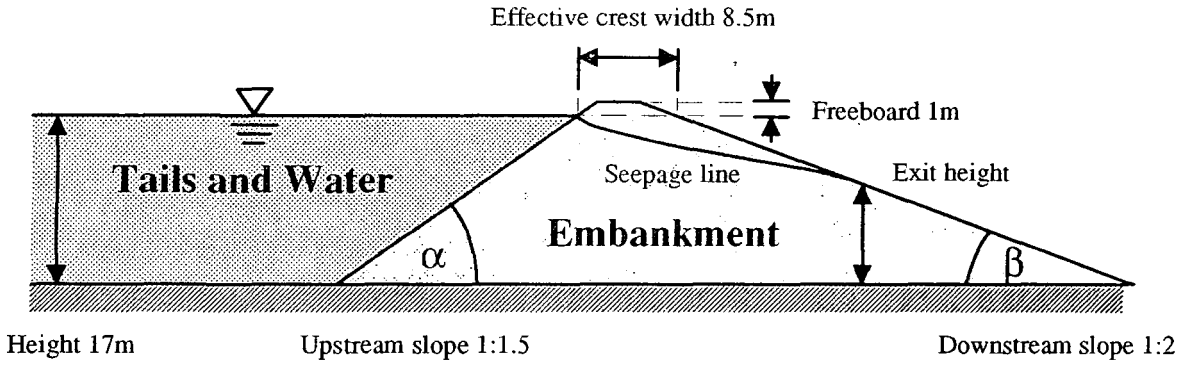

Figure 5.15 Limiting Geometry for a British Coal Type Dam

In addition to these material properties, the effect of changing the position of the lagoon pond was also investigated. The position of the pond can be expected to be the most important factor in determining the position of the seepage line within the dam because it controls the start and length of the shortest seepage path. No account will be taken of operating procedures such as hydraulic fill methods or other techniques which place water directly on the crest of the dam or the beach. This is in line with British Coal procedures (see Chapter 2). The accretion rate (evaporation-percolation balance) was also ignored. This may be an over-simplification for arid regions or where the precipitation and dam permeability are both high.

5.3.2. Beach Length and Tailings Permeability TD0-TD30

Simulations of the steady state seepage through a downstream type dam were performed using the "British Coal limiting geometry" for four different beach lengths (0, 10, 20, 30m) and a variety of different tailings to dam permeability ratios.

As the tailings permeability increases, the seepage discharge and seepage line exit point will rise. The limit is reached when the tailings offer no resistance to water flow. This situation is equivalent to that of an earth dam without tailings. A ratio of tailings to dam permeability of 50 was the highest used in the FE simulation. For short beach widths, this approaches the point where the presence of tailings makes little difference to the flow pattern. For a longer beach length, a higher ratio of permeabilities may be required.

At the other end of the scale, as the permeability of the tailings decreases relative to the dam, the effect of the dam on the seepage flow will become negligible. The problem becomes one of an overturned seepage face at the upstream dam slope. Unfortunately, the limiting case in this situation is not the hydrogeological limit but an inadequacy in

the program in dealing with near vertical or overturned seepage lines. Solutions to this problem have been implemented by Neuman & Witherspoon (1970).

In the case of the dam and tailings having a different permeability, the change in material properties was spread over a thin strip of the FE mesh. This was to satisfy the program material properties algorithm which requires a linear change in interpolated mesh values (see Chapter 4), and also cure an instability in the France algorithm (France et al, 1971) for moving the free surface. This instability was caused by the mismatch of the movement of seepage line nodes on adjacent zones of different permeability. A seepage line node passing from one permeability zone to another will have travelled an incorrect distance for a finite time step. The differential movement between adjacent nodes causes a perturbation in the seepage line which can create an unstable result. In the case where the tailings are of a lower permeability than the dam, fine tailings may be transported into the dam and trapped in a zone on the upstream face of the dam. For this reason, the strip of transitional permeability was located on the dam side of the embankment. The strip has an equivalent width of 1 metre.

Downstream tailings dam without a beach (**TD0**)

The analyses of a tailings dam without a beach were carried out for tailings/dam permeability ratios of 10, 5, 2, 1, 0.5, 0.4, 0.3 and 0.2. This problem proved one of the most difficult to solve. The seepage line enters the embankment perpendicular to the upstream face and then enters the zone of changing permeability. When the dam is more permeable than the tailings, this is not a problem. But when the dam is less permeable, the seepage line is deflected according to the law of refraction. The angle between the streamline and the transitional zone is greater on the side of low permeability than on the side of high permeability. The dam considered has an upstream slope of 1:1.5. When the permeability in the dam is higher than that in the tailings, the seepage line must be deflected from the vertical against the general direction of flow. The problem of an inverted seepage line proved very difficult to solve. The method using a pseudo time step to calculate seepage line movement (see Chapter 3) became unstable for large differences of permeability (see above). The unmodified Tailor/Brown method (Taylor & Brown, 1967) of moving the seepage line to satisfy the head requirement (see Chapter 3) was unable to cope with vertical or overhanging seepage lines. A ratio of dam to tailings permeability of 5 was the biggest which could be satisfactorily modelled.

For the ratio of tailings to dam permeability of 0.2, the fall of the seepage exit line (with respect to the homogeneous case) was about 20%. The rate of decrease in the exit

height on a log permeability scale is still high at a ratio of 0.2. Further reduction in tailings permeability would cause an appreciable further reduction in seepage line exit height.

The streamlines travelling close to the base of the dam have the furthest to travel through the less permeable tailings in which the head loss is greatest. Consequently, as the tailings permeability is decreased relative to the dam, flow is concentrated in the zone at the pond edge and reduced towards the base of the dam.

Downstream tailings dam without a 10m beach (**TD10**)

The analyses of a tailings dam without a 10m beach were carried out for tailings/dam permeability ratios of 10, 5, 2, 1, 0.5, 0.2 and 0.1. The last ratio (0.1) proved to have the same problems as the TD0 analysis. Where the seepage line crosses into the dam, the gradient of the seepage line is high (owing to the large negative hydraulic gradient). The seepage line is deflected by the permeability interface against the direction of flow. For this case, the Taylor/Brown seepage surface movement algorithm was used. The section of seepage line at the permeability interface has been constrained to move in a vertical direction only. This has truncated the form of the seepage line over a short section of its length. Although the accuracy here was not greatly affected, a smaller ratio of permeabilities was not attempted.

The seepage exit height for a tailings/dam permeability ratio of 0.1 was half that of the homogeneous case. The graphs indicate that the seepage line exit height will be reduced by a further rise in tailings dam permeability.

Downstream tailings dam without a 20m beach (**TD20**)

The analyses of a tailings dam without a 20m beach were carried out for tailings/dam permeability ratios of 10, 5, 2, 1, 0.5, 0.2, 0.1 and 0.05.

The effect of a reduction in tailings permeability is magnified by the additional distance travelled by pond water through the tailings before reaching the dam. In the case of a ratio of tailings/dam permeability of 0.05, half of the total head is lost within the tailings and the total reduction in seepage discharge is 76%.

Downstream tailings dam without a 20m beach (**TD30**)

The analyses of a tailings dam without a 30m beach were carried out for tailings/dam permeability ratios of 10, 5, 2, 1, 0.5, 0.2, 0.1, 0.05 and 0.02.

The trend of TD30 is identical to that of TD20. With the addition of a much lower ratio of tailings to dam permeability, it is evident that the hydrogeological limit for seepage

exit height is being approached. Over 70% of the total head is lost within the tailings dam. The graphs indicate that the rates of seepage exit height and seepage discharge reduction with decreasing tailings permeability (log scale) are also decreasing,

Summary

- The length of beach (distance between the pond and tailings dam) is of crucial importance in assessing the position of the seepage line within the dam, as long as the tailings are not much more permeable than the dam.
- The seepage lines for tailings embankments with tailings of lower permeability than the dam are concave upwards. This is because the head loss is concentrated in the low permeability tailings, and the gradient of the seepage line is almost equal to the hydraulic gradient. This effect is exaggerated by the influence of a longer beach. The water levels within the dam itself are reduced compared to an earth dam, but the slope of the seepage line itself is quite flat.
- The effect of tailings of higher permeability than the dam is not very significant compared to the converse case. The seepage discharge and seepage line exit height cannot be greater than that in an earth dam. The length of seepage line within the dam itself shows the classic earth dam configuration.
- The graph of seepage discharge mirrors the graph of seepage exit height (this is considered later).
- Further work with low tailings permeability, short beach length and a modified program should be considered.

5.3.3. Decrease of Permeability from Dam to Pond (TDDIHIC)

Chapter 2 describes how the permeability of the tailings deposited at the crest decreases from the dam to the lagoon pond. The effect of this lateral variation in permeability was investigated with the dam geometry having a 20m beach length. It was assumed that the distance from the pond to the dam remains constant; this means that the pond transgresses over tailings deposited on the beach. As a consequence, the permeability in the region between the pond sediments and the dam actually decreases downwards.

The dam to tailings permeability ratios tested were 1, 2, 5, 10 and 20. The converse problem with tailings increasing in permeability from the crest to the centre does not occur in conventional tailings dams (see Chapter 2) and was not investigated. In these simulations, the tailings permeability at the edge of the dam is equal to that of the dam itself. This is unlikely in practice, but the choice of another arbitrary value would be no

more valid. The effect of a jump change in permeability is analysed in the previous section (albeit with some modification).

The simulations were carried out using the Taylor/Brown method for seepage line movement (see Chapter 3). As in the previous analysis, the effect of this is to truncate the overhanging seepage line created by the refraction of the streamlines. In this case, the effect on the flow net appears to be negligible (the flow nets still conform to the rules for hand-drawn flow nets).

The graphs indicate an exponential decrease in seepage discharge and seepage line exit height for relative decreases in pond tailings permeability from 1/2 to 1/20. Once again these two graphs mirror one another. There is a 65% decrease in seepage line exit height for pond tailings having 1/20th of the permeability of the dam.

The water flow is concentrated in the zone close to the pond edge. The seepage line plummets from the pond to the upstream slope of the dam. The water level in the dam itself is relatively flat but is lower than that for an earth dam.

5.3.4. Vertical (Downwards) Decrease in Tailings Permeability (TDDIVID)

Consolidation of the tailings in the embankment may be responsible for a reduction in the permeability of coarse tailings by 5% and of fine tailings by 10% (Vick, 1983).

The effect of this vertical variation in permeability was investigated with the dam geometry and a 20m beach length. As before, it was assumed that the distance from the pond to the dam remains constant. The tailings top/base permeability ratios tested were 1, 2, 5, 10 and 20, 50 and 100. In these simulations, the tailings permeability at the top of the embankment is equal to that of the dam itself. Although unlikely in practice, this is an attempt to isolate just the effect of the vertical variation in permeability.

The graphs of seepage discharge and seepage exit point fall as the permeability of the base tailings decreases. This reduction occurs at a decreasing rate as the permeability ratio (top/base) increases on a log scale. The maximum reduction in seepage exit height (ratio of 100) is 10%. Water flow is concentrated into the zone near to the pond, where the permeability is highest. The flow nets show an almost imperceptible change in flow pattern for an increase in permeability ratio with a permeability ratio (top/base) of greater than 10. The corresponding reduction in seepage exit height is 8%.

5.3.5. Anisotropic Dam and Tailings Permeability (TDUAOHC)

All previous simulations have involved isotropic problems. One distinguishing feature commonly found in tailings embankments is the presence of a distinct difference in vertical and horizontal permeabilities (see Chapter 2). This property is important to

model because it is responsible for raising the level of water within a tailings dam above that of an earth dam (Abadjiev, 1976).

The TDUAOHC simulations model the effect of anisotropy in both the dam and the tailings (which are given the same permeability). The ratios of horizontal to vertical permeability chosen are 1, 2, 5, 10, 15 and 20. According to Kealy & Busch (1979), ratios of 10 are quite common. A beach length of 20m was simulated.

The flow nets produced for this simulation indicate that, as expected, the flow lines and equipotentials are no longer orthogonal. The actual position of the seepage line is not much affected by the anisotropy of the embankment. For ratios of horizontal to vertical permeability of 1 to 10, the seepage exit height increases with increasing ratio. At a ratio of 10 there is an increase of 9% in the seepage line exit height. This is close to the maximum rise of 10% predicted by Abadjiev (1976). As the permeability ratio increases above 10, the seepage exit height begins to fall sharply. This effect is due to the reduction in head from the pond, because water must travel vertically down from the pond through the tailings. For the range of horizontal to vertical permeabilities tested, the anisotropic condition always leads to a higher seepage line exit point than in the isotropic case.

The seepage discharge is reduced by a decrease in vertical permeability. While the seepage exit height for a ratio of horizontal to vertical permeability of 20 causes an increase in the seepage exit height (from the isotropic condition) of 5%, the seepage discharge is reduced by 46%.

In the anisotropic case, the seepage exit height and seepage discharge graphs are not identical in form.

5.3.6. Anisotropic Tailings Permeability (TDDAOID)

This analysis involves the case in which the tailings are anisotropic and the dam is isotropic. This is closer to the case of the downstream construction method, although in reality the dam is likely to be anisotropic but to a lesser degree. Once again a beach length of 20m was used.

The tailings horizontal to vertical permeability ratios that have been examined are 1, 2, 5, 10, 15, and 20. The border between the dam and the tailings properties is again spread over a 1m wide zone of the dam. In this case, there is no physical justification in using a transition zone rather than an abrupt break in material properties. In a real tailings dam, the permeability of the dam is unlikely to be the same as the horizontal

component of the permeability of the tailings. Again, this simplification is made so that one parameter may be examined to the exclusion of others.

The flow nets for TDDAOID are much the same as those for TD20 which is an isotropic embankment with a tailings permeability lower than the dam permeability. Within the tailings, the flow nets are nearly identical to those of the previous case (TDUAOHC) with an anisotropic dam. Hence the problem can be seen to be one of two halves. This is emphasized by the observation that the seepage discharge and seepage line exit height graphs mirror one another. In this case, the graphs indicate that the effect of anisotropy increases as the log permeability ratio of the tailings (top/base) increases. This suggests that a considerably greater drop of seepage exit height and seepage discharge could be expected for a higher anisotropic ratio.

The effect of an anisotropic ratio of top to base tailings permeability of 20 is roughly equivalent to an inhomogeneous dam (TD20) with a ratio of tailings to dam permeability of 5. One notable difference in the two simulations can be found in the locus of the seepage line at the interface of the dam and the embankment. In simulation TDDAOID, the seepage line drops suddenly at the upstream dam slope. This reflects the change in permeability over the 1m transition zone. The anisotropic conditions seem to have exaggerated the streamline refraction in the transition zone. Seepage line inversion for TDDAOID occurs with a relatively flat seepage line, while for TD0, TD10 and TDDIHIC the seepage line was inverted where it was entering the transition zone at a steep angle.

5.3.7. Relationship Between Seepage Discharge and Seepage Line Exit Height

For all the foregoing analyses (with the exception of the TDUAOHC), the graph of seepage discharge and seepage line exit height mirrored each other. TDDAOID is an interesting case in point. Although TDDAOID has anisotropic tailings, the dam is isotropic. It would seem that this property of symmetry depends only on having isotropic and homogeneous conditions adjacent to the downstream slope.

The seepage discharge/permeability of the downstream portion of the dam is plotted against the seepage line exit height for all the simulations of this section (see Figure 5.16). A best fit line through the origin is plotted for the isotropic dams. Despite the wide range of permeability conditions, the fit is extremely good with a coefficient of multiple determination (r^2) of 0.9987 for 41 data points. The graph for the anisotropic dam has also been plotted (TDUAOHC). These dams do not fit the general data trend. An object of a future study could be to determine the relationship between seepage discharge and seepage line exit height for an anisotropic dam.

The reciprocal of the gradient (seepage/exit height) for the isotropic tailings models is 0.3987. This value should equal $\lambda\beta$ of the previous section (where λ is the regression parameter and β is the downstream slope). The actual value of $\lambda\beta$ predicted in the previous section for a downstream slope gradient of 1:2 is 0.3951, so the difference is less than 1%.

5.3.8. Conclusions

- The position of the pond has a fundamental impact on the level of the seepage line within the dam. Maintaining a long beach is an effective way of keeping a low seepage line.
- When the tailings permeability is lower than the dam permeability, a concave upwards seepage line develops within the tailings. The seepage line in the dam itself is reduced and follows the classic convex upward line found in an earth dam. The overall appearance in the tailings embankment is one of a concave upwards seepage line.
- A large increase (in the direction of flow) of permeability at the tailings dam interface or a large increase in permeability in the tailings from beach to dam causes an abrupt drop of the seepage line. This has been widely reported in the literature (see Chapter 2).
- Decreasing tailings permeability downwards due to consolidation could be responsible for a maximum fall of 10% in the seepage line for the geometry investigated (compared to the isotropic case with an impervious base).
- For the upstream tailings dam, anisotropy may be responsible for an increase in the seepage line exit height of up to 9% (with respect to the isotropic case) for this geometry (Abadjiev (1976) gives a general figure of 10%).
- In the case of a downstream tailings dam, tailings anisotropy decreases the height of the seepage line.
- For isotropic and homogeneous tailings dams, the seepage discharge/permeability to seepage line exit height is proportional to the downstream slope angle.

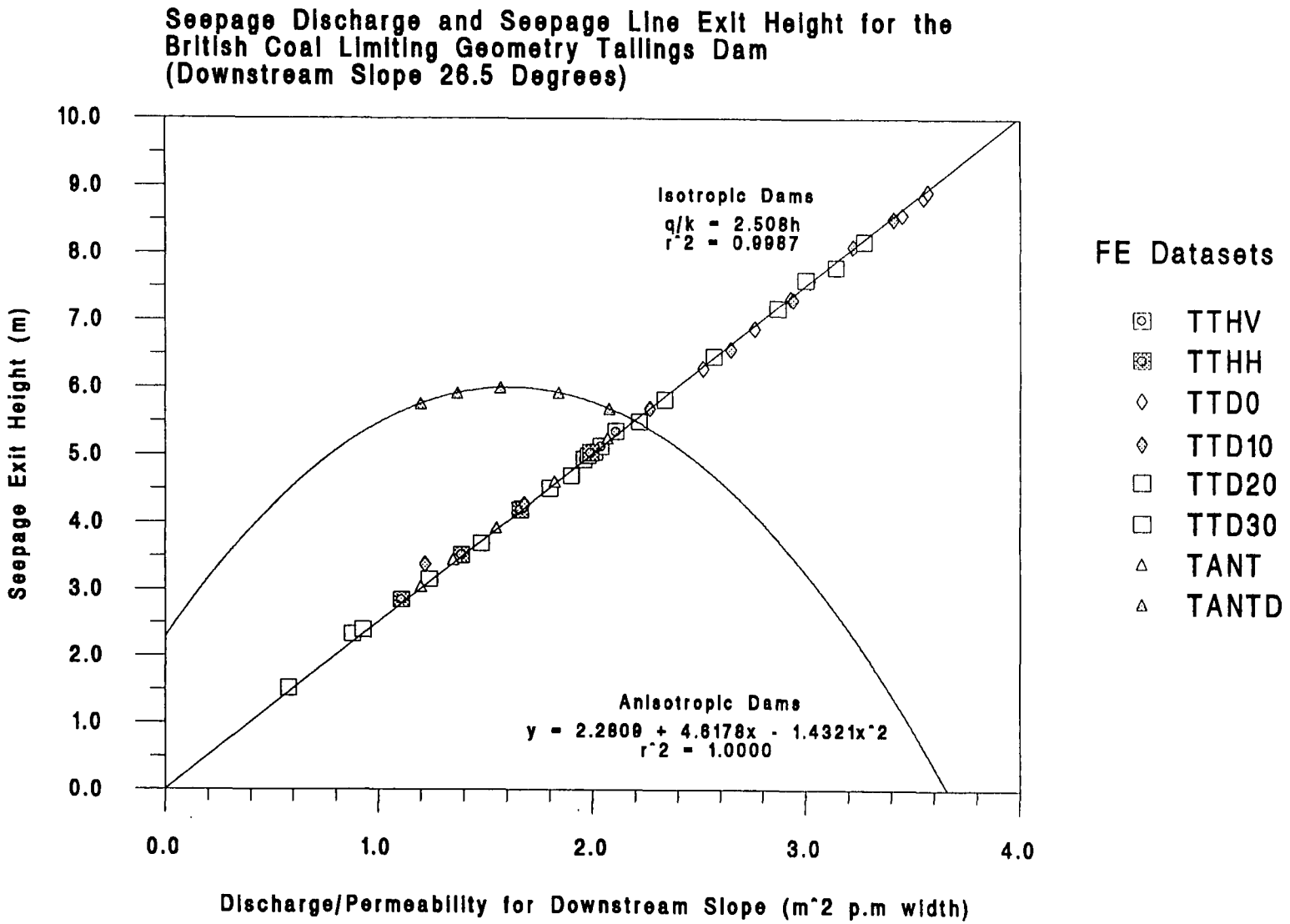

Figure 5.16 Graph of Seepage Characteristics for Tailings Dam Models

5.4. Miscellaneous Dam Flow Problems

This section of the thesis deals with additional cases which have been studied in order to examine some of the assumptions made in the preceding analyses. The object is not to provide a complete study of the influence of these new parameters. The following problems concern the permeability of the foundation below the dam (see Table 5.11) and the influence of a toe drain.

Code	Description
DVB	Earth dam geometry, isotropic, homogenous, variable depth of permeable base.
DVBK	Earth dam geometry, isotropic, inhomogenous, base depth equal to dam height, base of high permeability

Table 5.11 Identification Codes for Earth Dam Analyses

5.4.1. Influence of Permeable Base Thickness (DVB)

In the previous examples it has been assumed that the foundation below the dam is impervious to the flow of water. The geometry as examined corresponds to the "British Coal limiting geometry" used in the previous analyses. The particular example is an earth dam (without tailings) in which both the dam and the foundation are homogenous and isotropic. The simulated parameters involve depth of permeable base to dam height ratios of 2.0, 1.0, 0.5 and 0 (no base). The natural water table is assumed to be at ground level. Graphs, figures and flow nets for the analysis are presented in Appendix 3.

Flow from the reservoir may travel either through the dam, the permeable foundation, or both. The result is an increase in the total seepage discharge as the depth of the base is increased. Furthermore, the flow lines extend further out in the upstream and downstream directions. The seepage line exit height drops with increasing depth of permeable base but at a decreasing rate. For a base depth of twice the dam height, the seepage line exit point is 40% lower than the case with an impervious base. Based on this limited information, the maximum fall in seepage exit point height is not likely to be over 50% in this case.

The study shows that in the absence of artesian pressures, the effect of a permeable base will be to lower the seepage line in the dam and increase the seepage discharge.

The seepage discharge and exit height are not of a fixed ratio.

5.4.2. Influence of Base Permeability (DVBK)

The previous study (**DVB**) involved a dam situated on a base having a permeability identical to that of the dam. The case involving a base of a higher permeability is considered here. The problem is otherwise identical to the preceding analysis. Only a base depth to dam height ratio of 1 is considered. The ratios of base to dam permeabilities tested were 1, 5, 10, 20 and 50.

The flow nets for this problem (see Appendix 3) are spoilt by an artefact of the algorithm which calculates the flow lines. Flow lines are calculated by integrating the product of the streamline gradient function and the permeability across the FE mesh (see Chapter 4). The quality of this calculation depends on the route taken for the integration. The algorithm integrates to the next node using the shortest total path length (measured in whole element sides). If the path of the integration travels across a node with a singularity, then a dislocation in the flow line values occurs between this integration path and other paths which have not crossed the same singularity. This error may be cured for individual problems by repositioning the starting node for the integration. In this case, the error in the flow net is left as a demonstration of this phenomenon.

The seepage line exit point and seepage discharge are both lowered by an increase in base permeability. The rate of change of discharge and exit height decreases with increasing base to dam log permeability ratio. With a permeability (base to dam) ratio of 50, the seepage line exit point is lowered by 60%. This is in excess of the maximum likely fall in the seepage line for the previous homogenous case.

5.4.3. Influence of Drainage Toe on Tailings Dam Seepage Line

The final steady state case to be analysed involves the simulation of water flow through a tailings dam incorporating a toe dam. The studied examples mirror the problems **TD0**, **TD10**, **TD20**, **TD30** investigated in a previous section. The geometry of the dams is identical to these problems with the exception of a high permeability toe situated at the base of the downstream toe (see Figure 5.17).

A beach length of 0, 10, 20, and 30m was investigated. For each case, tailings permeabilities are equal to that of the dam, 10 times higher than that of the dam, and 10 times lower than that of the dam. For the case without a beach, the last two permeability ratios could not be satisfactorily computed (see case TD0).

The flow nets for these dams are presented in Figures 5.18, 5.19 and 5.20.

The toe drain is effective in preventing seepage out of the downstream slope. However, the seepage line may still be high within the dam. The trend is identical to the cases without a toe drain described previously.

- The beach length has a major effect in controlling the level of the seepage line within the dam.
- The seepage line is concave upwards for the case with low permeability tailings.
- High permeability tailings have only a small effect on the position of the seepage line (for a reasonably short beach).

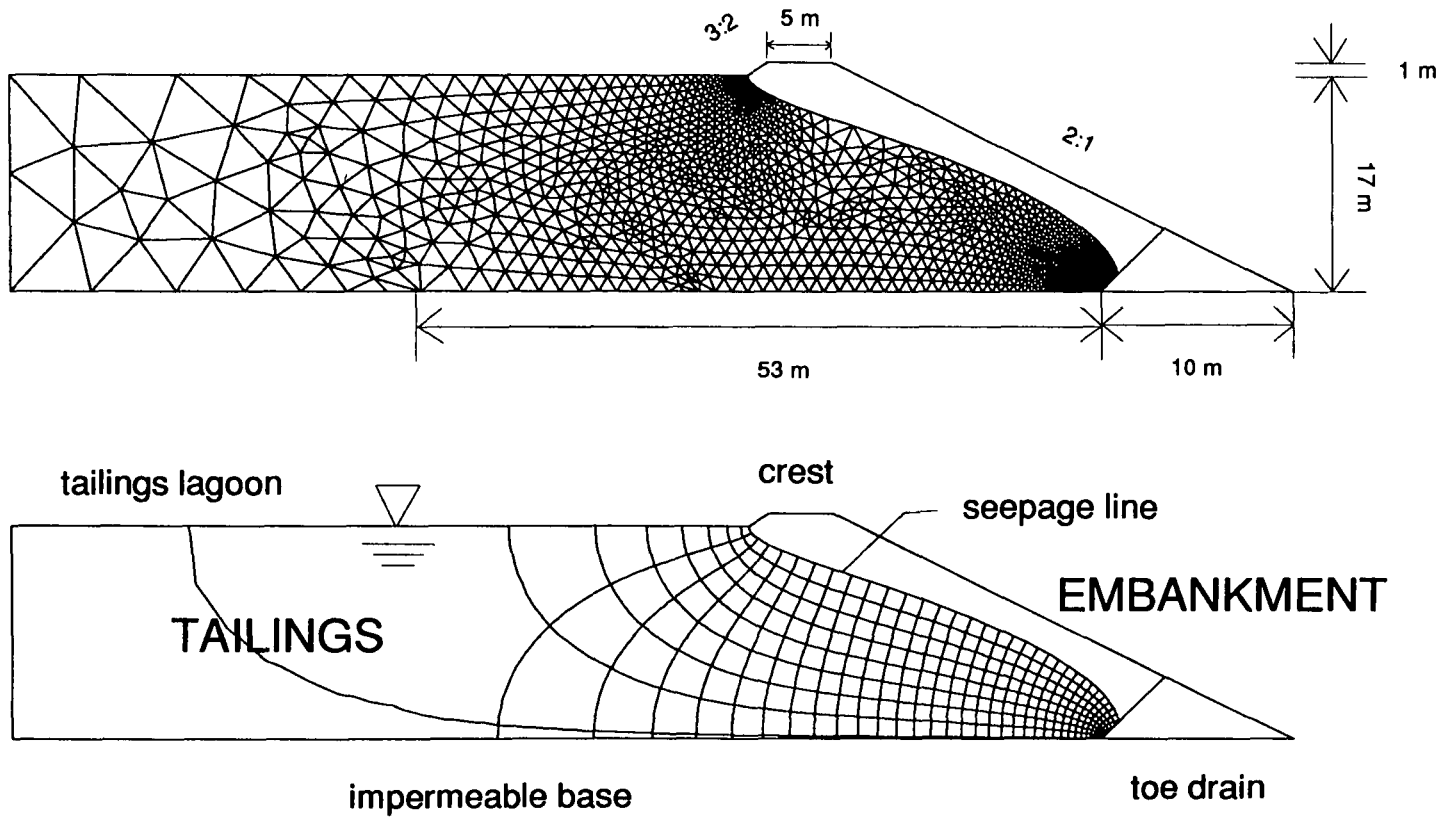

Figure 5.17 Toe Drain Problem Geometry

Downstream Tailings Dam With Toe Drain

Influence of Beach Length on Flow Net

Tailings permeability = Embankment permeability

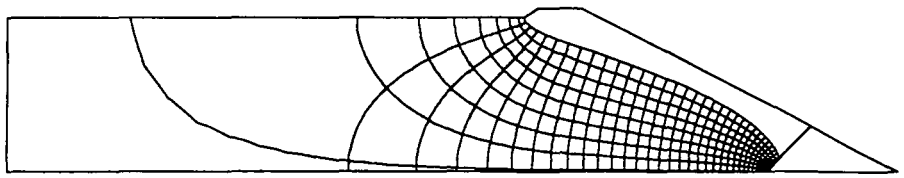

a) Beach length 0m

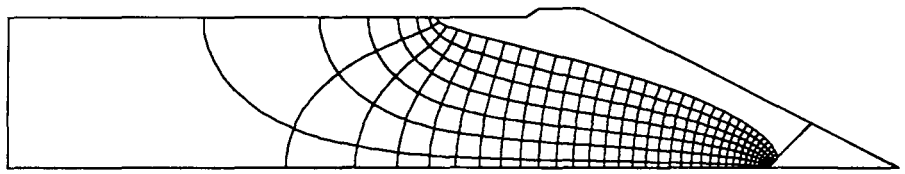

b) Beach length 10m

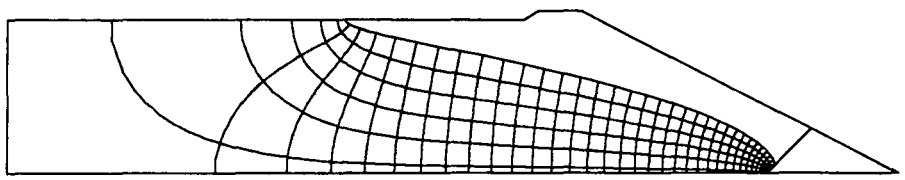

c) Beach length 20m

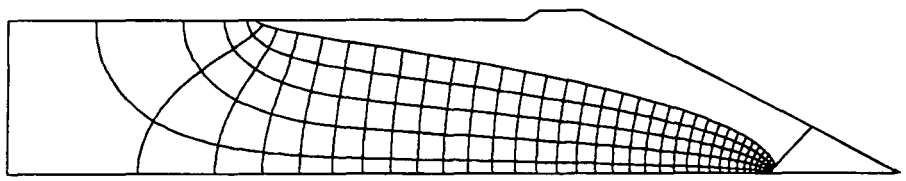

d) Beach length 30m

Figure 5.18 Toe Drain in Homogeneous Embankment

Downstream Tailings Dam With Toe Drain

Influence of Beach Length on Flow Net

Tailings permeability = Embankment permeability / 10

N o P l o t A v a i l a b l e

a) Beach length 0m

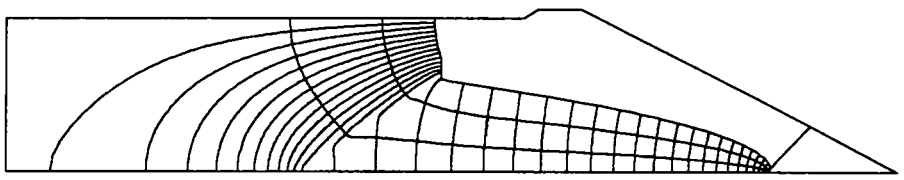

b) Beach length 10m

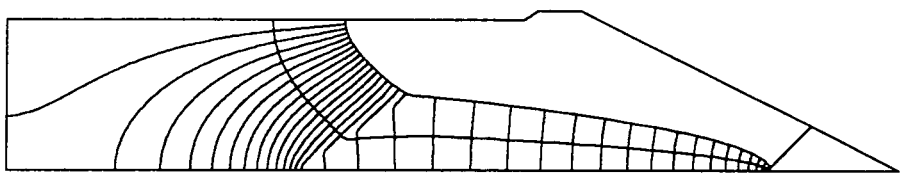

c) Beach length 20m

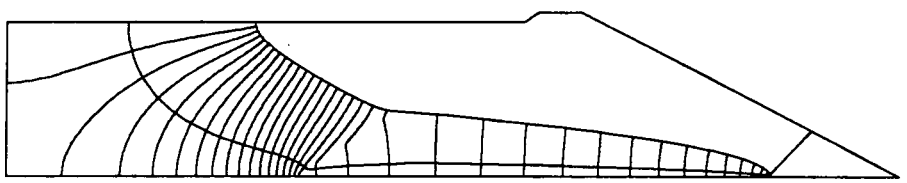

d) Beach length 30m

Figure 5.19 Toe Drain with Low Permeability Tailings

Downstream Tailings Dam With Toe Drain

Influence of Beach Length on Flow Net

Tailings permeability = Embankment permeability x 10

N o P l o t A v a i l a b l e

a) Beach length 0m

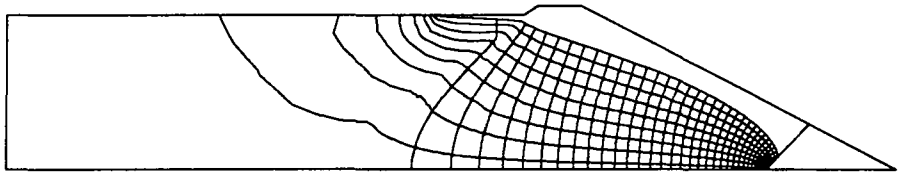

b) Beach length 10m

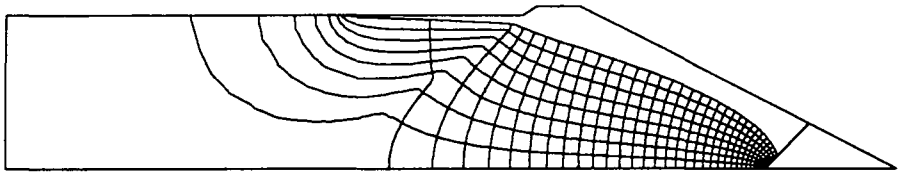

c) Beach length 20m

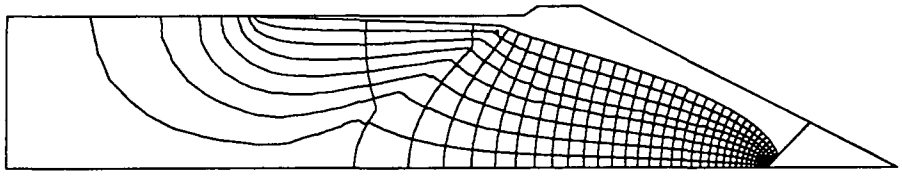

d) Beach length 30m

Figure 5.20 Toe Drain with High Permeability Tailings

5.5. Sudden Fill Earth Dam

The influence on the seepage line advance of the upstream slope angle was investigated using the FE model. The factors taken into consideration are:

a. Upstream slope angle

b. Displacement of the seepage line

c. Time taken in simulation

d. Numerical Accuracy.

Permeability and effective porosity have a linear scaling effect on the time/displacement relationship and so they need not be incorporated into the analysis at this early stage.

An equation for the seepage line movement is obtained using a regression analysis and is then compared with an approximate solution proposed by Huang (1986).

5.5.1. Model Assumptions

Geometry

To make a parametric study of all possible earth dam geometries would be beyond the scope of any reasonable study. The effect of base permeability, dam length and downstream slope angle are not considered here. Obviously the assumption that the foundations are impervious does limit the applicability of this study (this is no worse an assumption than that commonly made in standard groundwater hydrology). A redeeming feature is that this is the worst case scenario if only the detrimental effects of saturated flow within the earth embankment itself are being considered (e.g. for slope stability). The analysis does not consider the form of the seepage line after it has reached the downstream face of the dam. This has the advantage that all lengths of dam may be considered in a single simulation (so long as the length does not exceed the height by a factor of more than 10). However, the results only fit the dam in question up to the time when the seepage line crosses the downstream face. The section dealing with steady state analysis considers the quantity of discharge and maximum height of the seepage line. The actual times taken to reach steady state (and intermediate discharge rates) are not considered. If this information is required then it must be based on an in-depth analysis of the particular dam in question. The assumptions already made allow an examination of the general case (i.e. the influence of the factors discussed above), but a general analysis is not precise enough to provide such specific information. Figure 5.21 shows the cross section modelled for this analysis.

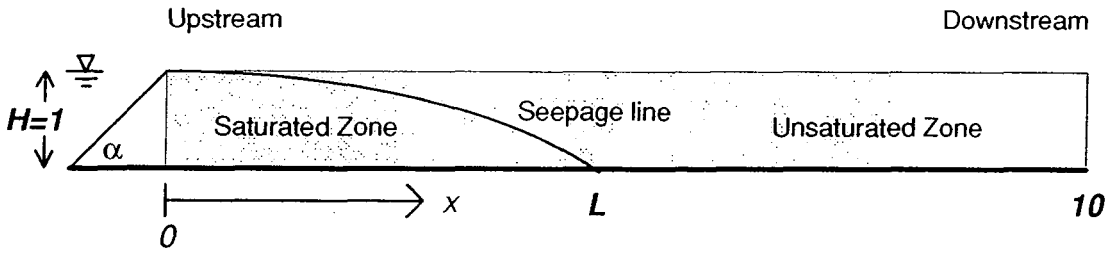

Figure 5.21 Cross-Section through an Idealized Earth Dam

Starting Conditions

At the instant when water is introduced into the pond, there will not be a finite saturated zone which could be modelled and the hydraulic gradient at the dam slope will be infinite. These conditions make it impossible to describe the initial conditions in the FE analysis. Furthermore, shortly after the flow has been initiated, an inverted phreatic surface must develop above the unsaturated upstream toe of the dam. It is evident that water may mound up in advance of the seepage line. As this analysis involves only a consideration of the saturated flow regime, it was necessary to start the simulation with the toe of the dam completely saturated (see Figure 5.22). The initial seepage conditions will be taken into consideration by a back analysis of the flow development.

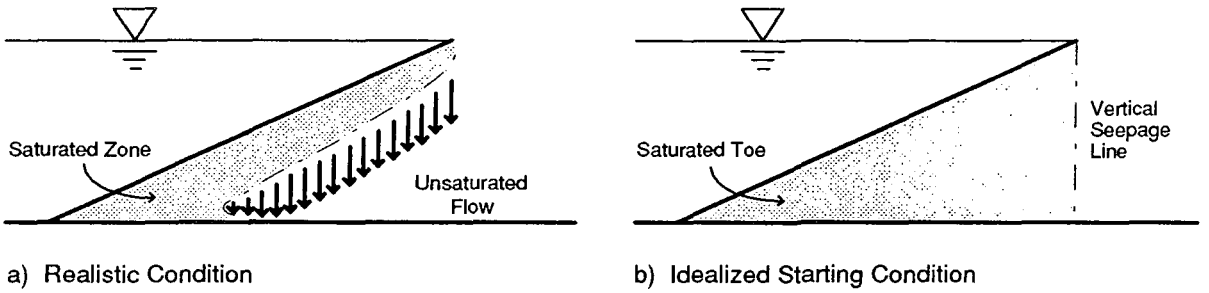

Figure 5.22 Initial Conditions for Transient Solution of Dam Flow

Material Properties

The velocity of the seepage line depends on the hydraulic gradient, permeability and effective porosity of the dam material. The effective porosity is used here to take into account the partial saturation of the dam. By this definition it represents the proportion of the total volume of the dam which is available for water storage. It does not include unconnected or saturated pore space. Darcy's equation can now be written for the velocity of the fluid in the porous medium:

$$\bar{v} = \frac{ki}{n} \qquad \text{Eq. 5.16}$$

where $\bar{v}$ is seepage line velocity in ms^{-1}, k is permeability (hydraulic conductivity) in ms^{-1}, i is the hydraulic gradient, and n is the effective porosity. The analysis deals only with homogeneous and isotropic material properties. The time units (t in days) and distance travelled (x in metres) of the FE simulation may be converted into "real units" by taking into account the permeability, effective porosity and dimensions of the dam:

$$t = t^* \frac{Hn}{k} \times 24 \times 60 \times 60 \text{ days}$$
$$x = x^* H \qquad \text{Eq. 5.17}$$

where t^* is simulation time, x^* is the simulated distance travelled, and H is the height of water from dam base (in metres).

5.5.2. Analysis of Numerical Error

Seepage line movement is calculated from the water velocity normal to the zero pressure line. The displacement of the fluid particles on the free surface is controlled by the hydraulic gradient, permeability, effective porosity, and the time step over which the movement is to be calculated. The algorithm employs an explicit (Euler) finite difference approximation which is affected by:

- Discretization error (mesh spacing)
- Time step length.

Unfortunately, these two factors are intimately connected; the stability and convergence of a fine mesh depends on having a sufficiently small time step. Where the geometry of the flow domain introduces a nonlinearity (or singularity) into the solution, an accurate solution of the partial differential equations depends on having a fine enough mesh to allow a smooth and rapid variation in potential gradient. Such a situation exists where the upstream slope angle is low and the seepage line, which must enter the dam perpendicular to the upstream face, turns rapidly on entering the dam. The stability of the time stepping routine depends on the size of the smallest element, so earth dams with low upstream angles require a smaller time step to achieve the same accuracy.

Note that the relative error of the solution is a measure of accuracy for the steady state solution between time steps, and not the accuracy of the time stepping routine. The accuracy of the time stepping algorithm depends on the ability of the mesh to model the geometry of the seepage line adequately. With linear elements, this means having enough degrees of freedom along the boundary. Meshes of elements of equal numerical error will be denser in all regions for greater degrees of accuracy, hence an automatic improvement in time stepping should occur for a more accurate mesh so long as the time step itself is not too great.

A number of solutions were obtained for the time taken for the seepage line to travel 10 times the height of the dam for upstream slope angles of 0, 45 and 85 degrees using different time steps and at different accuracies. The results are plotted in the Figure 5.23. The choice of data points that were examined was controlled by the length of time required for the simulation and the time step stability requirement. In the case of the zero degree upstream slope dam, the point at 3% relative error took several days to complete and could not be repeated for an increased time step.

The time steps are not constant throughout the simulation, shorter steps being used initially and longer steps towards the end. For this reason, only the ratio of the time steps between one simulation and another is given. A "quarter" time step produces about 14,000 mesh iterations.

Three trends are evident in the data:

I. As the relative error of the solution of the steady state problem decreases with increasing degrees of freedom, so the velocity of the seepage line increases.

II. Decreasing the time step reduces the velocity of the seepage line.

III. High slope angles exhibit a greater variation in travel time.

It is assumed that the correct solution is achieved at the limit, i.e. with zero error and infinitely small time steps. While the case for the former is strong, it has not been proven that the accuracy of the solution will necessarily improve with a reduction in the time step. It is logical to assume that numerical errors will rise below some time step length threshold. As previously stated, as the slope angle increases, so the singularity at the seepage entry point decreases. This means that the meshes for the zero degree slope angle are denser than meshes for 45 and 85 degrees at the same accuracy. In this instance, the zero degree slope dam had approximately 10 times as many nodes as the 85 degrees slope dam in the early stages. At the end of the simulation, the zero degree slope mesh had twice as many nodes along the boundary as did the 85 degree slope. As

a consequence, the time stepping routine for low angles can be expected to be more accurate for a reasonable time step. This explains why the travel time against relative error plots are steeper for lower angled upstream slopes.

5.5.3. Results of the Numerical Simulation

Simulations of seepage line displacement are presented for earth dams having an upstream slope angle α of 0, 15, 30, 45, 60, 75 and 85 degrees (see Appendix 4). The simulations were all computed to an accuracy of below 3% relative error. The time step used was roughly the same in all cases and equivalent to the "half" step used in the preceding error analysis (and reduced for zero and 15 degree angled slopes). For each simulation there is a graph of the distance travelled along the base of the dam by the seepage line (L) against time, and a plot of the seepage line profile achieved after travelling 10 multiples of the dam height (H=1). The points in bold on the upper graph indicate the next stage in the development of the seepage line as plotted in profile below. The upper graph consists of points describing the position of the seepage line base at approximately 8,000 time intervals. Minor numerical instability is evident in the "fuzziness" of the curves for dams with high upstream slopes (due to the sparseness of the FE mesh).

All graphs show the same parabolic form of curve for seepage line base displacement (top graph). The initial portion of the curve is steep, indicating that seepage into the dam is fastest at an early stage. Lower angled dams have a shallower seepage line slope, reflecting a reduced water velocity. This is due to the longer average seepage path length to the ponded water and a consequent reduction in potential gradient (head potential/seepage path length).

The seepage line profiles show how the angle of the upstream slope affects the seepage line entry angle. Water enters the dam at an angle normal to the slope. Hence, initially the curves for low angled slopes (< 45 degrees) are concave upwards, while high angled slopes (> 45 degrees) have convex upward seepage line profiles. However, at the end of their travel (L=10H) all the seepage line profiles are in an average sense minutely convex upwards, except the initial portion of seepage lines in low angled dams which are concave.

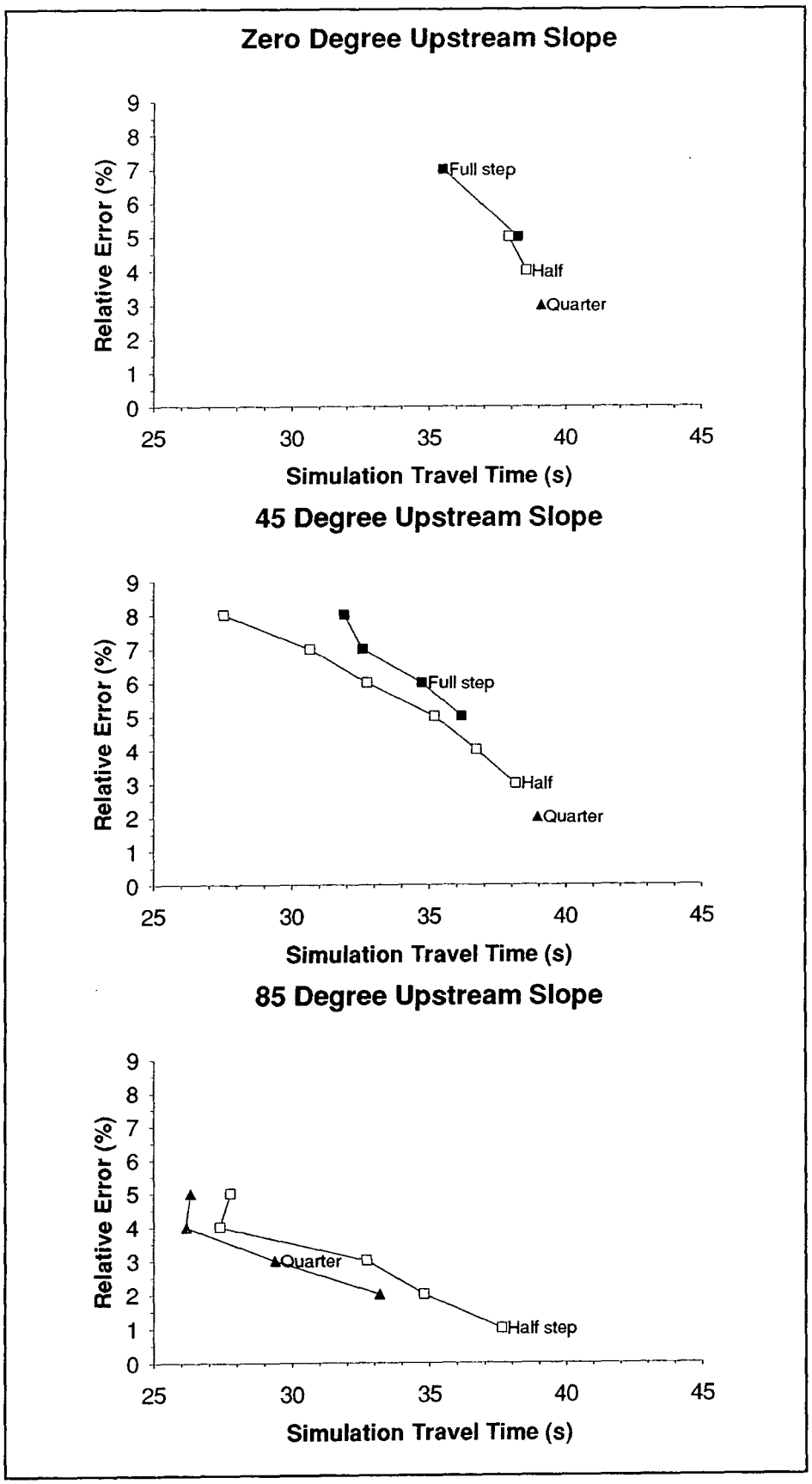

Figure 5.23 Accuracy and Time Step for Transient Solutions

In addition to the plots for simulations at below 3% relative error, a further plot for the slope of 85 degrees is presented for a relative error of below 1%. This plot differs significantly in the absolute travel time predicted in the simulation (37.63 seconds compared to 32.71 for 3% relative error). The seepage line profiles are similar, but slightly more curved. This supports the contention that the accuracy of seepage line movement depends on having sufficient degrees of freedom on the free boundary.

5.5.4. Analysis of Seepage Line Movement

The displacement of the base of the seepage line appears to follow the path of a translated parabolic equation (translated because the curve is not perpendicular to the x axis at its intersection). In order to model the seepage line displacement, first a simple analytical model is proposed. This model is used in a regression analysis to study the divergence of the approximate complex model (FE) from the exact simplified model.

Analytical Solution

From the numerical solutions it is evident that the seepage line profiles are approximately straight lines. It is assumed that this is indeed the case. By definition, the seepage line has a relative pore water pressure of zero (atmospheric). The head potential equals the sum of the pore water pressure divided by the unit weight of water and the elevation above the datum. As a consequence, the potential gradient at the base of the seepage line profile is equal to the slope of the seepage line at the base:

$$i_{base} = \frac{\delta h}{\delta x} = \frac{\delta y}{\delta x} = \frac{H}{x} \qquad \text{Eq. 5.18}$$

where i_{base} is the potential gradient, h is the head potential, x and y are the usual space coordinates (horizontal and vertical respectively) and H is the height of the dam water. The velocity of the seepage line depends on the permeability and effective porosity of the dam:

$$\bar{v}_{base} = \frac{\delta x}{\delta t} = \frac{ki}{n} \qquad \text{Eq. 5.19}$$

where $\bar{v}_{base}$ is the seepage line velocity in ms^{-1}, and k is the dam permeability in ms^{-1}.

The potential gradient at the base of the seepage line is equal at that point to the gradient of the seepage line. Combining Equations 5.18 and 5.19:

$$\frac{\delta x}{\delta t} = \frac{kH}{xn} \qquad \text{Eq. 5.20}$$

Integrating Equation 5.20, taking into account that x=0 at t=0:

$$t = \frac{n}{kH}\frac{x^2}{2} \qquad \text{Eq. 5.21}$$

Equation 5.23 describes the parabolic form evident in the numerical results.

Regression Analysis

The FE analysis does not assume that the seepage line forms a straight line. In addition, the angle of the upstream slope will have an influence on the real seepage line displacement. It is assumed, for the sake of the regression model, that the difference between the analytical model and the numerical results is an unknown slope factor λ. Furthermore, because the starting position for the numerical model was arbitrary, the problem will also be solved for initial values of x and t *at* (x_0, t_0) :

$$t - t_0 = \frac{\lambda n}{2kH}(x - x_0)^2 \qquad \text{Eq. 5.22}$$

Converting Equation 5.22 to simulation units (see Equation 5.17):

$$t^* = \frac{\lambda}{2}(x^* - x_0^*)^2 + t_0^* \qquad \text{Eq. 5.23}$$

Values of λ, x_0 and t_0 are presented together with the standard error for each equation as calculated (noting that for this simulation H=k=n=1 and so $x_0 \equiv x_0^*$ and $t_0 \equiv t_0^*$). The results were obtained using the nonlinear regression package NONLIN (Sherrod, 1992). The graphs were sampled at 0.2m intervals, giving 51 observation points for each analysis.

Slope Angle (degrees)	λ (dimensionless)	x_0 (m)	t_0 (s)	Standard Error (s)
0	0.66	-0.98	-0.50	0.078
15	0.67	-0.86	-0.41	0.085
30	0.66	-0.82	-0.37	0.074
45	0.66	-0.69	-0.27	0.055
60	0.61	-0.90	-0.49	0.122
75	0.59	-0.81	-0.44	0.107
85	0.56	-0.85	-0.48	0.157
85*	0.73	-0.17	-0.05	0.025

* 1% Relative Error

Table 5.12 Regression Analysis of Slope Angle Effect on Seepage Line Displacement

Despite the goodness of fit, the x_0 and t_0 values exhibit an unexpectedly wide variation. It would be expected that both x_0 and t_0 would decrease as the dam slope angle increases (and the seepage path length decreases). For high angled upstream slopes, the value of x_0 would be expected to be approximately equal to the distance between the base of the slope and the perpendicular dropped from the dam-side pond edge. The solution for 1% relative error is included for the 85 degree slope angle dam. It is clear that this simulation gives a more satisfactory answer for x_0 and t_0 ; the value of -0.17m for x_0 compares better with the 0.09m distance between the base of the slope and the starting position. The difference between the 3% and 1% relative error for this case reflects the lower accuracy in the time step routine for steep angled dams (page 185).

It is recommended that the value of x_0 is taken as $-H\cos\alpha$ (where H is the height of water in the dam, and α is the upstream slope angle). The rationale behind this is that the value loosely fits the figures for x_0 obtained from the finite element simulations, and it represents the shortest distance between the reservoir and the point at which the numerical simulations were initiated.

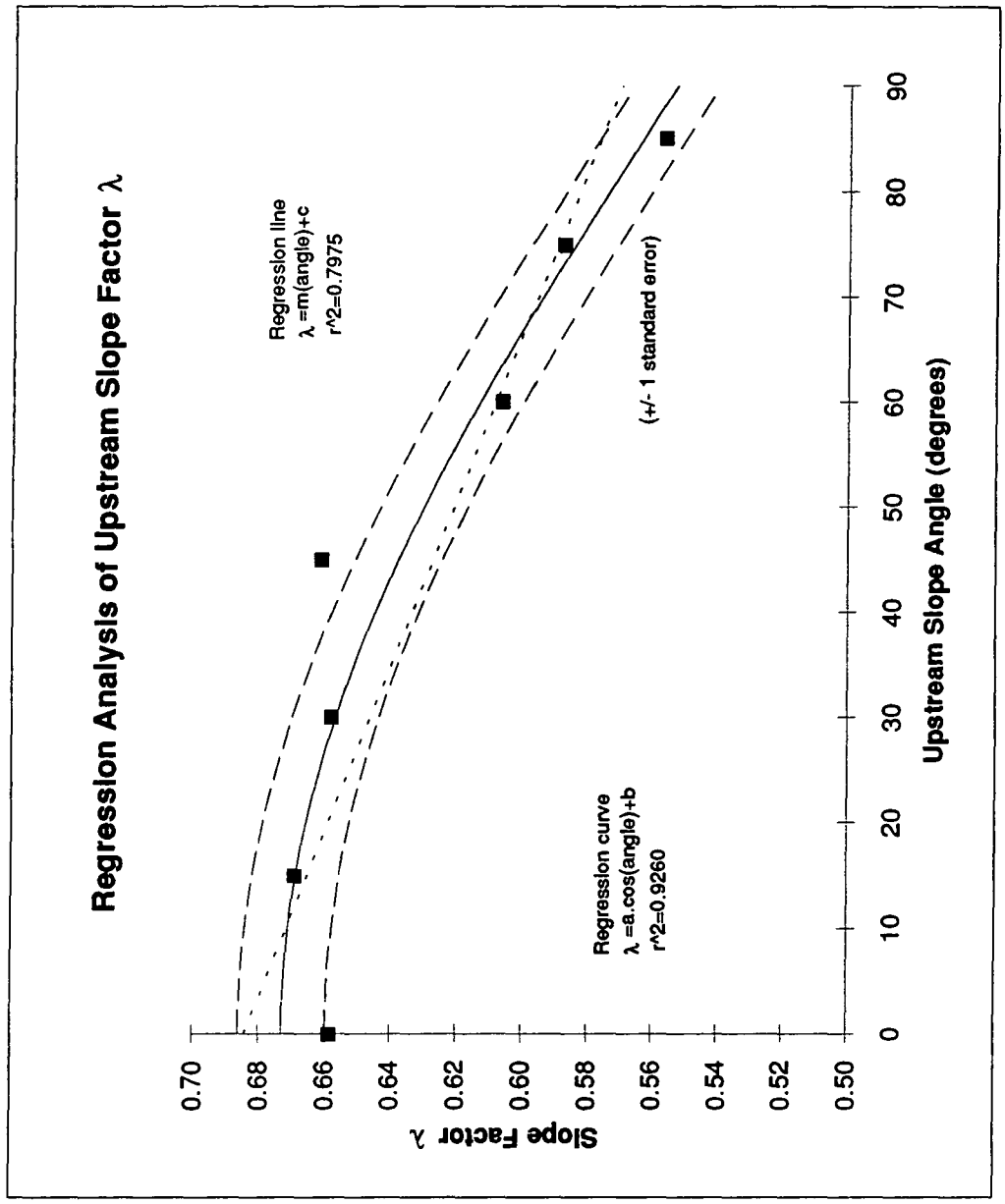

Figure 5.24 Regression Analysis of Upstream Slope Factor λ

The slope influence factor λ shows a more consistent variation than do the values of x_0 and t_0. A second regression analysis was performed to obtain an equation relating the slope influence factor with the slope angle α. The equation should fulfil the following criteria:

- Values of λ should decrease monotonically for increasing slope angle.
- Variation of λ should be low for low values of α and high for high angles.

The reason for the first objective is obvious; the velocity of the seepage line must increase as the average path length for flow decreases. The second objective is based on a visual interpretation of the data. By a process of trial and error using the NONLIN regression program, Equation 5.24 was found to give the best fit (see Figure 5.24). The best fit line through the data is also given for comparison. The curve of Equation 5.24 (for the analysis at 3% relative error) has a coefficient of multiple determination of 0.9260, which is significantly different from the value of 0.7975 for the straight line fit.

$$\lambda_{3\%} = 0.12\cos\alpha + 0.55 \qquad \text{Eq. 5.24}$$

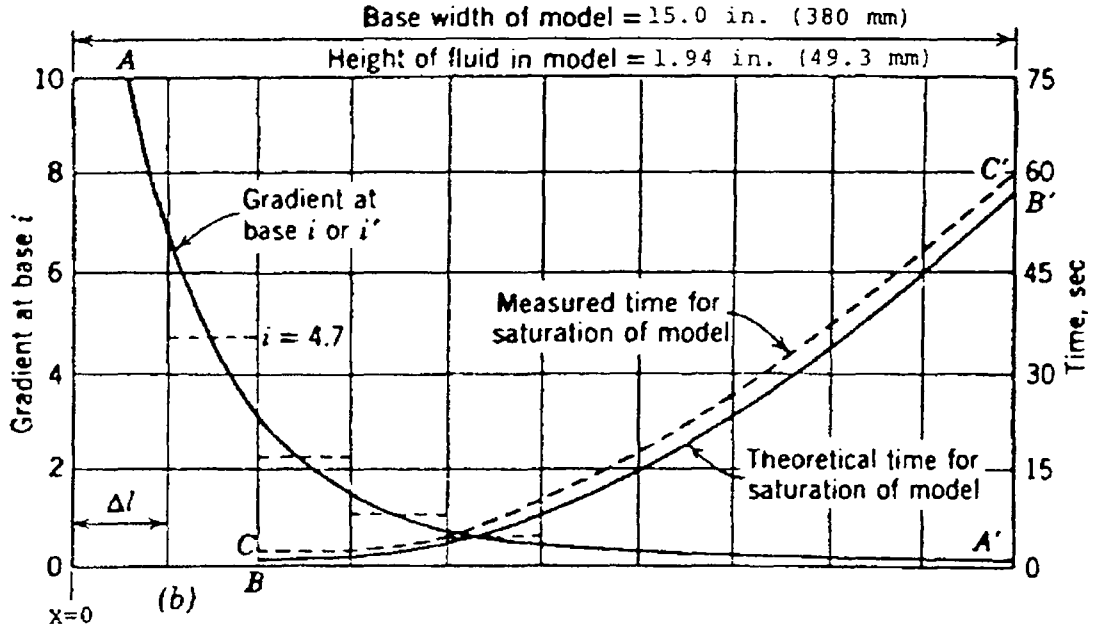

Figure 5.25 Hydraulic Gradient and Time for Saturation - Theory and Model

(from Huang [1986], after Cedergren [1977])

5.5.5. Comparison with Huang's Method

Huang (1986) proposed an approximate solution for transient flow in an earth dam based on a transient flow net solution (Cedergren, 1977). Huang's model was based on a dam with an upstream gradient of 2:1, although it was claimed that the solution could be safely extended to other geometries by making conservative assumptions concerning the flow regime. Huang assumed that the seepage line may be approximated by a straight line. A chart of hydraulic gradient against distance travelled for the seepage base was constructed from a viscous flow model (see Figure 5.25). The dam concerned was divided into vertical strips, and the time taken for the seepage line to travel through each strip was calculated from the strip length, permeability, effective porosity and hydraulic gradient read from the chart (see Equation 5.16).

Huang (1986) used his approximate solution to model the flow through a simple dam geometry (see Figure 5.26).

Huang's example is solved in order to demonstrate a calculation of seepage line movement by the proposed method, and provide a comparison of results. Note that Huang's solution is derived from a flow analogue, not an analytical solution.

Q. Figure 5.26 shows a temporary dam on a horizontal impervious base. The dam has a permeability of 9.1×10^{-7} ms^{-1} and an effective porosity of 0.2. If the dam is used for only 5 years, determine the location of the unsteady state seepage line at the end of the fifth year.

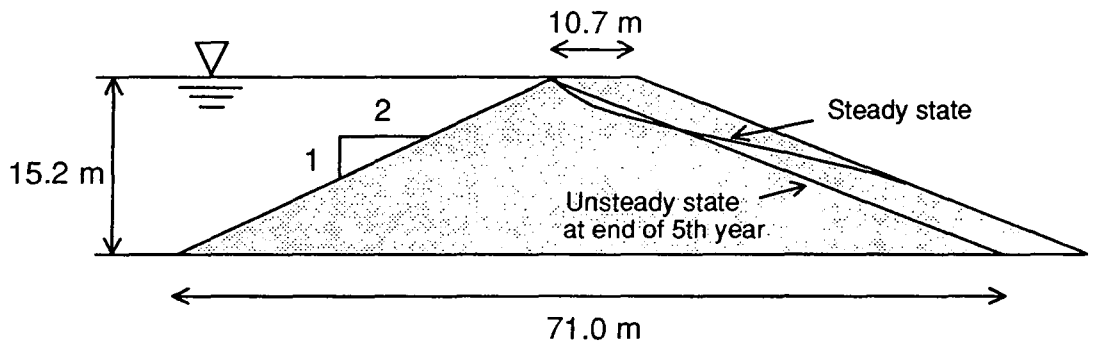

Figure 5.26 Location of the Free Surface using Huang's Method

(adapted from Huang, 1986)

A. First the time (t) is transformed to obtain a solution for a problem with a permeability (k) of 1 ms^{-1}, height (H) of 1 m, and a transformed time of t* in seconds:

$$t^* = t \times \frac{k}{nH} = 5 \times 365 \times 24 \times 60 \times 60 \times \frac{9.1 \times 10^{-8}}{0.2 \times 15.2} = 4.72s.$$

This represents the total time, including the time required to achieve a vertical seepage surface. The upstream slope factor λ is calculated from Equation 5.24:

$$\lambda = 0.12\cos\alpha + 0.55 = 0.657$$

Equation 5.23 is used to calculate the distance travelled from the unknown equivalent starting position in the transformed units:

$$x^* = \sqrt{\frac{2t^*}{\lambda}} = \sqrt{\frac{2 \times 4.72}{0.657}} = 3.79$$

Finally, the distance is multiplied by the dam height (15.2 m) to give a preliminary answer of 57.6 m. This is the distance travelled along the base from the vertical seepage line position plus the equivalent distance from the pond to the vertical position. To calculate the equivalent starting position, the following approximation is used:

$$x_0 = -H\cos\alpha = -15.2 \times 0.8944 = -13.6$$

The distance travelled from the base of the upstream slope is therefore

57.6-13.6+(15.2×2)=74.4 m.

The answer computed by Huang for this problem is 71.0 m, about 5% lower.

5.5.6. Conclusions

- The curves for the seepage line base movement (Appendix 4) show that displacement is proportional to the square root of the time elapsed.
- The time stepping routine used in the algorithm is shown to be sensitive to the FE mesh density and size of time step.
- Figure 5.23 suggests that simulations performed at 3% relative error may overestimate the distance travelled by the seepage line base by as much as 10%. This means that the equation should give a conservative (more advanced) estimate of the position of the seepage line.
- The influence of the upstream slope angle may be taken into account using Equation 5.24. The initial point from which to calculate the seepage line movement has not yet been clearly defined, but it is suggested that x_0 should be taken as $-H\cos\alpha$ (where H is the height of water in the dam, and α is the upstream slope angle measured from the base) from the point on the base directly below the dam-side edge of the pond. Equation 5.24 is not suitable for the early stages of flow development when the seepage line is inverted or sharply inclined.
- In the early stages of flow development, the form of the seepage line is strongly dependent on the upstream slope angle. After the seepage line base has travelled twice the height of the dam, the seepage lines are almost straight (before they meet the downstream face of the dam and a seepage surface develops).
- The regression model based on the FE data gives a similar value for seepage line base displacement to results obtained using Huang's method (Huang, 1986). The advantage of the method presented here is its ability to model any upstream slope of between zero (tailings dam geometry) and 90 degrees. It should also be noted that results of the FE program have also been compared favourably with experimental and numerical results presented by France et al (1971) for a transient problem (in a previous section).

5.6. Transient Analysis of Flow through a Downstream Construction Tailings Dam with a Gradual Lagoon Fill

The previous analysis concerning the transient flow of water through an earth dam assumed that the reservoir is filled instantaneously. Even in a water retaining dam this is unlikely to be true. In the case of a tailings dam it is extremely unlikely. Chapter 2 describes how a tailings dam is constructed in stages while tailings are being placed behind the embankment. This section considers how three factors affect the movement of water within the dam:

I. Rate of rise of the tailings pond

II. Permeability of the tailings embankment

III. Effective porosity of the tailings embankment.

5.6.1. Model Assumptions

The object of the analysis is not to provide a universal solution for the transient flow condition for a tailings dam. Accurate solutions are only possible when the particular site conditions are adequately modelled. Rather, the object is to look for general properties of the transient state:

- Form of the seepage line.
- How the **relative** rate of movement depends on the factors simulated.

Various assumptions are made once again to limit the number of parameters involved in the simulation.

- The foundation is deemed to be impervious to the flow of water. This is a conservative assumption as long as artesian conditions do not prevail (Brawner and Campbell, 1973). If drainage measures such as pipes, a drainage blanket or even a drainage toe are in place, then the advance of the seepage line may be halted within the dam.
- The tailings are assumed to be homogeneous and isotropic. This restriction would seem to be a quite serious one, as tailings are generally not homogeneous and the analysis is only directly relevant to the downstream construction geometry (see Chapter 2). In the downstream construction technique, the properties of materials used in the construction of the tailings dam are controlled by the engineer. Commonly, coarse mine waste, cycloned sand or borrow is used to build the dam; these materials will not show the variation seen in the permeability of the tailings. The dam construction materials are laid down at as low a moisture content as

possible (subject to adequate compaction) (NCB, 1970). Tailings are saturated at the point of deposition and do not slow down the passage of the seepage line (this simulation assumes that the water from the pond is adequate to replenish free draining water in the tailings). In the upstream construction tailings dam, the dam zone may be very narrow and the dam material itself may be laid down wet (hydraulic cell construction, e.g. Nyren et al, (1978)). An upstream embankment does not in general provide a long term check to the development of the seepage line; the steady state analyses are more appropriate.

- The pond is kept at the same position throughout the life of the dam. This condition is necessary to provide a general solution to the problem. The pond itself is considered to be of negligible depth.

5.6.2. Numerical solution

The problem pictured below in Figure 5.27 was simulated using the FE program. All the analyses were carried out with less than 3% relative error for each FE mesh. It is assumed that the error in the time stepping algorithm is of the same magnitude as the case with a constant height of reservoir. The starting conditions for the simulation are a 1 metre high lagoon having a vertical seepage line. The simulation was stopped when the lagoon had reached a height of 20 metres. The introduction of two time-based parameters (permeability and lagoon fill rate) preclude a single scaleable solution to the problem. As in the previous section, the permeability is divided by the effective porosity to provide a single flow parameter. The range of permeability/porosity ratios was bounded by considering what would be a reasonable minimum value in a British Coal dam , and what ratio would be considered relatively impermeable over a 20 year period ($10^{-8}ms^{-1}$). The values for lagoon fill rate (1, 2, 3 & 4 metres/year) straddle the typical fill rate of 2 metres per year in a British Coal dam (Bacon, 1987).

The graphs plotted for distance travelled/time and the profiles of the seepage line at discrete values for seepage line base displacement are in Appendix 5. After a short initially curved section, they all indicate that the rate of movement of the seepage line is nearly constant. The seepage line reaches a dynamic equilibrium with the rising lagoon level; the increase in hydraulic gradient due to the rise in lagoon height equals the drop in hydraulic gradient due to the increase in seepage path length. The gradients calculated for the linear sections of the graphs are presented in Table 5.13.

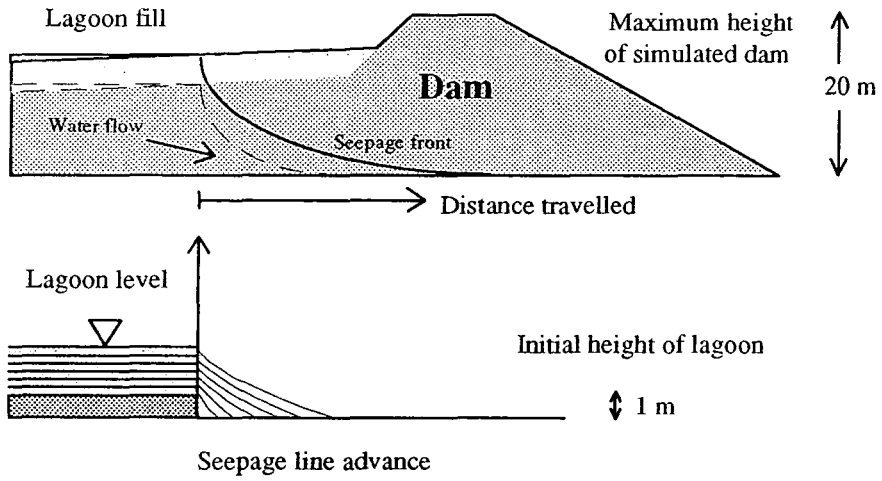

Figure 5.27 Transient Flow through a Tailings Dam with Gradual Lagoon Fill

All the seepage line profiles are to some extent concave upwards. The trend is for seepage lines in dams with lower permeability/porosity ratios and higher lagoon fill rates to be more concave. This relationship is difficult to quantify because a mathematical function chosen to describe the magnitude of the seepage line concavity would not help in visualising the data. An arbitrary boundary would have to be chosen to distinguish those curves which were concave, but would be described by an engineer as approximately straight. Besides, the engineer is interested in the form of the seepage line in relation to the whole dam. Even a convex upward seepage line which had progressed only a little way through the dam would appear to be low (and concave) for most of the dam's length to an engineer observing from the surface (see line X-X' in Figure 5.28).

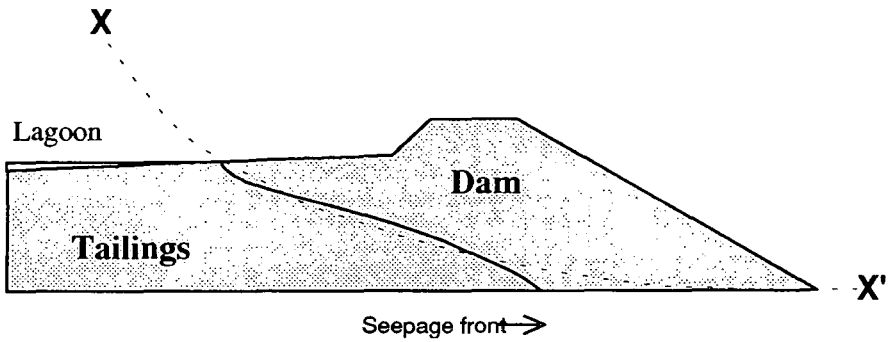

Figure 5.28 Apparent Concavity of Transient Seepage Line

Rate of Lagoon Fill (m/year)	Permeability/Porosity Ratios (ms^{-1})				
	1×10^{-6}	5×10^{-7}	1×10^{-7}	5×10^{-8}	1×10^{-8}
1	5.1	3.63	1.52	1.02	0.36
2	7.35	5.03	2.04	1.33	0.44
3	8.83	6.1	2.39	1.52	0.49
4	10.09	6.91	2.66	1.9	0.54

Table 5.13 Rate of Advance of Seepage Line in a Tailings Dam with Gradual Rise of Lagoon

5.6.3. Analysis of Results

The values of the gradient (or seepage line base velocity v) of the linear section of each of the 20 distance/time graphs is plotted against the permeability/porosity (k/n) being considered. (see Figure 5.29). The permeability/effective porosity ratio has been placed on the x-axis to allow the calculation of a quadratic curve of the form:

$$k/n = a_0 v + a_1 v^2 \qquad \text{Eq. 5.25}$$

The form of this curve was calculated for each of the four lagoon fill rates (R). It would have been preferable if the independent variable had been on the right-hand side of the equation. A least squares best fit regression analysis indicated that all four of the curves have correlation coefficients (r^2) in excess of 0.999 (for 5 data points).

The four curves of Figure 5.29 appear to follow a general trend. However, it proved impossible to construct a polynomial equation of the form:

$$k/n = a_0 v + a_1 v^2 + a_2 R + a_3 R^2 + a_4 vR \qquad \text{Eq. 5.26}$$

which would provide a good model for the data.

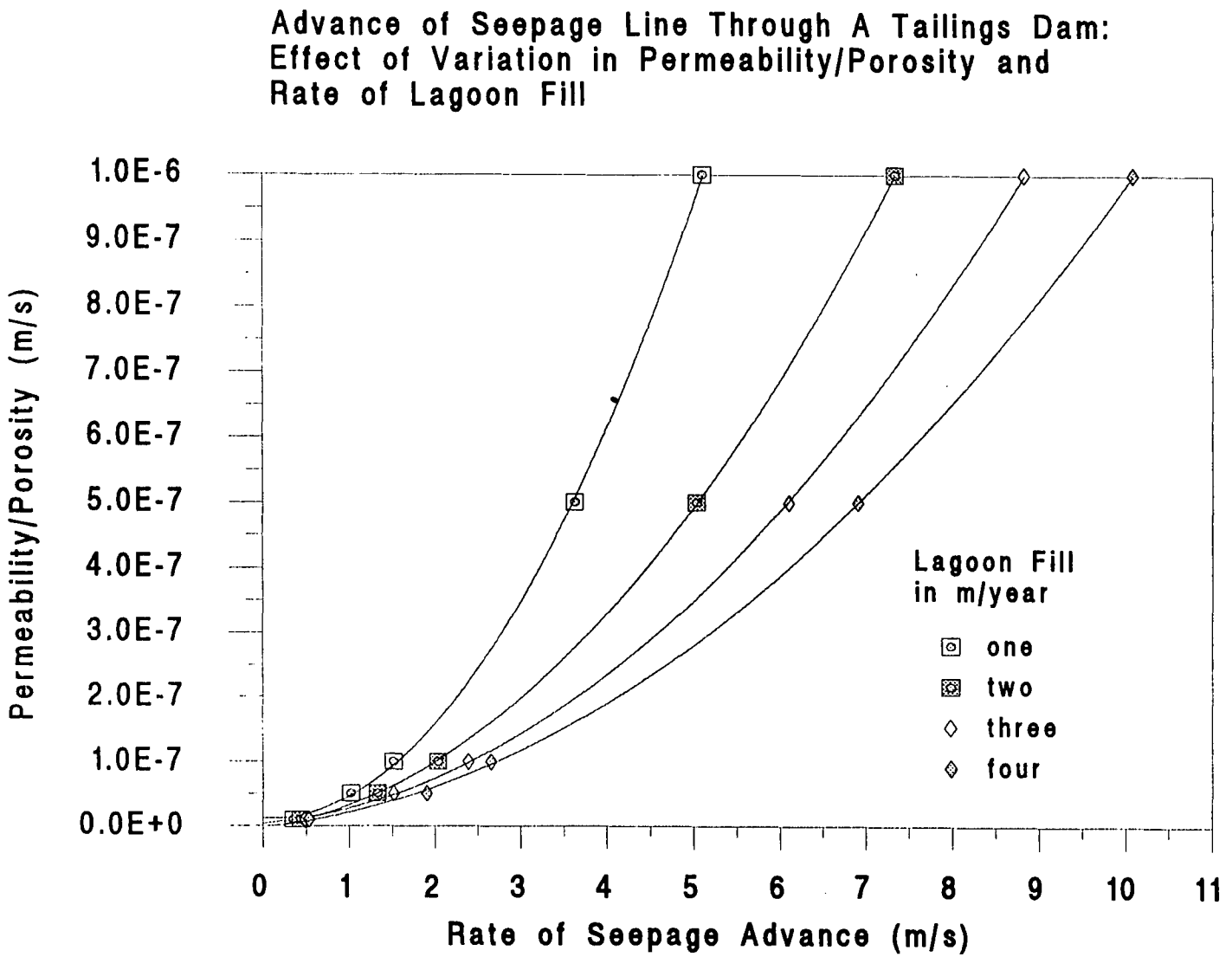

Figure 5.29 Graphs of k/n against Seepage Base Velocity for 4 Lagoon Fill Rates

The data were analysed using an automatic least squares program written by Dr Steve Lavelle (Research Assistant in the School of Engineering and Computer Science at Durham University). The program searches for linear combinations of the variables, their ratios, and transformations (logarithms and so on) which act as good predictors for the independent variable. The best fit (least squares) equation was found to be:

$$k/n = \frac{b_0 v^2}{R} + b_1 v + \frac{b_2 v}{R}$$

$$b_0 = 0.034 \times 10^{-6}$$
$$b_1 = 0.011 \times 10^{-6}$$
$$b_2 = 0.007 \times 10^{-6}$$

$$\begin{bmatrix} 10^{-6} \leq k/n \leq 10^{-8} \\ 0 < v \leq 12 \\ 1 \leq R \leq 4 \end{bmatrix} \qquad \text{Eq. 5.27}$$

where k is the permeability (ms^{-1}), n is the effective porosity, v is the velocity of the seepage line base (m/year), and R is the rate of lagoon rise (m/year). The regression statistics for this analysis are presented in Table 5.14.

$k/n = \frac{b_0 v^2}{R} + b_1 v + \frac{b_2 v}{R}$				
Number of Points	**Standard Error**	**Average Deviation**	**Maximum Deviation**	**r^2**
20	0.0097×10^{-6}	0.0056×10^{-6}	0.024×10^{-6}	0.9994

Table 5.14 Regression Statistics for Seepage Line Advance in a Tailings Dam with an Increasing Lagoon Height

The coefficient of multiple determination (0.9994) for 20 data points shows a very strong fit for the equation. The maximum deviation of the data from the equation occurs for the highest permeability. The percentage error between the equation and the data is never more than 2.5% and is most commonly less than 1%.

Unfortunately, this equation is not expressed in terms of the independent variable (seepage line base velocity). The least squares regression algorithm is designed to measure the distance between a function and the independent variable. Where the error term in the regression is very low (as in this case), the inaccuracy introduced by an arbitrary choice of a dependent variable on the right hand side is not significant.

Equation 5.27 can be used as an interpolating function for the FE data. It is not a predictive model outside the bounds of the FE analysis. For example, if the lagoon fill rate is very low, then Equation 5.27, which has the lagoon fill rate as the denominator, cannot be used. In this case, the previous analysis with a fixed lagoon level is more appropriate. The model can only deal with cases where the dynamic equilibrium of seepage base movement and lagoon fill is achieved. Conversely, the model may well be applicable for much larger lagoon fill rates, but these have not been tested.

A graph is presented in Figure 5.30 to allow a solution to Equation 5.27 via a graphical method. The vertical axis (permeability/effective porosity) is also contoured on the *xy* plane (Seepage rate and lagoon fill rate). The following instructions describe how to obtain a seepage rate for the seepage line base point:

(1) Mark the lagoon fill rate axis at the value of fill rate to be investigated.

(2) Place a straight edge on the value marked on the lagoon fill axis in (1) and draw a line parallel to the seepage rate axis.

(3) Find or interpolate the appropriate permeability/porosity contour (some of these have been numbered with the corresponding value) and mark the intersection of the interpolated contour and the line drawn in (2).

(4) Draw a line through the point marked in (3) parallel to the lagoon fill rate axis.

(5) Read off the seepage rate value at the intersection of the line marked in (4) and the seepage rate axis.

5.6.4. Conclusions

The transient seepage line in a homogeneous and isotropic tailings dam with a rising lagoon (>1m/year) and having an intermediate to low permeability/effective porosity ratio ($<10^{-6}$ ms^{-1}) has a concave upward form. Taking the whole dam into account, this concavity is greatly exaggerated.

The velocity of the seepage line base in a tailings dam with increasing lagoon height (and within the limits examined) is (after an initial short period of equilibration) constant for a particular permeability/porosity ratio and lagoon fill rate.

Figure 5.30 Seepage Line Advance in a Tailings Dam

Chapter 6
Conclusion

This conclusion covers four aspects of the work of this thesis:

(1) Seepage line profile in a tailings dam

(2) Regression equations obtained from the finite element analyses

(3) Finite element program

(4) Future work.

The findings of previous chapters in the thesis are summarised in the following sections.

6.1. The Profile of the Seepage Line in a Tailings Embankment

The object of this thesis has been to ascertain which factors are responsible for the low seepage line commonly found in the tailings dam compared to that of a regular earth dam. Research has been directed primarily at a design of tailings dam used by British Coal. This type of dam merits new research because the dam is constructed of coarse waste at a relatively low moisture content. Transient flow conditions may exist within the embankment if the dam is of a sufficiently low permeability. Many of the factors which may be important for both earth and tailings dams (e.g. accretion and evaporation rates, unsaturated flow, general groundwater conditions and so on) have been ignored. This is valid for a study of the relative importance of the other factors in the general case, but a more complete analysis should be undertaken for a specific tailings embankment.

The factors which have been simulated are:

- Embankment Geometry
- Permeability
- Transient Flow Development.

6.1.1. Embankment Geometry

One of the most important controls on the position of the seepage line within a tailings embankment has proved to be the distance between the pond and the downstream slope.

The beach between the pond and dam extends the effective length of the dam, lowering the seepage line in the downstream portion.

This thesis has shown that for a long dam and/or beach, the upstream angle has little effect on the position of the seepage line (except in a small section adjacent to the pond). Although in a short dam having a low upstream angle, the seepage line may be concave, in the general case the seepage line is convex within homogeneous sections of the dam.

Dams having a lower downstream angle have a higher seepage line for the same dam base length (under steady state conditions). If the angle of the downstream slope is lowered (by the emplacement of additional material of a similar permeability) to improve slope stability or decrease seepage, then the eventual steady state height of the seepage line will be higher. However, the seepage line takes longer to achieve this position.

6.1.2. Permeability

The effect of permeability on the seepage line is seen to be equivalent to changing the effective length of the flow path. Kealy & Busch (1971) investigated the influence of lateral variation in permeability for the case of the upstream construction method. This study confirms that an increasing downstream permeability causes the seepage line to become progressively less steep (in the direction of flow). This effect is stronger for longer beach lengths even for the same permeability ratio (ratio of downstream to pond slime permeability). At some critical permeability ratio, the effect of changing permeability counteracts the "natural" convex shape of the seepage line and a concave upwards form develops.

The step change in permeability which occurs in the case of a downstream construction dam had not been thoroughly investigated before this thesis. A large jump in permeability from the tailings to the dam causes a steep fall of the seepage line within the tailings (from the pond to the tailings/dam interface). The fall of the seepage line within the tailings may be concave upwards, despite the fact that the permeability is treated as constant within the tailings themselves. This concavity is due to a combination of factors:

- Vertical fall of the seepage line at the edge of the pond.
- Lateral compression of the seepage line (compared to the homogeneous transformed section for the entire structure).
- Shortening of the flow lines through the tailings to reach the extended upstream "toe" of the dam.

The steepness of the seepage line in the tailings and its low level in the dam increase the apparent concavity (as observed from the surface).

The study confirms the assertion by Abadjiev (1976) that anisotropic dam permeability (greater horizontal than vertical permeability) raises the seepage line by no more than 10%. Moreover, it has been shown that, in the case of a downstream tailings dam, the anisotropy of the tailings (if we take the vertical permeability to be reduced relative to the horizontal permeability) has a depressing effect on the level of the seepage line within the dam. This effect is due to the overall reduction in seepage discharge in the upstream section of the embankment where the flow of water is directed downwards.

Vick (1983) suggested that the vertical variation of permeability due to the consolidation of the tailings was unlikely to have a significant effect on the position of the seepage line. This thesis has shown this to be the case where the foundation is relatively impervious to flow. The presence of low permeability tailings below the pond concentrates the flow of water at the dam-side edge of the pond. The tailings at the base of the embankment play a lesser role in determining the flow pattern. Where the foundation is much more permeable than the tailings structure, the flow pattern within the embankment may be changed from one being predominantly horizontal to one that is vertical (within the tailings structure). The seepage line becomes highly concave upwards in shape.

6.1.3. Transient Flow Development

If the tailings lagoon remains at the same level for some extended period of time, then the seepage line's rate of movement decreases as it moves through the dam. This result is widely recognised, having been observed in flow models and predicted by theoretical and numerical models. The seepage line may be concave upwards in the early stages, but will be straight (in homogeneous dams) by the time it has travelled twice the height of the dam. The model confirms that the common assumption of a straight (transient) seepage line is a reasonable approximation for a homogeneous dam.

For a rising lagoon (greater than 1 metre per year) and tailings of intermediate to low permeability/porosity ratio (less than 10^{-6} ms^{-1}), the seepage line is concave upwards.

The rate of movement of the seepage line remains almost constant (for a homogeneous dam) except for a short initial period.

The concavity of the seepage line is much greater if the whole length of the dam is considered; this is because of the combination of a fairly steep concave seepage line and a flat dam base.

As the transient seepage line is straight or concave upwards, the seepage surface will develop up from the toe in the case of a homogeneous dam without benches.

6.1.4. Determining Factors

From the factors of embankment geometry, permeability and transient flow development, the main causes for a concave seepage line are (in order of importance):

- A highly permeable base (relative to the tailings structure). This effect is significant if the tailings do not consolidate to form a low permeability barrier to flow (Kealy & Busch, 1971).
- Transient development of the seepage line in the case of downstream construction and a relatively impermeable dam.
- Tailings having a lower permeability than the dam (in the case of a downstream dam construction).
- Tailings decreasing in permeability from the dam to the pond (due to method of tailings disposal).

The effective length of the dam (dam length plus beach) has a crucial effect on the strength of these factors (excluding the first). Maintaining a long beach is the best way of reducing the height of the seepage line.

Two factors of a lesser importance are:

- Anisotropy of tailings permeability
- Upstream slope angle in the case of a short dam (e.g. upstream tailings construction).

Special drainage measures may also affect the position of the seepage line. A semi-permeable slimes barrier placed on the upstream slope is equivalent to increasing the effective length of the dam, reducing the level of the seepage line within the dam. A drainage blanket laid under the dam and/or the tailings is equivalent to a permeable foundation described earlier. With an effective drain, the seepage line can be expected to be much reduced, even completely failing to exit the downstream face of the dam.

6.2. Seepage Line Prediction from FE Regression statistics

Four equations to predict the seepage exit point height or position have been presented in the thesis. The merits and limitations of these formulae are discussed in the following sections.

6.2.1. Seepage Line Exit Height in an Earth Dam

An old relationship between the seepage exit height and the seepage discharge/permeability ratio for an isotropic and homogeneous dam on a horizontal impermeable base (without drainage measures) has been rediscovered.

Figure 6.1 below shows the geometry of the downstream portion of an earth dam.

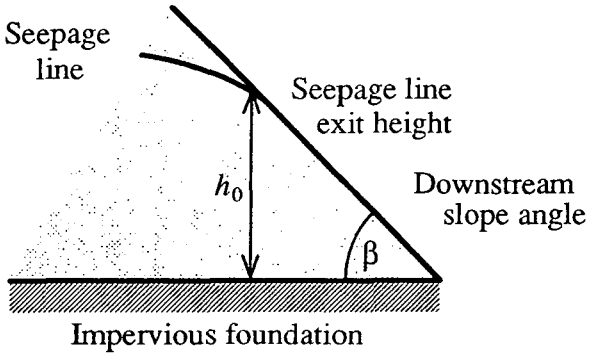

Figure 6.1 Seepage Exit Height in Homogeneous Isotropic Earth Dam

The equation based on a regression analysis of the finite element results is shown below:

$$q/k = \lambda\beta h_0 \qquad 0° \le \beta \le 90° \qquad \text{(Eqns. 5.13 \& 5.14)}$$
$$\lambda = 0.0149$$

where q is the seepage discharge (m^3s^{-1} per metre width), k is the permeability (ms^{-1}), h_0 is the seepage exit height (m), and β is the downstream slope angle (degrees).

For this range of downstream slope angles, the FE regression equation is approximately equal to the gradient of 0.0143 calculated analytically by S.V. Falkovich (in Polubarinova-Kochina, 1962, pp 307-307) for slope angles between 0 and 80 degrees. The FE regression equation is superior to the conventional formulae in all respects; it is simple, more accurate and more general. Its only deficiency is in the prediction of the

seepage line exit height for a short dam (i.e. when the dam length is shorter than the dam height) with a steep downstream slope (greater than 60 degrees). For these conditions, the FE regression equation is still superior to the Schaffernak and Casagrande formulae. The FE regression equation is also applicable when only the downstream portion of the dam may be considered homogeneous and isotropic.

The equation contains two unknown variables (seepage discharge and seepage line exit height) for most problems of common interest. The following section presents a second equation which may be used to calculate a complete solution.

6.2.2. Seepage Discharge in an Isotropic and Homogeneous Earth Dam

A new equation with which to calculate the seepage discharge through an isotropic and homogeneous earth dam (with an impervious horizontal base and no drainage measures) has been presented. The equation is based on the Dupuit solution for flow through an earth dam. Slope factors are incorporated into the equation to take into consideration the upstream and downstream dam slopes. When the dam slopes are vertical, the slope factors disappear and the result obtained is the analytically correct solution.

The FE regression equation obtained (see below) refers to the dam geometry pictured in Figure 6.2.

$$q^* = \frac{1 + 0.84 h_0^{*2} \cos\beta}{2\left(\ell^* + 0.518\cos\alpha + \cot\beta\right)} \qquad \text{(Eq. 5.15)}$$

where q^* is the seepage discharge/(permeability×dam height) per unit width (q/kH), h_0^* is the seepage exit height/dam height ratio (h_0/H), ℓ^* is the effective crest length/dam height (ℓ^*/H), and α and β are the upstream and downstream slope angles, respectively.

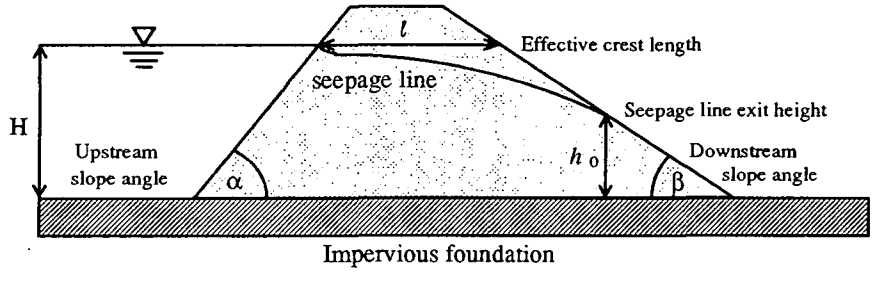

Figure 6.2 Earth Dam Geometry

The above equation may be combined with the relationship between the seepage discharge, permeability and seepage line exit height to obtain both seepage discharge and seepage exit height. The equation obtained is a rather involved quadratic formula which can be solved directly without iteration. As an alternative, an iterative method (similar to that used in a programmed solution to Schaffernak's or Casagrande's method) may be used to obtain the two unknown values simultaneously.

The regression model fits the finite element data almost exactly. The calculated values for seepage discharge are particularly accurate. The established equations of Schaffernak and Casagrande do not correlate well with the finite element data, although they are closer to the FE data than they are to each other. These other methods provide solutions in only a limited range of circumstances (combinations of upstream slope angle, downstream slope angle and crest width).

The flow nets obtained from the program provide an independent visual check to the accuracy of the finite element data. The program has obtained the analytically correct solution (to a reasonable degree of accuracy) when such a result was known. Consequently, there is no reason to doubt that the equations presented offer a significant advance over the previous approximate solutions.

6.2.3. Seepage Line Advance for a Fixed Level Reservoir

The computer simulations have shown a consistent relationship between the permeability and porosity of the dam, the height of the reservoir, the angle of the upstream slope, and the rate of advance of the seepage line through the partially saturated dam. A method of interpolating the finite element results for an isotropic and homogeneous earth dam resting on a horizontal impervious base (see Figure 6.3), has been presented in equation form:

$$x = H\left(\sqrt{\frac{2t^*}{\lambda}} - \cos\alpha\right)$$

$$\text{where} \quad t^* = \frac{tk}{nH} \qquad \text{(Eqns. 5.23 \& 5.24)}$$

$$\lambda = 0.12\cos\alpha + 0.55 \ ,$$

and where x is the distance travelled from the perpendicular dropped from the dam-side pond edge (in metres), t is the time passed since filling the reservoir (in seconds), H is

the effective height of the dam (m), k is the permeability (ms^{-1}), and n is the effective porosity of the dam.

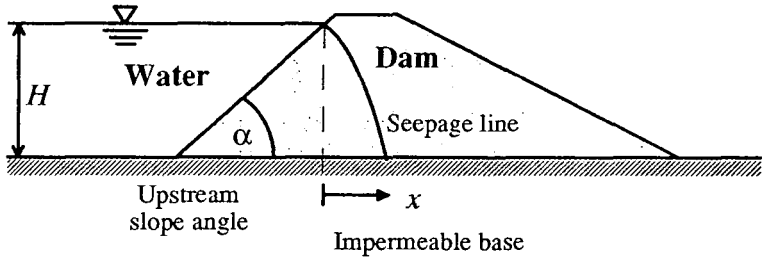

Figure 6.3 Transient Flow in an Earth Dam

The indications are that this model is slightly conservative. The equation has given a result which is in good agreement with the solution of Huang (1986) for a dam with an upstream slope of 2:1. The advantage of this solution is that it may be used for dams of any upstream slope (between 0 and 90 degrees), including the tailings dam geometry. Although the equation is not directly applicable to inhomogeneous dams, it may be possible to extend the solution to a transformed dam section based on the difference in permeability/effective porosity ratios.

The single biggest drawback of the model is the difficulty in obtaining data for the ratio of permeability to effective porosity. It is expected that any error in the model will be far outweighed by the problem of determining accurate average material properties. However, the prospect does exist for using this theoretical model to perform back analyses with either field or model problems in order to obtain the appropriate lumped values.

6.2.4. Seepage Line Advance for a Downstream Tailings Embankment

Two important factors differentiate the development of the seepage line within a tailings dam and a water retaining dam.

- Tailings dams have a very shallow "upstream slope" because the ponded water rests on top of tailings deposits.
- The tailings dam lagoon rises monotonically throughout the lifetime of the structure.

The finite element results predict that the base of the seepage line in a tailings dam (under these conditions of rising pond level and for the range of material properties considered) will move at a constant rate.

The following equation relates the permeability/effective porosity ratio, the rate of seepage line advance and the rate of lagoon rise:

$$\frac{k}{n} = \frac{b_0 v^2}{R} + b_1 v + \frac{b_2 v}{R}$$

$$\text{where} \quad b_0 = 0.034 \times 10^{-6} \qquad \begin{bmatrix} 1 \le R \le 4 & \text{m/year} \\ 10^{-6} \le k/n \le 10^{-8} & \text{ms}^{-1} \end{bmatrix} \qquad \text{(Eq. 5.27)}$$

$$b_1 = 0.011 \times 10^{-6}$$

$$b_2 = 0.007 \times 10^{-6} \ ,$$

and where k is the permeability (ms^{-1}), n is the effective porosity, v is the velocity of the seepage line base (m/year), and R is the rate of lagoon rise (m/year). Note that the units in this formula are mixed because these are the natural units of measurement, and a consistent system of SI units produces an equation involving very small numbers.

For low rates of lagoon rise, the dynamic equilibrium between seepage line advance and pond level cannot be maintained and the model breaks down. In this case, the previous analysis using a fixed pond level should be used as an alternative. The equation could be used for higher rates of lagoon rise. However, the equation is not based on any theoretical considerations and so such an extrapolation may not be as accurate outside the bounds of the FE analysis.

The upper limit for the ratio of permeability/porosity is not likely to be exceeded in British tailings dams. If a dam is built of material with a higher ratio, then the preceding warning against extrapolation of the results outside the problem set must be reiterated. The lower limit of permeability/porosity ratio may well be exceeded, but in this case the rate of advance is so slow that the movement of the seepage line is unlikely to be significant within the lifetime of the dam.

As in the previous equation, the formula presupposes that there is accurate enough data from which to calculate the rate of seepage line advance. In addition, the management of tailings disposal will have a direct effect on the seepage line advance. The actual rate of lagoon rise will not be constant and the mode of tailings disposal will also affect seepage within the dam. The most valuable contribution of this aspect of the study is the prediction that the advance of the seepage line will not necessarily slow down (as it would in the case of a fixed level water retaining dam).

6.3. The Finite Element Program

The variable mesh free surface method has been successfully combined with an automatic adaptive meshing algorithm using an unstructured mesh of linear triangular elements. The program provides accurate solutions to a range of different steady state and transient groundwater flow problems involving saturated conditions in a porous incompressible medium.

The main advantages of the program are:

- Ease of use, including the absence of a requirement to specify the finite element subdivision of the problem domain.
- Consistently high accuracy of the results obtained, including the precise prediction of the seepage line position.
- Ability to produce flow nets which provide both a visual check of the results and a dimensionless form of presentation which may be used for other sizes of structure and material properties.

The language of the finite element is easily understood by structural engineers, but the method is not so accessible to geotechnical or hydrogeological personnel. This thesis demonstrates two ways in which this barrier may be broken down:

- Development of a program requires no specialist knowledge outside the field of investigation to operate. The adopted finite element technique should be invisible to the user.
- Utilization of the finite element method to obtain accurate empirical solutions which may be applied without a second resort to the finite element method.

6.4. Future Work

- Modifications of the program to improve performance and extend the types of problem which may be studied are outlined in Chapter 4. These improvements are of an incremental nature requiring only a modest adaption of the current program. Conversion of the program to deal with axisymmetric problems and solution of the Boussinesq equation offer the greatest increase in the range of problems which may be considered.
- Seepage analysis using the current program is likely to reap further dividends. Falkovich's equation concerning the relationship between the seepage exit height and the seepage discharge (and permeability) could be verified for inverted downstream slopes (occurring in flow into toe drains and flow though inclined dam

cores). A more original contribution could come from the investigation of the seepage exit height for anisotropic dams. Inhomogeneous and anisotropic permeability might also be incorporated into the equation for seepage discharge. This may lead to a simple solution to dam flow through conventional zoned embankments and tailings embankments.

- Actual flow problems could be modelled and then compared with real field data in order to verify (or otherwise) the validity of the various simplifying assumptions. Steady state solutions are widely recognised as being useful tools in the investigation of groundwater problems. It is not so clear that the transient solutions will prove as useful in practice because they lack the conservatism of the steady state analysis.
- Flow net construction may be improved by the use of a relaxation technique in order to smooth the error inherent in the integration procedure. This should reduce the computational cost of obtaining an adequate flow net. The calculation of flow nets involving singularities requires further research in order to improve their accuracy. One possibility is to assess the error in each element in order to control both the direction and order of the integration procedure.

References

Abadjiev Ch. B. (1976), "Seepage Through Mill Dams", 12th Int. Conf. on Large Dams, Mexico; 381-393,

Almes R.G. (1978), "An Overview of Coal Tailings Disposal in the Eastern United States", in *Tailings Disposal Today v2, Proc. 2nd Int. Tailings Symp., Denver, Colorado,* ed. G.O. Argall Jnr., Miller Freeman Publ., San Francisco; 13-53.

Aziz N.M., C.H. Juang & S. Sinharoy (1992), "Polynomial Approximation of Equipotential Lines for Flow Under a Dam", Technical Note, *Computers & Geotech.*, **13**; 119-133.

Babuska I. & A.K. Aziz (1976), "On the Angle Condition in the Finite Element Method", *Math. of Computation*, **24** (112); 809-820.

Babuska I. & M. Shri (1990), "The p- and h-p Versions of the Finite Element Method, An Overview", *Comp. Meth. in Appl. Mech. & Eng.*, **80**; 5-26.

Babuska I. & W.C. Rheinboldt (1978), "A Posteriori Error Estimates for the Finite Element Method", *Int. J. Num. Meth. Eng.*, **12**; 1597-1615.

Bacon A.R. (1987) Head of Civil Engineering Services, British Coal, Burton, Personal Communication.

Baiocchi C., V. Comincioli, E. Magnes & G.A. Pozzi (1973), "Free Boundary Problems in the Theory of Fluid Flow through Porous Media, Existence & Theorems", *Anna. Mat. Pura. Appl.*, **96** (4); 1.

Bathe K. & M.R. Khoshgoftaar (1979), "Finite Element Free Surface Seepage Analysis Without Mesh Iteration", *Int. J. Num. Anal. Meth. Geomech.*, **3**; 13-22.

Berry P.L. & D. Reid (1987) *An Introduction to Soil Mechanics*, McGraw-Hill, London, 317p.

Brawner C.O. & D.B. Campbell (1973), "The Tailings Structure and its Characteristics", in *Tailing Disposal Today, Proc. 1st Int. Symp., Tucson, Arizona,* eds. C.L. Aplin & G.O. Argall Jnr., Miller Freeman Publ., San Francisco; 59-96.

Burkley V.J. & J.C. Bruch Jnr. (1991), "Adaptive Error Analysis in Seepage Problems", *Int. J. of Num. Meth. Eng.*, **31**; 1333-1356.

Cargill K.W. & K. Hon-Yim (1983), "Centrifugal Modelling of Transient Water Flow", *J. Geotech. Eng., ASCE,* **109** (4); 536-555.

Casagrande A. (1940) "Seepage Through Dams", in *Contributions to Soil Mechanics 1925-1940*, Boston Society of Civil Engineers, Boston; 295-337.

Casagrande L. & B.N. McIver (1971) "Design and Construction of Tailings Dams", *Proc. 1st Int. Conf. Stability in Open Pit Mining*, Vancouver B.C., Canada, eds. C.O. Brawner & V. Milligan, Society of Mining Engineers (Publ.), New York; 181-203.

Cavendish J.C. (1974), "Automatic Triangulation of Arbitrary Planar Domains for the Finite Element Method", *Int. J. Num. Meth. Eng.*, **8**; 679-696.

Cavendish J.C., D.A. Field & W.H. Frey (1985), "An Approach to Automatic Three-Dimensional Finite Element Mesh Generation", *Int. J. Num. Eng.*, **21**; 329-347.

Cedergren H.R. (1977), *Seepage, Drainage and Flow Nets*, John Wiley & Sons, Second Edition, New York.

Chung K.Y. & N. Kikuchi (1987), "Adaptive Methods to Solve Free Boundary Problems of Flow through Porous Media", *Int. J. Num. Anal. Meth. Geomech.*, **11**; 17-31.

Cividini A. & G. Gioda (1989), "On the Variable Mesh Finite Element Analysis of Unconfined Seepage Problems", *Geotechnique*, **39** (2); 251-267.

Clough R.W. (1960), "The Finite Element Method in Plane Stress Analysis", *Proc. Electronic Computation, ASCE, 2nd Conf. Pittsburgh; 345-378.*

Connor J.J. & C.A. Brebbia (1976), *Finite Element Techniques for Fluid flow*, Newnes-Butterworths, London, p. 310.

Craig A.W., M. Ainsworth, J.Z. Zhu & O.C. Zienkiewicz (1989), "h and h-p Version Error Estimation and Adaptive Procedures from Theory to Practice", *Engineering with Computers,* **5**; 221-234.

Cuthill E. & J. McKee (1969), "Reducing the Bandwidth of Sparse Symmetrical Matrices", *Proc. 24th ACM Nat. Conf.*, Barndon Systems Press; 157-172.

Davis L.A. (1980), "Computer Analysis of Seepage and Groundwater Response Beneath Tailings Impoundments", *NSF/RA-800054 U.S. Department of Commerce, National Technical Information Service*; 1-89.

De Wiest R.J.M. (1965), *Geohydrology*, John Wiley & Sons, Inc., New York, p. 366.

Deju R.A. (1974), *Extraction of Minerals and Energy: Today's dilemmas*, Ann Arbor, Science Publishers, Inc., Ann Arbor, Michegan, Chapter 5; 43-47.

Department of the Environment (1988), *Development of Evaluative Framework amd Review of Existing Spoil Disposal Procedures*, Mining Planning Research Project PECD 7/1/118-180/83, HMSO, London; 70-178.

Desai C.S. & J.F. Abel (1972), *Introduction to the Finite Element Method - A Numerical Method for Engineering Analysis*, Van Nostrand Reinhold Co., New York, p. 306.

Desai C.S. (1976), "Finite Element Residual Schemes for Unconfined Flow", Short Communication, *Int. J. Num. Meth. Eng.*, **10**; 1415-1418.

Desai C.S. (1983), "A Residual Flow Procedure and Application for Free Surface Flow in Porous Media", *Int. J. Adv. Water Res.* **6**; 27-35.

Donaldson G.W. (1959), "The Effects on Foundation Conditions on Seepage Flow Through Earth Dams and Other Embankments", *Proc. 2nd African Regional Conf. on Soil mechanics and Foundation Engineering,* Laurenco Marques, Mocambique; 21-26.

Donaldson G.W. (1960), "The Stability of Slimes Dams in the Gold Mining industry", *J. South African Inst. of Mining & Metallurgy*, October; 183-199.

Down C.G. & J. Stocks (1976), "The Environmental Problems of Tailings Disposal at Metal Mines", *Department of the Environment Research Report 17,* HMSO; 1-29.

Down C.G. & J. Stocks (1977), "Methods of Tailings Disposal", *Mining Magazine*, May; 345-359.

Fan Y., F.D. Tompkins, E.C. Drumm & R.D. Von Bernuth (1992), "Generation of Flownets using FEM Nodal Potentials and Bilinear Shape Functions", *Int. J. Num. Anal. Meth. Geomech.*, **16**; 425-437.

Finn W.D.L. (1967), "Finite Element Analysis of Seepage Through Dams", *J. Soil Mech. Found. Div., Proc. of ASCE,* **93** (SM6); 41-48.

Fipps G. & R.W. Skaggs (1990), "Pond Seepage in Two and Three Dimensions", *J. Hydr.*, **117**; 133-151.

France P.W., C.J. Parekh, J.C. Peters & C. Taylor (1971), "Numerical Analysis of Free Surface Seepage Problems", *J. Irr. & Drain. Div., Proc. of ASCE,* **97** (PIRI); 165-179.

Galpin A.L. (1971), "The Control of Water in Tailings Dams", *2nd Int. Conf. on Stability in Open Pit Mining,* Vancouver; 173-196.

Green P.V. (1980), "The Need for Long Term Lagoons - A Literature Survey", *Warren Springs laboratory, Dept. Industry Report LR 326(MP), 45p.*

Griffiths D.V. (1990), "On the Variable Mesh Finite Element Analysis of Unconfined Seepage Problems", Discussion, *Geotechnique*, **40** (N3); 523-526.

Harr M.E. (1962), *Groundwater and Seepage,* McGraw-Hill Inc., New York, 315p.

Hinton E. & J.S. Campbell (1974), "Local and Global Smoothing of Discontinuous Finite Element Functions Using a Least Squares Method", *Int. J. Num. Meth. Eng.*, **8**; 461-480.

Huang Y.H. (1986), "Unsteady State Phreatic Surface in Earth Dams", *J. Geotech. Eng., ASCE,* **112** (1); 93-98.

ICOLD (1982), "Manual on Tailings Dams and Dumps", *Bulletin - International Commission on Large Dams No. 45*, Paris; 13-215.

ICOLD (1989), "Tailing Dam Safety - Guidelines", *Bulletin - International Commission on Large Dams No. 74,* Paris; 11-49.

International Water Power Dam Construction (1985), "Tailings Dams : Improved Methods for Upstream Construction", *37 (12); 34-36.*

Isaacs L.T. (1980), "Location of Seepage Free Surface in Finite Element Analyses", *Civil Eng. Trans., The Institute of Engineers, Australia,* **CE 22** (1); 9-16.

Ishtok J. (1989), *Groundwater Modelling by the Finite element Method,* American Geophysical Union, Water Resources Monograph, Washington D.C., 495p.

Kealy C.D. & R.E. Williams (1971a), "Mathematical Models of Groundwater Flow as an Aid for Predicting Slope Stability in Tailings-Pond Embankments", *Proc. 8th Annual Symp. Eng. Geol. & Soil Eng.,* Pocatello, Idaho Dept. of Highways, Idaho, 7 (1); 143-154.

Kealy C.D. & R.E. Williams (1971b), "Flow through a Tailings Pond Embankment", *Water Resources Res.*, **7** (1); 143-154.

Kealy C.D., R.A. Busch & M.M. McDonald (1974), "Seepage-Environmental Analysis of the Slime Zone of a Pond", *Bureau of Mines Report of Investigations RI 7939, Dept. of the Interior*; 1-89.

Kealy C.D. & R.A. Busch (1971), "Determining Seepage Characteristics of Mill-Tailings by the Finite Element Method", *Bureau of Mines Report of Investigations RI 7477, Dept. of the Interior*; 1-73.

Kealy C.D. & R.A. Busch (1979), "Evaluation of Mine Tailings Disposal", *Current Geotechnical Practice in Mine Waste Disposal,* ASCE Geotechnical Engineering Division, New York; 181-201.

Kealy C.D. & R.E. Williams (1971a), "Mathematical Models of Groundwater Flow as an Aid for Predicting Slope Stability in Tailings Pond Embankments", *Proc. 8th Ann. Symp. Eng. Geol & Soil Eng, Pocatello, Idaho, Idaho Department of Highways, Idaho, USA;* 21-36.

Kealy C.D. & R.E. Williams (1971b), "Flow Through a Tailings Pond Embankment", *Water Resources Res.*, **7** (1)*; 143-154.*

Klohn E.J. (1972), "Design and Construction of Tailings Dams", *Can. Min. & Met. Bull.*, April; 28-44.

Klohn E.J. (1979), "Seepage Control for Tailings Dams", *Proc. 1st Int. Mine Drainage. Symp., Denver, Colorado; 671-725.*

Klohn E.J. (1980), "The Development of Current Tailings Dam Design and Construction Methods", *Seminar on Design and Construction of Tailings Dams,* Colorado School of Mines, Colorado; 1-52.

Krizec M. & P. Neittaanmaki (1987), "On Superconvergence Techniques", *Acta Applicandae mathematicae, **9**; 175-198.*

Levine N. (1985), "Superconvergent Recovery of the Gradient from Piecewise Linear FE Approximations", *IMA J. Num. Anal.*, **5**; 407-427.

Longhurst J.W.S. (1983), "An Assessment of the Potential Environmental Impact of Colliery Spoil Production in the South Warwickshire Prospect", *Ph.D. Thesis*, Department of Minerals Engineering, Faculty of Science and Engineering, University of Birmingham (UK).

MacKinnon R.J. & G.F. Carey (1990), "Nodal Superconvergence and Solution Enhancement for a Class of Finite Element and Finite Difference Nodes", *SIAM J. Sci. Stat. Comput.*, **11** (2); 343-353.

Mantei C.L. (1985), "Seepage Control for Embankment Dams : USBR Practice", *Proc. Symp. Geotech. Div., ASCE, New York,* eds. Volpe R.L. & Kelly W.E.; 299-314.

McWhorter D.B. (1985), "Seepage in the Saturated Zone : A Review", in *Seepage and Leakage from Dams and Impoundments, Proc. of Symp. of Geotech. Div.*, ASCE, New York, N.Y., eds. R.L. Volpe & W.E. Kelly; 200-219.

Minns A. (1988), "A Review of Tailings Disposal Practices in North America and Australia", in *Hydraulic Fill Structures, Conf. Geotech. Eng. Div.,* ASCE, Colorado State University, eds. D.J.A. Van Zyl & S.G. Vick; 52-68.

Mitchell A.R. (1973), "An Introduction to the Mathematics of the Finite Element Method" in *The Mathematics of Finite Elements and Applications,* Academic Press Inc. (London) Ltd.; 37-58.

Mittal H.K. & N.R. Morgenstern (1976), "Seepage Control in Tailings Dams", *Can. Geotech. J.*, **13**; 277-293.

Mittal H.K. & N.R. Morgenstern (1977), "Design and Performance of Tailings Dams", *Proc. Geotechnical Practice for Disposal of Solid Waste Materials,* Ann Arbor, Michegan, ASCE; 475-492.

Morgenstern N.R., R.W. Hendry, C.B. Abadjiev, Y Perlea & E. Botea (1985), "Tailings Dams : Improved Methods for Upstream Construction", *Water Power & Dam Construction,* 1st Conf. Soil Mechanics and Foundation Engineering, San Francisco, USA;34-36.

Morgenstern N.R. & A.A.G. Kupper (1988), "Hydraulic Fill Structures - A Perspective", in *Hydraulic Fill Structures, Conf. Geotech. Eng. div.,* ASCE, Colorado State University, eds. D.J.A. Van Zyl & S.G. Vick; 1-31.

NCB (1970), *Spoil Heaps and Lagoons*, National Coal Board, 232p.

Nelson J.D., T.A. Shepherd & W.A. Charlie (1977), "Parameters Affecting Stability of Tailings Dams", *Proc. Conf. on Geotech. Pract. for Disposal of solid Waste, ASCE, University of Michegan, Ann Arbor, MI; 444-460.*

Neuman S.P. & P.A. Witherspoon (1970), "Finite Element Method of Analyzing Steady Seepage with a Free Surface", *Water Resource Res.*, **6**; 889-897.

Neuman S.P. & P.A. Witherspoon (1971), "Analysis of Nonsteady Flow with a Free Surface Using the Finite Element method", *Water Resources Res.*, **6**; 611-623.

Neuman S.P. (1973), "Saturated-Unsaturated Seepage by Finite Elements", *J. Hydr. Div., ASCE*, **99** (HY12); 2233-2250.

Norrie D.H. & G. de Vries (1978), *An Introduction to Finite Element Analysis,* Academic Press, Inc. (London) Ltd., p. 301.

Nyren R.H., K.A. Haakonson & H.K. Mittal (1978), "Disposal of Tar Sand Tailings at Syncrude Canada Ltd.", in *Tailings Disposal Today, v2, Proc. 2nd Int. Tailings Symp.*, Denver, Colorado, Miller-Freeman, San Franciso; 54-74.

Onate E. & J. Castro (1991), "Adaptive Mesh Refinement Techniques for Structural Problems", in *Finite Elements in the 1990's,* eds. E. Onate, J. Peraire & A .Samuelson, Springer-Verlag/CIMNE, Barcelona; 133 - 144.

Parsons M.L. (1980), "Groundwater Aspects of Tailings Impoundments", *Seminar on Design & Construction of Tailings Dams*, Colorado School of Mines; 119-126.

Peraire J., M. Vahdati, M. Morgan & O.C. Zienkiewicz (1987), "Adaptive Remeshing for Compressible Flow Computations", *J. Computational Physics; 449-466.*

Pettibone H.C. & C.D. Kealy (1971), "Engineering Properties of Mine Tailings", *J. Soil Mech. & Found. Div.*, ASCE, **97** (SM9); 1207-1225.

Polubarinova-Kochina P. YA. (1962), *Theory of Ground Water Movement*, Princeton University Press, Princeton, New Jersey, Translation by J.M.R. De Wiest, 613p.

Ramstad H. (1970), "Convergence and Numerical Accuracy with Special Reference to Plate Bending", Chapter 6 in *Finite Elements in Stress Analysis,* eds. I. Holland & K. Bell, Tapir Press, Trondheim - Norway; 179-211.

Rank E. & H. Werner (1986), "An Adaptive Finite Element Approach for the Free Surface Seepage Problem", *Int. J. Num. Meth. Eng.*, **23**; 1217-1228.

Raudkivi A.J. & Callender R.A. (1976), *Analysis of Groundwater flow*, Edward Arnold (Publ.) Ltd., London.

Rivara M.C. (1986), "Adaptive Finite Element Refinement and Fully Irregular and Conforming Triangulations", Chapter 20 in *Accuracy Estimates and Adaptive Refinements in Finite Element Computations", eds. I. Babuska, O.C. Zienkiewicz, J. Gago and E.R. de A. Oliveira, John Wiley & Sons Ltd.*

Rubinchic Ya.A. (1960), "Stability of Reservoirs for Fine Grained Tailings", TSETNAYA METALLURGIYA, **33** (4); 3-7, (English translation).

Sherrod P.H. (1992), *NONLIN Nonlinear Regression Analysis Program Manual*, Shareware Program, 4410 Gerald Place, Nashville, TN, 37205-3806.

Smith I.M. & D.V. Griffiths (1988), *Programming the Finite Element Method*, Second Edition, John Wiley & Sons, Chichester, p. 469.

Stauffer P.A. & J.P. Obermeyer (1988), "Pore Pressure Conditions In Tailings Dams", in *Hydraulic Fill Structures, Conf. Geotech. Eng. Div.*, ASCE, Colorado State University, eds. D.J.A. Van Zyl & S.G. Vick; 924-939.

Stello M.W. (1987), "Seepage Charts for Homogeneous and Zoned Embankments", *J. Geotech. Eng.*, **113** (9); 996-1012.

Strang G. & G.J. Fix (1973), *An Analysis of the Finite Element Method*, Prentice-Hall, Inc., Englewood Cliffs, N.J., p. 306.

Strang G. (1972), "Approximation in the Finite Element Method", *Numer. Math.*, **19**; 81-98.

Swaisgood J.R. & G.C. Toland (1973), "The Control of Water in Tailings Structures", in *Tailing Disposal Today, Proc. 1st Int. Symp., Tucson, Arizona,* eds. C.L. Aplin & G.O. Argall Jnr., Miller Freeman Publ., San Francisco; 138-163.

Taylor R.L. & C.B. Brown (1967), "Darcy Flow Solutions with a Free Surface", *J. Hydr. Div., Proc. of ASCE,* **93** (HY2); 25-33.

Thacker W.C. (1980), "A Brief Review of Techniques for Generating Irregular Computational Grids", *Int. J. Num. Mech. Eng.*, **15**; 1335-1341.

Vick S.G. (1977), "Rehabilitation of a Gypsum Tailings Embankment", *Proc. Conf. on Geotechnical Practice for Disposal of Solid waste,* ASCE, Michegan University, Ann Arbor, Michegan; 697-714.

Vick S.G. (1983), *Planning, Design and Analysis of Tailings Dams*, Wiley Interscience, John Wiley & Sons, New York.

Whiteman J.R. & G. Goodsell (1987), "Some Gradient Superconvergence Results in the Finite Element Method", in Turner P.R. "Numerical Analysis and Parallel Processing" from *Lecture Notes in Mathematics 1397*, eds. A Dold & B. Eckmann, Lancaster, Springer-Verlag, Berlin.

Windolph F. (1973), "Operation of the Tailings System and Characteristics of the Tailings Structure", in *Tailing Disposal Today, Proc. 1st Int. Symp., Tucson Arizona,* eds. C.L. Aplin & G.O. Argall Jnr., Miller Freeman Publ., San Francisco; 203-210.

World Mining Equipment (1985), "Ways to Improve Mine Safety", October; 37-43.

Yerry M.A. & M.S. Shephard (1983), "A Modified Quadtree Approach to Finite Element Mesh Generation", *IEEE Computer Graphics and Applications*, **3** (1); 39-46.

Zhu J.Z., O.C. Zienkiewicz & A.W. Craig (1987), "Adaptive Techniques in Finite Element Analysis", in *Numerical Techniques for Engineering Analysis and design,* Proc. of the Int. Conf. on Numerical Methods in Engineering, Swansea, Martinus Nijhoff Publishers, Lancaster, (S3); 1-10.

Zhu J.Z. & O.C. Zienkiewicz (1990), "Superconvergence Recovery Techniques and A Posteriori Error Estimators" *Int. J. Num. Meth. Eng.*, **30**, 1321-1339.

Zienkiewicz O.C., B.M. Irons, J. Ergatoudis, S. Ahmad & F.C. Scott (1970), "Iso-Parametric and Associated Element Families for Two- and Three-Dimensional Analysis", in *Finite Element Methods in Stress Analysis*, eds. I. Holland & K. Bell, Tapir Press, Trondheim - Norway; 390-393.

Zienkiewicz O.C. & D.V. Phillips (1971), "An Automatic Mesh Generation Scheme for Plane and Curved Element Domains", *Int. J. Num. Meth. Eng.*, **3**; 519-528.

Zienkiewicz O.C. & J.Z. Zhu (1987), "A Simple Error Estimator and Adaptive Procedure for Practical Engineering Analysis", *Int. J. Num. Meth. Eng.*, **24**; 337-357.

Zienkiewicz O.C. & R.L. Taylor (1989), *The Finite Element Method*, Fourth Edition, Volume 1, "Basic Formulation and Linear Problems", McGraw-Hill Book company, London, p. 648.

Appendix 1
Seepage Line Profiles for a Rectangular Section Dam

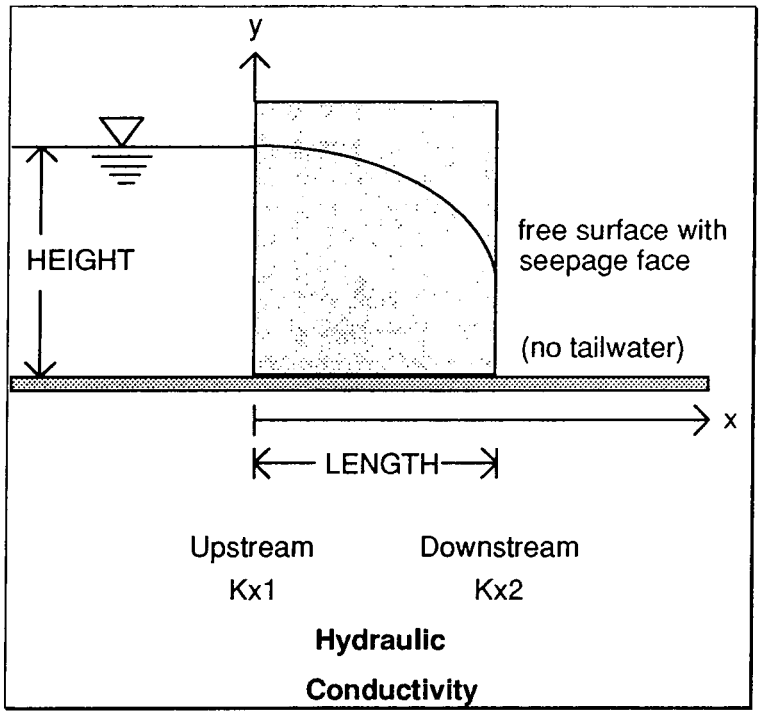

The units for height, length and seepage discharge per unit width of dam have been divided by the height of the dam. The seepage discharge has also been divided by the permeability at the upstream slope. The plots may be used for any height of dam or permeability by multiplying space dimensions by the true height of the water in the dam. The seepage discharge should be multiplied by the true height of the dam and the permeability measured in compatible units.

Rectangular Dam with Linear Horizontal Variation in Hydraulic Conductivity

Kx2/Kx1=.02 .05 .1 .2 .5 1 2 5 10 20 50

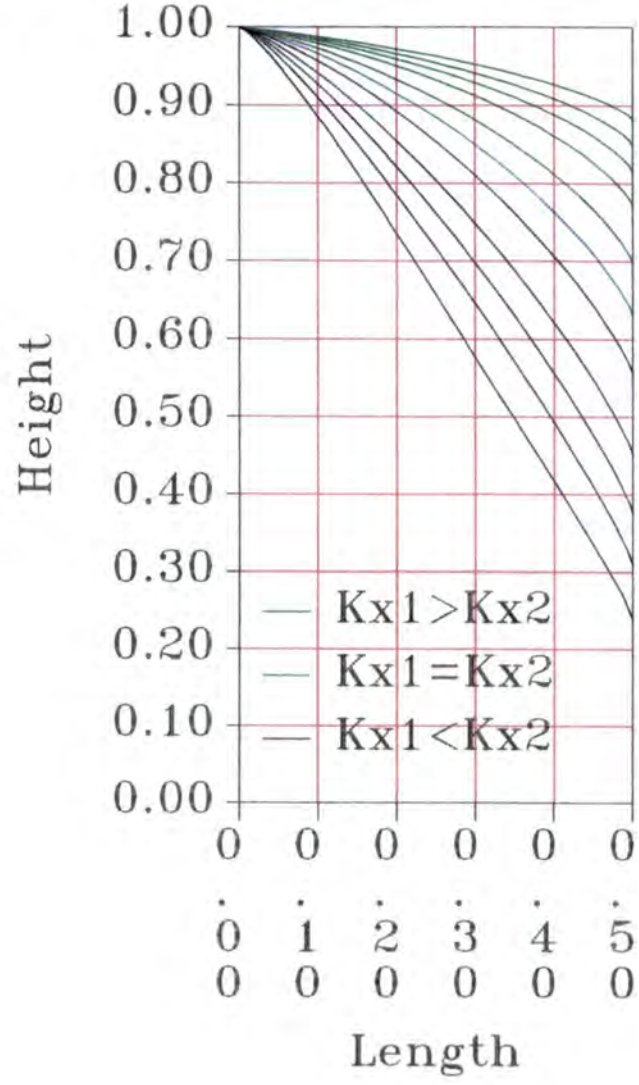

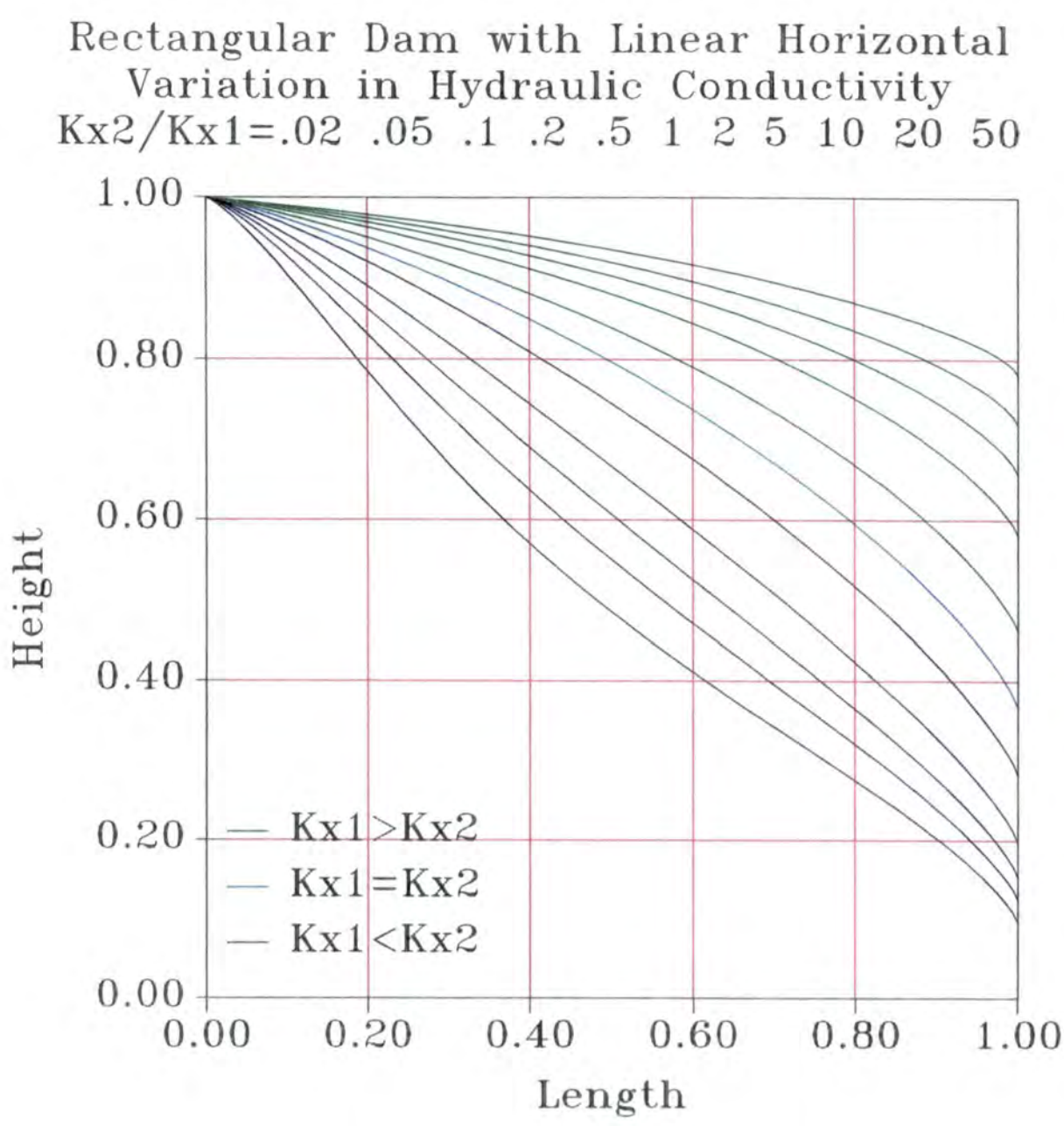
Rectangular Dam with Linear Horizontal Variation in Hydraulic Conductivity
Kx2/Kx1=.02 .05 .1 .2 .5 1 2 5 10 20 50
1.00
0.80
0.60
0.40
0.20
0.00
Height
Kx1>Kx2
Kx1=Kx2
Kx1<Kx2
0.00
0.20
0.40
0.60
0.80
1.00
Length

Rectangular Dam with Linear Horizontal
Variation in Hydraulic Conductivity
Kx2/Kx1=.02 .05 .1 .2 .5 1 2 5 10 20 50

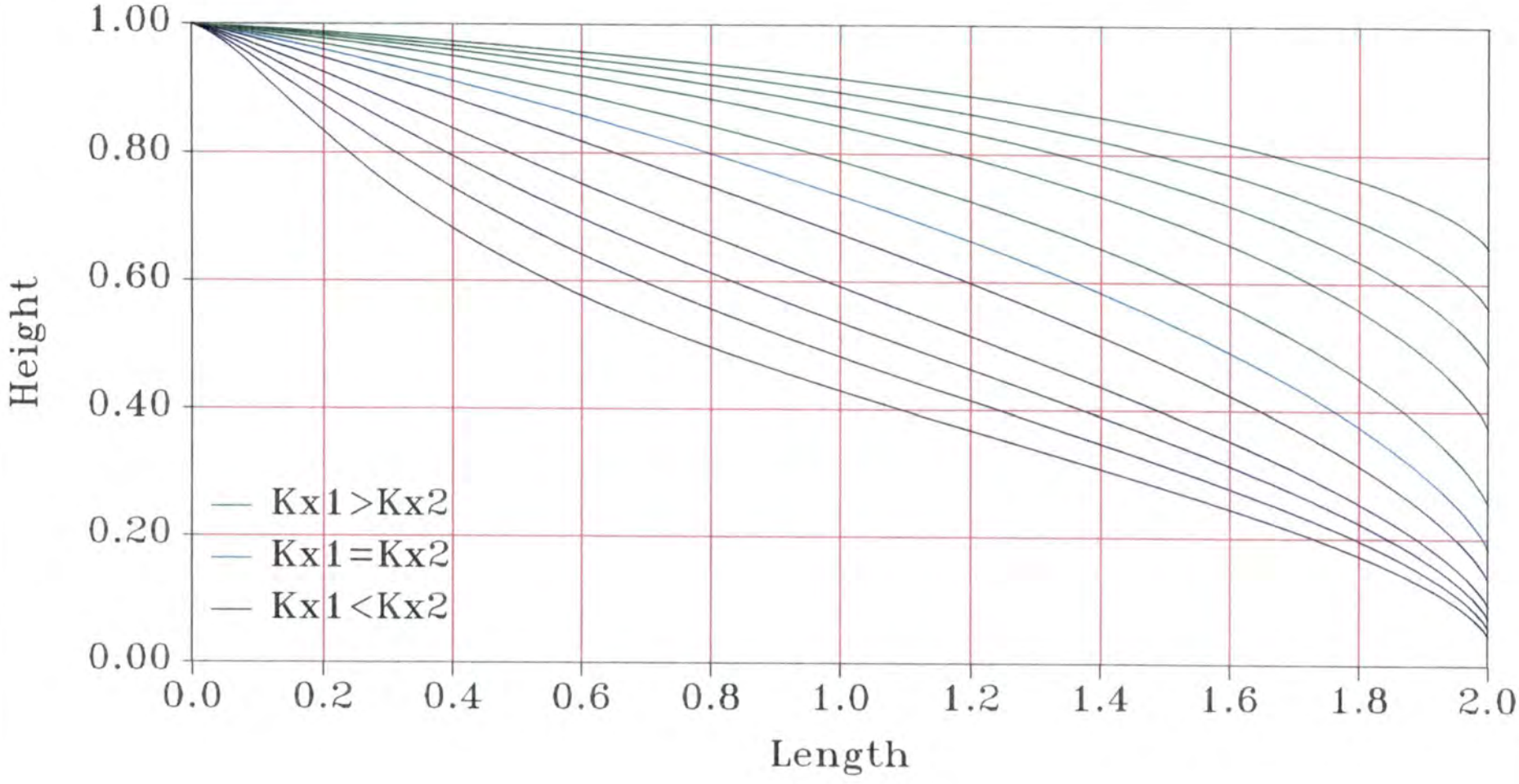

Rectangular Dam with Linear Horizontal
Variation in Hydraulic Conductivity
Kx2/Kx1=.02 .05 .1 .2 .5 1 2 5 10 20 50

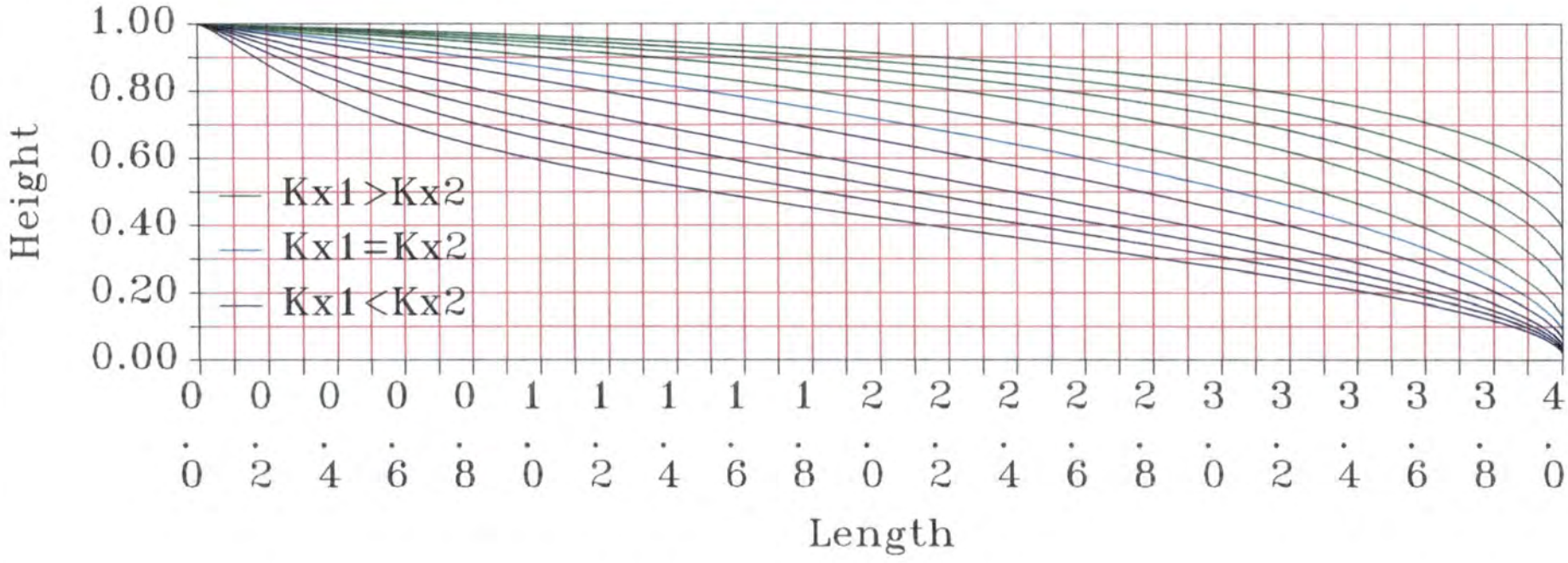

Rectangular Dam – Seepage Exit Heights
Linear Variation in Horizontal Hydraulic Conductivity

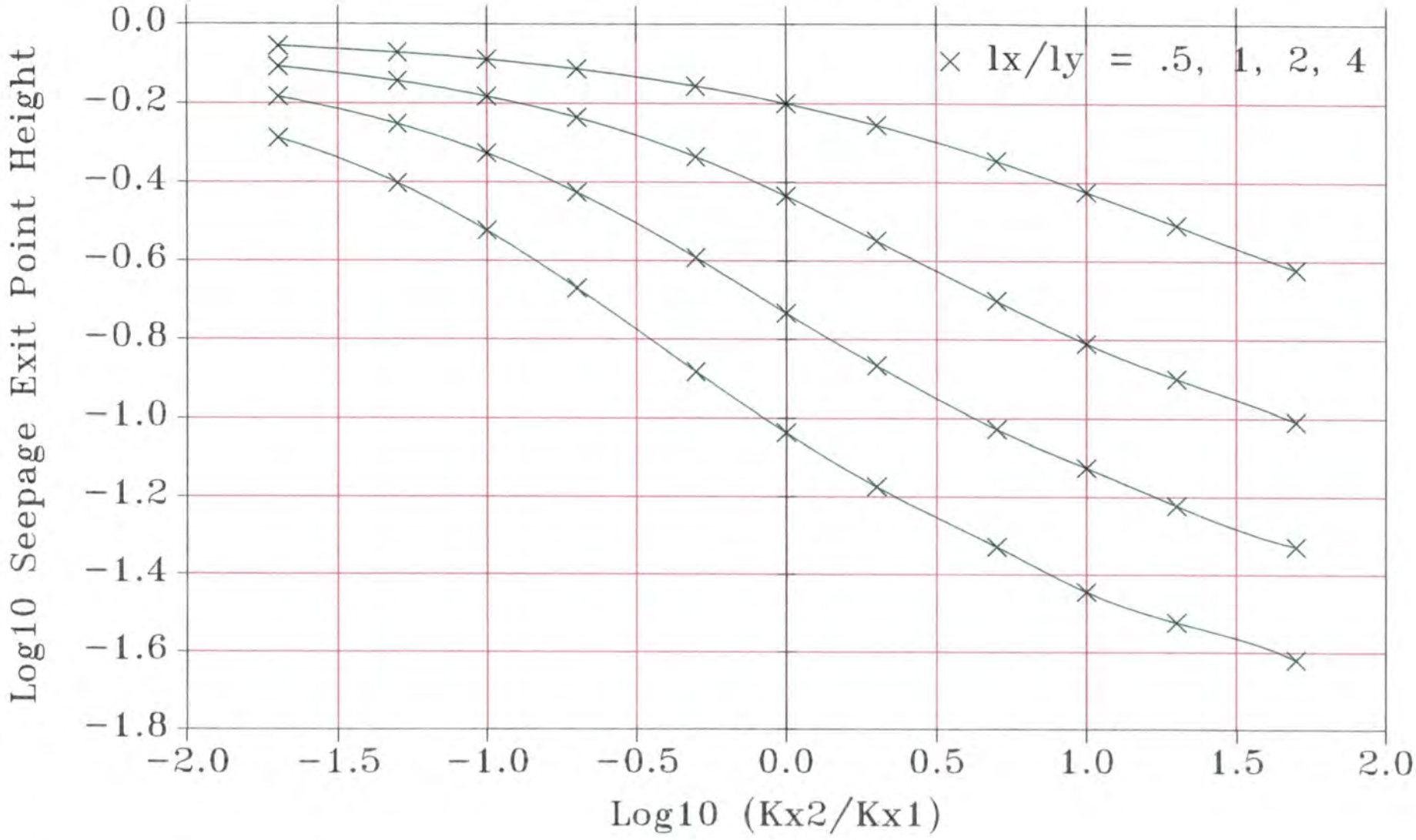

N.B. The height/length ratio lx/ly of the dam is 0.5 for the uppermost graph increasing down through the lower graphs

Rectangular Dam – Seepage Discharge
Linear Variation in Horizontal Hydraulic Conductivity

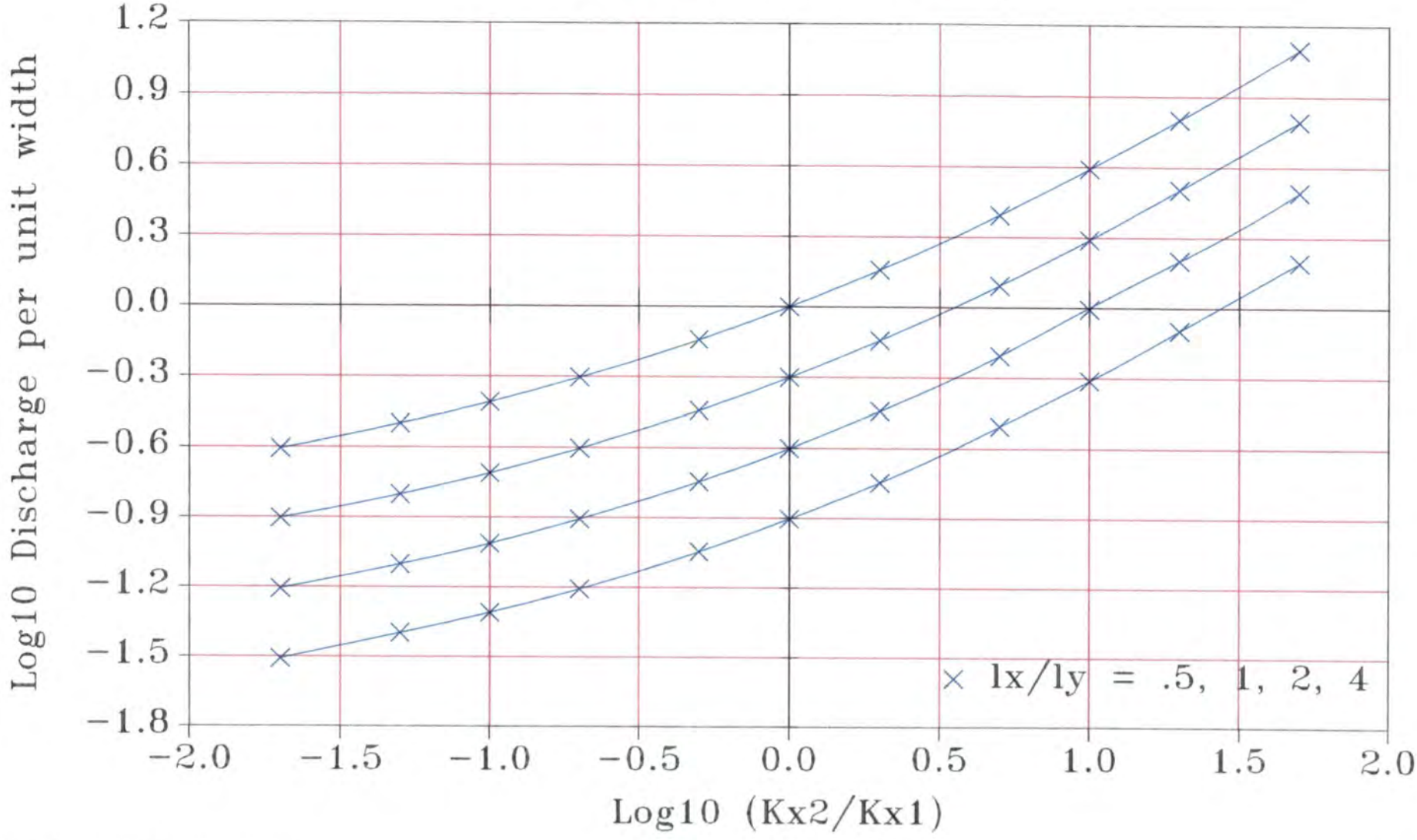

N.B. The height/length ratio lx/ly of the dam is 0.5 for the uppermost graph increasing down through the lower graphs

Appendix 2
Anisotropic and Homogeneous Earth Dams
Seepage Lines, Seepage Exit Heights and Seepage Discharge

The plots in this appendix refer to the anisotropic and homogeneous dam pictured below. The foundation is considered to be impervious.

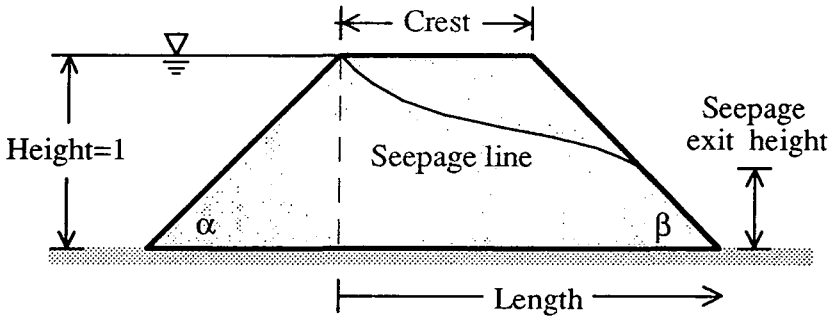

The space dimensions and seepage discharge per unit width of dam are all scaled with respect to the height of water behind the dam. The seepage discharge is also scaled with respect to the permeability which has a value of 1 in these calculations. In order to obtain the appropriate values of seepage discharge and seepage line height from the values plotted, the following transformations should be used:

$$h_e = h_0 H$$
$$q_d = qkH$$

where h_e is the seepage line height (in metres), h_0 is the height read from the plot, H is the height of the earth dam (in m), q_e is the seepage discharge, q is the seepage discharge from the plot (m^3s^{-1} per metre width), and k is the permeability (in ms^{-1}).

The seepage line plots are grouped according to the downstream slope angle β. As the graphs are traversed from top to bottom, the upstream slope angle α decreases in value from 90 to 0 degrees as indicated.

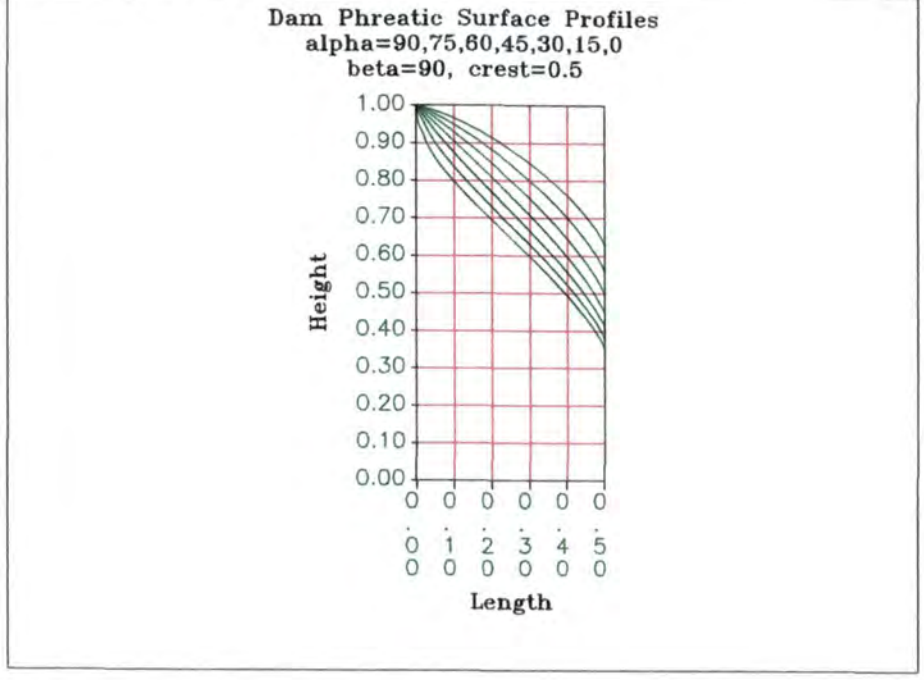
Dam Phreatic Surface Profiles
alpha=90,75,60,45,30,15,0
beta=90, crest=0.5
Height
1.00
0.90
0.80
0.70
0.60
0.50
0.40
0.30
0.20
0.10
0.00
0.0 0.1 0.2 0.3 0.4 0.5
Length

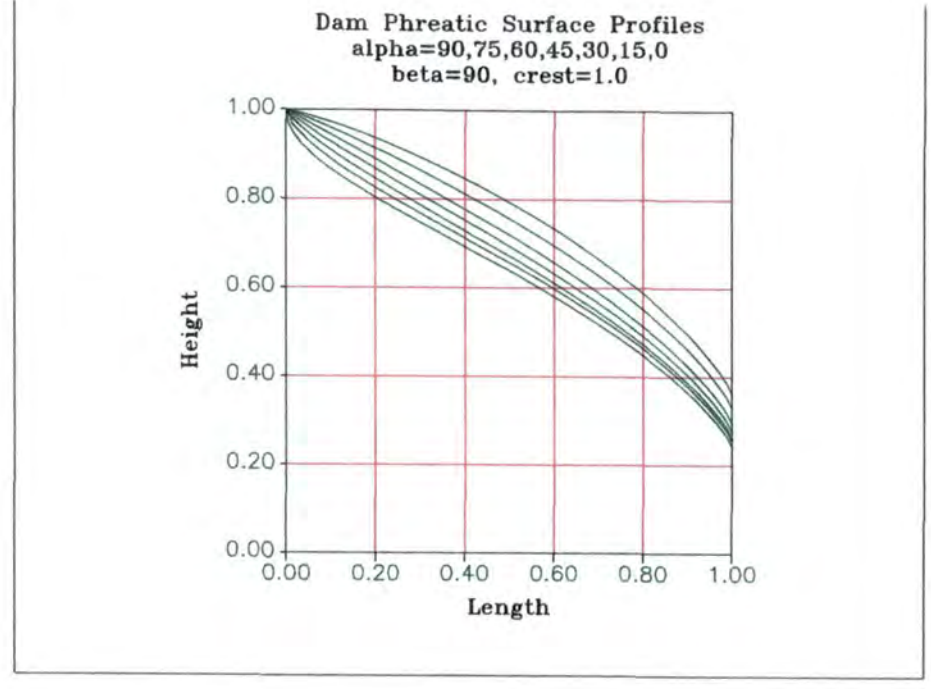
Dam Phreatic Surface Profiles
alpha=90,75,60,45,30,15,0
beta=90, crest=1.0
Height
1.00
0.80
0.60
0.40
0.20
0.00
0.00 0.20 0.40 0.60 0.80 1.00
Length

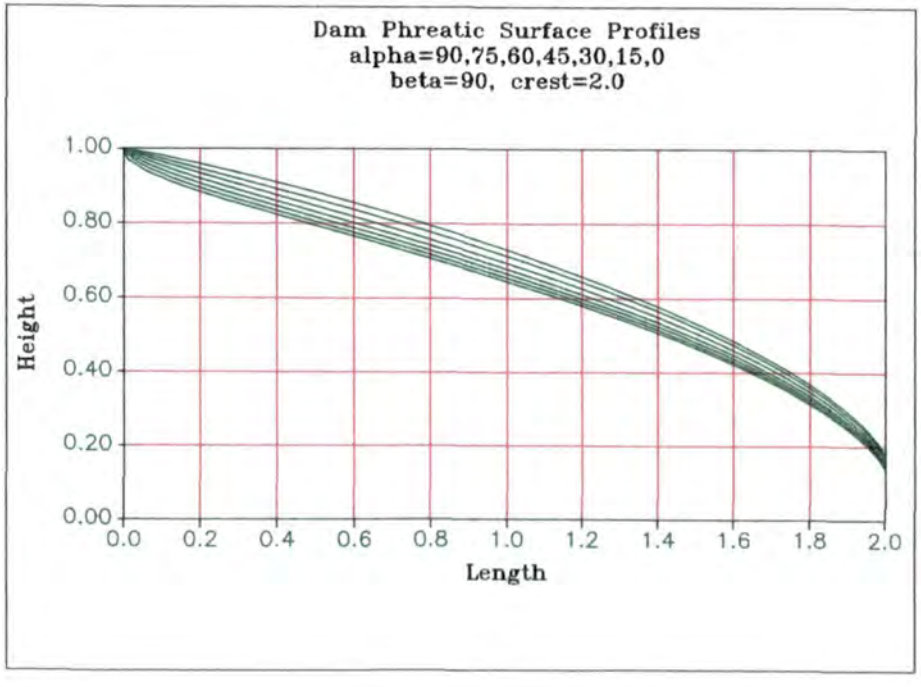
Dam Phreatic Surface Profiles
alpha=90,75,60,45,30,15,0
beta=90, crest=2.0
Height
1.00
0.80
0.60
0.40
0.20
0.00
0.0 0.2 0.4 0.6 0.8 1.0 1.2 1.4 1.6 1.8 2.0
Length

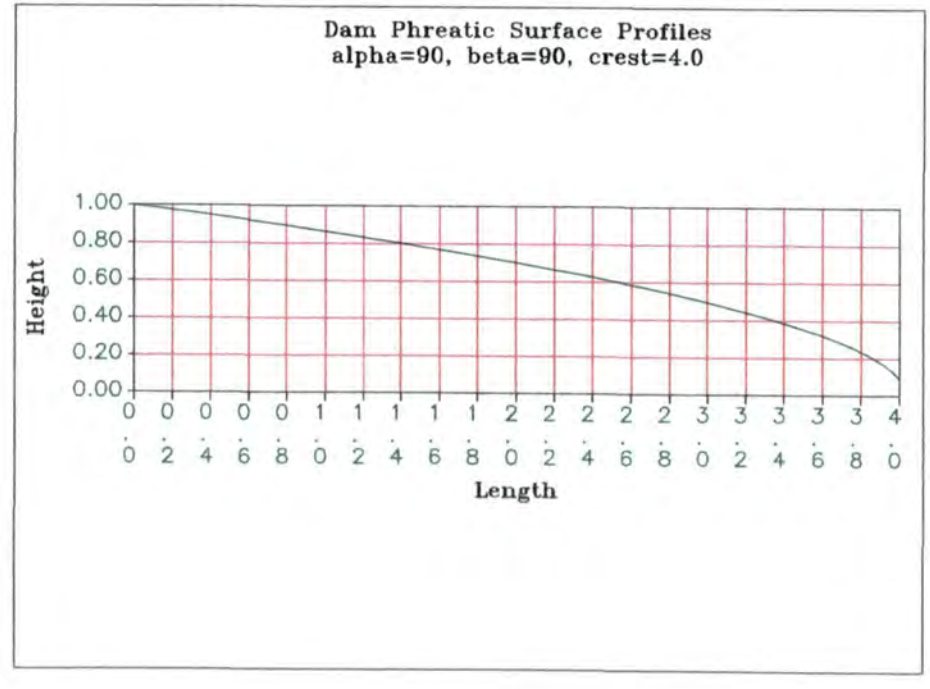
Dam Phreatic Surface Profiles
alpha=90, beta=90, crest=4.0
Height
1.00
0.80
0.60
0.40
0.20
0.00
0.0 0.2 0.4 0.6 0.8 1.0 1.2 1.4 1.6 1.8 2.0 2.2 2.4 2.6 2.8 3.0 3.2 3.4 3.6 3.8 4.0
Length

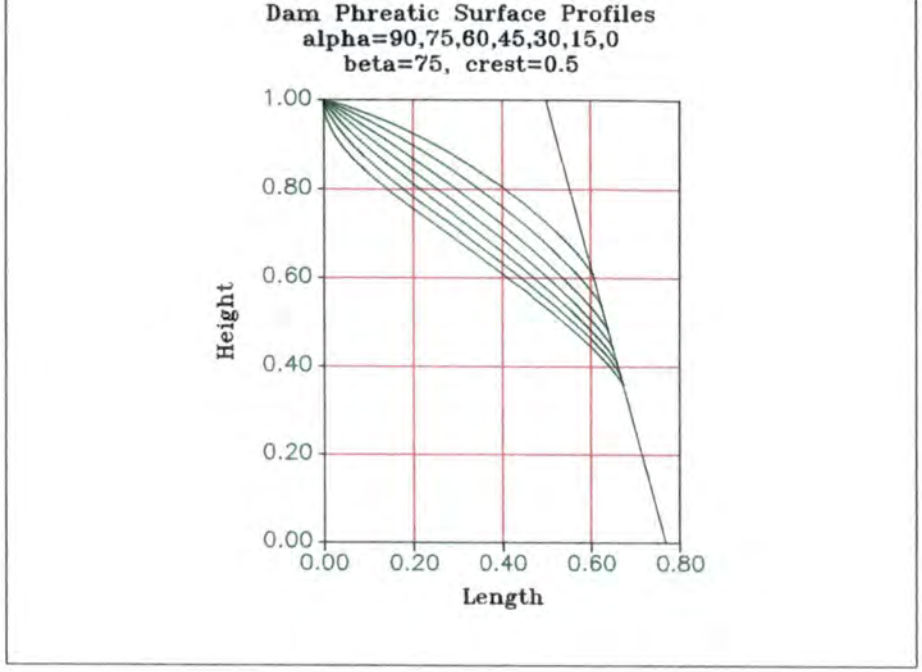
Dam Phreatic Surface Profiles
alpha=90,75,60,45,30,15,0
beta=75, crest=0.5
Height
1.00
0.80
0.60
0.40
0.20
0.00
0.00
0.20
0.40
0.60
0.80
Length

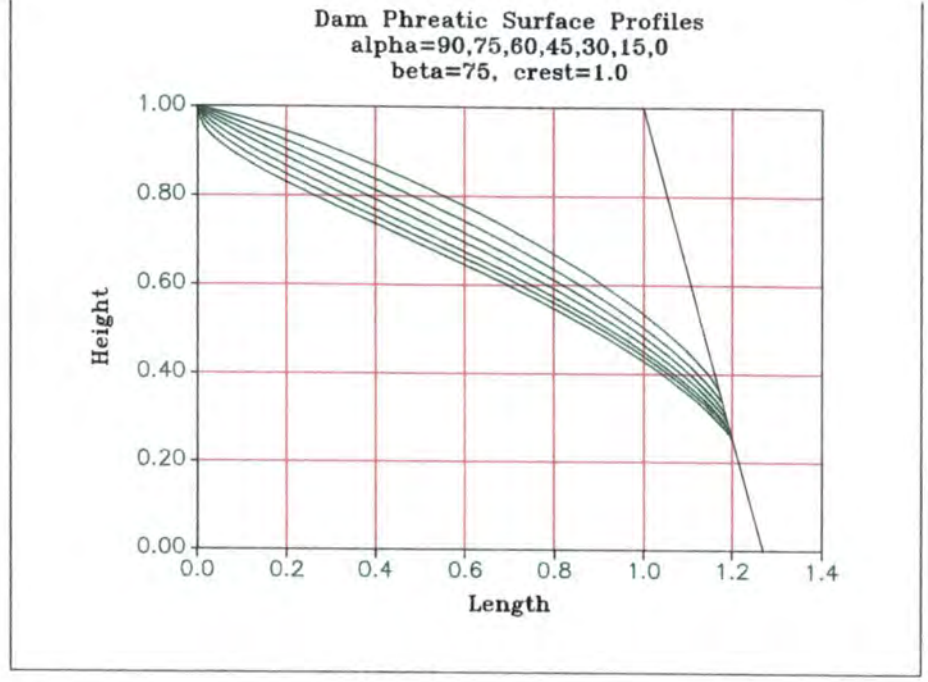
Dam Phreatic Surface Profiles
alpha=90,75,60,45,30,15,0
beta=75, crest=1.0
Height
1.00
0.80
0.60
0.40
0.20
0.00
0.0
0.2
0.4
0.6
0.8
1.0
1.2
1.4
Length

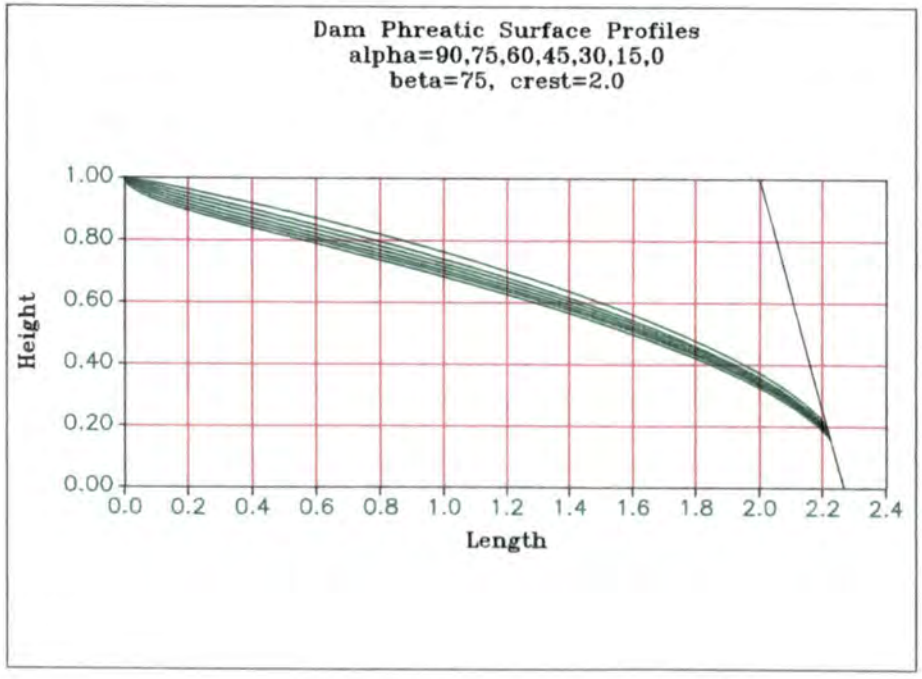
Dam Phreatic Surface Profiles
alpha=90,75,60,45,30,15,0
beta=75, crest=2.0
Height
1.00
0.80
0.60
0.40
0.20
0.00
0.0
0.2
0.4
0.6
0.8
1.0
1.2
1.4
1.6
1.8
2.0
2.2
2.4
Length

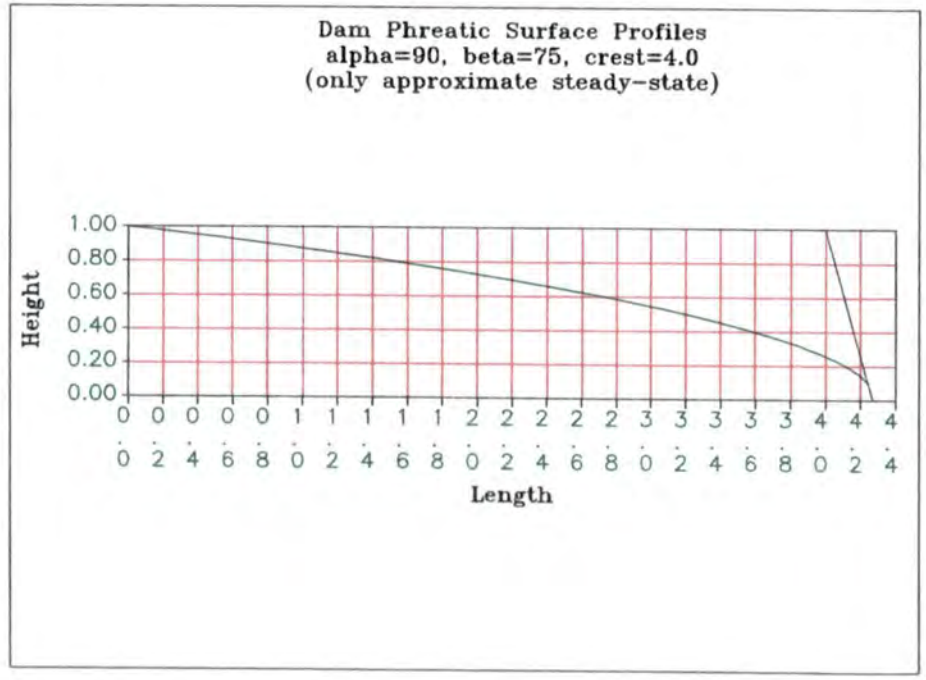
Dam Phreatic Surface Profiles
alpha=90, beta=75, crest=4.0
(only approximate steady-state)
Height
1.00
0.80
0.60
0.40
0.20
0.00
0 0 0 0 0 1 1 1 1 1 2 2 2 2 2 3 3 3 3 3 4 4 4
. . . .
0 2 4 6 8 0 2 4 6 8 0 2 4 6 8 0 2 4 6 8 0 2 4
Length

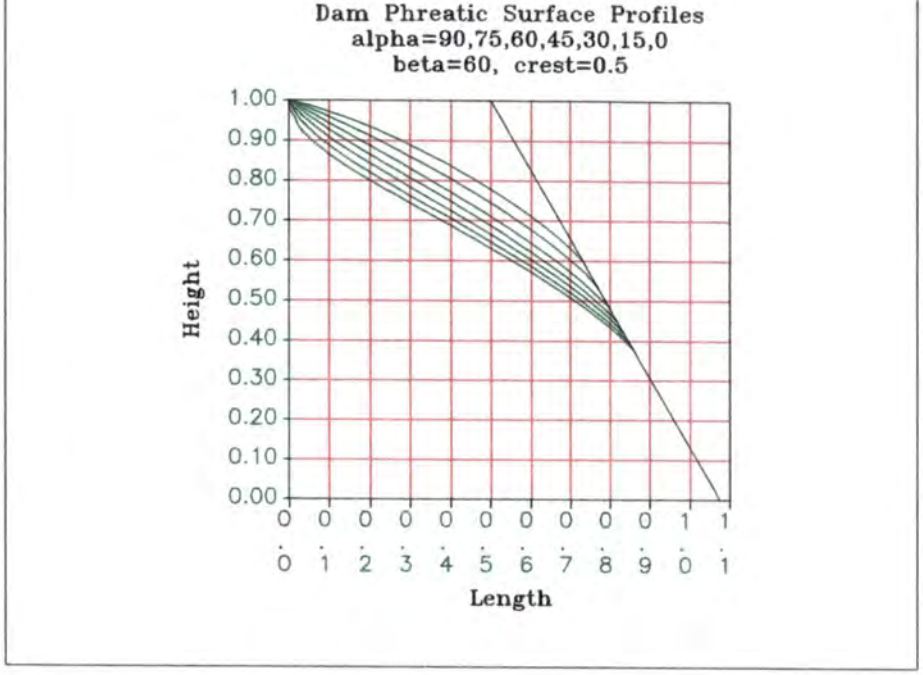
Dam Phreatic Surface Profiles
alpha=90,75,60,45,30,15,0
beta=60, crest=0.5
Height
1.00
0.90
0.80
0.70
0.60
0.50
0.40
0.30
0.20
0.10
0.00
0 0 0 0 0 0 0 0 0 0 1 1
0 1 2 3 4 5 6 7 8 9 0 1
Length

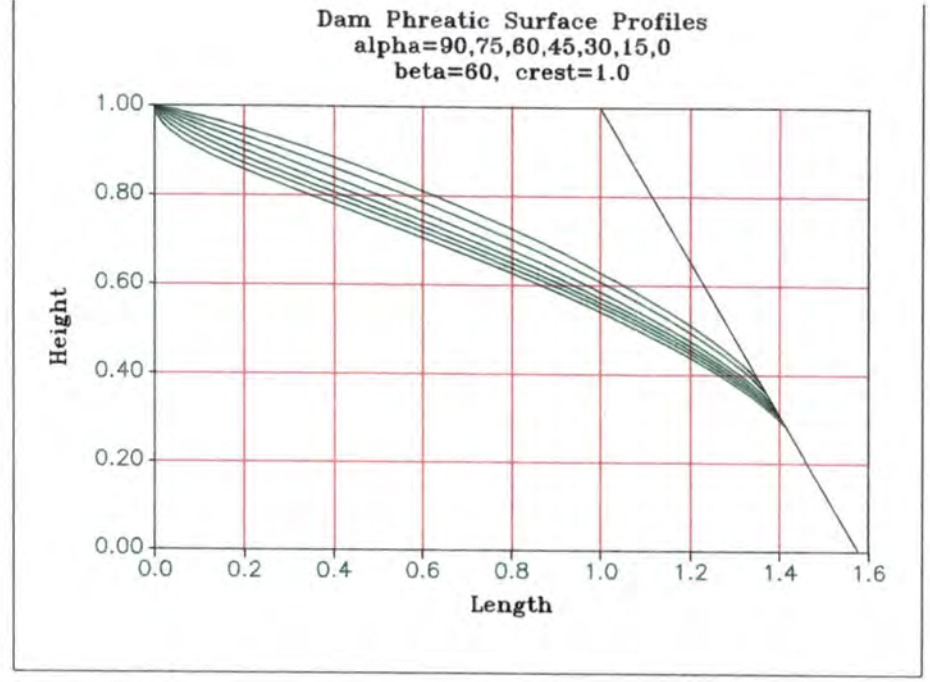
Dam Phreatic Surface Profiles
alpha=90,75,60,45,30,15,0
beta=60, crest=1.0
Height
1.00
0.80
0.60
0.40
0.20
0.00
0.0 0.2 0.4 0.6 0.8 1.0 1.2 1.4 1.6
Length

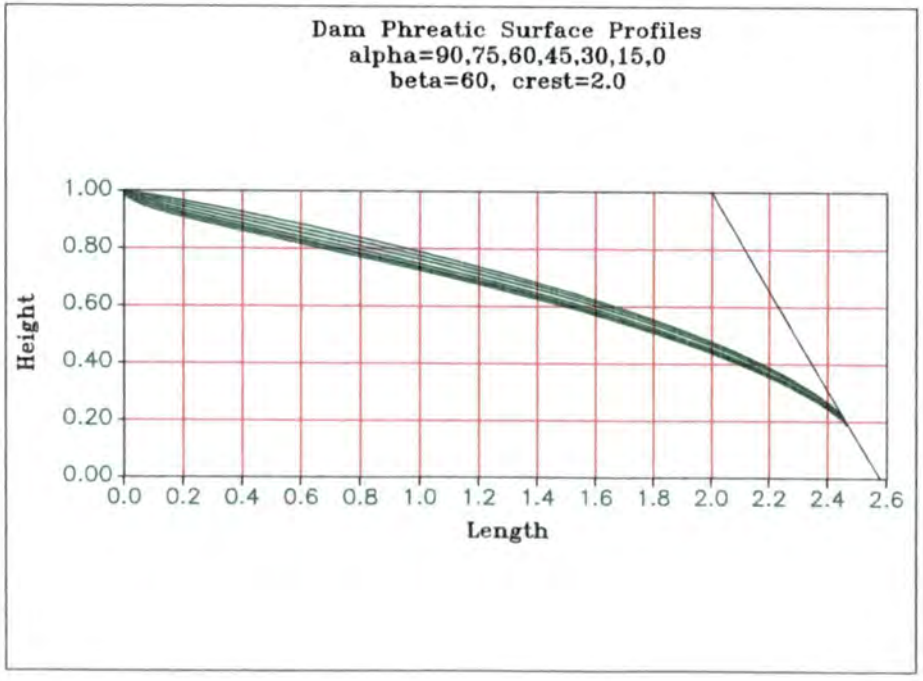
Dam Phreatic Surface Profiles
alpha=90,75,60,45,30,15,0
beta=60, crest=2.0
Height
1.00
0.80
0.60
0.40
0.20
0.00
0.0 0.2 0.4 0.6 0.8 1.0 1.2 1.4 1.6 1.8 2.0 2.2 2.4 2.6
Length

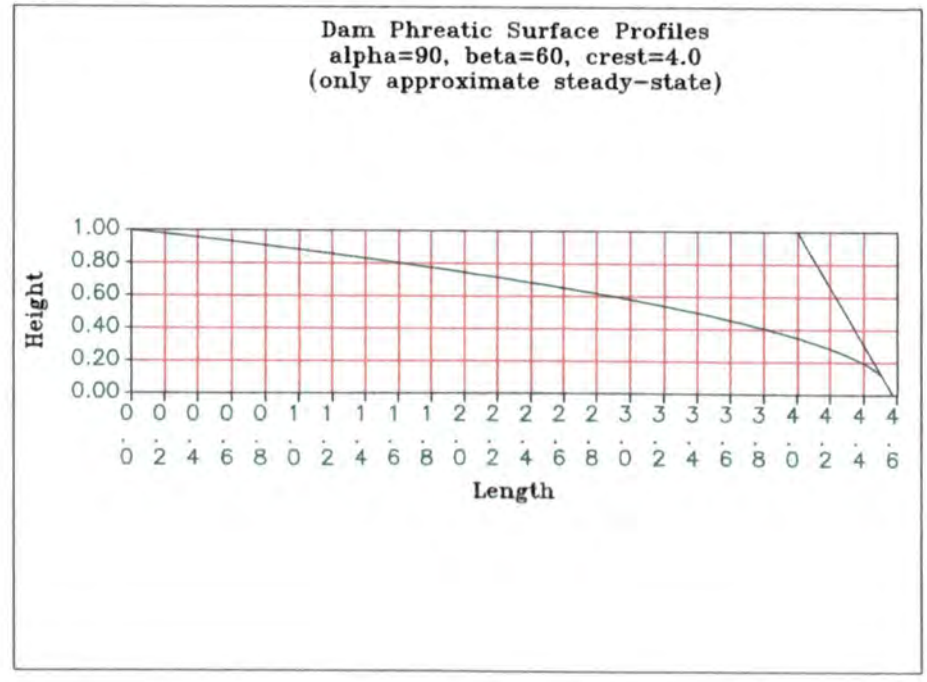
Dam Phreatic Surface Profiles
alpha=90, beta=60, crest=4.0
(only approximate steady-state)
Height
1.00
0.80
0.60
0.40
0.20
0.00
0 0 0 0 0 1 1 1 1 1 2 2 2 2 2 3 3 3 3 3 4 4 4 4
0 2 4 6 8 0 2 4 6 8 0 2 4 6 8 0 2 4 6 8 0 2 4 6
Length

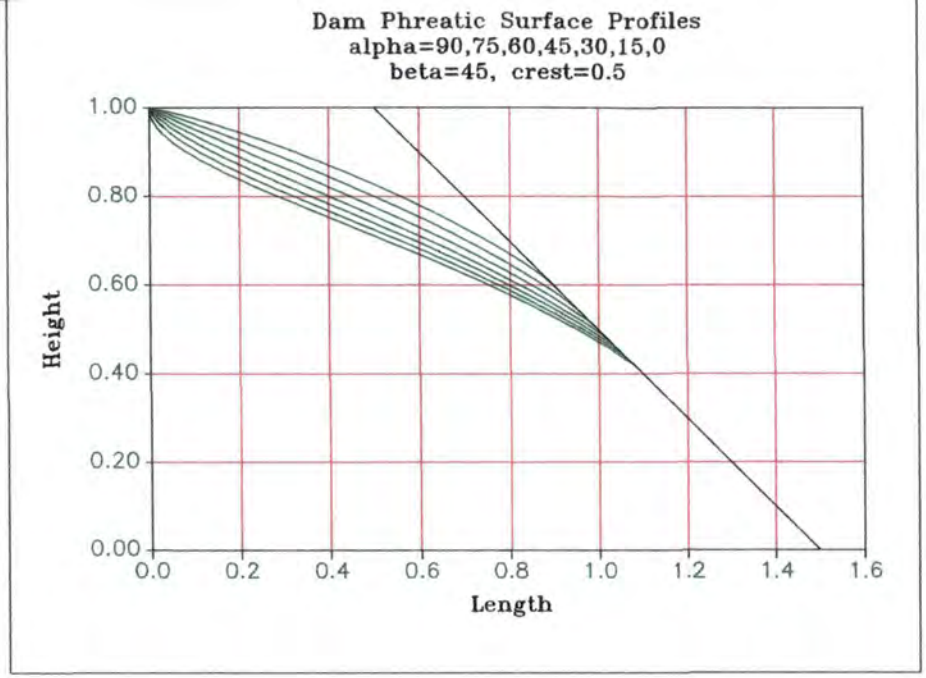
Dam Phreatic Surface Profiles
alpha=90,75,60,45,30,15,0
beta=45, crest=0.5
Height
1.00
0.80
0.60
0.40
0.20
0.00
0.0
0.2
0.4
0.6
0.8
1.0
1.2
1.4
1.6
Length

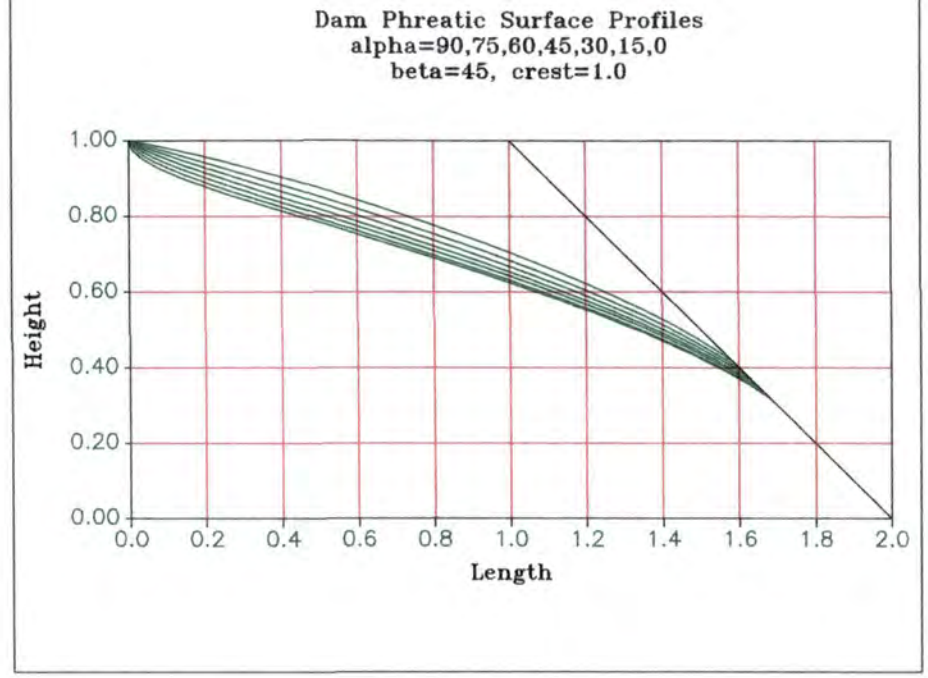
Dam Phreatic Surface Profiles
alpha=90,75,60,45,30,15,0
beta=45, crest=1.0
Height
1.00
0.80
0.60
0.40
0.20
0.00
0.0
0.2
0.4
0.6
0.8
1.0
1.2
1.4
1.6
1.8
2.0
Length

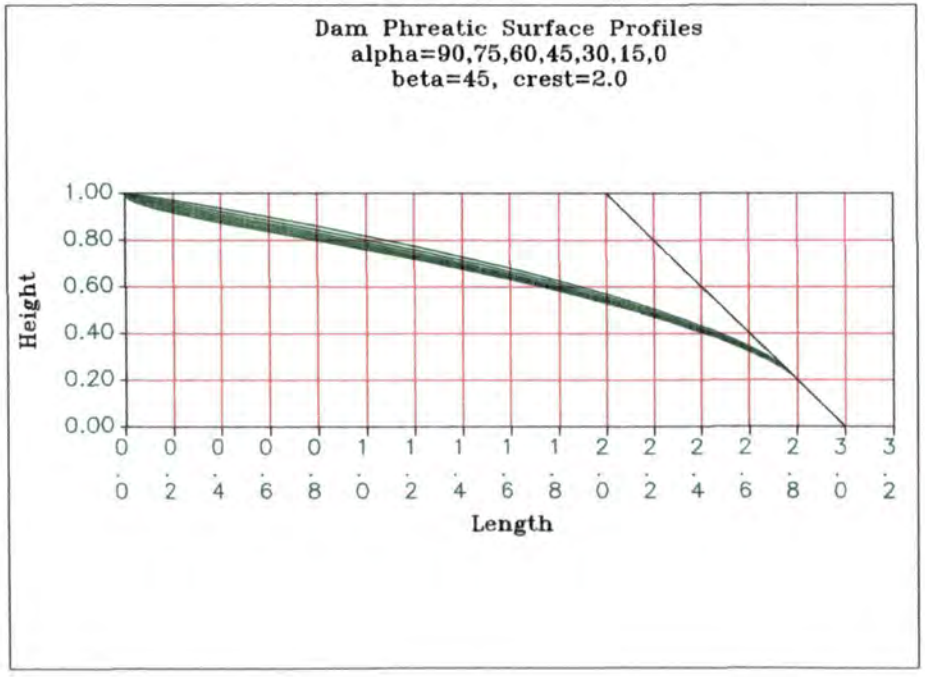
Dam Phreatic Surface Profiles
alpha=90,75,60,45,30,15,0
beta=45, crest=2.0
Height
1.00
0.80
0.60
0.40
0.20
0.00
Length

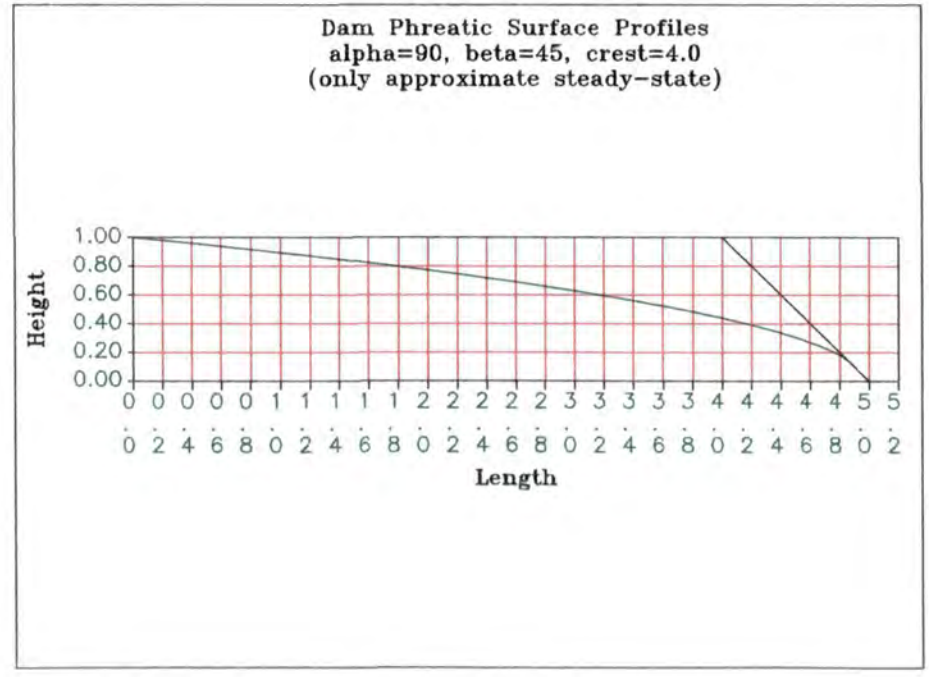
Dam Phreatic Surface Profiles
alpha=90, beta=45, crest=4.0
(only approximate steady-state)
Height
1.00
0.80
0.60
0.40
0.20
0.00
Length

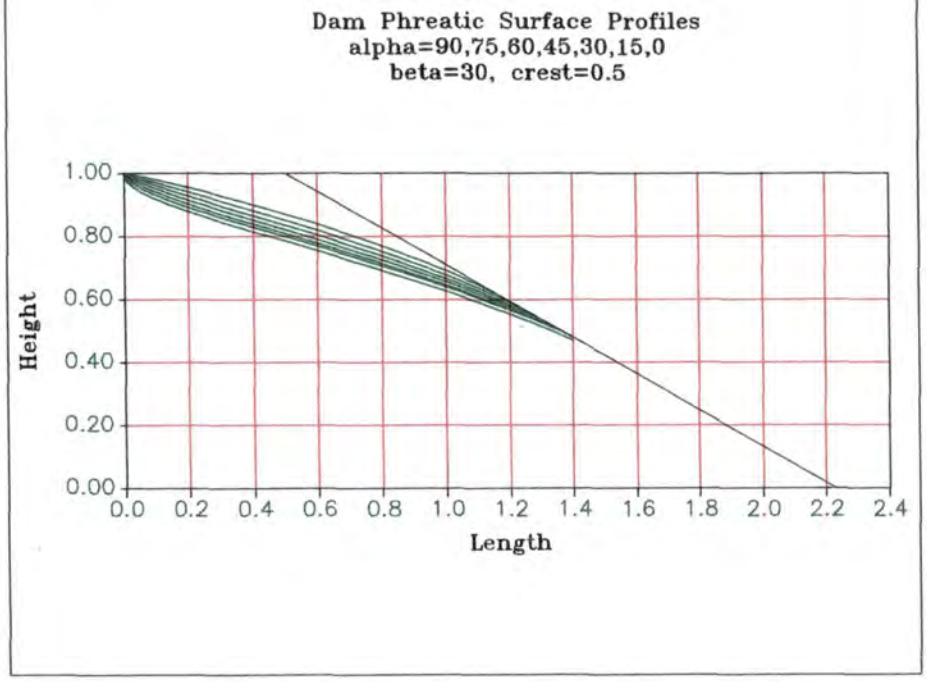
Dam Phreatic Surface Profiles
alpha=90,75,60,45,30,15,0
beta=30, crest=0.5
Height
1.00
0.80
0.60
0.40
0.20
0.00
0.0 0.2 0.4 0.6 0.8 1.0 1.2 1.4 1.6 1.8 2.0 2.2 2.4
Length


Dam Phreatic Surface Profiles
alpha=90,75,60,45,30,15,0
beta=30, crest=1.0
Height
1.00
0.80
0.60
0.40
0.20
0.00
0 0 0 0 0 1 1 1 1 1 2 2 2 2 2
0 2 4 6 8 0 2 4 6 8 0 2 4 6 8
Length

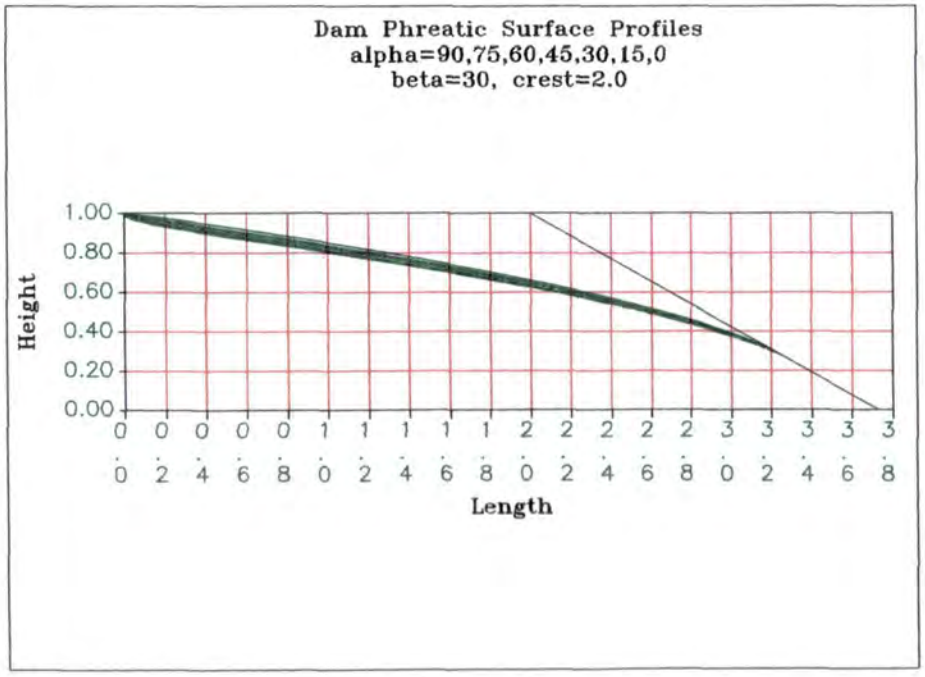
Dam Phreatic Surface Profiles
alpha=90,75,60,45,30,15,0
beta=30, crest=2.0
Height
1.00
0.80
0.60
0.40
0.20
0.00
0 0 0 0 0 1 1 1 1 1 2 2 2 2 2 3 3 3 3 3
0 2 4 6 8 0 2 4 6 8 0 2 4 6 8 0 2 4 6 8
Length

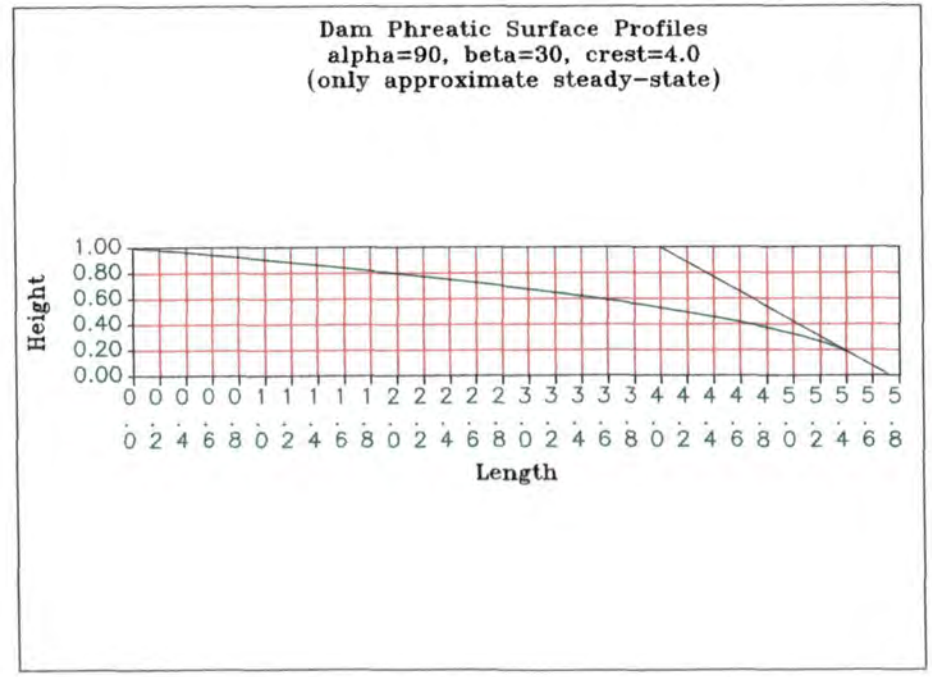
Dam Phreatic Surface Profiles
alpha=90, beta=30, crest=4.0
(only approximate steady-state)
Height
1.00
0.80
0.60
0.40
0.20
0.00
0 0 0 0 0 1 1 1 1 1 2 2 2 2 2 3 3 3 3 3 4 4 4 4 4 5 5 5 5 5
0 2 4 6 8 0 2 4 6 8 0 2 4 6 8 0 2 4 6 8 0 2 4 6 8 0 2 4 6 8
Length

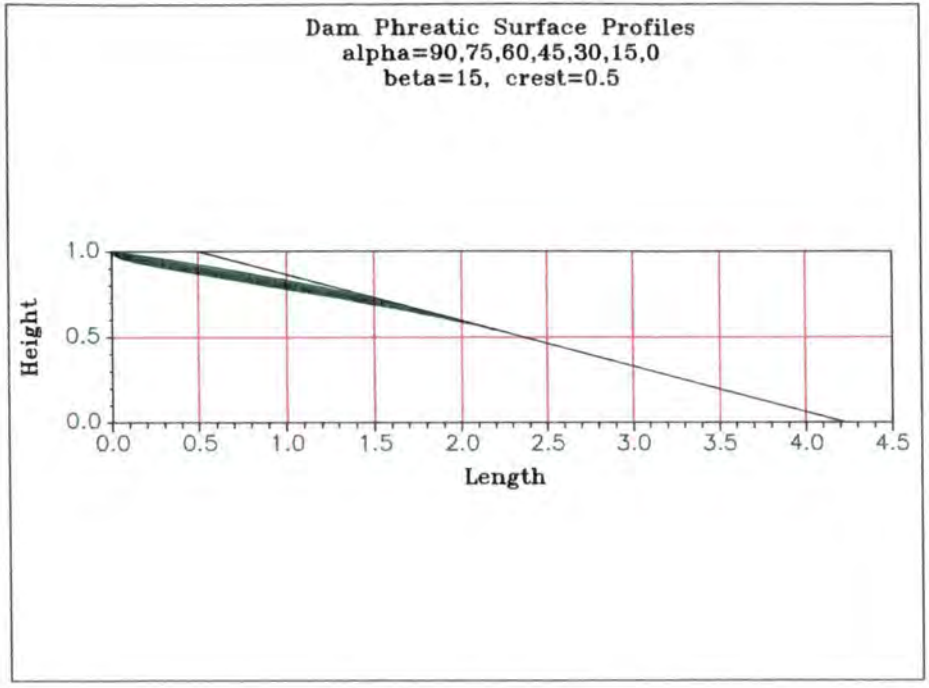
Dam Phreatic Surface Profiles
alpha=90,75,60,45,30,15,0
beta=15, crest=0.5
Height
1.0
0.5
0.0
0.0 0.5 1.0 1.5 2.0 2.5 3.0 3.5 4.0 4.5
Length

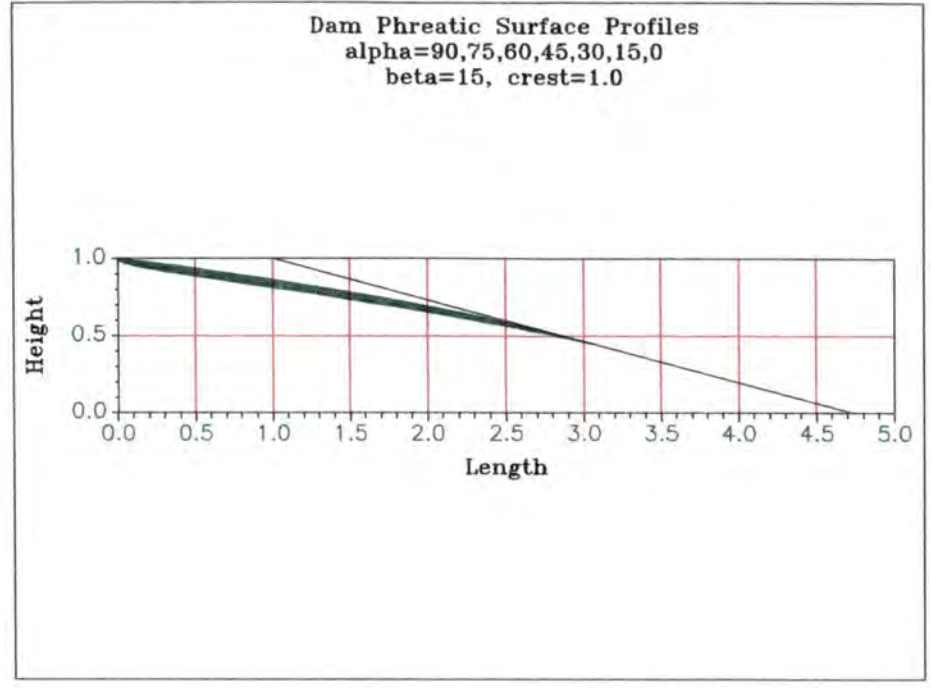
Dam Phreatic Surface Profiles
alpha=90,75,60,45,30,15,0
beta=15, crest=1.0
Height
1.0
0.5
0.0
0.0 0.5 1.0 1.5 2.0 2.5 3.0 3.5 4.0 4.5 5.0
Length

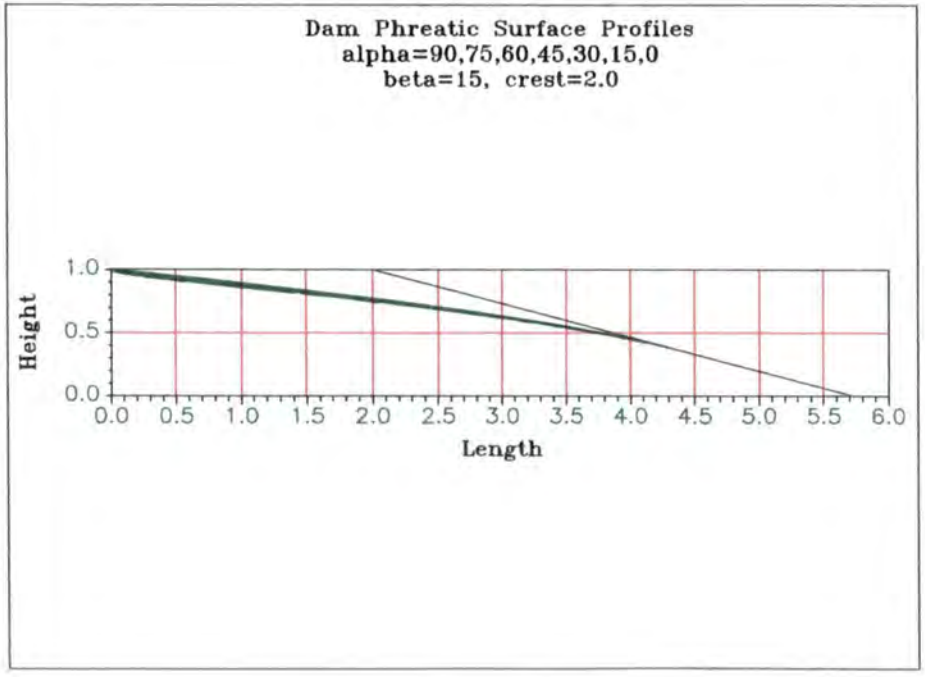
Dam Phreatic Surface Profiles
alpha=90,75,60,45,30,15,0
beta=15, crest=2.0
Height
1.0
0.5
0.0
0.0 0.5 1.0 1.5 2.0 2.5 3.0 3.5 4.0 4.5 5.0 5.5 6.0
Length

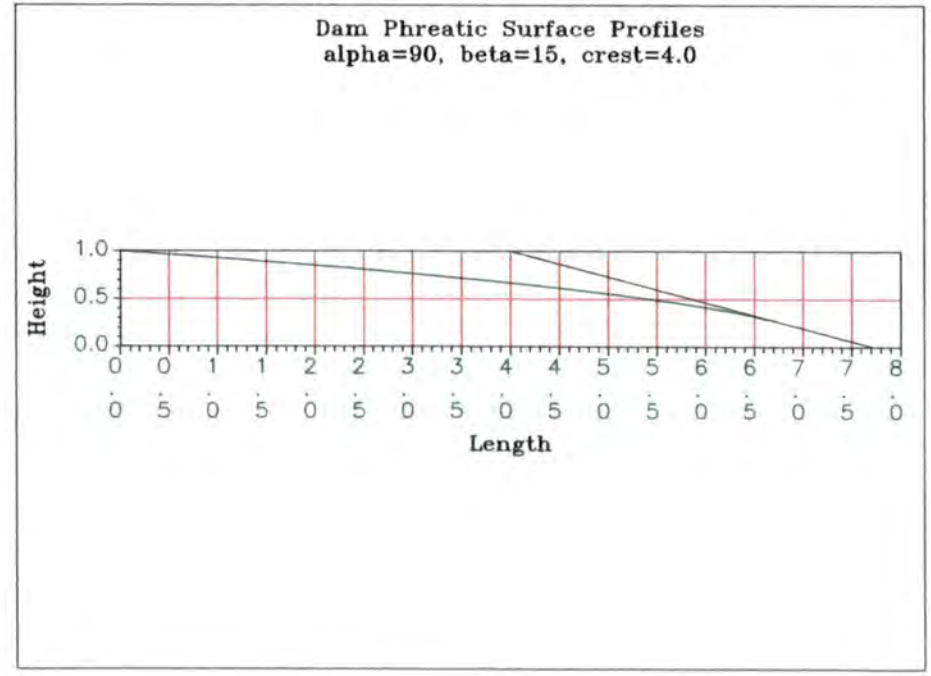
Dam Phreatic Surface Profiles
alpha=90, beta=15, crest=4.0
Height
1.0
0.5
0.0
0.0 0.5 1.0 1.5 2.0 2.5 3.0 3.5 4.0 4.5 5.0 5.5 6.0 6.5 7.0 7.5 8.0
Length

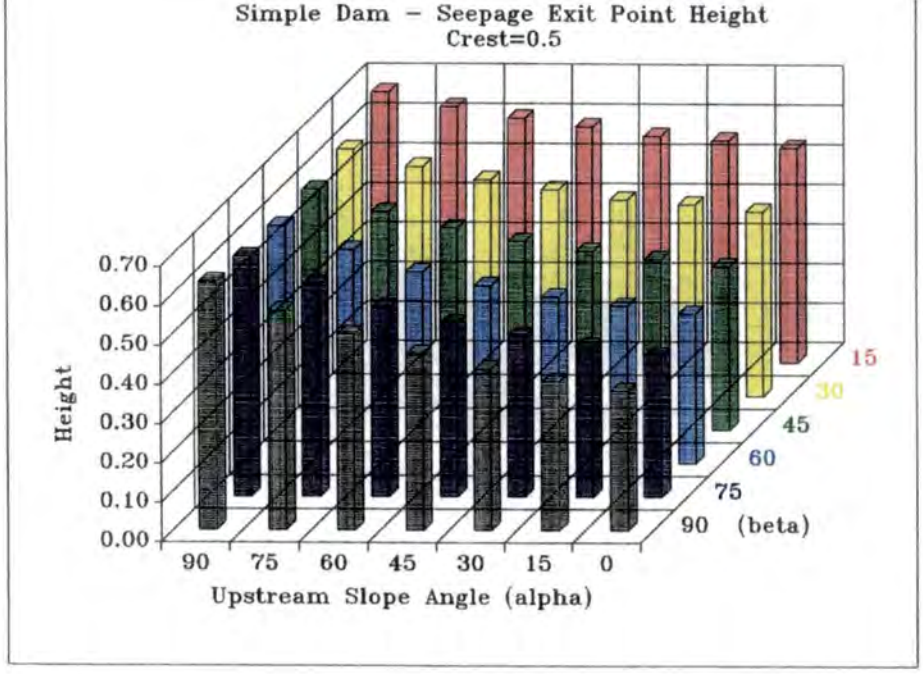
Simple Dam – Seepage Exit Point Height
Crest=0.5
Height
0.70
0.60
0.50
0.40
0.30
0.20
0.10
0.00
90 75 60 45 30 15 0
Upstream Slope Angle (alpha)
15
30
45
60
75
90 (beta)

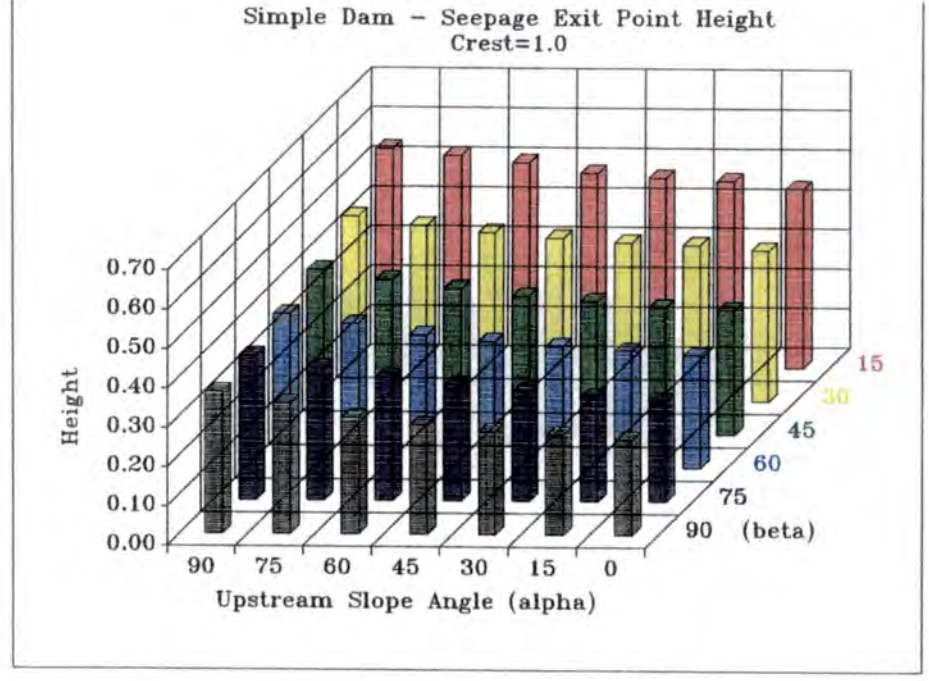
Simple Dam – Seepage Exit Point Height
Crest=1.0
Height
0.70
0.60
0.50
0.40
0.30
0.20
0.10
0.00
90 75 60 45 30 15 0
Upstream Slope Angle (alpha)
15
30
45
60
75
90 (beta)

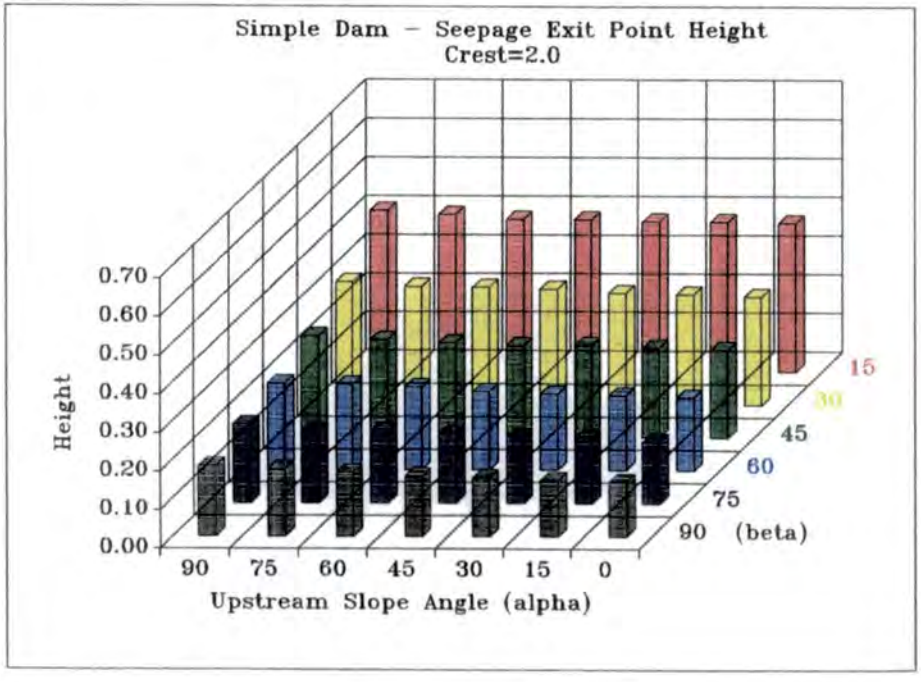
Simple Dam – Seepage Exit Point Height
Crest=2.0
Height
0.70
0.60
0.50
0.40
0.30
0.20
0.10
0.00
90 75 60 45 30 15 0
Upstream Slope Angle (alpha)
15
30
45
60
75
90 (beta)

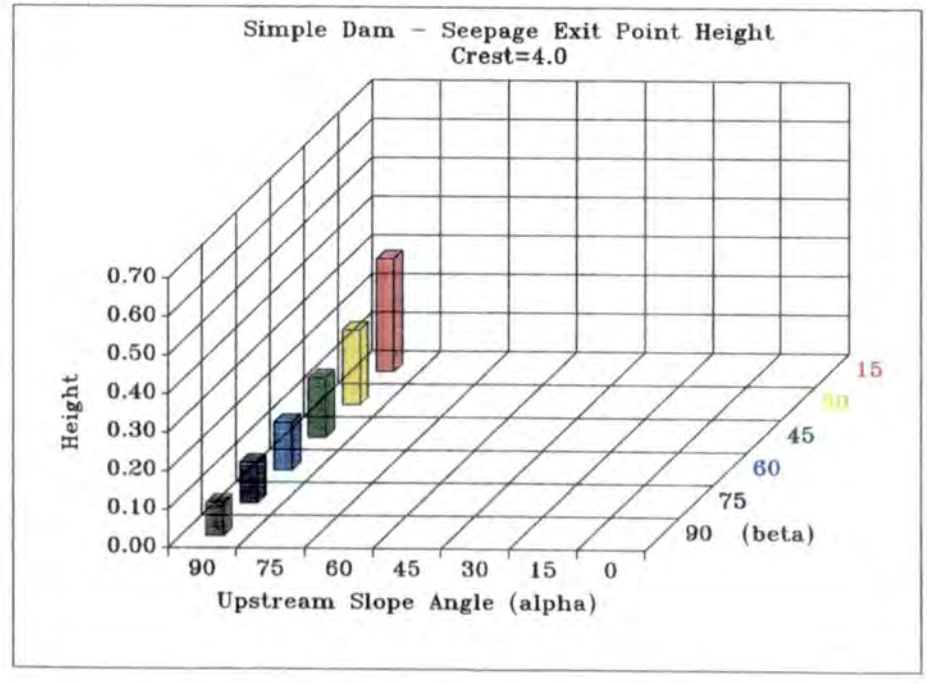
Simple Dam – Seepage Exit Point Height
Crest=4.0
Height
0.70
0.60
0.50
0.40
0.30
0.20
0.10
0.00
90 75 60 45 30 15 0
Upstream Slope Angle (alpha)
15
30
45
60
75
90 (beta)

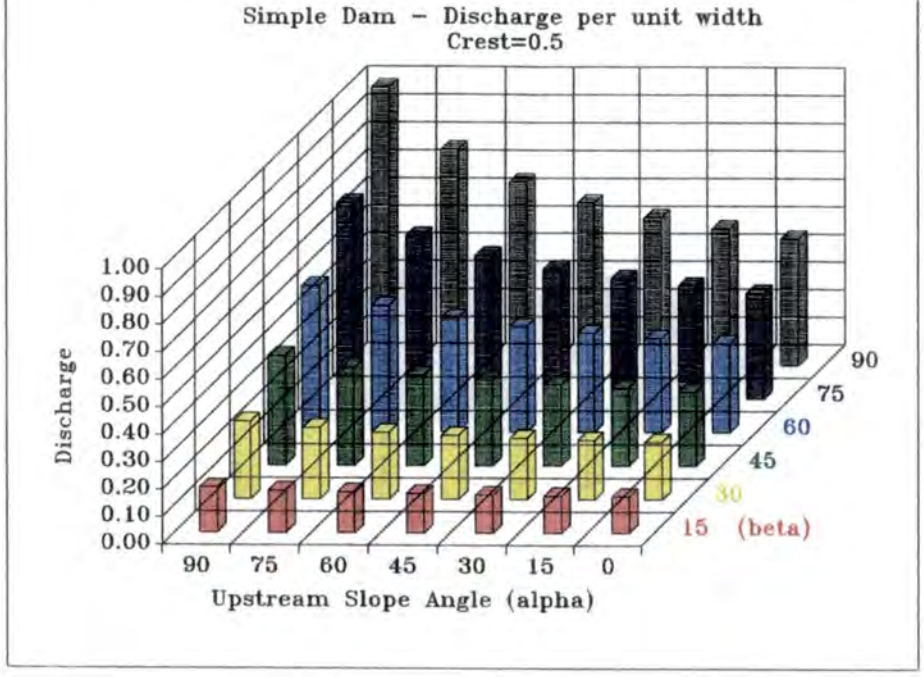
Simple Dam – Discharge per unit width
Crest=0.5
Discharge
1.00
0.90
0.80
0.70
0.60
0.50
0.40
0.30
0.20
0.10
0.00
90 75 60 45 30 15 0
Upstream Slope Angle (alpha)
90
75
60
45
30
15 (beta)

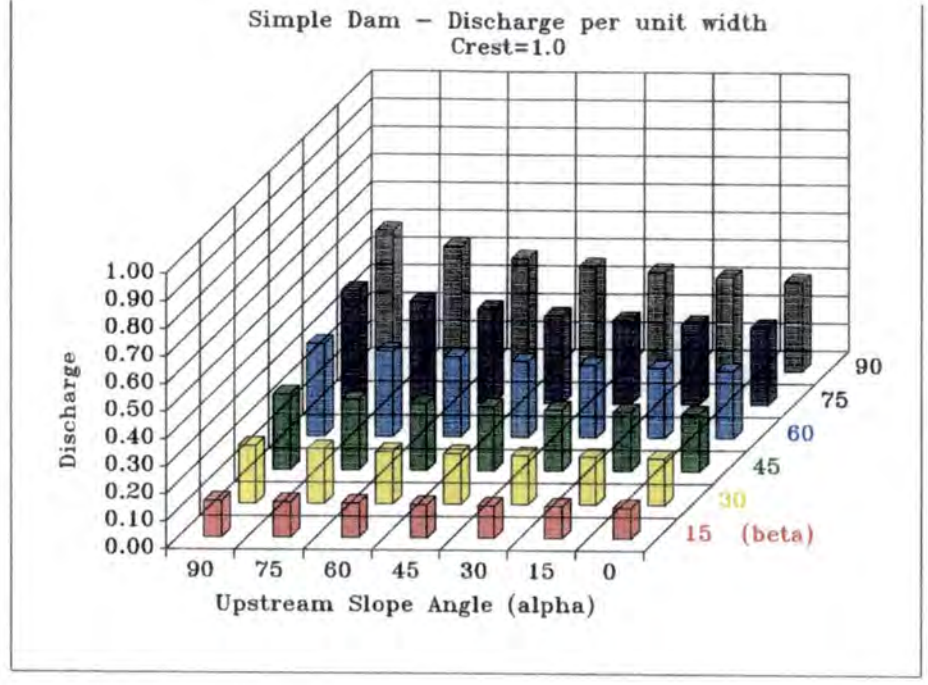
Simple Dam – Discharge per unit width
Crest=1.0
Discharge
1.00
0.90
0.80
0.70
0.60
0.50
0.40
0.30
0.20
0.10
0.00
90 75 60 45 30 15 0
Upstream Slope Angle (alpha)
90
75
60
45
30
15 (beta)

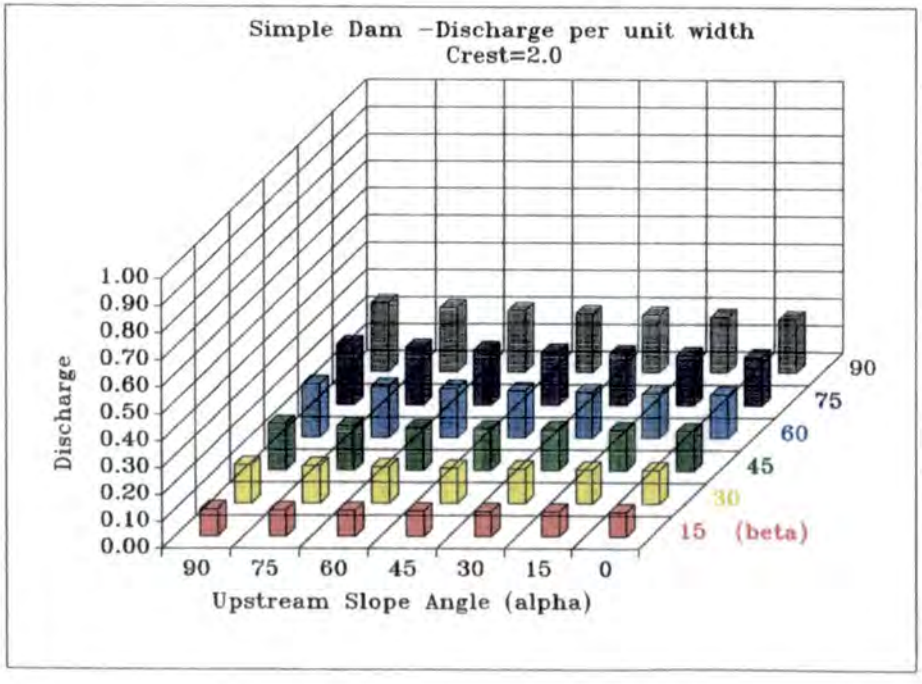
Simple Dam –Discharge per unit width
Crest=2.0
Discharge
1.00
0.90
0.80
0.70
0.60
0.50
0.40
0.30
0.20
0.10
0.00
90 75 60 45 30 15 0
Upstream Slope Angle (alpha)
90
75
60
45
30
15 (beta)

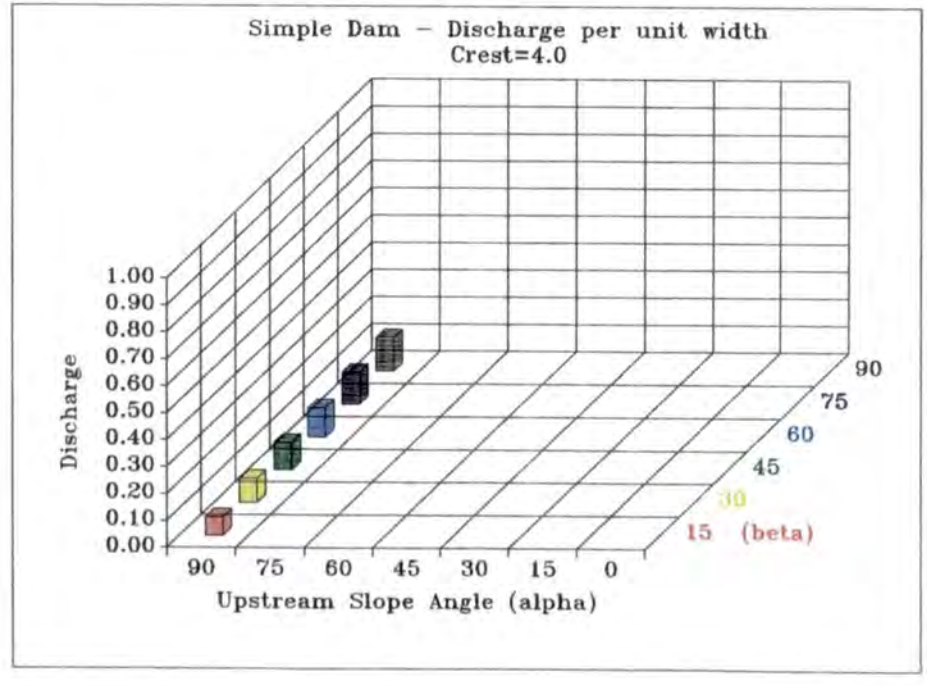
Simple Dam – Discharge per unit width
Crest=4.0
Discharge
1.00
0.90
0.80
0.70
0.60
0.50
0.40
0.30
0.20
0.10
0.00
90 75 60 45 30 15 0
Upstream Slope Angle (alpha)
90
75
60
45
30
15 (beta)

Appendix 3

Flow Nets for Tailings Dams and Earth Embankments

Graphs of Seepage Discharge and Seepage Line Exit Height

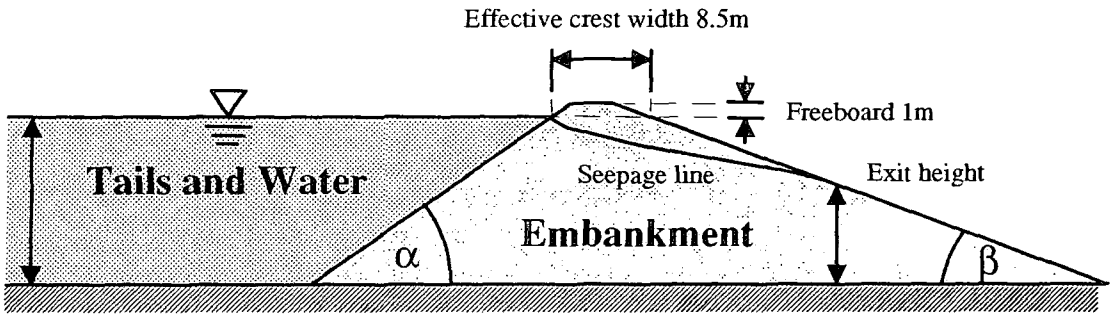

Height 17m Upstream slope 1:1.5 Downstream slope 1:2

not to scale

Dam Geometry Modelled in Finite Element Analyses

Analysis of the Effect of Tailings Permeability and Beach Length
Limiting Geometry British Coal Dam - Zero Beach
TD0

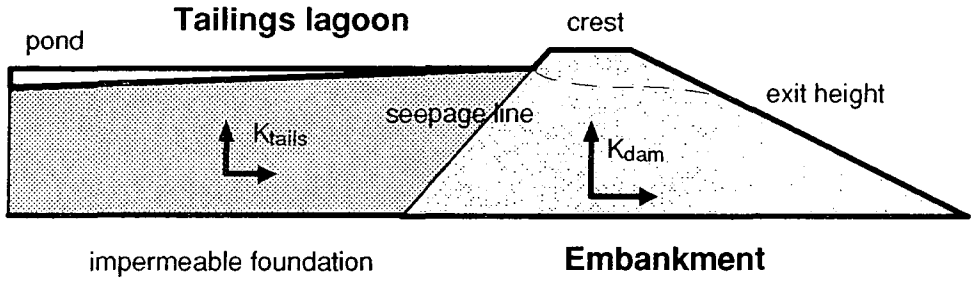

Ktails/Kdam	discharge *	exit height **	K log ratio	rel. discharge
10	3.57	8.92	1.00	1.09
5	3.55	8.84	0.70	1.08
2	3.45	8.57	0.30	1.05
1	3.28	8.18	0.00	1.00
0.5	3.02	7.60	-0.30	0.92
0.4	2.93	7.33	-0.40	0.89
0.3	2.76	6.88	-0.52	0.84
0.2	2.52	6.29	-0.70	0.77

* discharge in m^3/s per m width for a dam permeability of 1 m/s ** exit height in metres

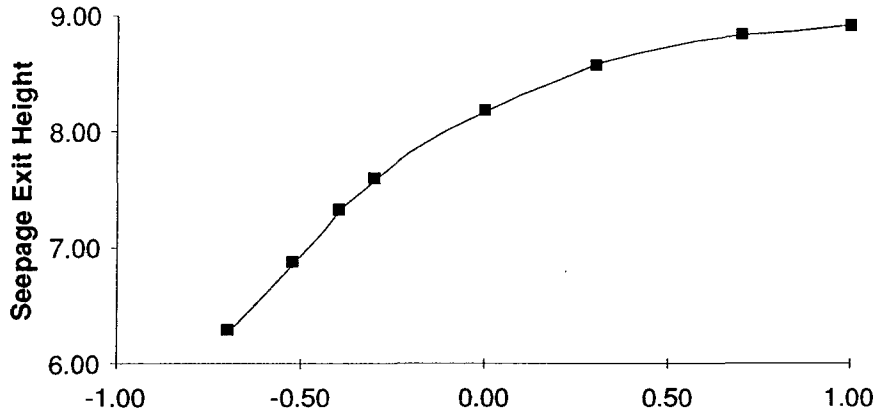

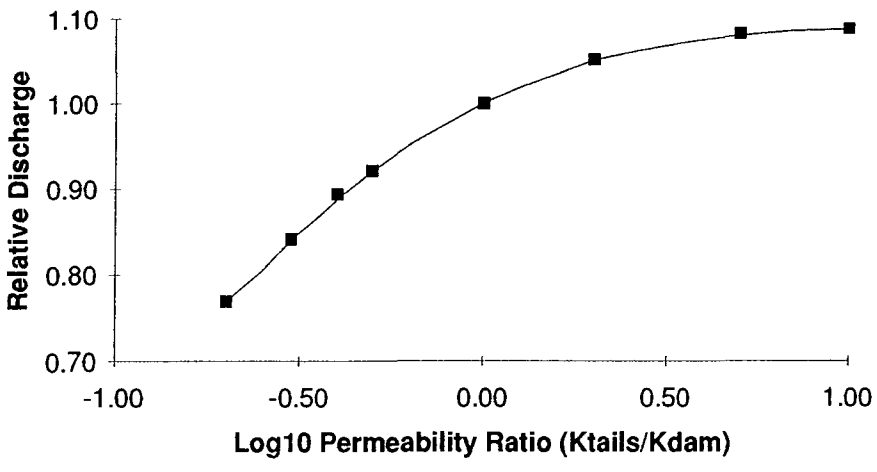

Tailings Dam Geometry (with pond against dam) TD0
Step change in permeability from tailings to dam.
Ratio k(tailings)/k(dam)

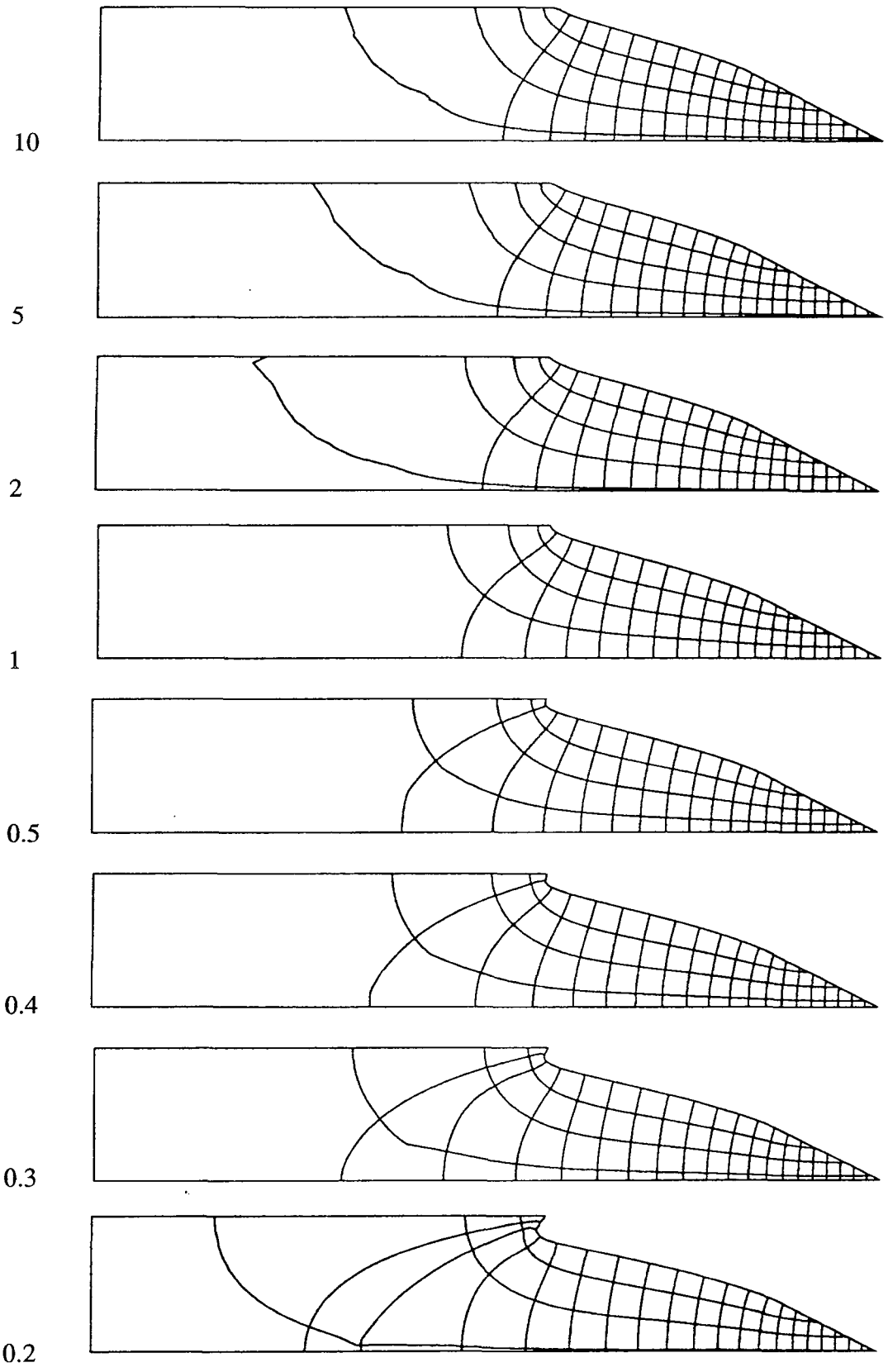

Analysis of the Effect of Tailings Permeability and Beach Length
Limiting Geometry British Coal Dam - 10m Beach
TD10

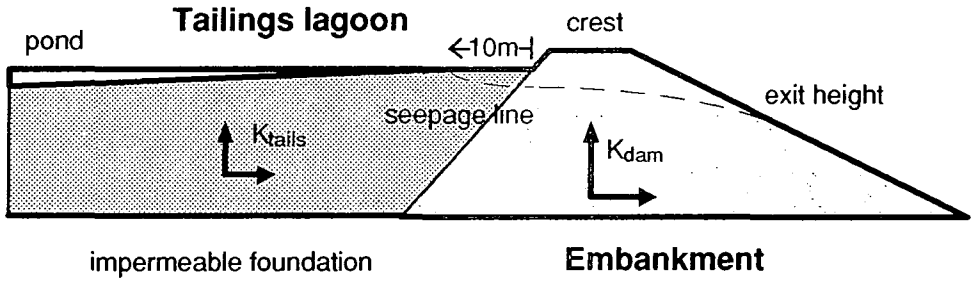

Ktails/Kdam	discharge *	exit height **	K log ratio	rel. discharge
10	3.41	8.51	1.00	1.29
5	3.22	8.10	0.70	1.22
2	2.94	7.31	0.30	1.11
1	2.65	6.57	0.00	1.00
0.5	2.27	5.70	-0.30	0.86
0.2	1.68	4.27	-0.70	0.63
0.1	1.22	3.38	-1.00	0.46

* discharge in m^3/s per m width for a dam permeability of 1 m/s ** exit height in metres

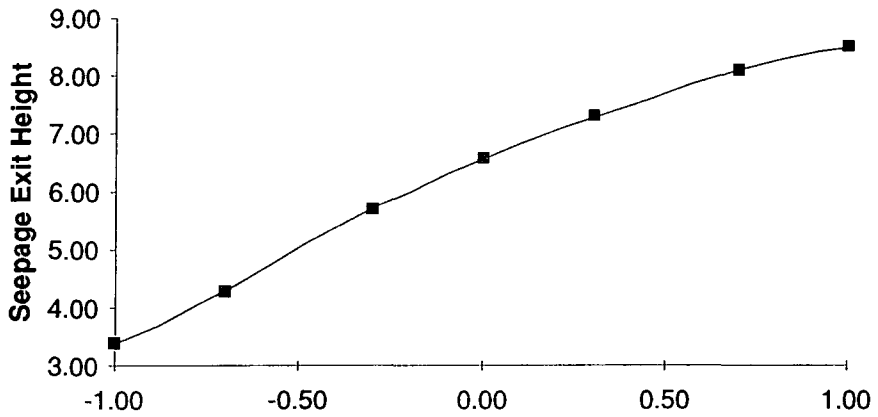

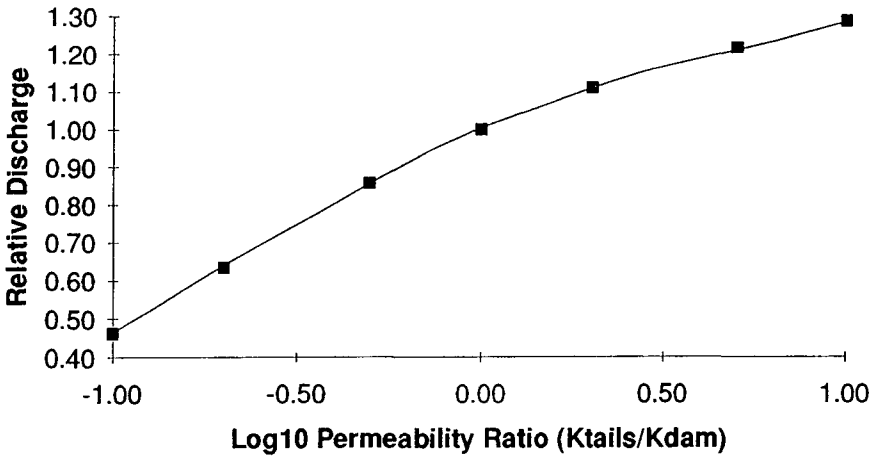

Tailings Dam Geometry (with pond 20m from dam) TD10
Step change in permeability from tailings to dam.
Ratio k(tailings)/k(dam)

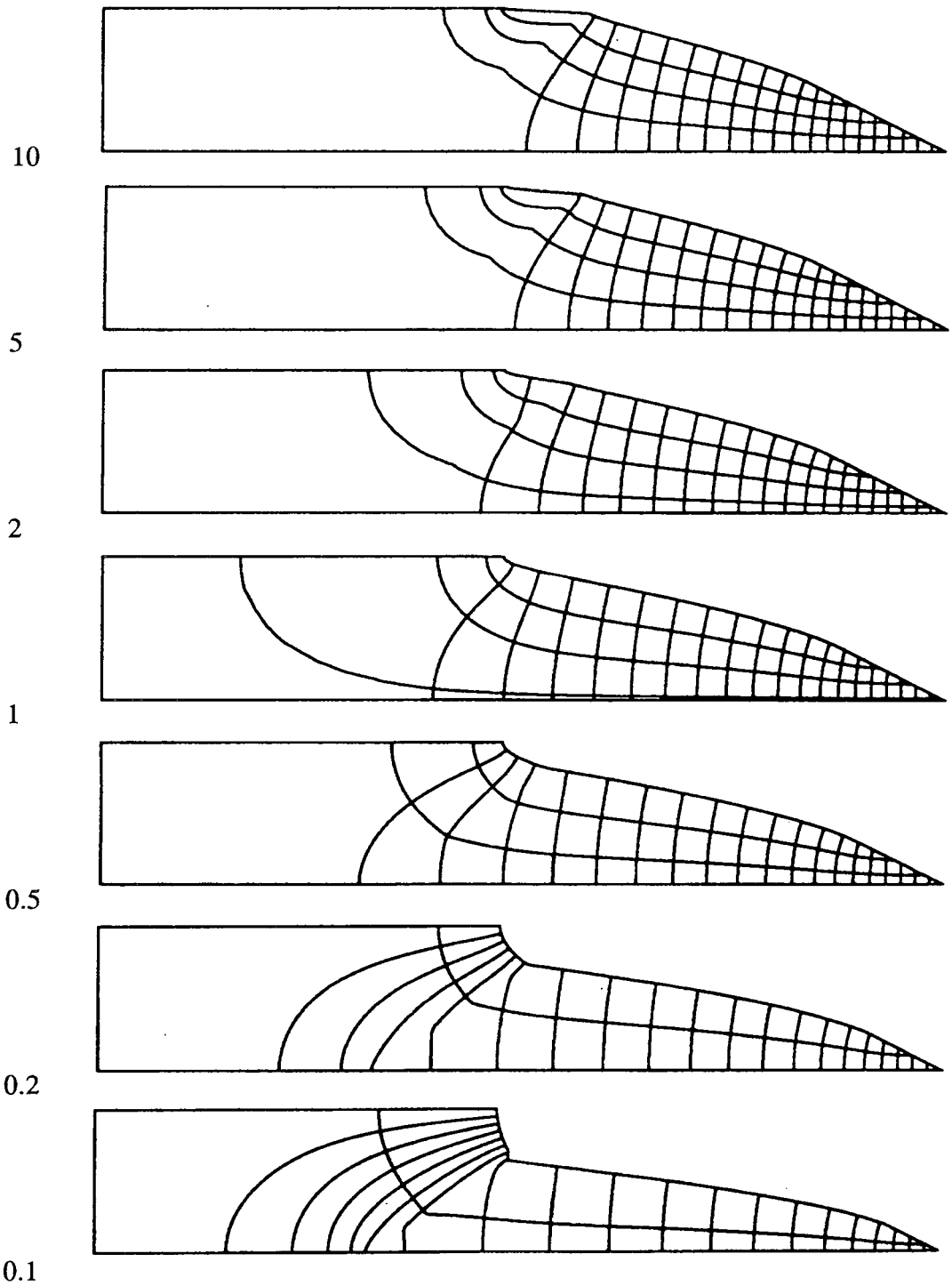

Analysis of the Effect of Tailings Permeability and Beach Length
Limiting Geometry British Coal Dam - 20m Beach
TD20

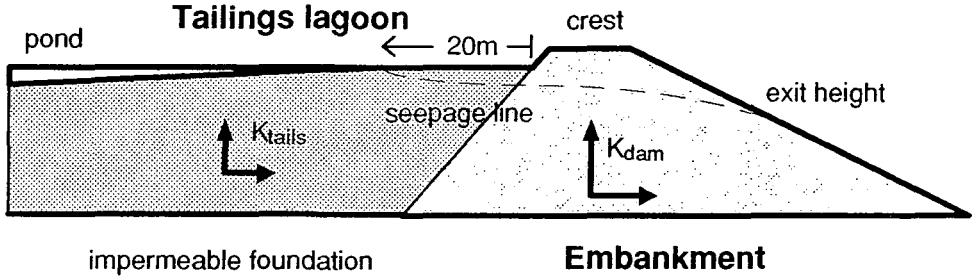

Ktails/Kdam	discharge *	exit height **	K log ratio	rel. discharge
10	3.27	8.18	1.00	1.47
5	3.00	7.61	0.70	1.35
2	2.57	6.47	0.30	1.16
1	2.22	5.50	0.00	1.00
0.5	1.80	4.51	-0.30	0.81
0.2	1.24	3.16	-0.70	0.56
0.1	0.88	2.33	-1.00	0.40
0.05	0.53	1.37	-1.30	0.24

* discharge in m^3/s per m width for a dam permeability of 1 m/s ** exit height in metres

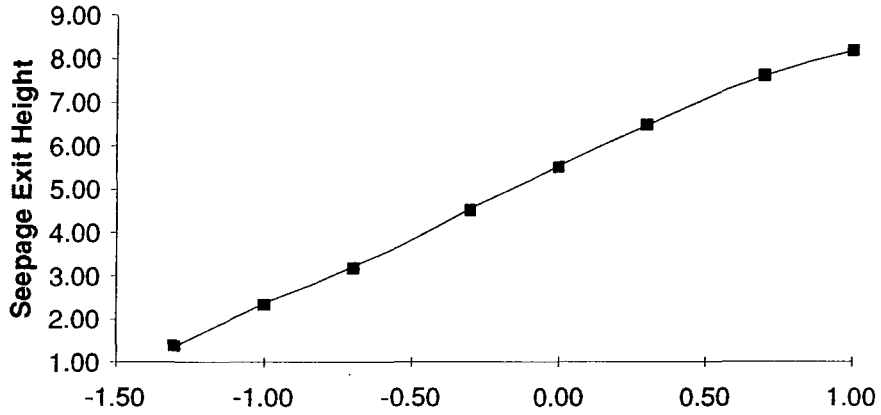

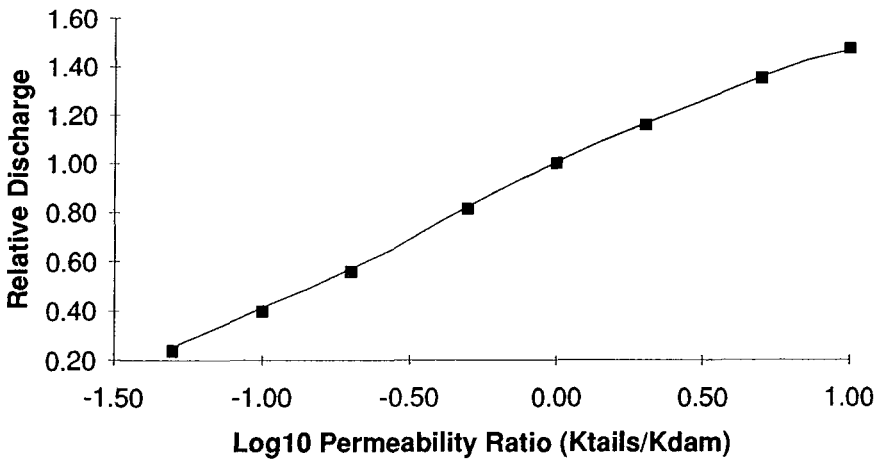

Tailings Dam Geometry (with pond 20m from dam) TD20
Step change in permeability from tailings to dam.
Ratio k(tailings)/k(dam)

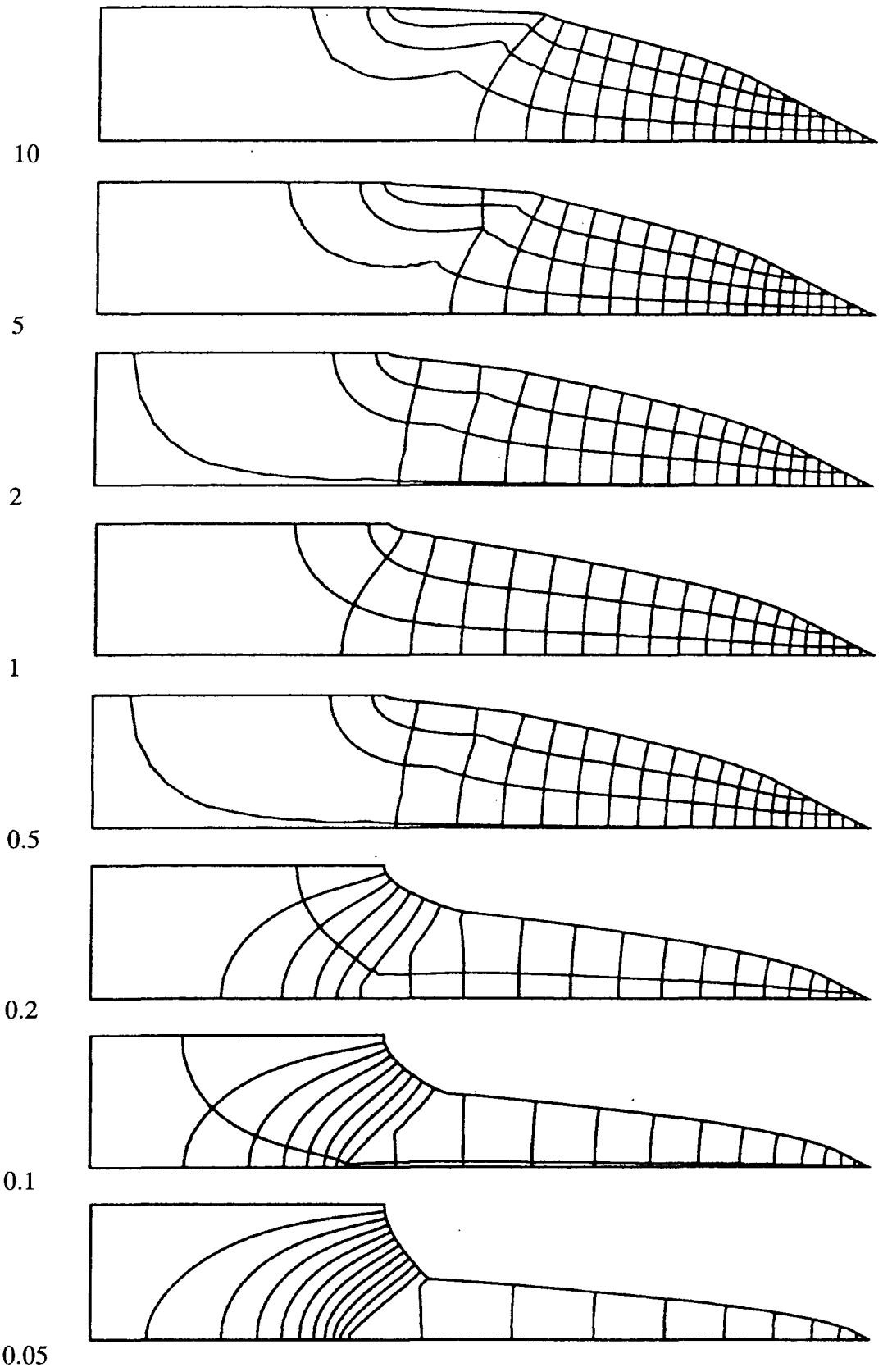

Analysis of the Effect of Tailings Permeability and Beach Length
Limiting Geometry British Coal Dam - 30m Beach
TD30

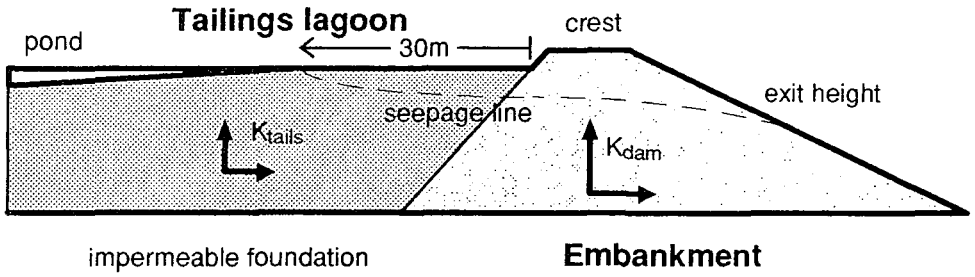

Ktails/Kdam	discharge *	exit height **	K log ratio	rel. discharge
10	3.14	7.80	1.00	1.65
5	2.87	7.19	0.70	1.51
2	2.34	5.83	0.30	1.23
1	1.90	4.70	0.00	1.00
0.5	1.48	3.70	-0.30	0.78
0.2	0.93	2.40	-0.70	0.49
0.1	0.58	1.52	-1.00	0.31
0.05	0.35	0.93	-1.30	0.18
0.02	0.16	0.43	-1.70	0.08

* discharge in m^3/s per m width for a dam permeability of 1m/s ** exit height in metres

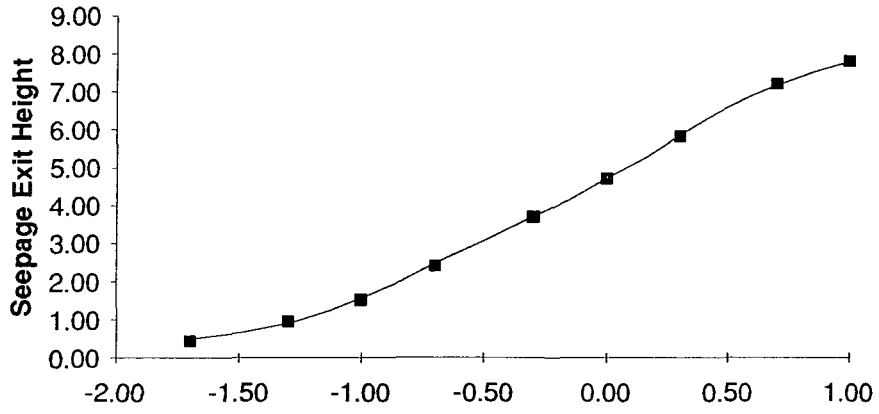

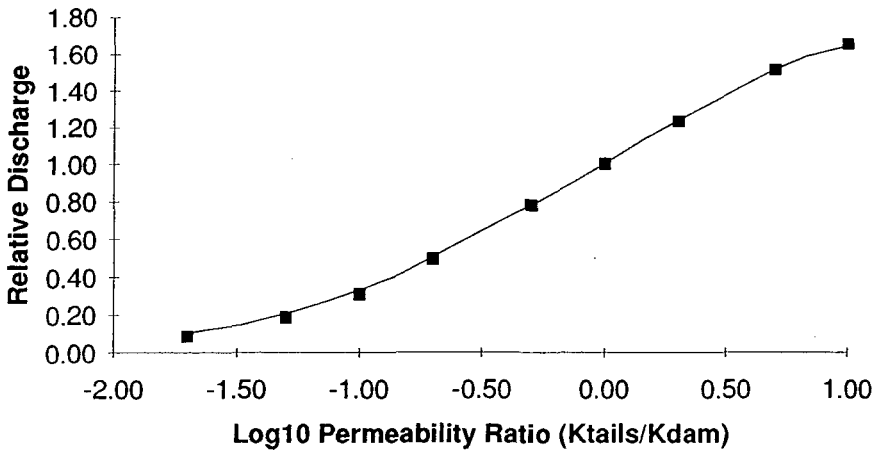

Tailings Dam Geometry (with pond 30m from dam) TD30
Step change in permeability from tailings to dam.
Ratio k(tailings)/k(dam)

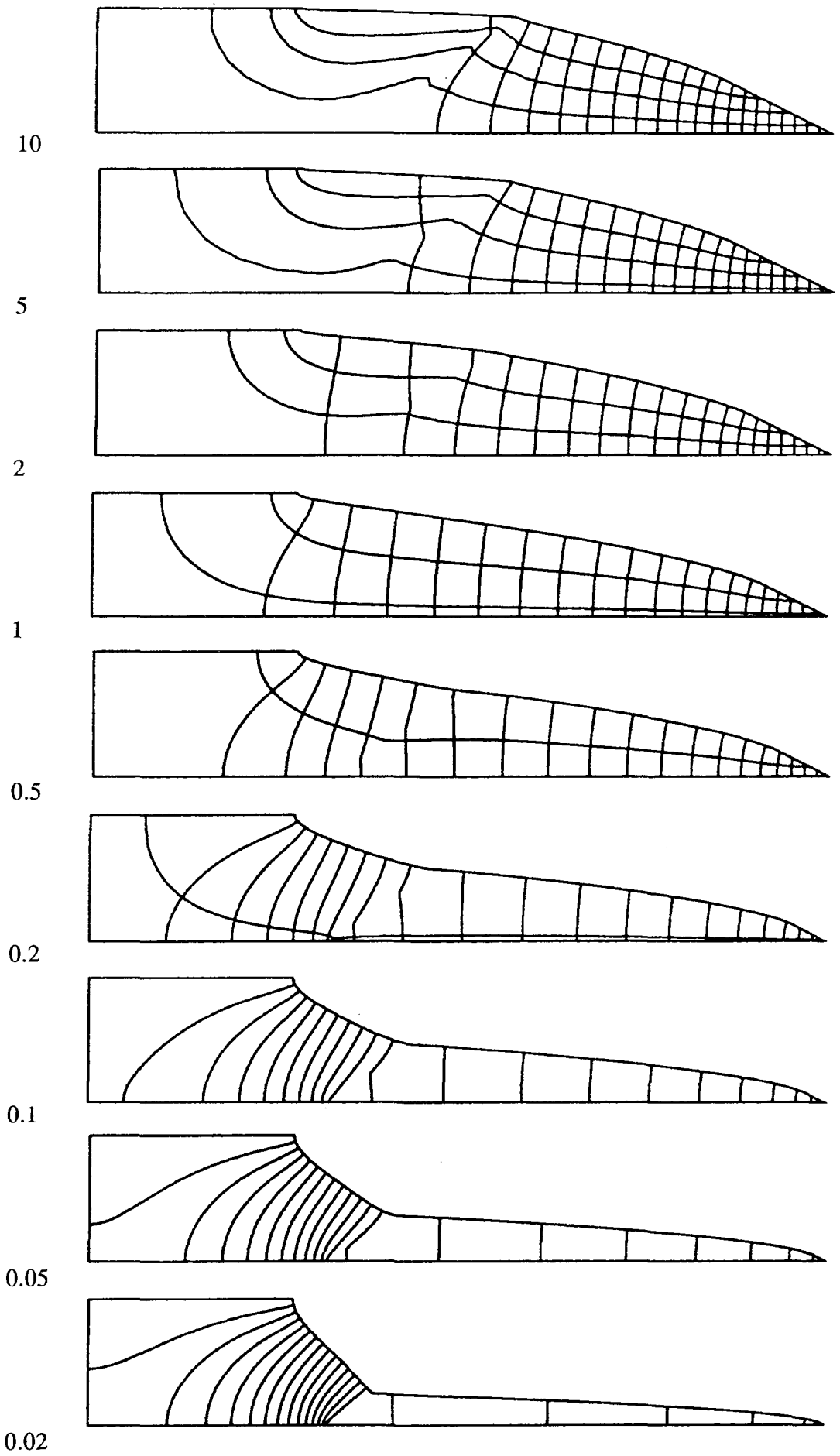

Analysis of the Effect of Horizontal Variation in Tailings Permeability
Limiting Geometry British Coal Dam
TDDIHIC

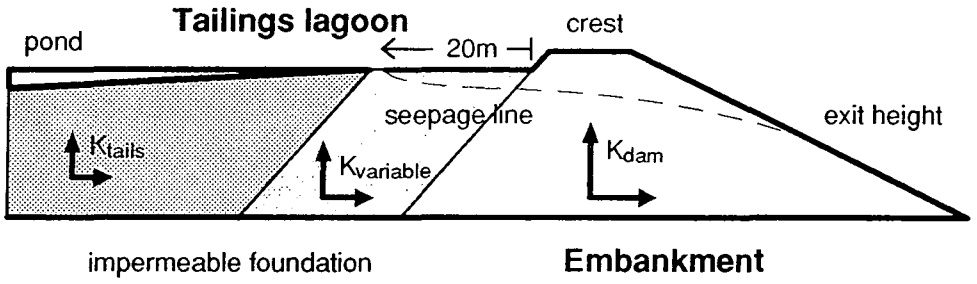

Kdam/tails	discharge	exit height **	K log ratio	rel. discharge
1	3.28	8.18	0.00	1.00
2	1.99	5.04	0.30	0.61
5	1.66	4.20	0.70	0.51
10	1.39	3.52	1.00	0.42
20	1.11	2.85	1.30	0.34

* discharge in m^3/s per m width for a dam permeability of 1 m/s ** exit height in metres

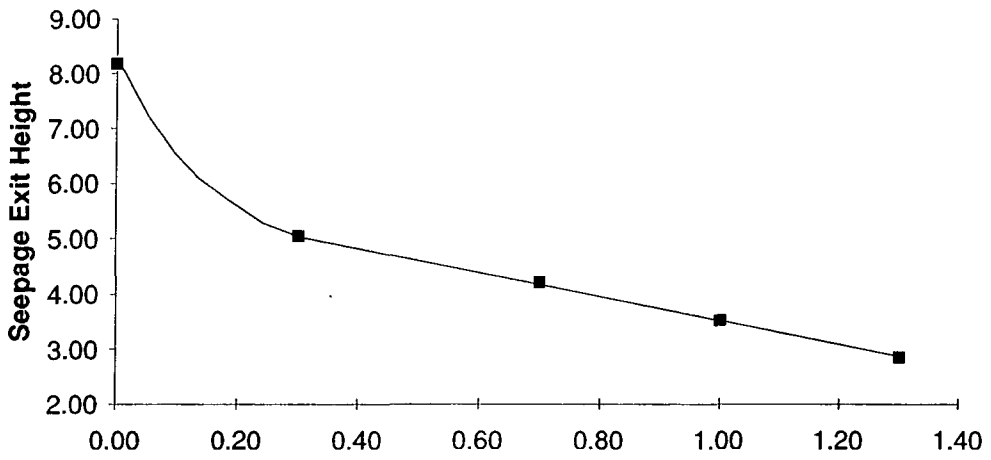

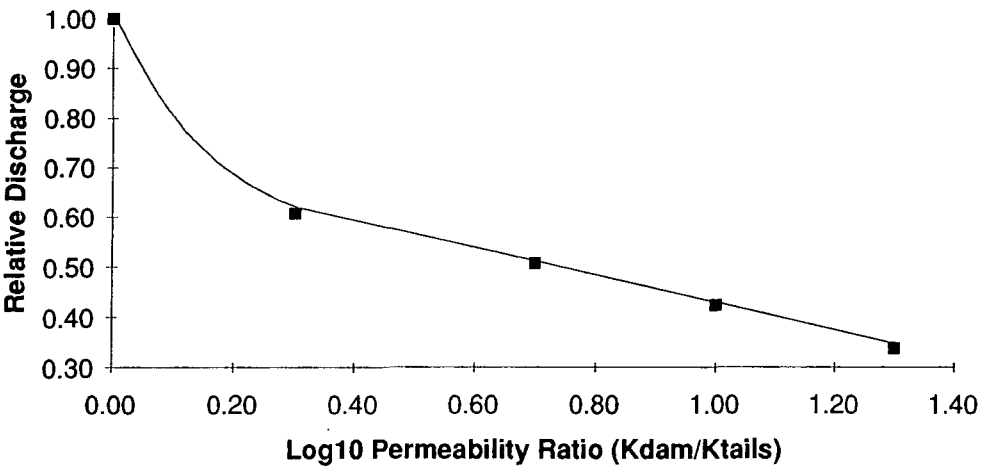

Tailings Dam Geometry (with pond at 20m from dam) TDDIHIC
Tailings permeability increasing from pond to dam.
Ratio k(pond)/k(dam)

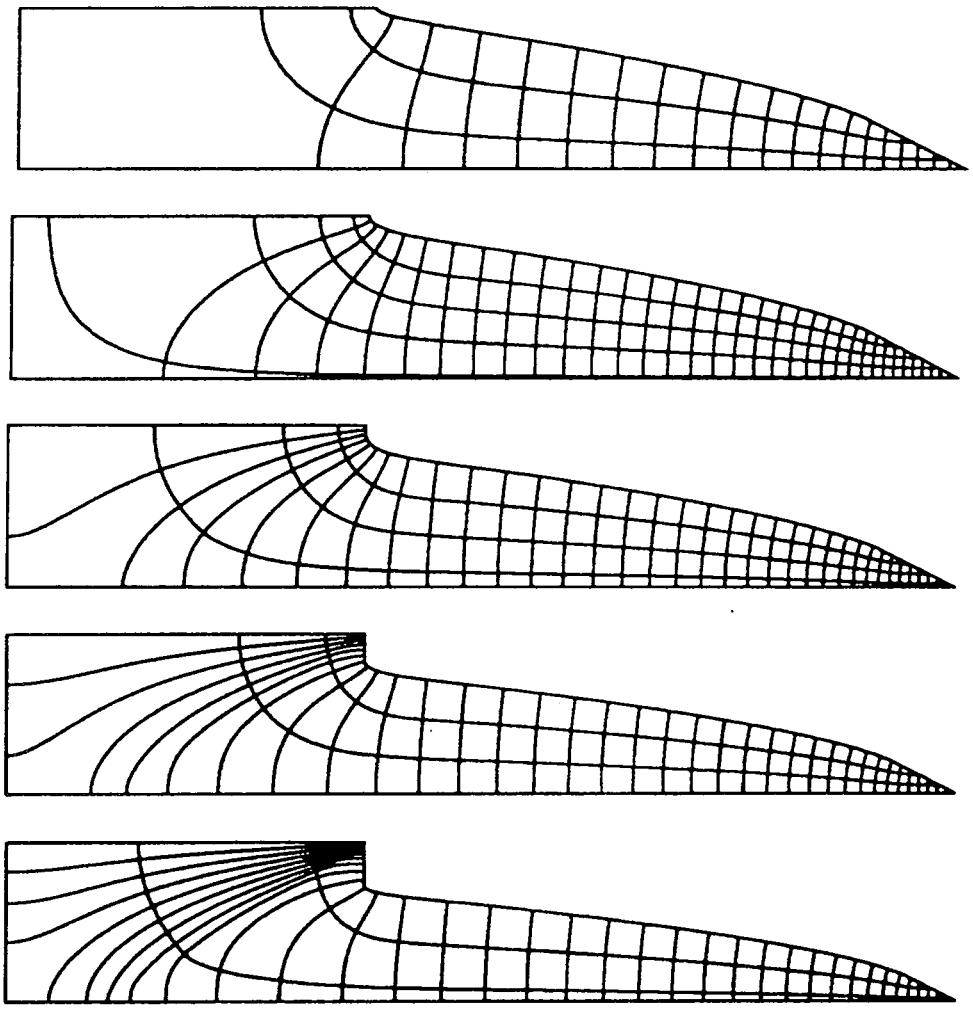

Analysis of the Effect of Vertical Variation in Tailings Permeability
Limiting Geometry British Coal Dam
TDDIVID

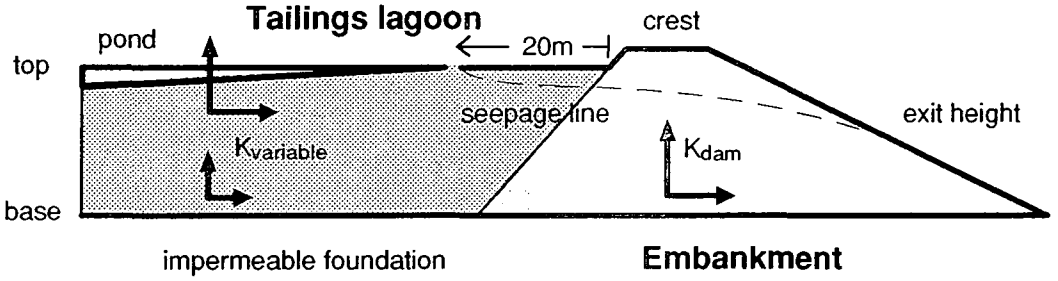

Ktop/Kbase	discharge *	exit height **	K log ratio	rel. discharge
1	2.22	5.50	0.00	1.00
2	2.11	5.36	0.30	0.95
5	2.04	5.14	0.70	0.92
10	2.01	5.05	1.00	0.91
20	1.98	5.00	1.30	0.89
50	1.96	4.95	1.70	0.88
100	1.96	4.94	2.00	0.88

* discharge in m^3/s per m width for a dam and top permeability of 1m/s ** exit height in metres

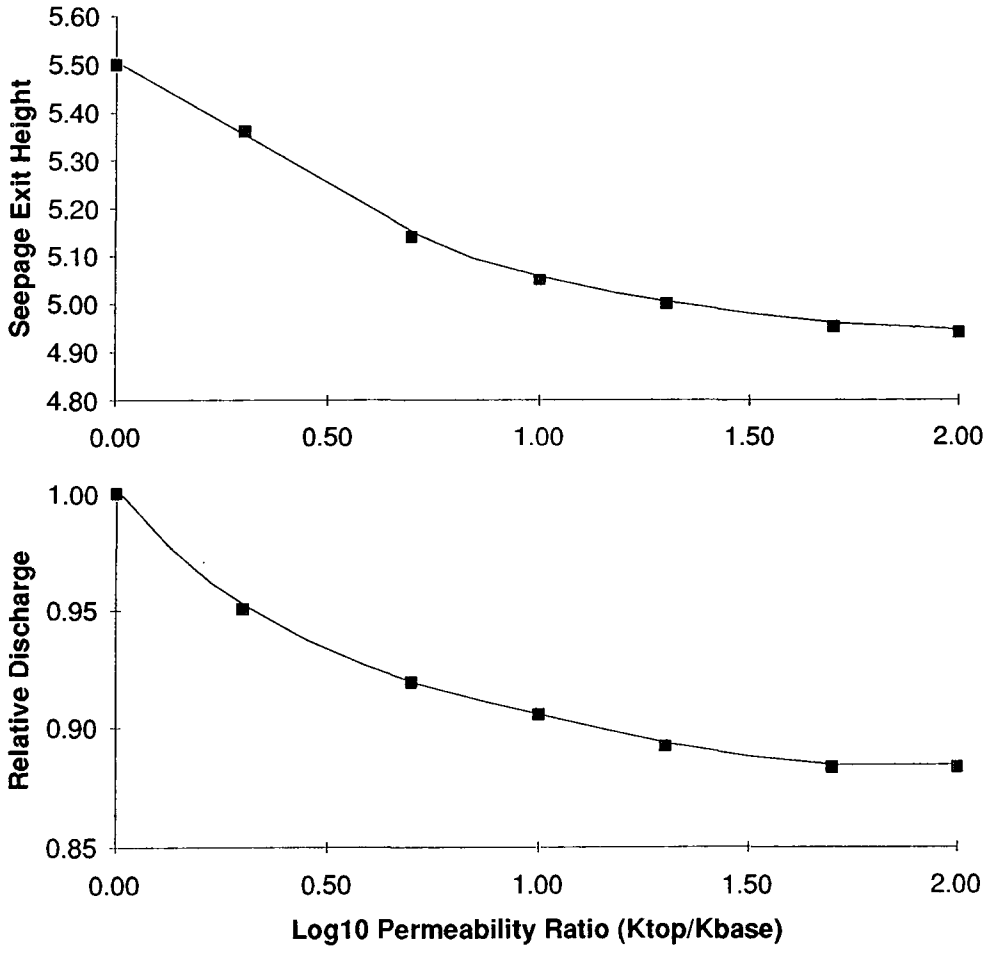

Tailings Dam Geometry (with pond at 20m from dam) TDDIVID
Tailings permeability decreasing with depth..
Ratio k(top)/k(base)

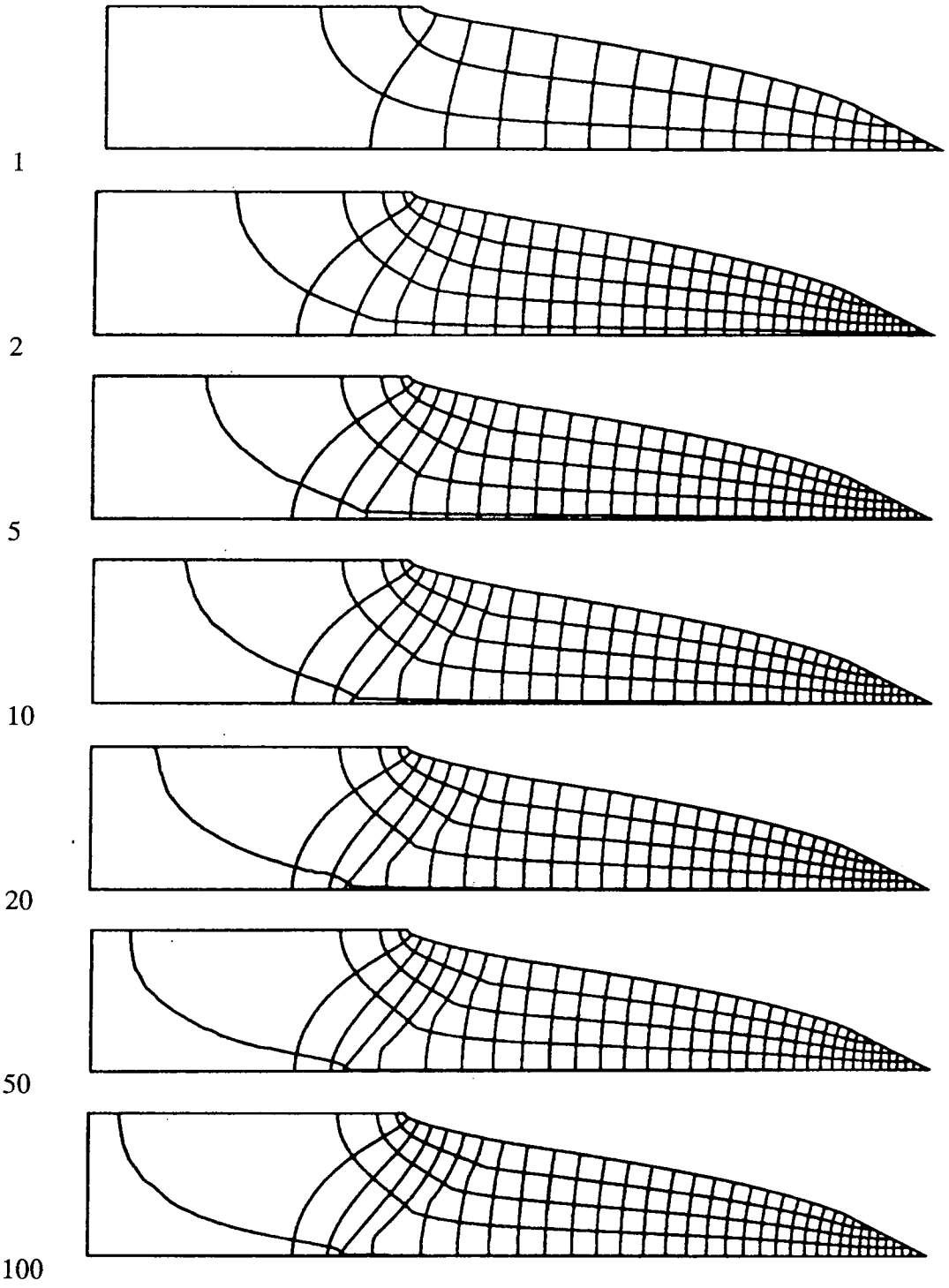

Analysis of the Effect of Anisotropy in Tailings & Dam Permeability Limiting Geometry British Coal Dam

TDUAOHC

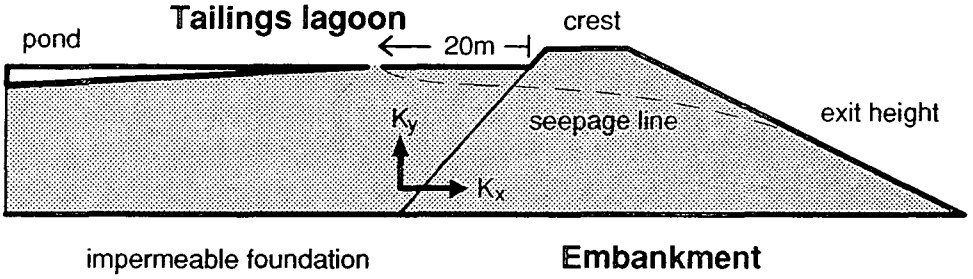

Kx/Ky	discharge *	exit height **	K log ratio	rel. discharge
1	2.22	5.50	0.00	1.00
2	2.08	5.69	0.30	0.94
5	1.84	5.93	0.70	0.83
10	1.57	6.00	1.00	0.71
15	1.37	5.92	1.18	0.62
20	1.20	5.76	1.30	0.54

* discharge in m^3/s per m width for a horizontal permeability of 1m/s ** exit height in metres

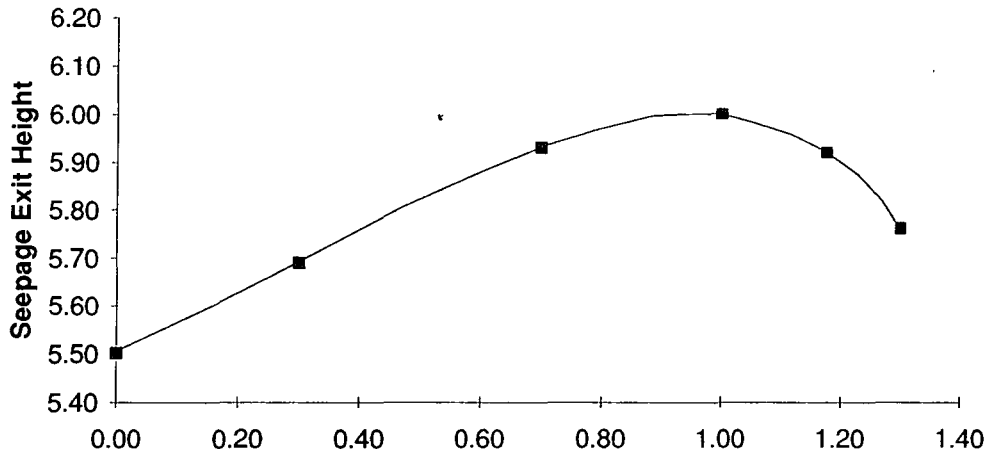

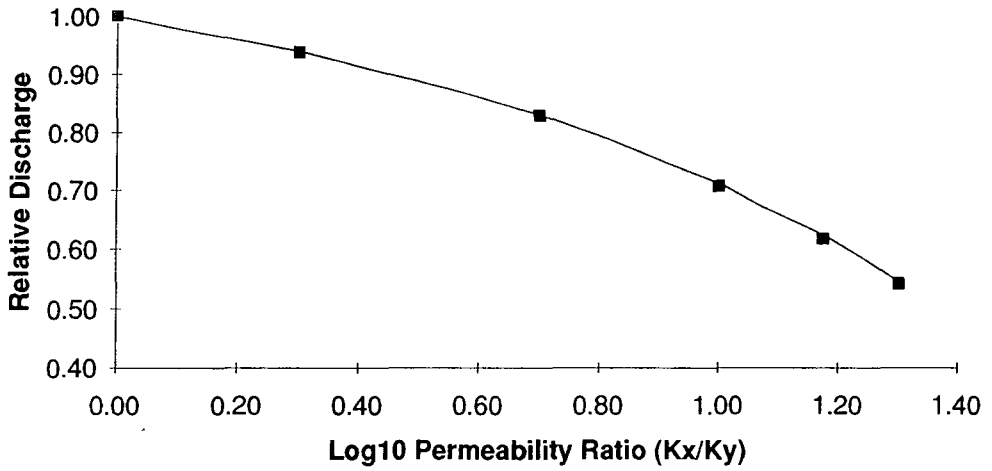

Tailings Dam Geometry (with pond at 20m from dam) TDUAOHC
Anisotropic dam and tailings.
Ratio k(horizontal)/k(vertical)

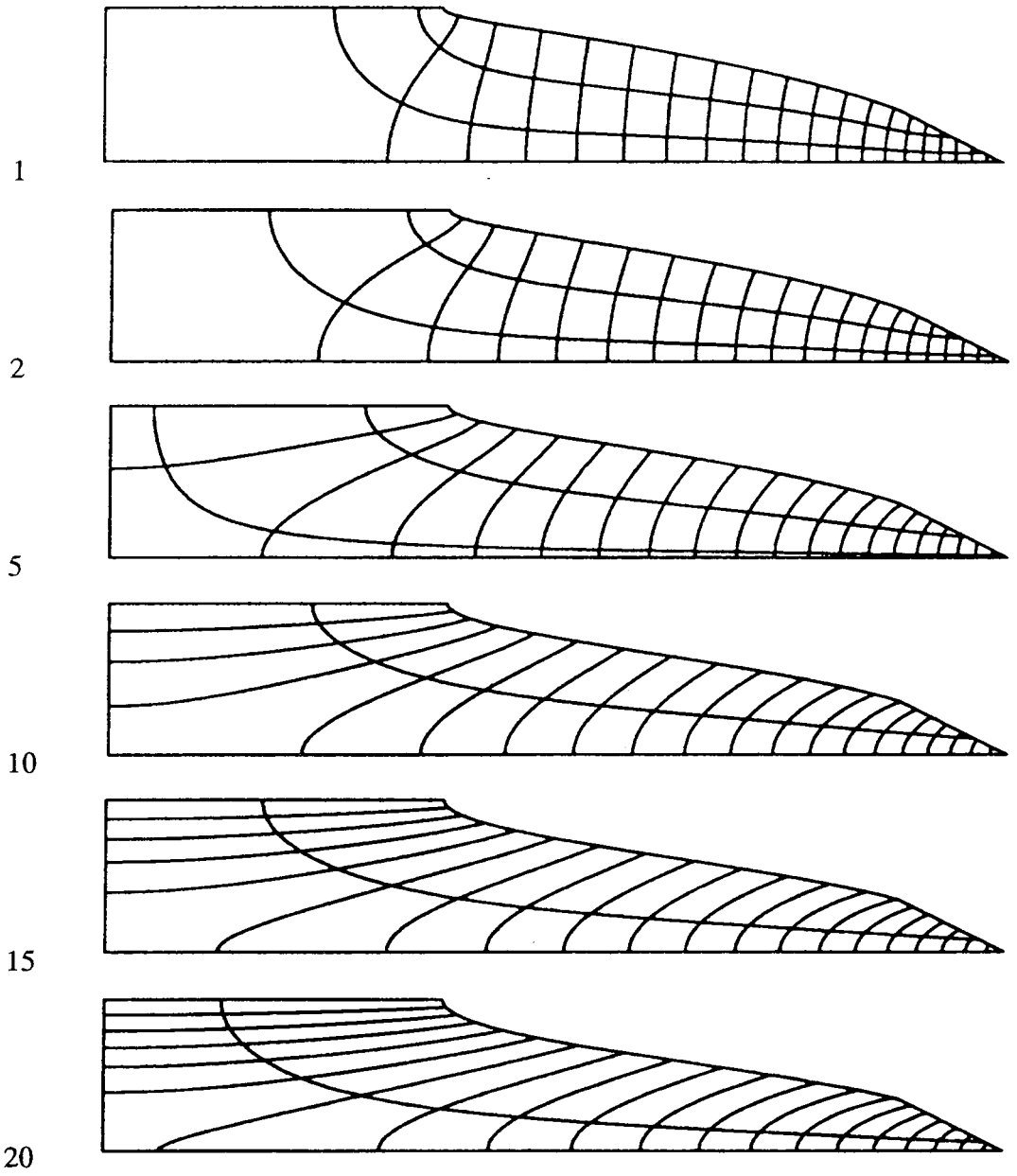

Analysis of the Effect of Anisotropy in Tailings Permeability
Limiting Geometry British Coal Dam
TDDAOID

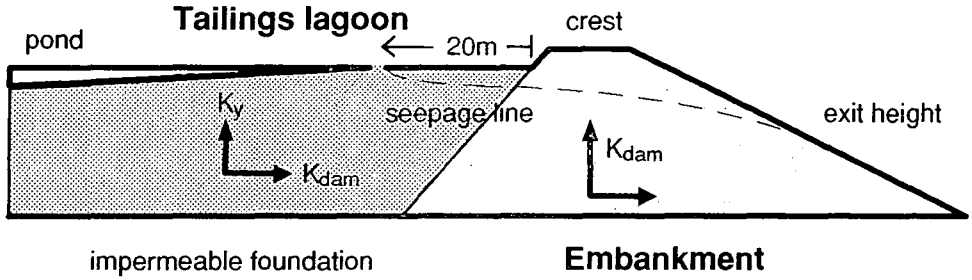

Kdam/Ky	discharge *	exit height **	K log ratio	rel. discharge
1	2.22	5.50	0.00	1.00
2	2.07	5.26	0.30	0.93
5	1.82	4.61	0.70	0.82
10	1.55	3.93	1.00	0.70
15	1.35	3.45	1.18	0.61
20	1.20	3.05	1.30	0.54

* discharge in m^3/s per m width for a dam permeability of 1 m/s ** exit height in metres

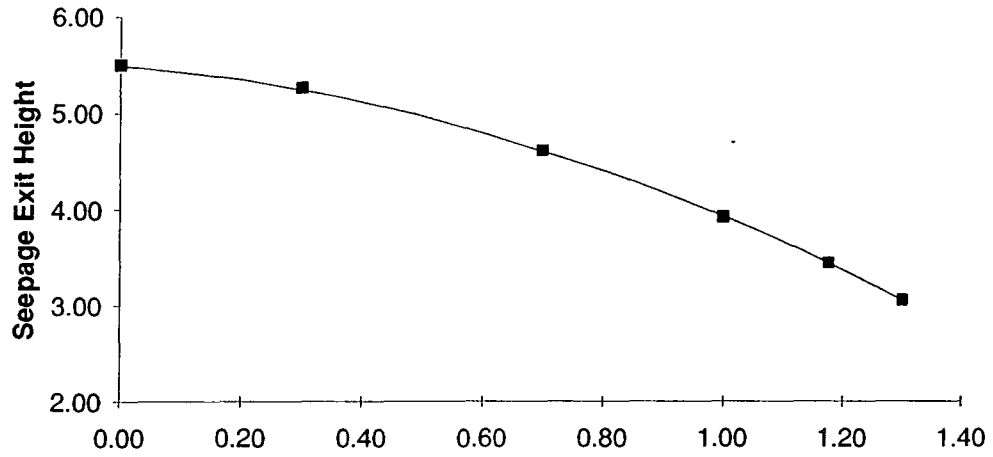

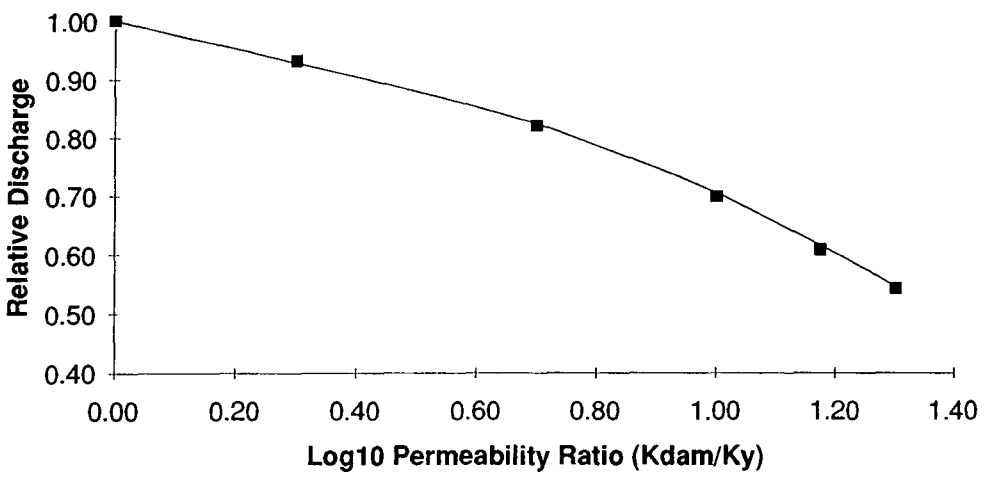

Tailings Dam Geometry (with pond at 20m from dam) TDDAOID
Anisotropic tailings.
Ratio k(horizontal)/k(vertical)

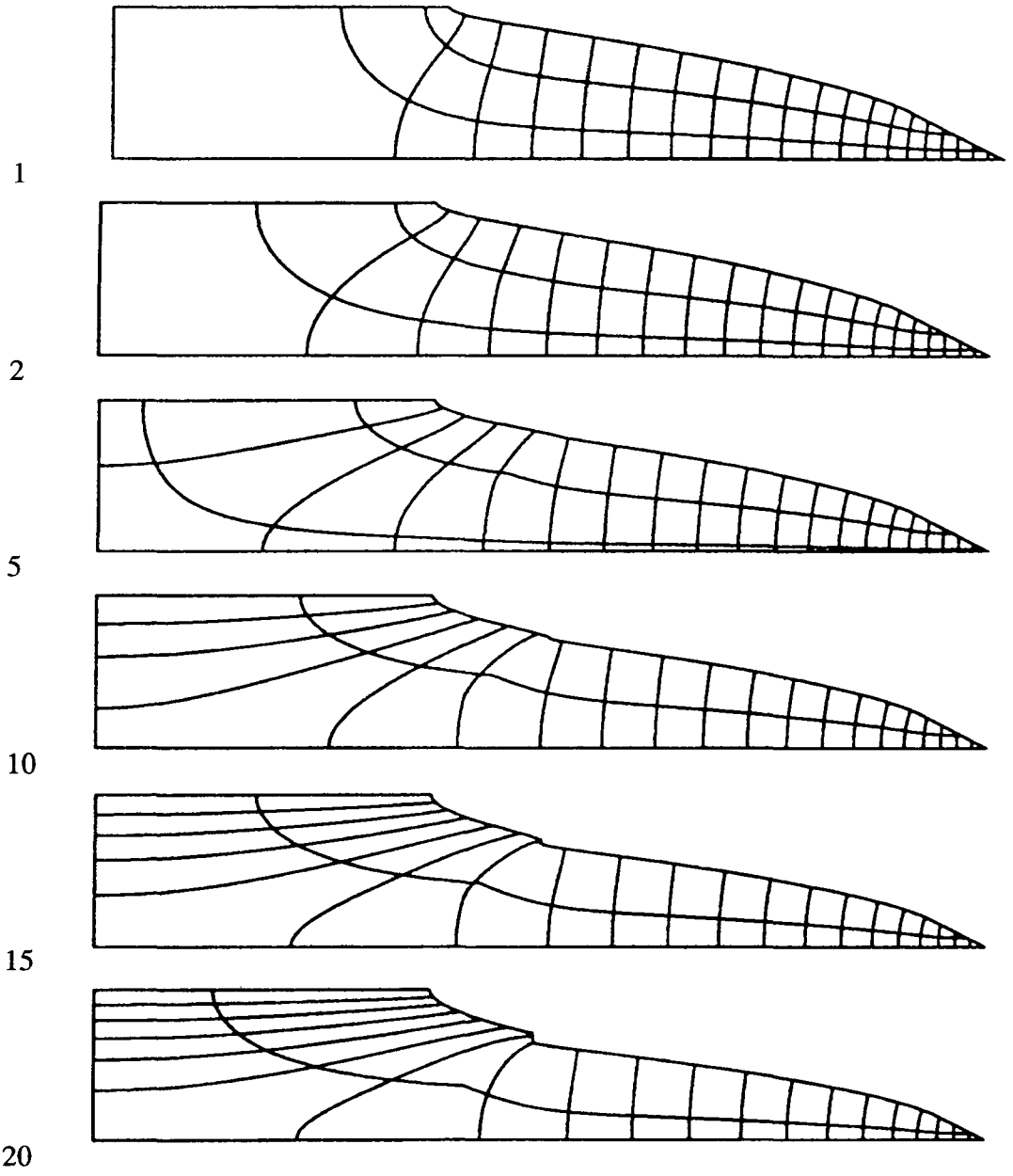

Analysis of the Effect of a Permeable Base below Earth Dam
Limiting Geometry British Coal Dam
DVB

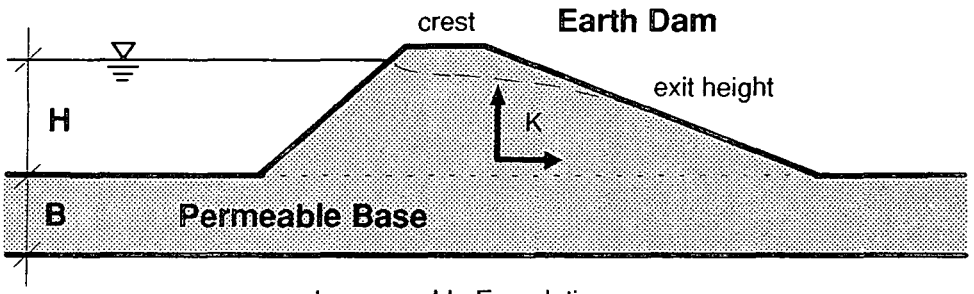

B/H	discharge *	exit height **	rel. discharge
0	3.52	9.78	1.00
0.5	5.69	6.67	1.62
1	7.53	6.00	2.14
2	10.30	5.80	2.93

* discharge in m^3/s per m width for a uniform permeability of 1m/s ** exit height in metres

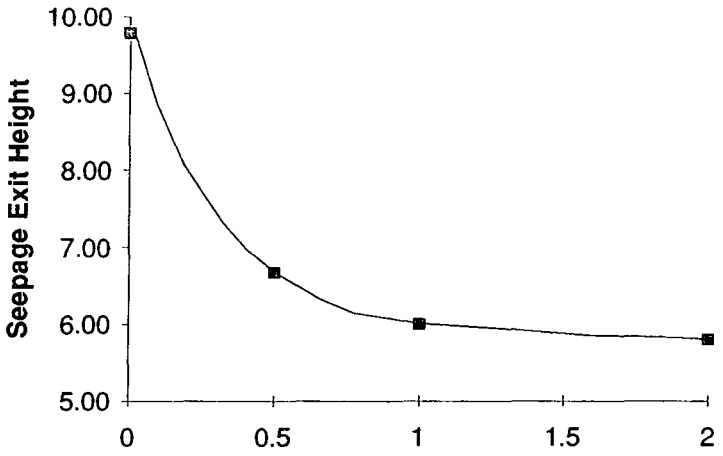

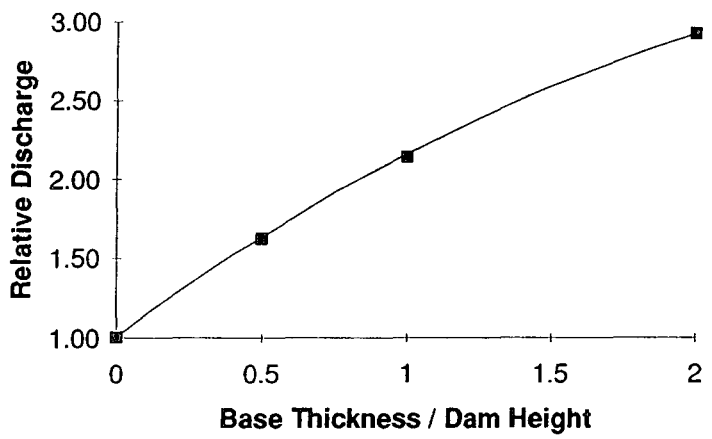

Tailings Dam Geometry (with pond at 20m from dam) DVB
Variation in permeable base depth.
Ratio base depth/dam height

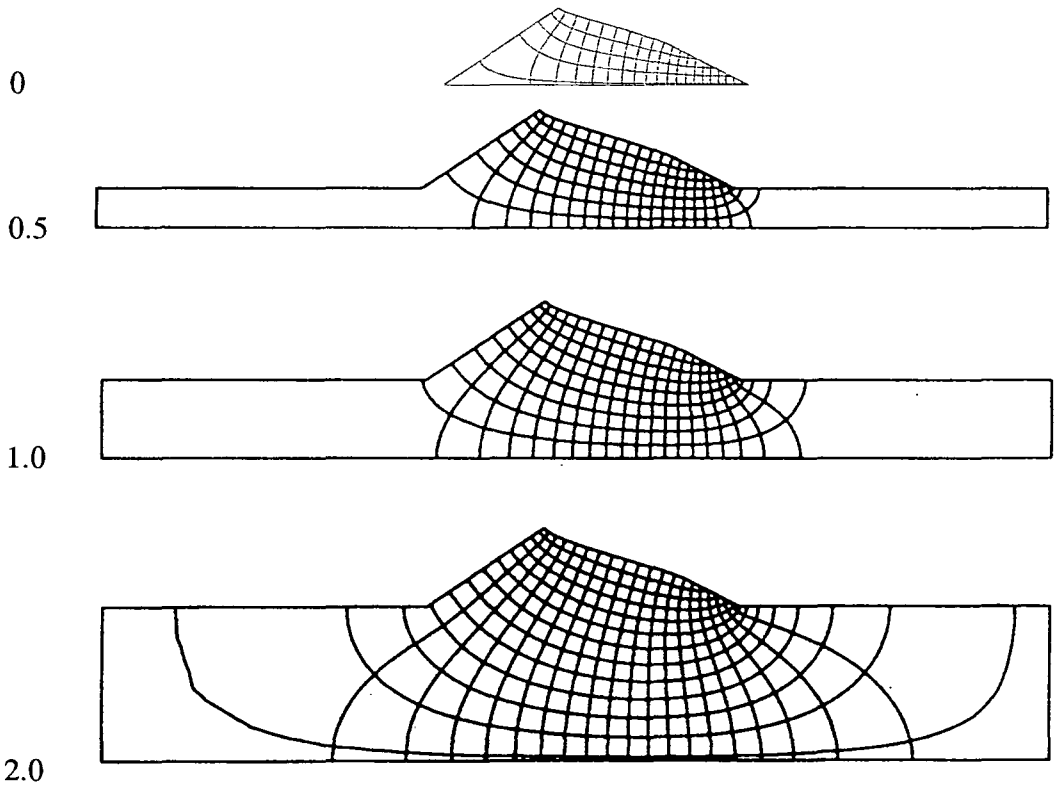

Analysis of the Effect of a Lower Permeability Base below Earth Dam
Limiting Geometry British Coal Dam
DVBK

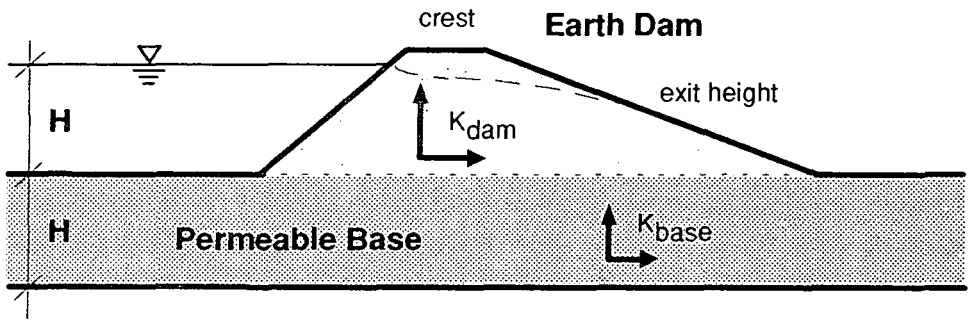

Kbase/Kdam	discharge *	exit height **	K.log.ratio	rel. discharge
1	7.50	6.11	0.00	1.00
5	4.40	3.47	0.70	0.59
10	3.93	2.90	1.00	0.52
20	3.63	2.60	1.30	0.48
50	3.48	2.45	1.70	0.46

* discharge in m^3/s per m width for a dam permeability of 1m/s ** exit height in metres

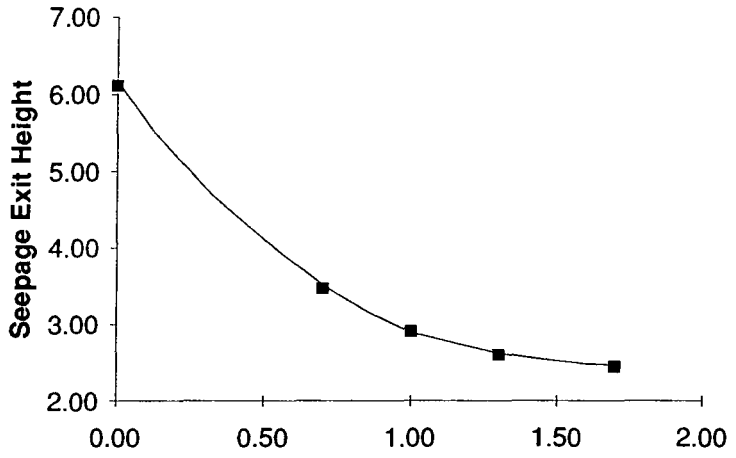

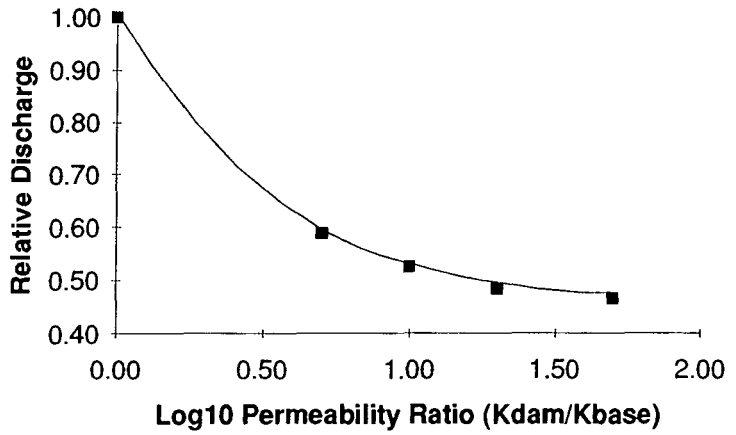

Tailings Dam Geometry (with pond at 20m from dam) DVBK
Variation in permeability of base.
Ratio k(base)/k(dam)

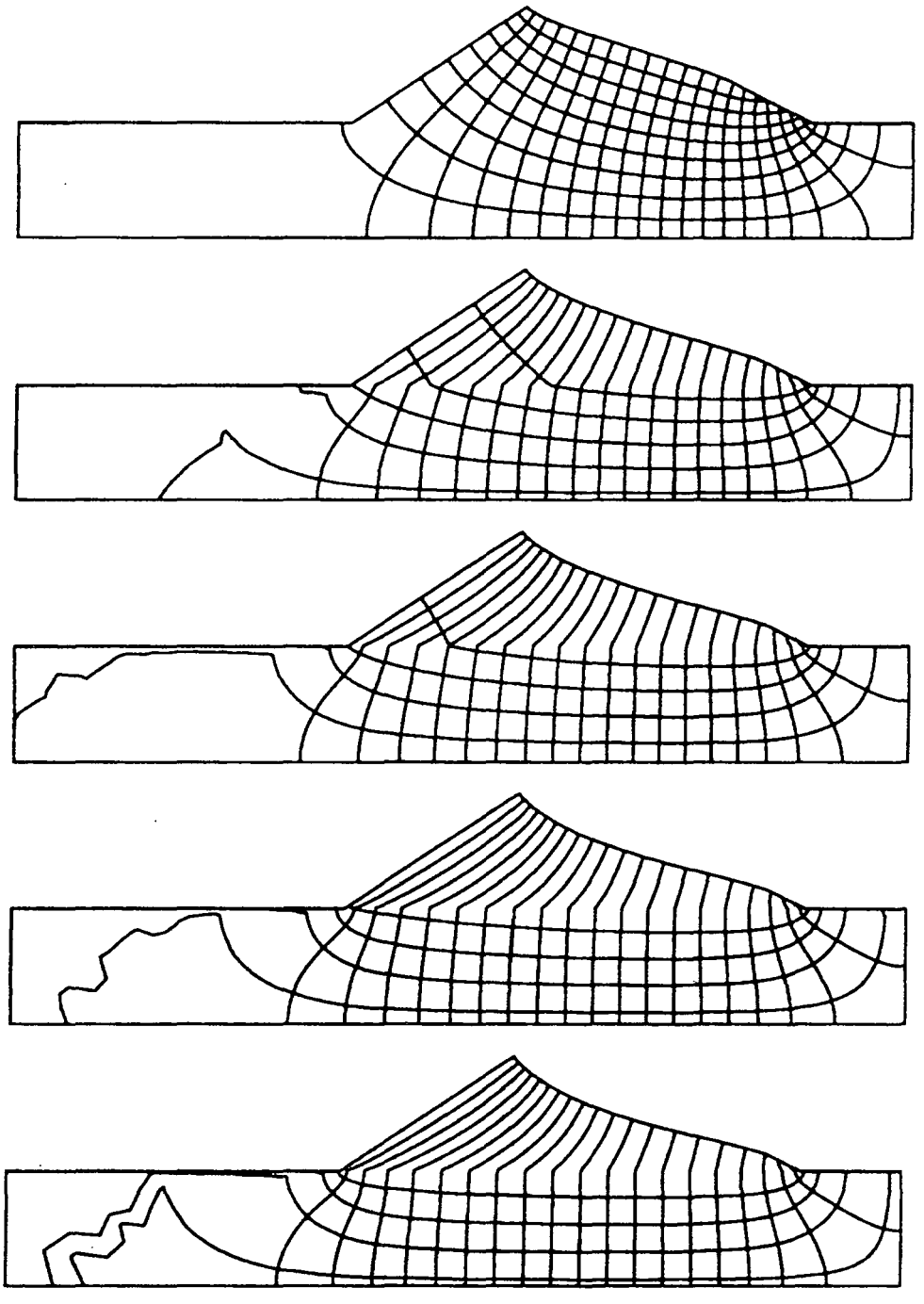

Appendix 4
Advance of Seepage Line Through an Idealized Earth Dam with Constant Head

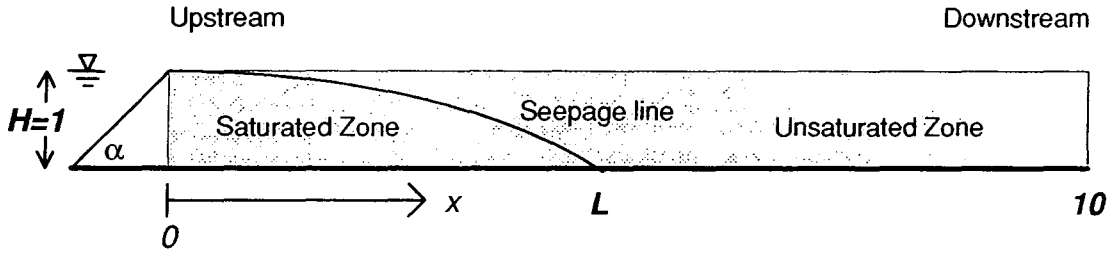

The height of the water in the dam (H) and displacement (L) of the seepage line base are in dimensionless units. To convert distances (x) from the figures to real units ($\bar{x}$) the following transformation is used:

$$\bar{x} = \overline{H}x$$

where $\overline{H}$ is the height of the dam in the same units as s (e.g. in metres).

The travel time is scaled with respect to the permeability (k), effective porosity (n) and the height of the dam ($\overline{H}$). To convert time units from simulation time (t) to real time ($\bar{t}$) the following transformation is used:

$$\bar{t} = t\frac{\overline{H}n}{k}$$

where a compatible set of units is used (e.g. $\bar{t}$ in seconds, $\overline{H}$ in metres, k in ms^{-1} and n is dimensionless).

Advance of Seepage Line Base through an Idealized Earth Dam

With zero degree upstream slope angle (horizontal)

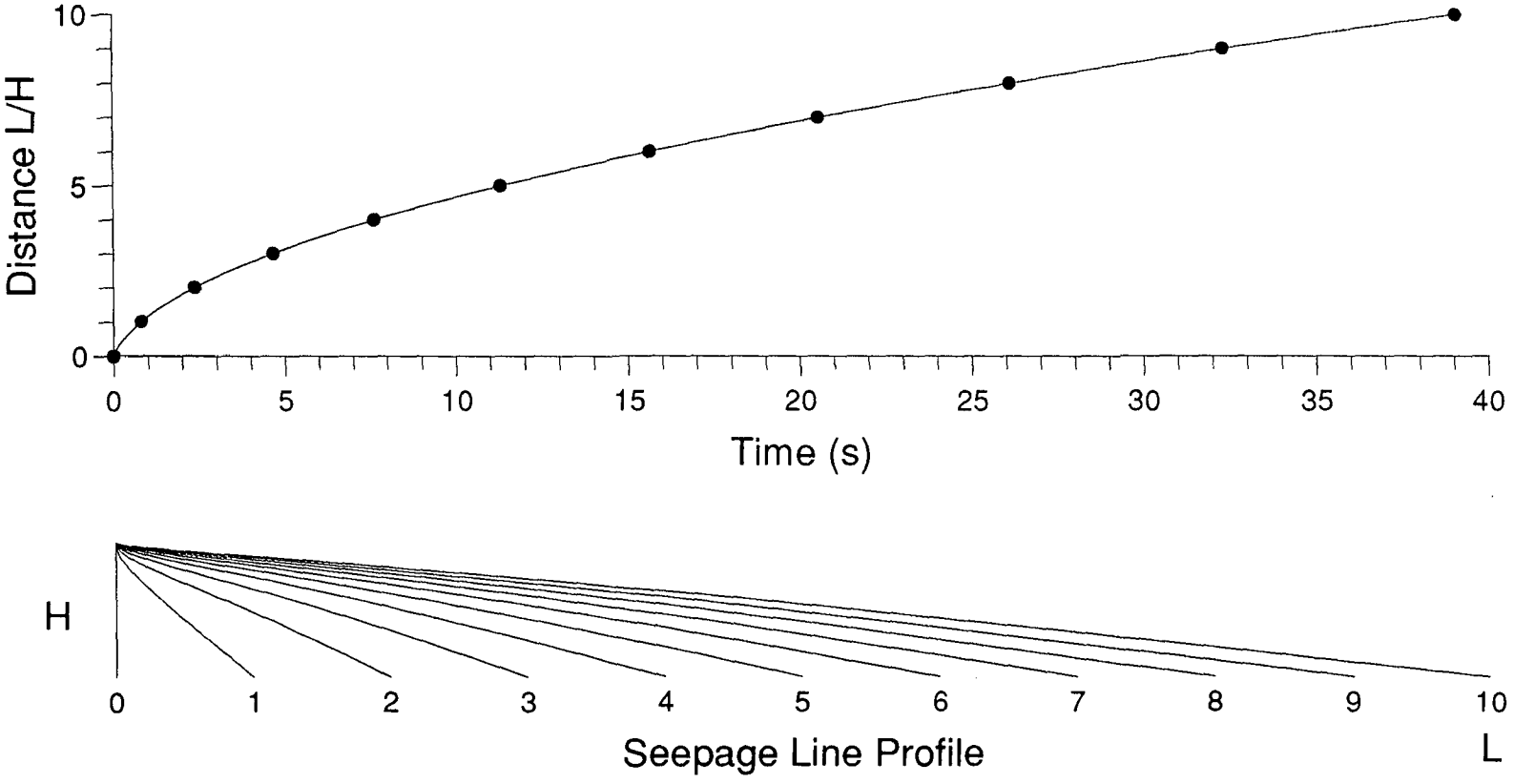

N.B. Distances are scaled with respect to permeability and porosity.

Advance of Seepage Line Base through an Idealized Earth Dam

With 15 degree upstream slope angle

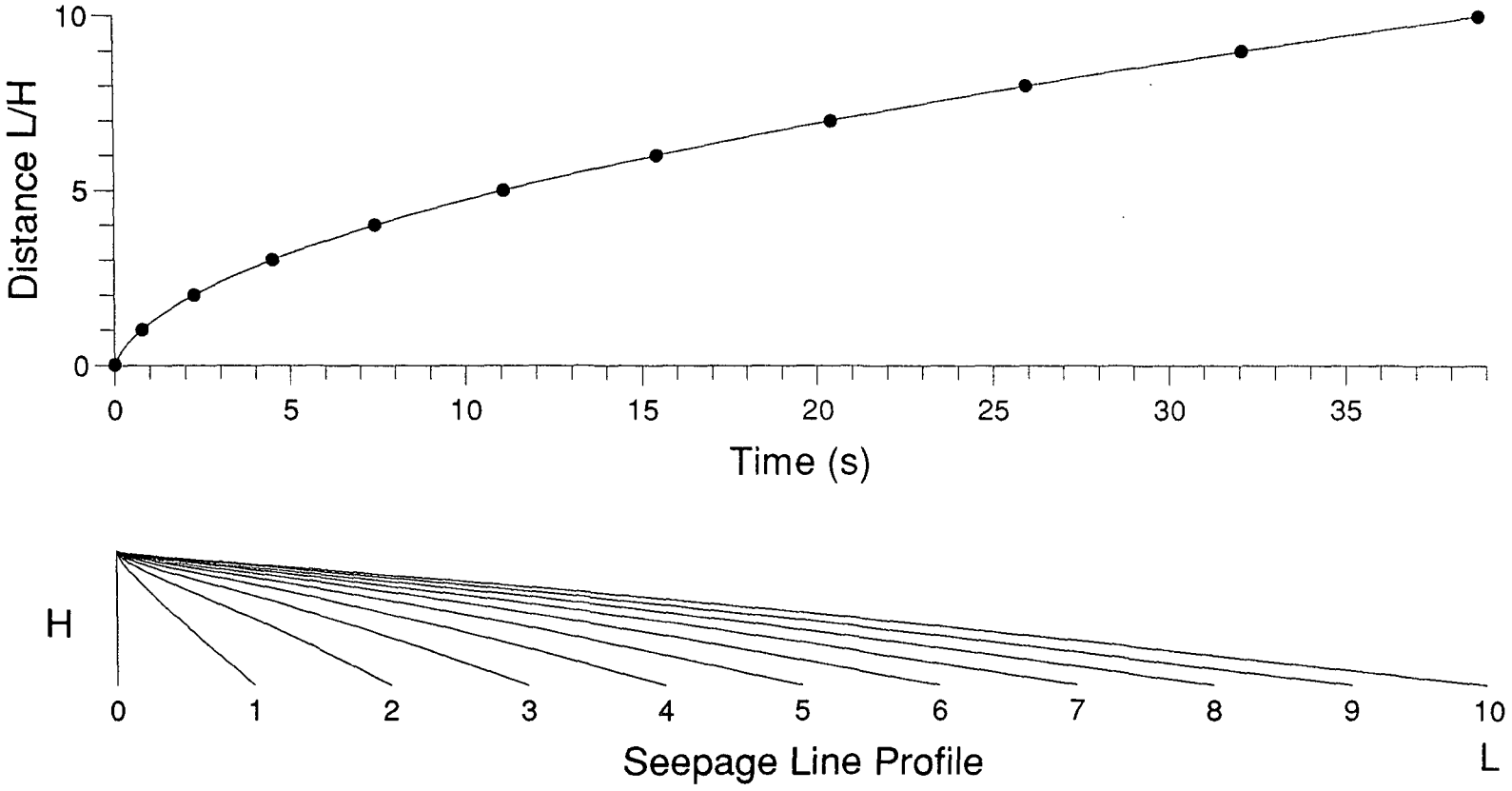

N.B. Distances are scaled with respect to permeability and porosity.

Advance of Seepage Line Base through an Idealized Earth Dam

With 30 degree upstream slope angle

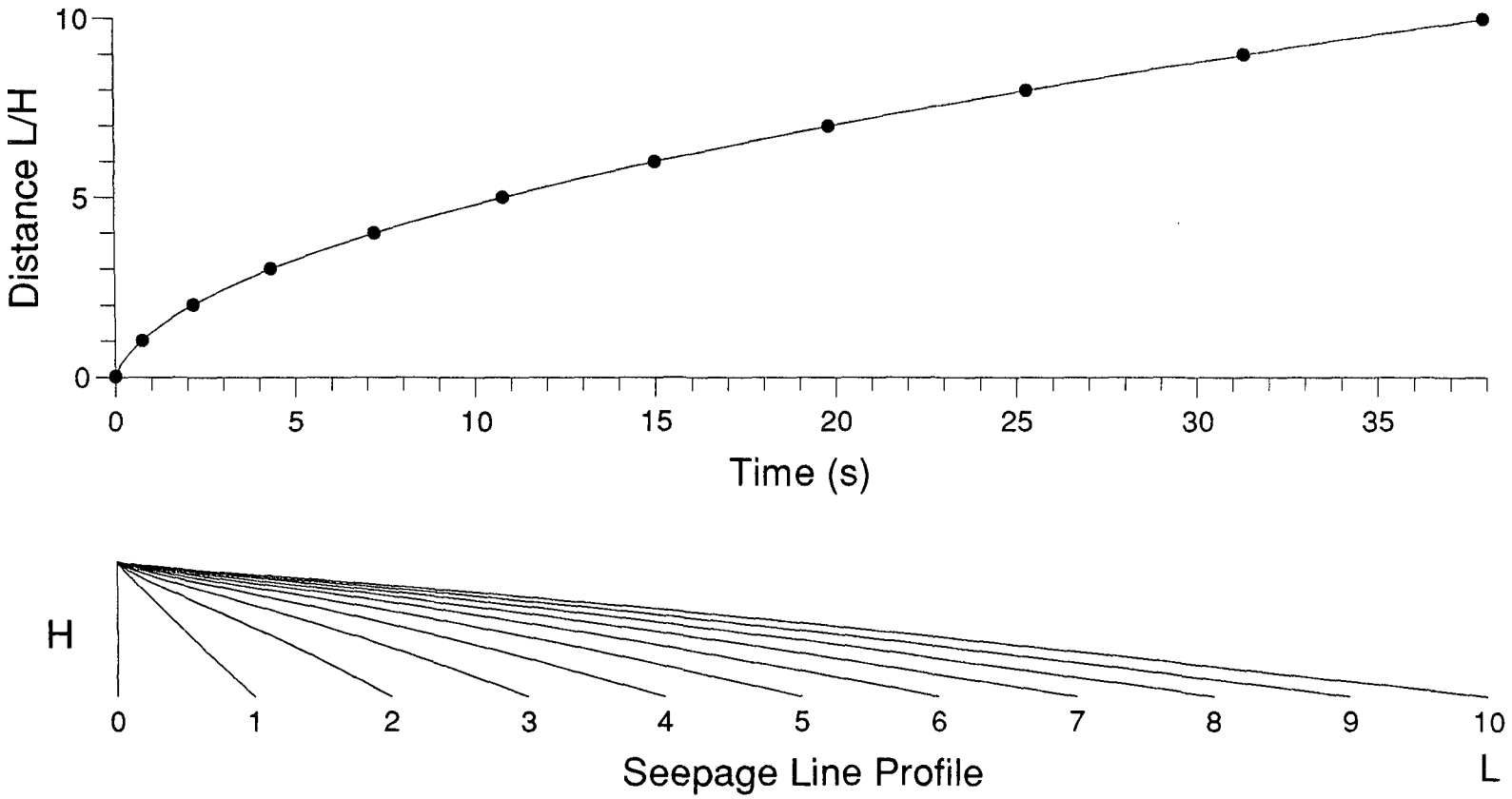

N.B. Distances are scaled with respect to permeability and porosity.

Advance of Seepage Line Base through an Idealized Earth Dam

With 45 degree upstream slope angle

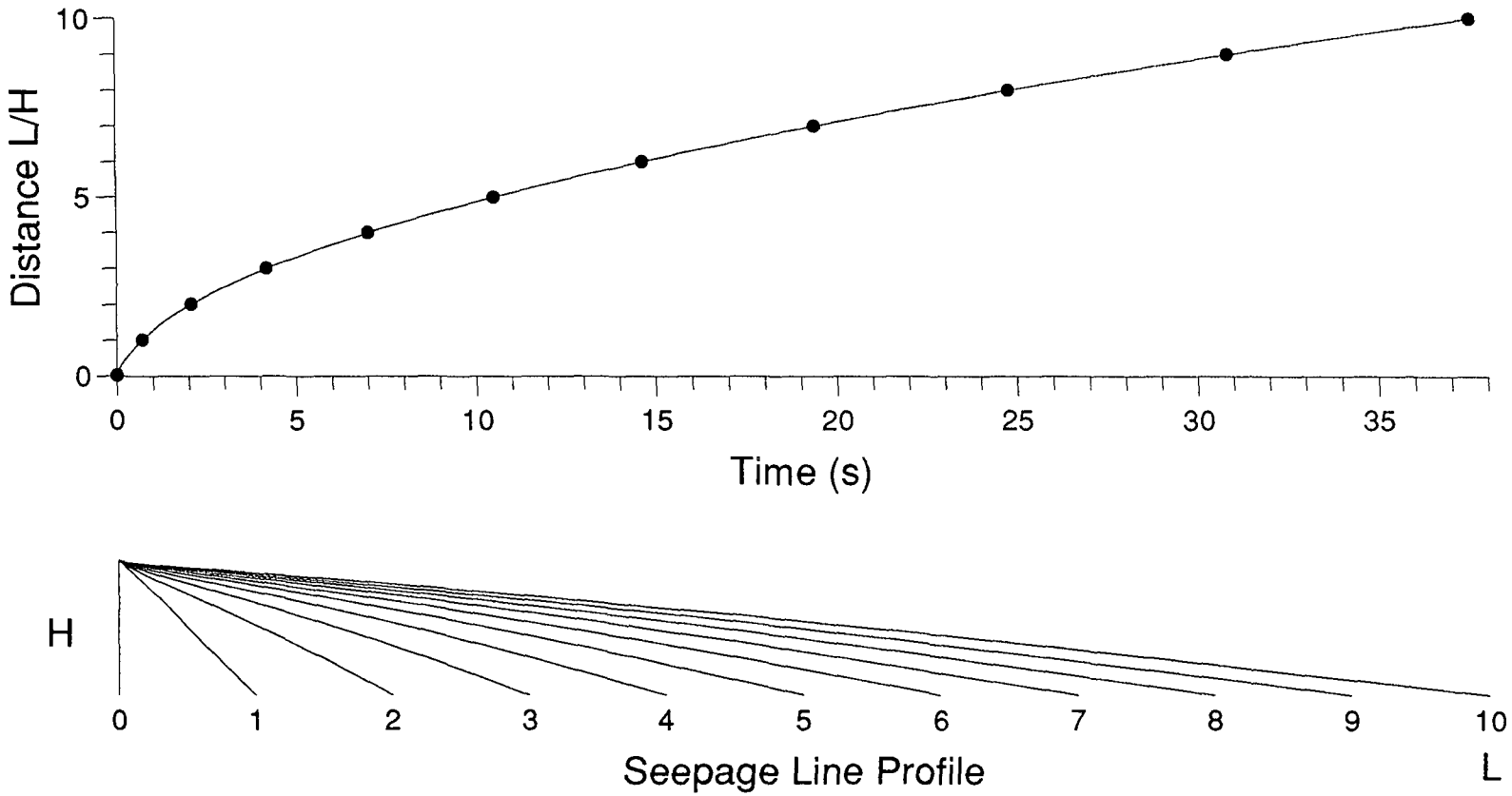

N.B. Distances are scaled with respect to permeability and porosity.

Advance of Seepage Line Base through an Idealized Earth Dam

With 60 degree upstream slope angle

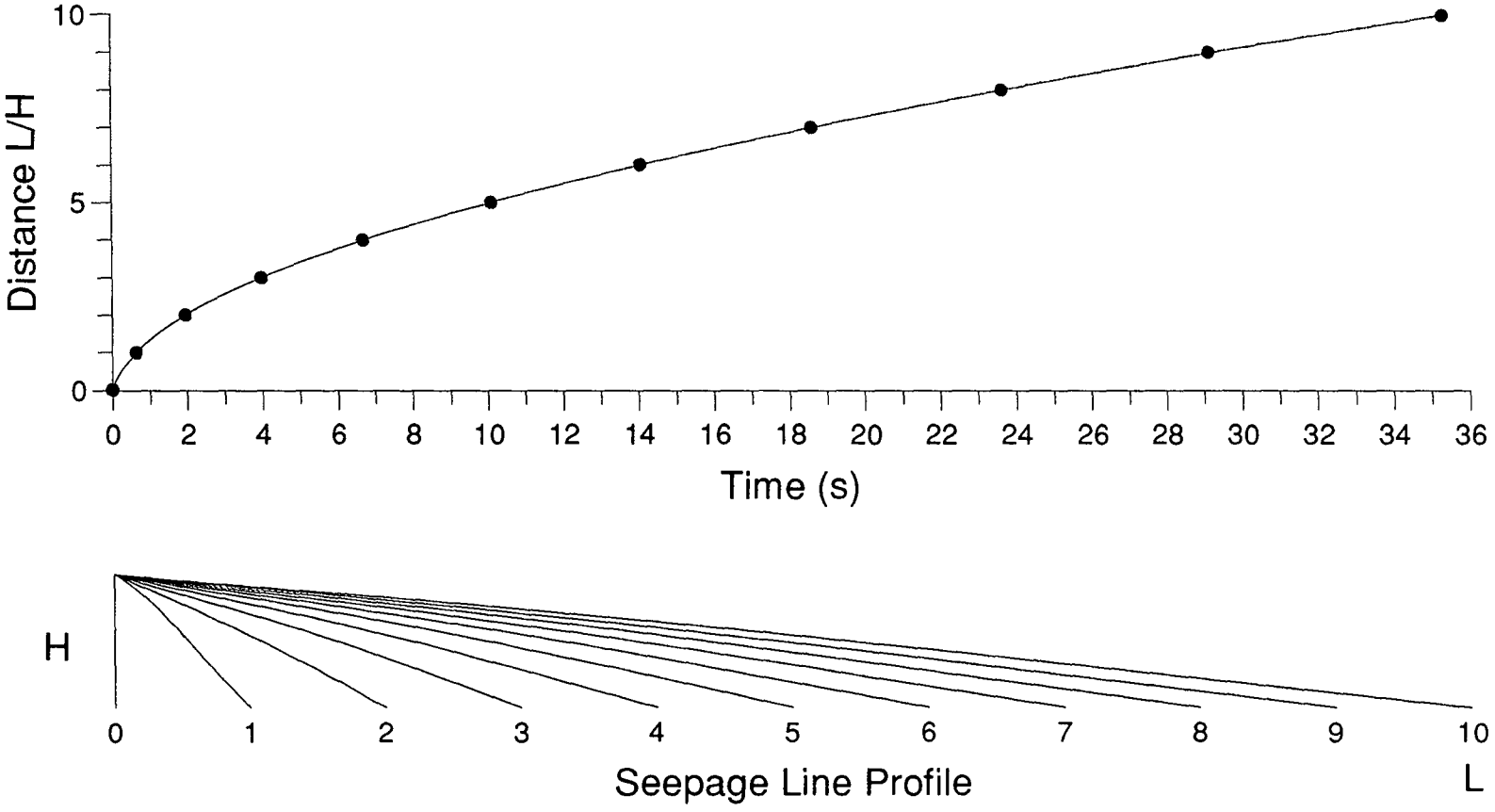

N.B. Distances are scaled with respect to permeability and porosity.

Advance of Seepage Line Base through an Idealized Earth Dam

With 75 degree upstream slope angle

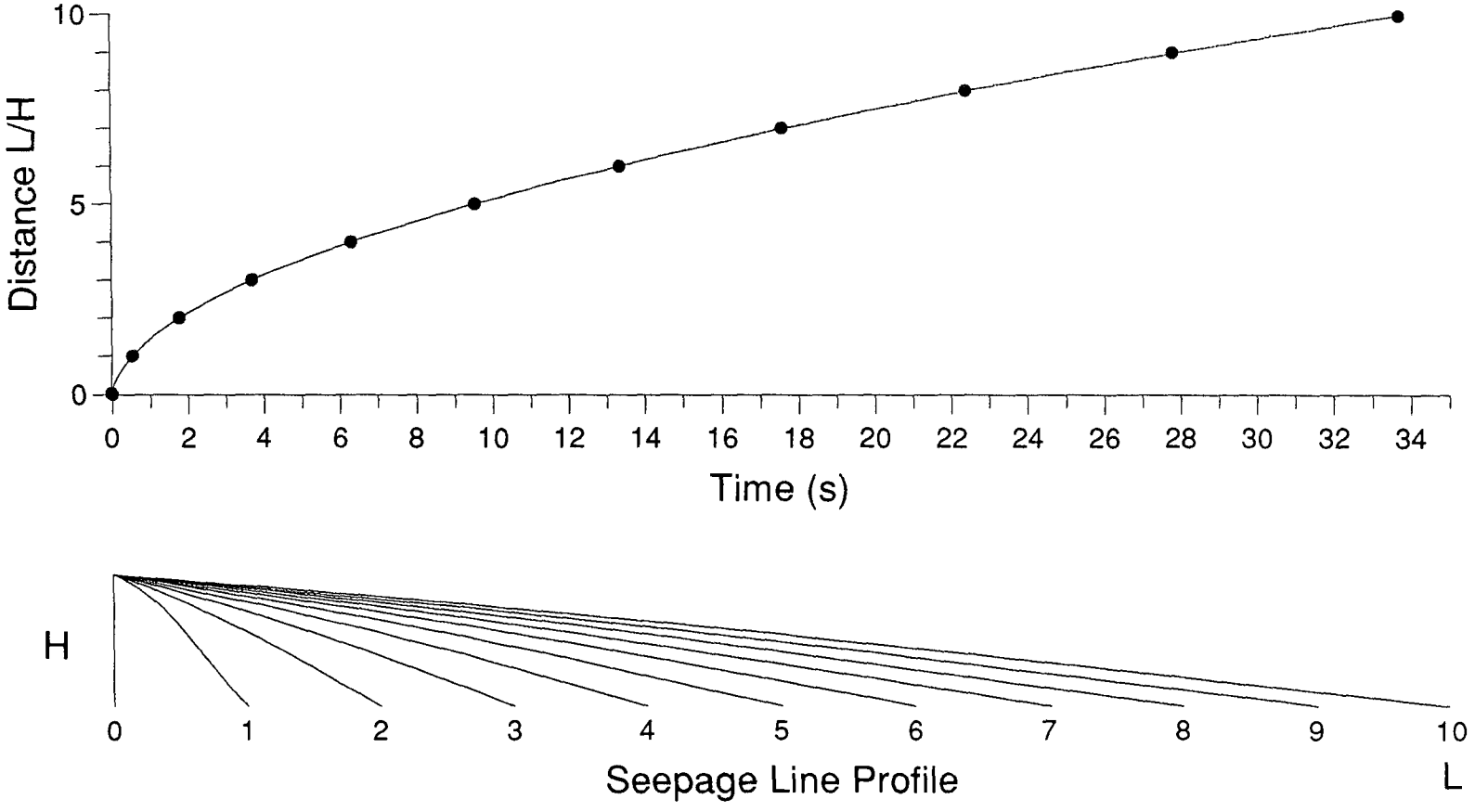

N.B. Distances are scaled with respect to permeability and porosity.

Advance of Seepage Line Base through an Idealized Earth Dam

With 85 degree upstream slope angle

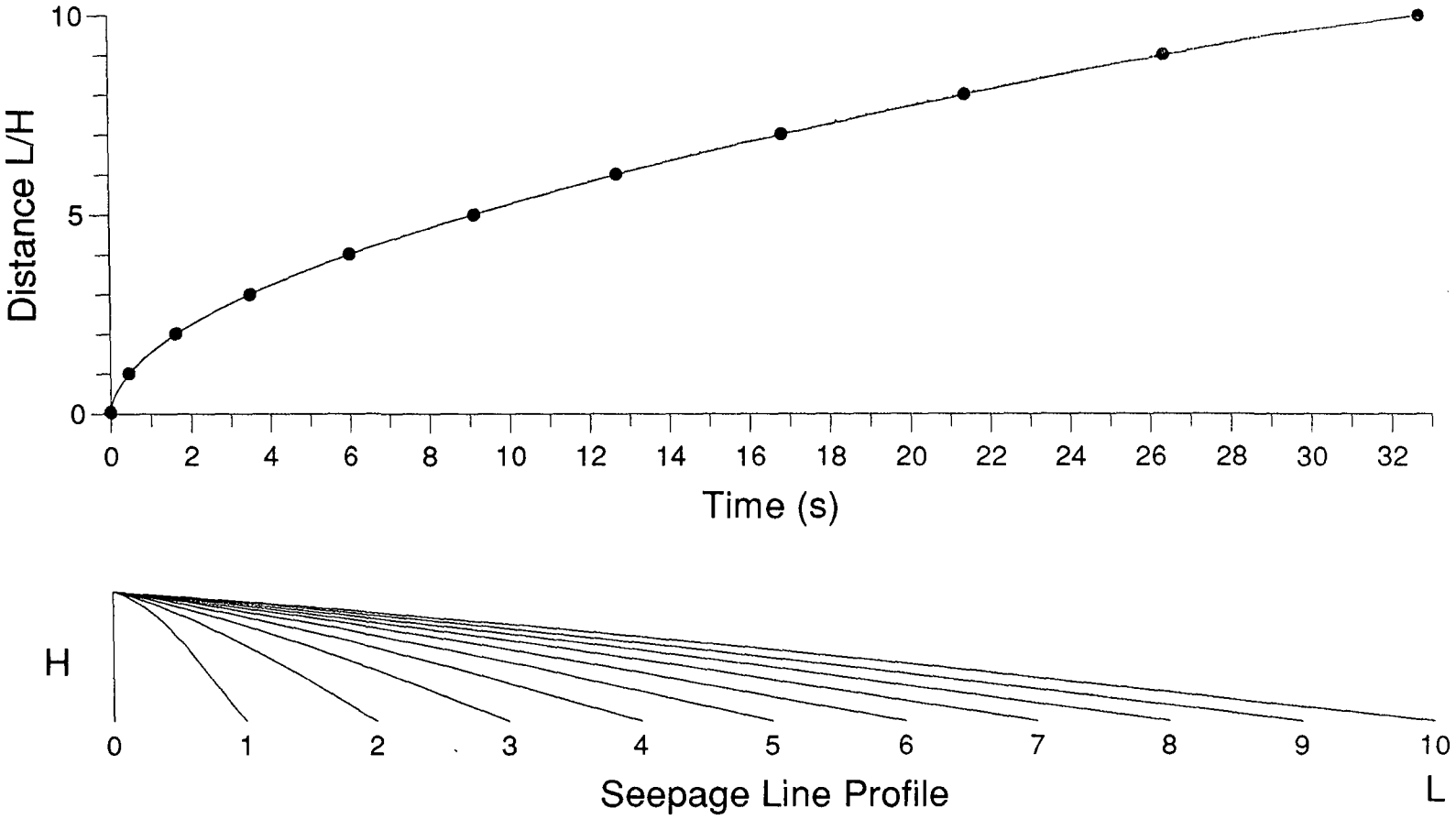

N.B. Distances are scaled with respect to permeability and porosity.

Advance of Seepage Line Base through an Idealized Earth Dam

With 85 degree upstream slope angle (1% Relative Error)

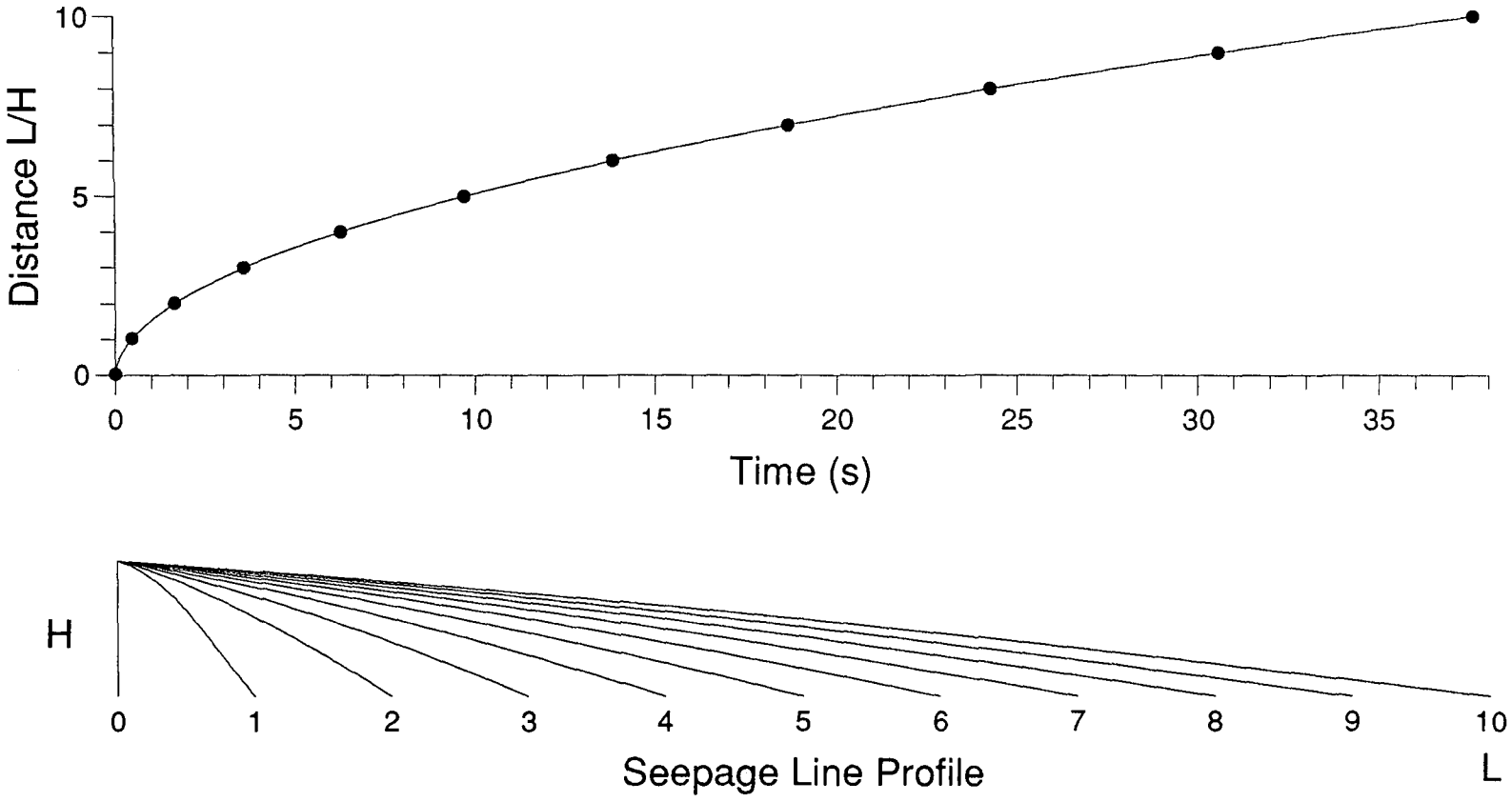

N.B. Distances are scaled with respect to permeability and porosity.

Appendix 5

Seepage Line Advance Through an Idealised Tailings Dam

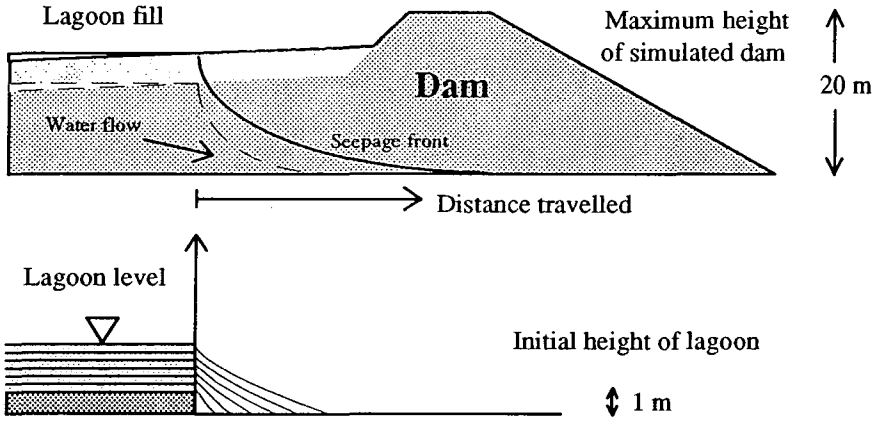

Seepage line profile corresponding to computer plots

Advance of Seepage Line through an Idealized Tailings Dam

With permeability/porosity of $10^{-6}ms^{-1}$ and tailings lagoon rise of 1m per year

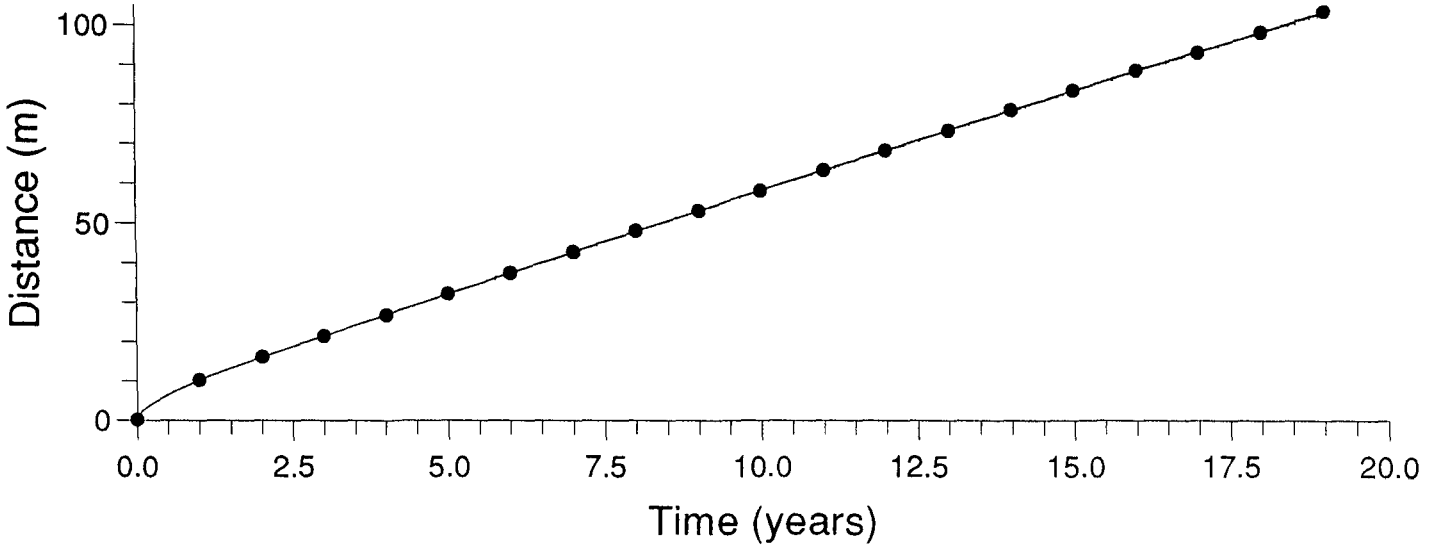

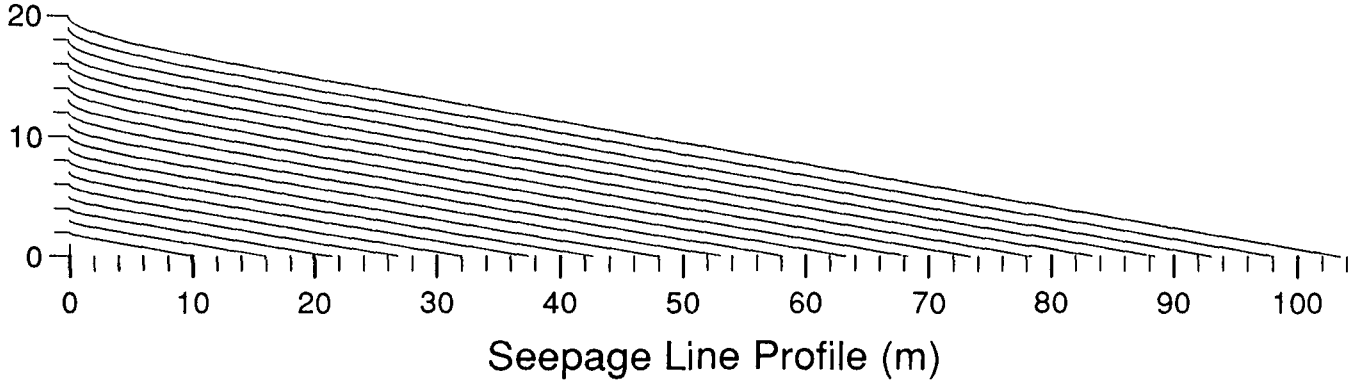

Advance of Seepage Line through an Idealized Tailings Dam

With permeability/porosity of $5 \times 10^{-7} ms^{-1}$ and tailings lagoon rise of 1m per year

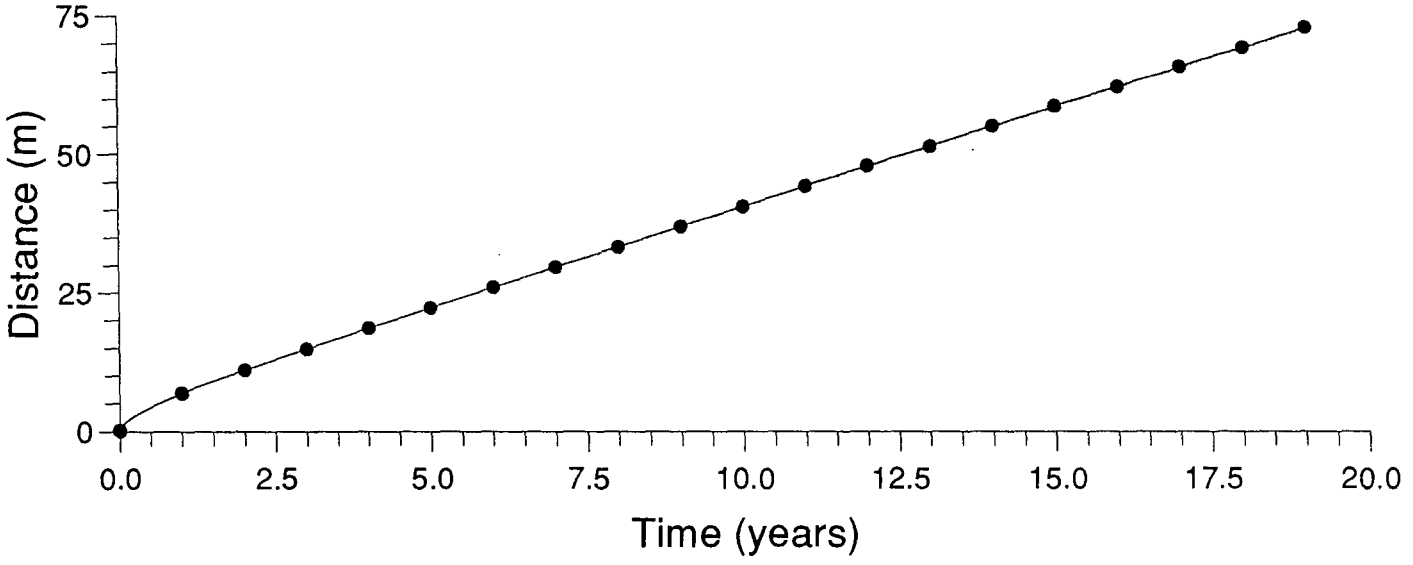

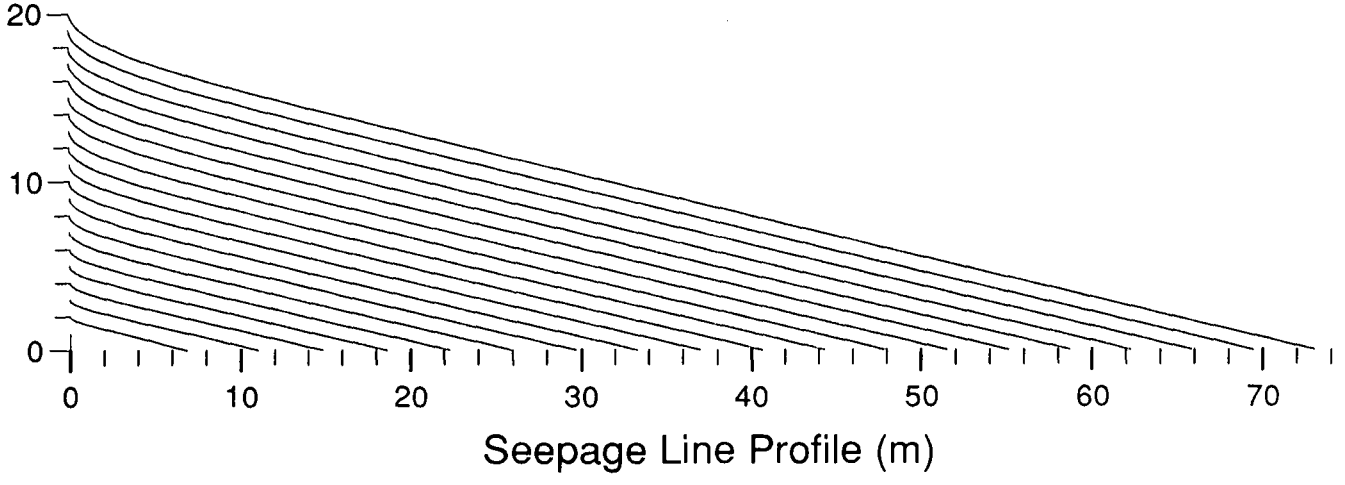

Advance of Seepage Line through an Idealized Tailings Dam

With permeability/porosity of $10^{-7}ms^{-1}$ and tailings lagoon rise of 1m per year

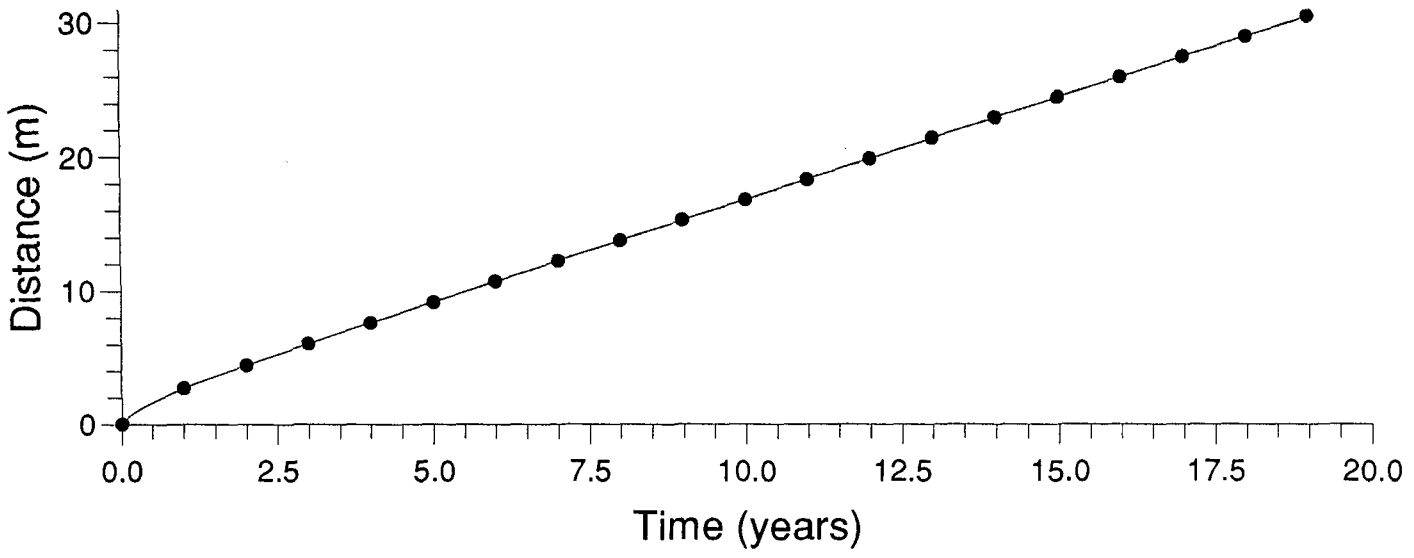

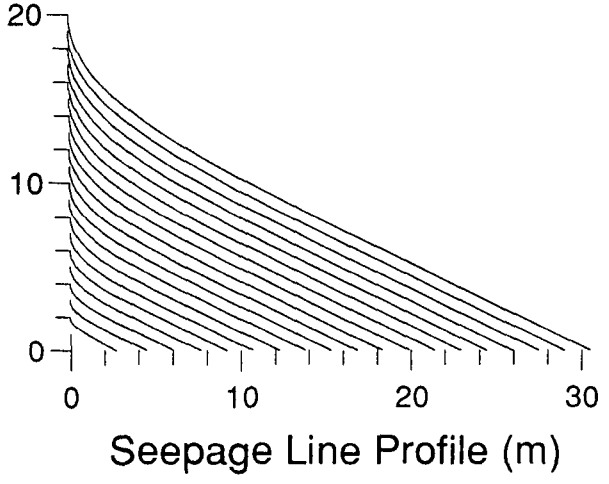

Advance of Seepage Line through an Idealized Tailings Dam

With permeability/porosity of $5 \times 10^{-8} ms^{-1}$ and tailings lagoon rise of 1m per year

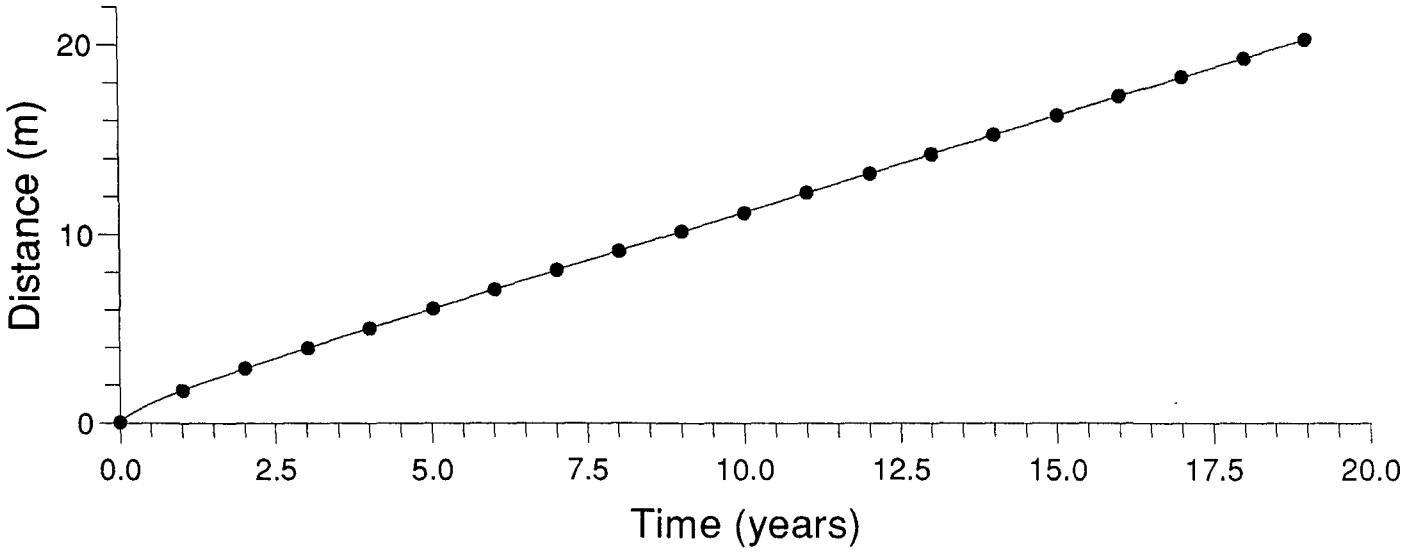

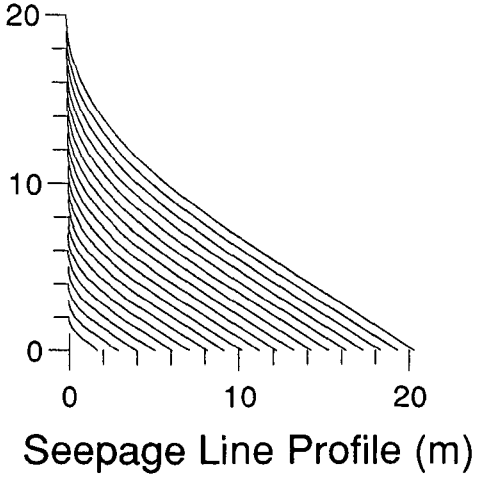

Advance of Seepage Line through an Idealized Tailings Dam

With permeability/porosity of $10^{-8}ms^{-1}$ and tailings lagoon rise of 1m per year

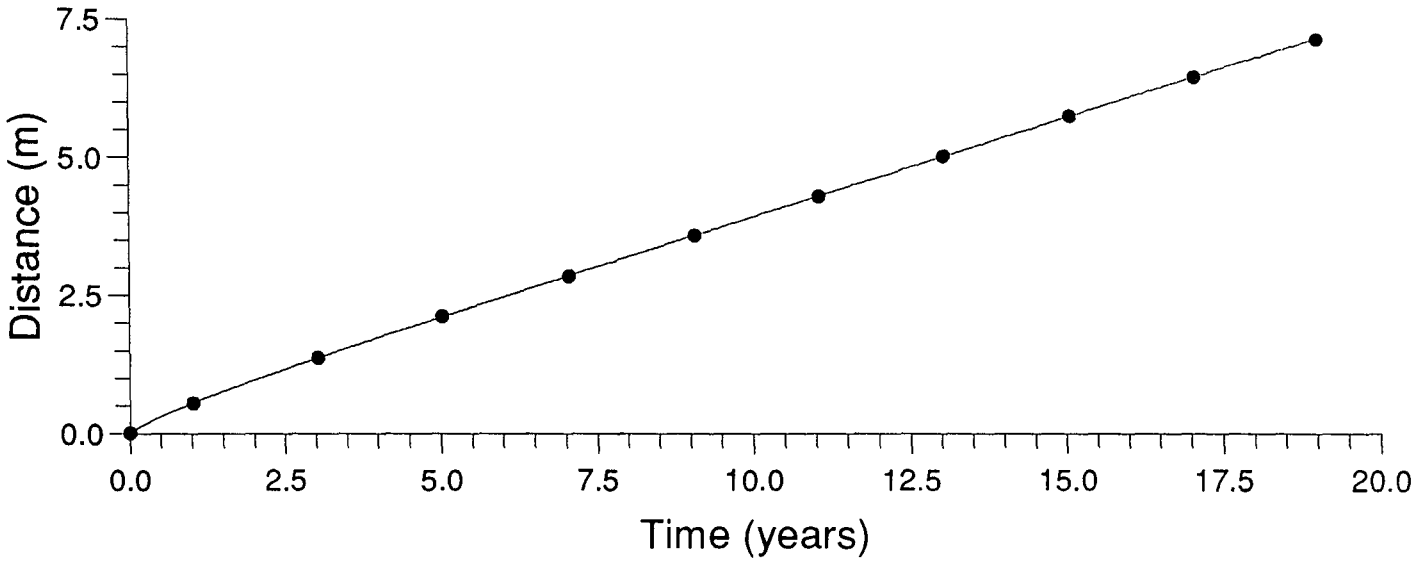

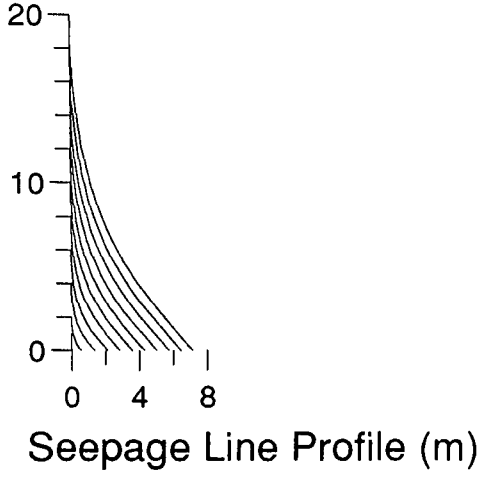

Advance of Seepage Line through an Idealized Tailings Dam

With permeability/porosity of $10^{-6}ms^{-1}$ and tailings lagoon rise of 2m per year

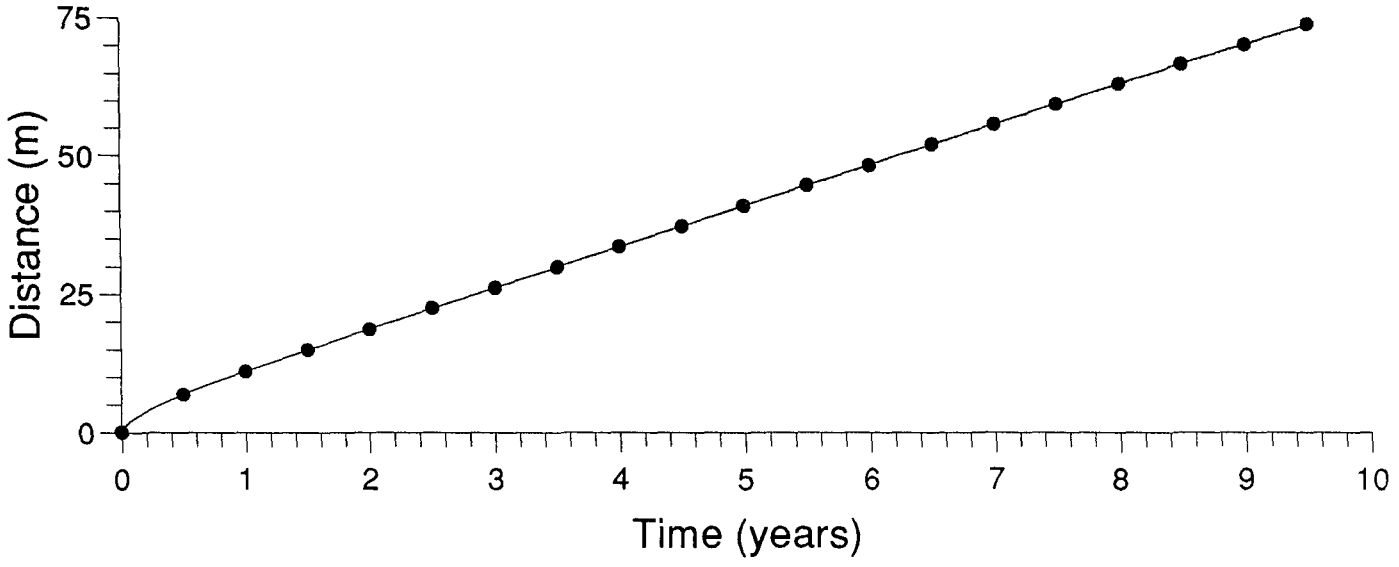

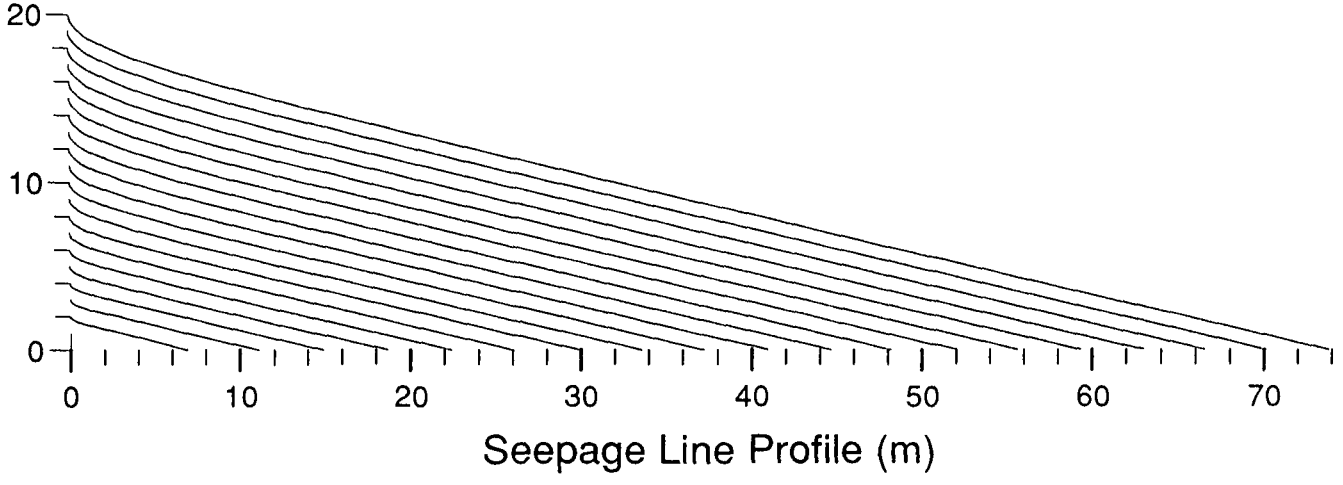

Advance of Seepage Line through an Idealized Tailings Dam

With permeability/porosity of $5 \times 10^{-7} ms^{-1}$ and tailings lagoon rise of 2m per year

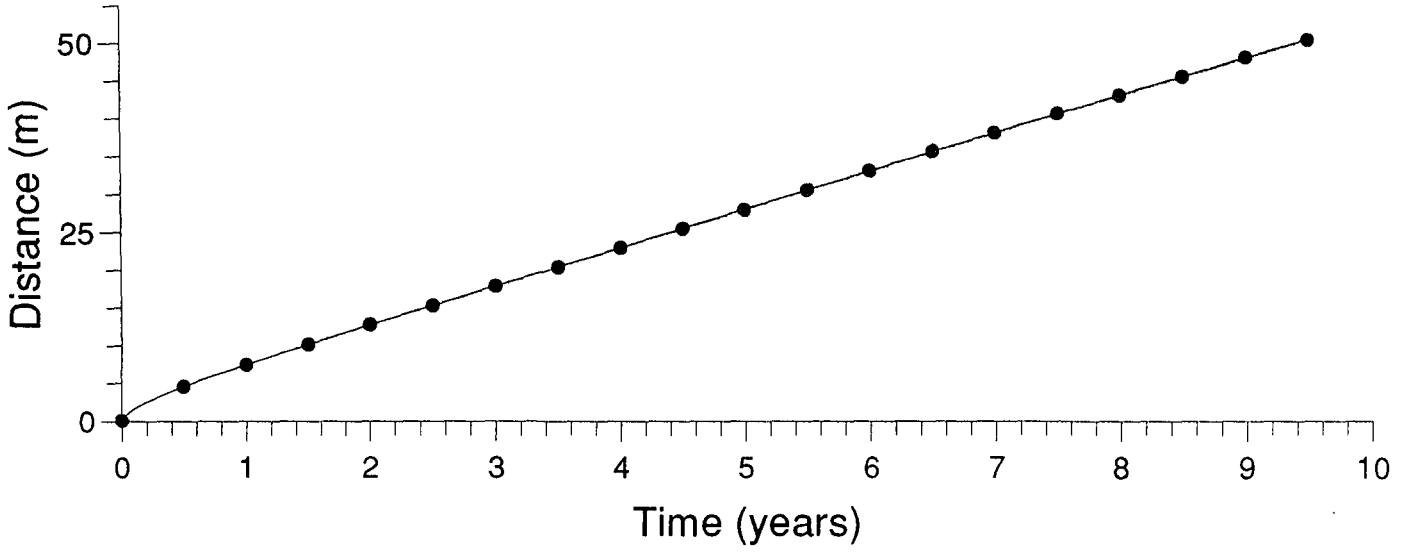

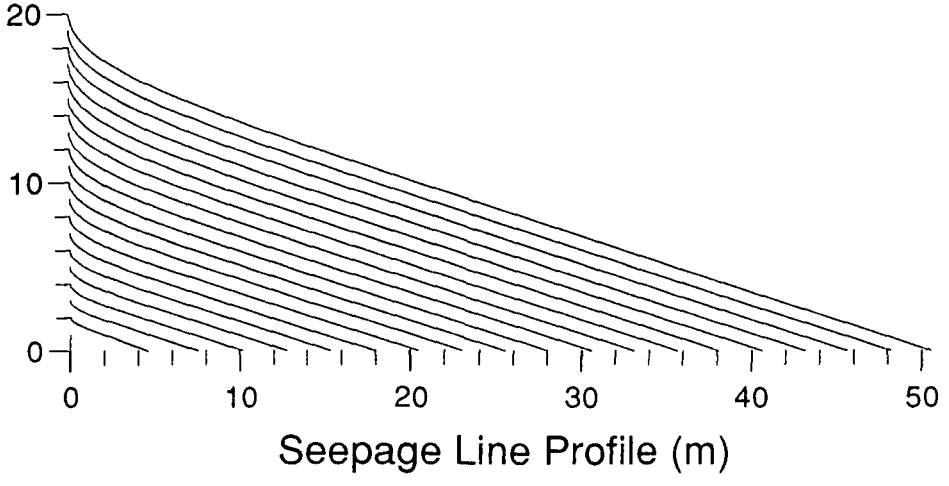

Advance of Seepage Line through an Idealized Tailings Dam

With permeability/porosity of $10^{-7}ms^{-1}$ and tailings lagoon rise of 2m per year

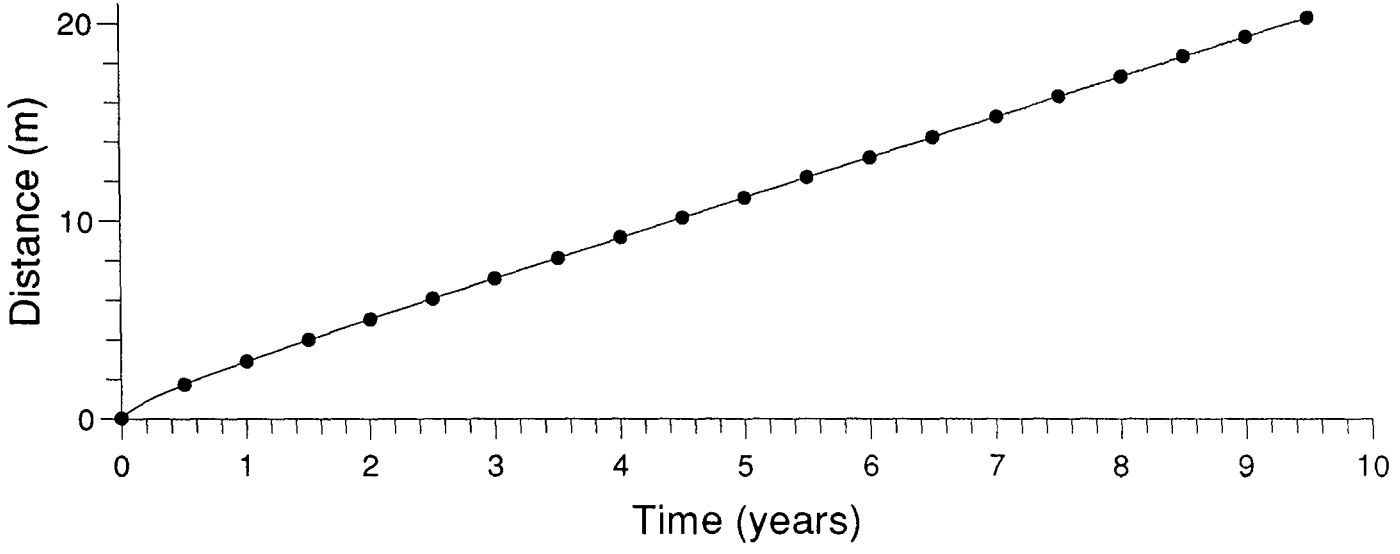

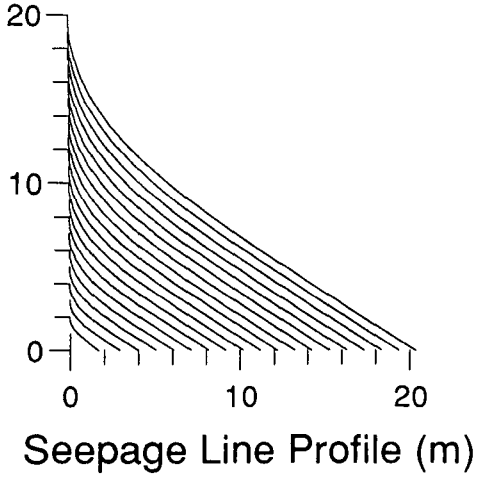

Advance of Seepage Line through an Idealized Tailings Dam

With permeability/porosity of $5 \times 10^{-8} ms^{-1}$ and tailings lagoon rise of 2m per year

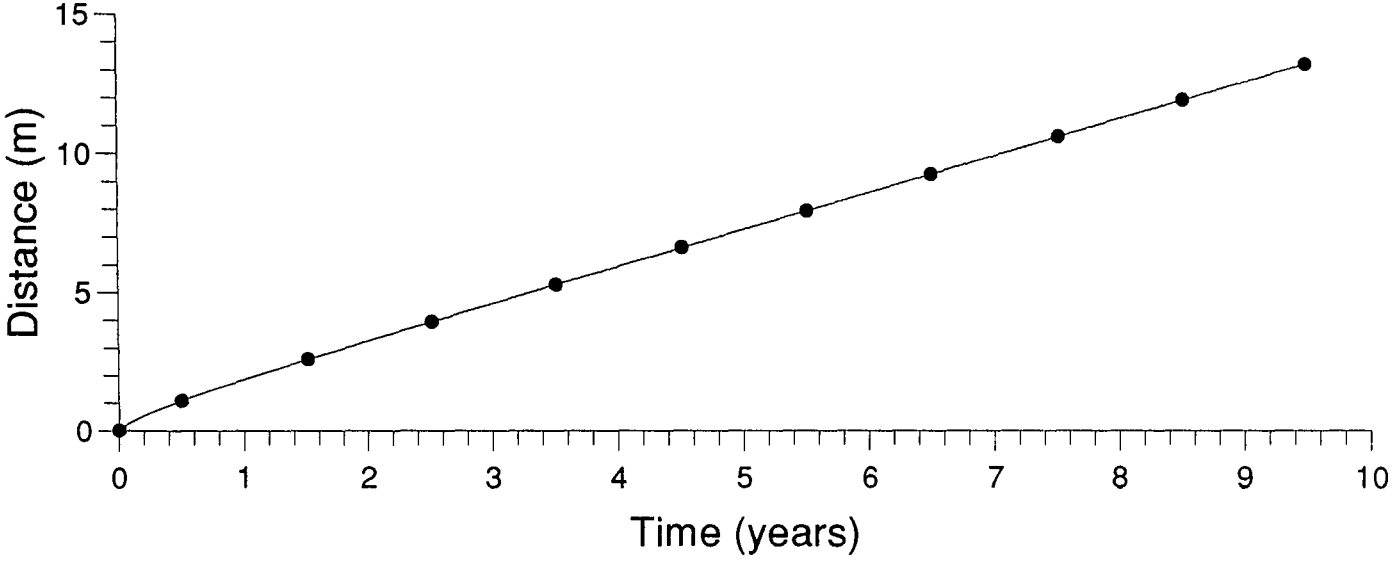

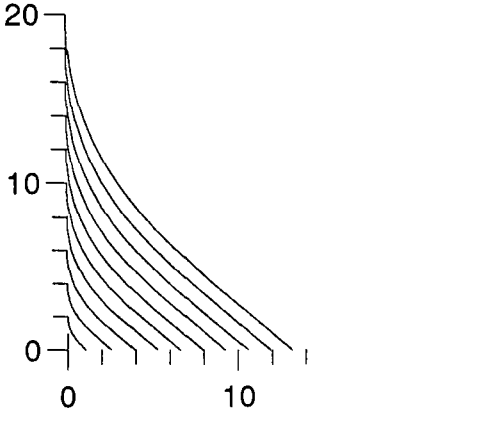

Advance of Seepage Line through an Idealized Tailings Dam

With permeability/porosity of $10^{-8}ms^{-1}$ and tailings lagoon rise of 2m per year

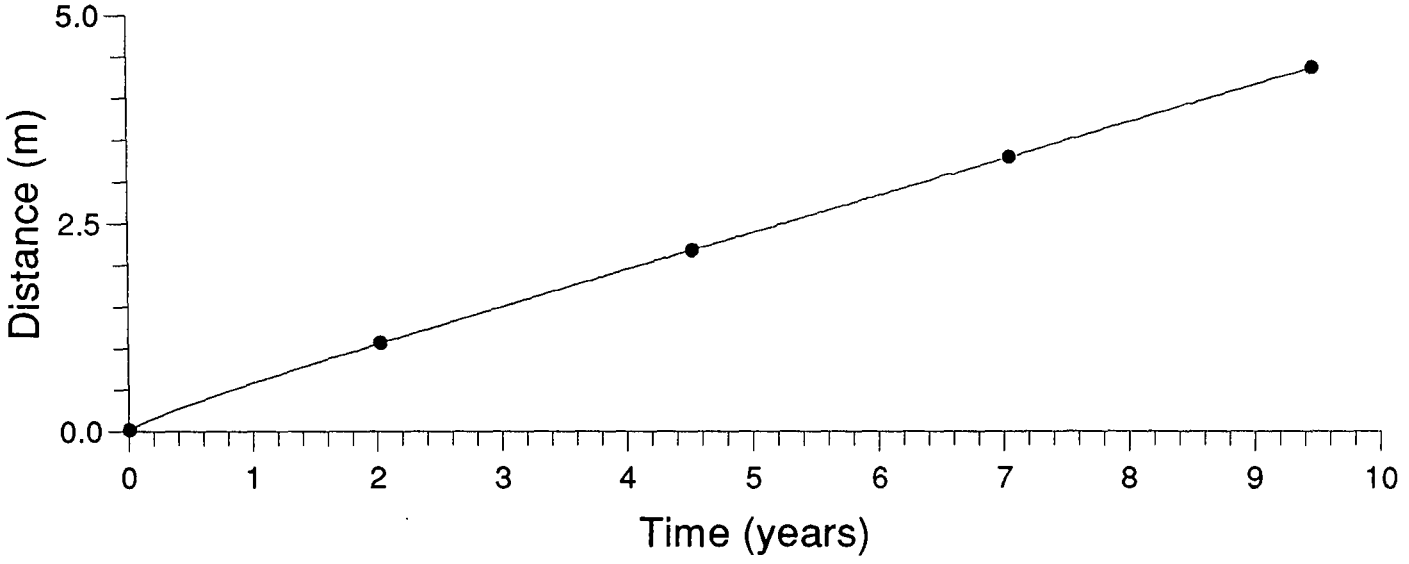

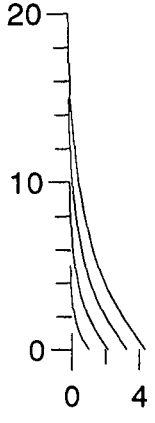

Seepage Line Profile (m)

Advance of Seepage Line through an Idealized Tailings Dam

With permeability/porosity of $10^{-6}ms^{-1}$ and tailings lagoon rise of 3m per year

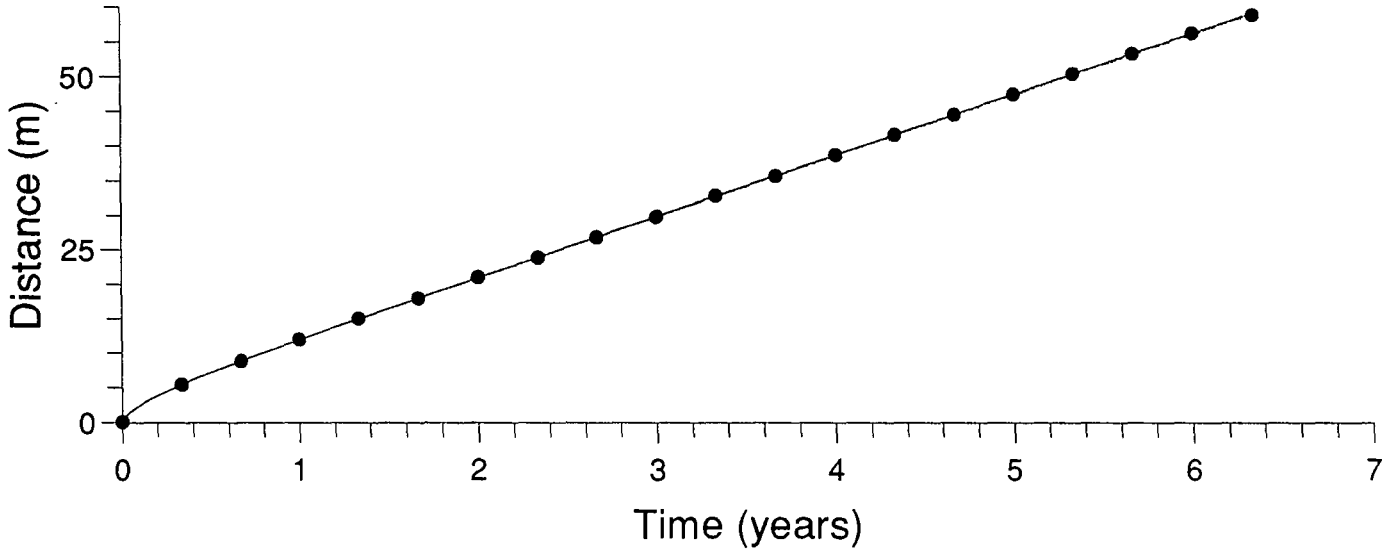

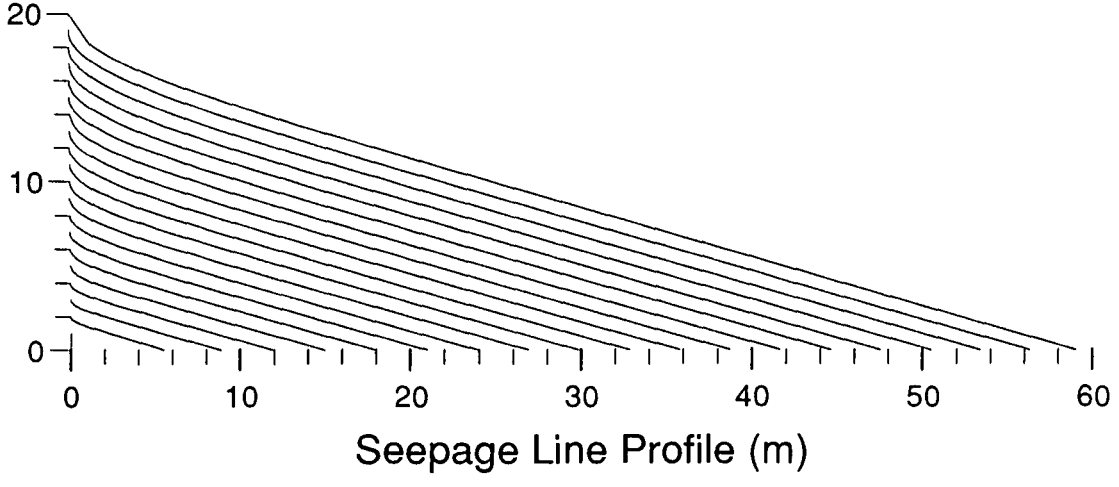

Advance of Seepage Line through an Idealized Tailings Dam

With permeability/porosity of $5 \times 10^{-7} ms^{-1}$ and tailings lagoon rise of 3m per year

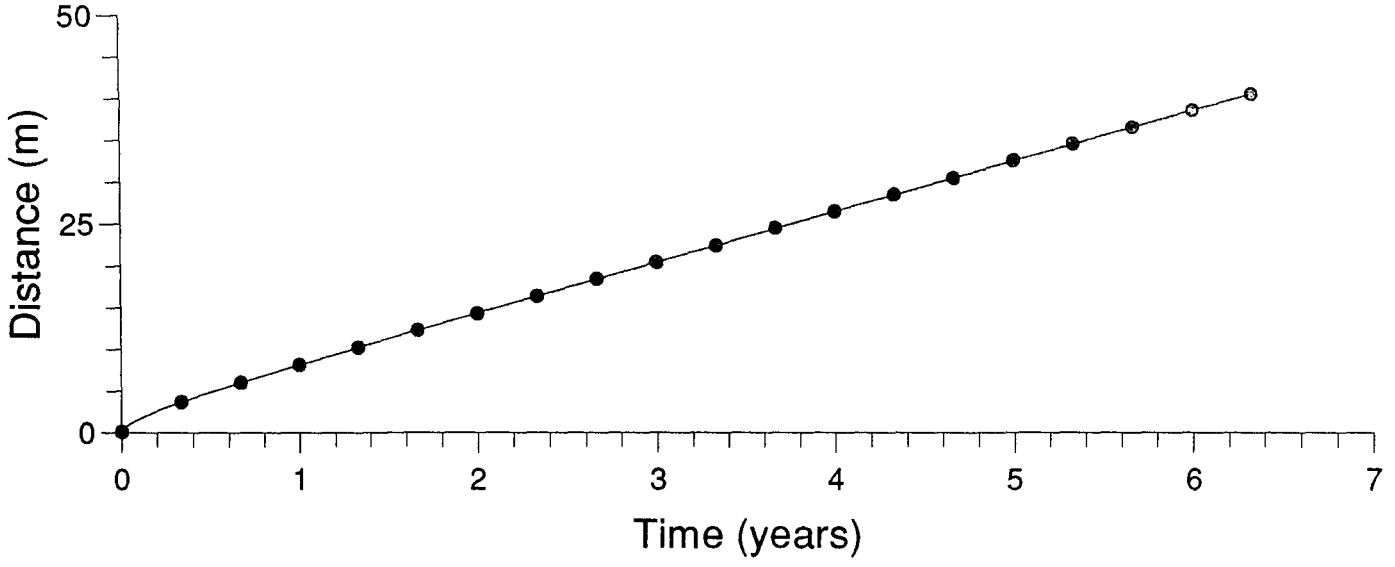

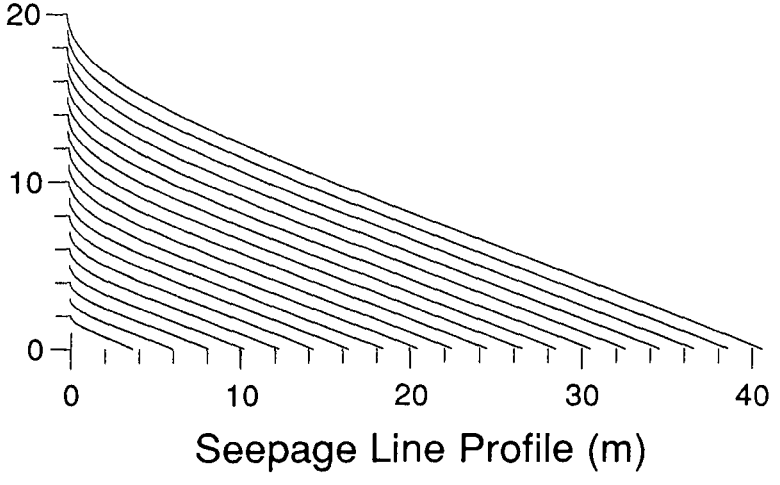

Advance of Seepage Line through an Idealized Tailings Dam

With permeability/porosity of $10^{-7}ms^{-1}$ and tailings lagoon rise of 3m per year

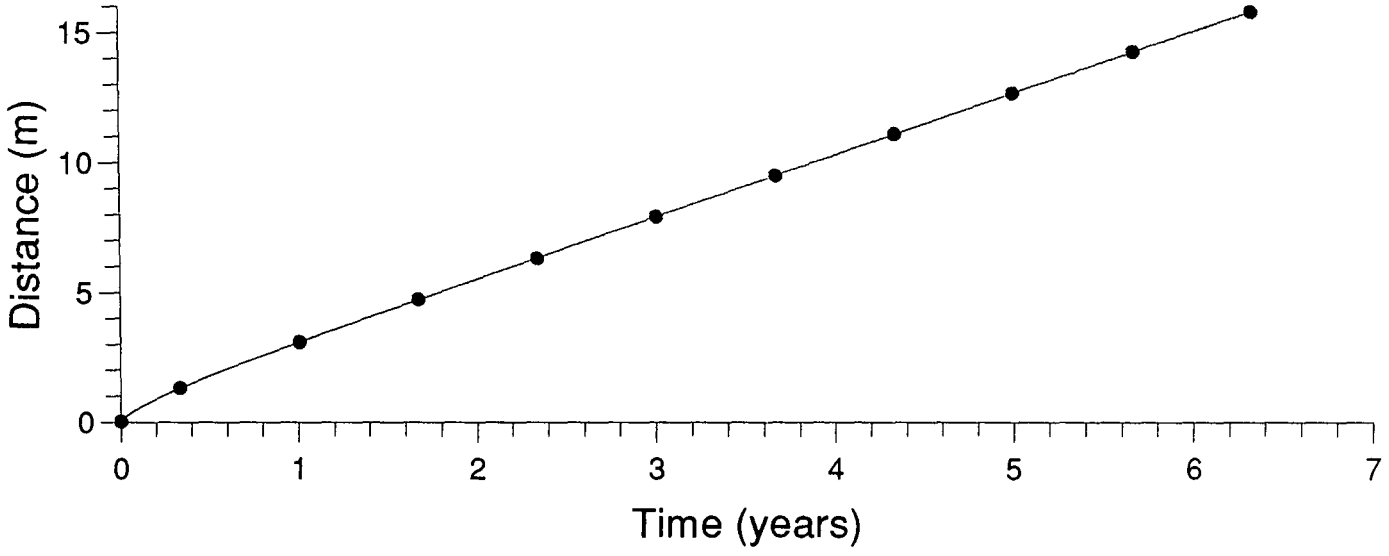

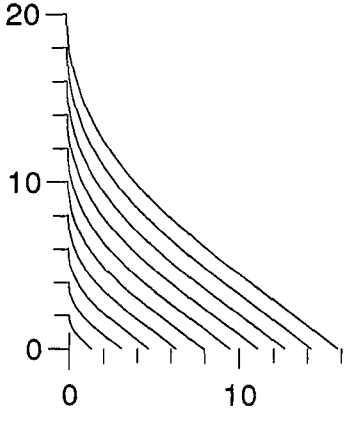

Seepage Line Profile (m)

Advance of Seepage Line through an Idealized Tailings Dam

With permeability/porosity of $5 \times 10^{-8} ms^{-1}$ and tailings lagoon rise of 3m per year

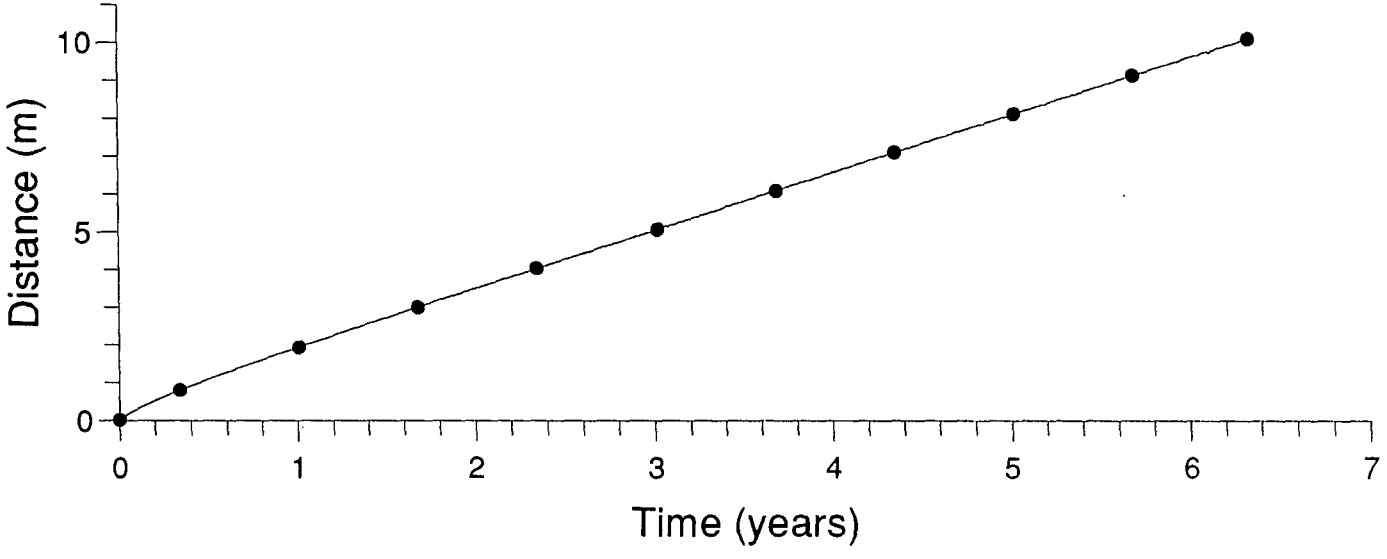

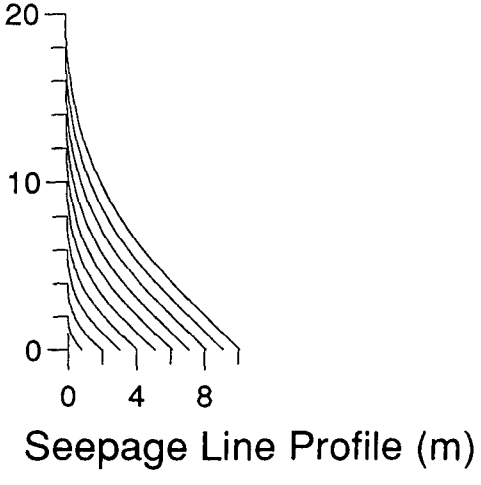

Advance of Seepage Line through an Idealized Tailings Dam

With permeability/porosity of $10^{-8}ms^{-1}$ and tailings lagoon rise of 3m per year

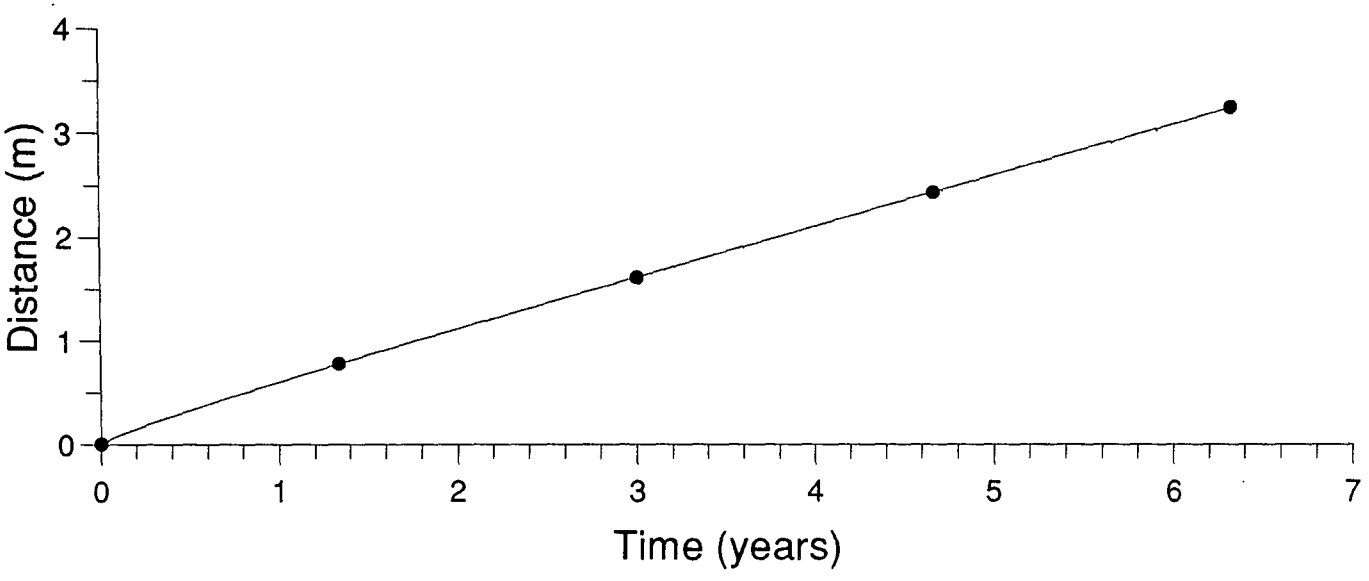

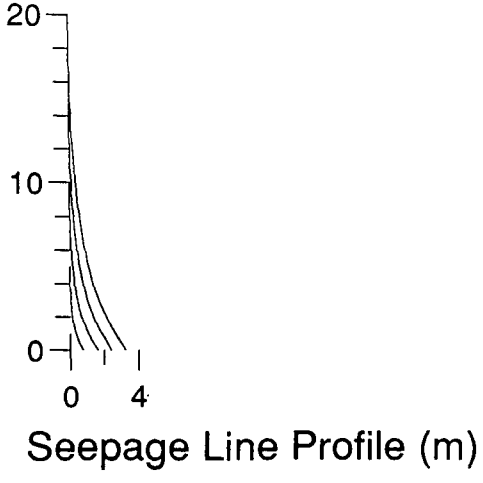

Advance of Seepage Line through an Idealized Tailings Dam

With permeability/porosity of $10^{-6}ms^{-1}$ and tailings lagoon rise of 4m per year

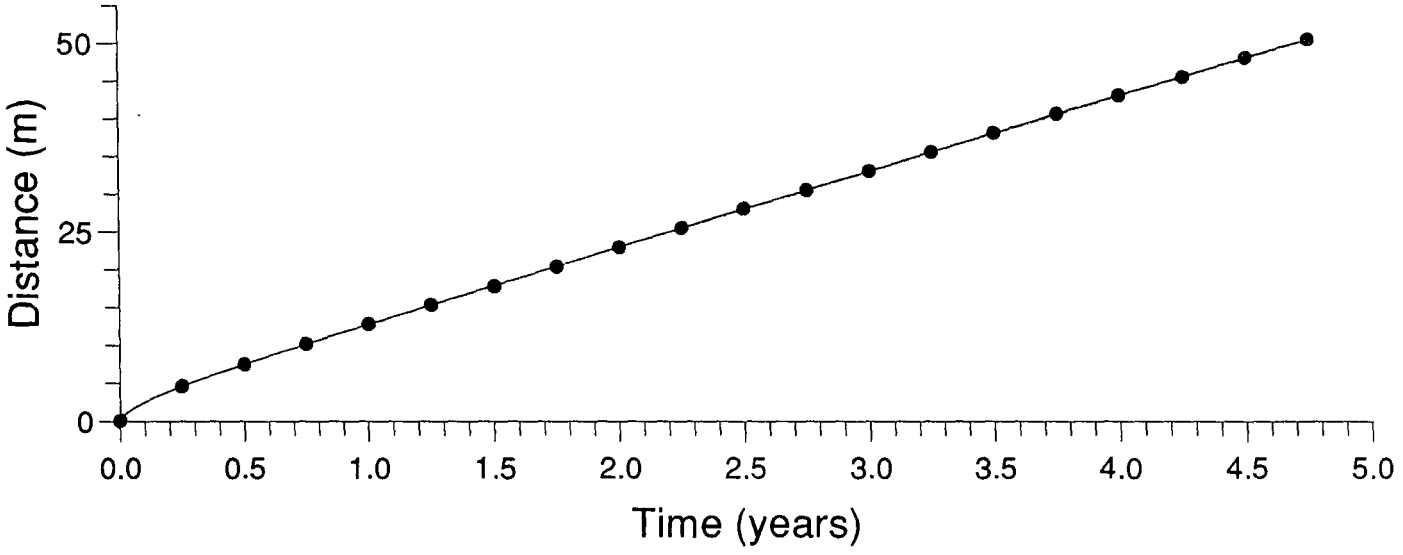

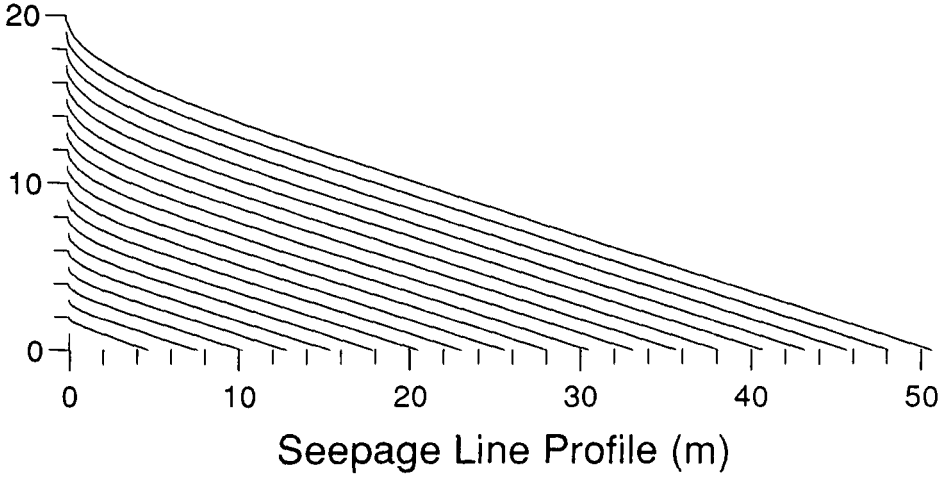

Advance of Seepage Line through an Idealized Tailings Dam

With permeability/porosity of $5 \times 10^{-7} ms^{-1}$ and tailings lagoon rise of 4m per year

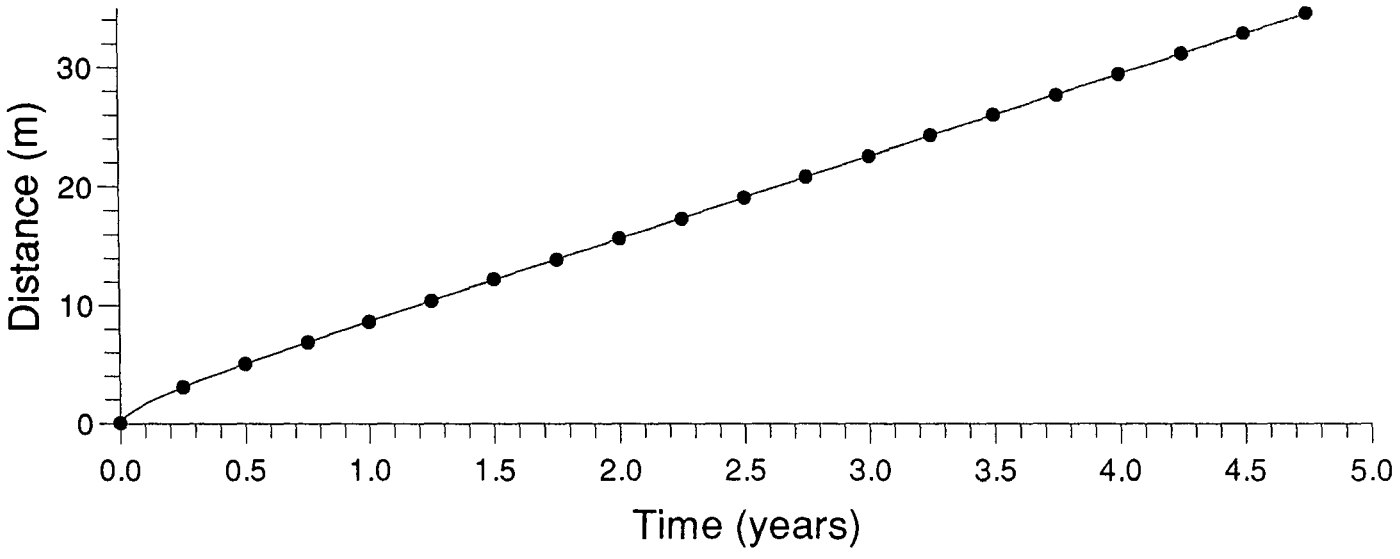

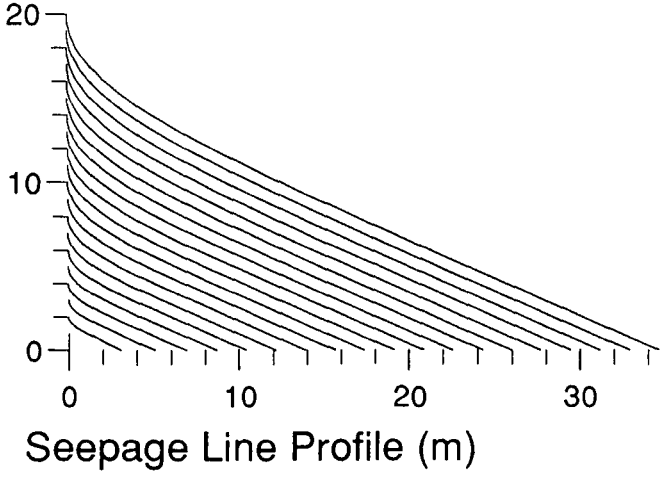

Advance of Seepage Line through an Idealized Tailings Dam

With permeability/porosity of $10^{-7}ms^{-1}$ and tailings lagoon rise of 4m per year

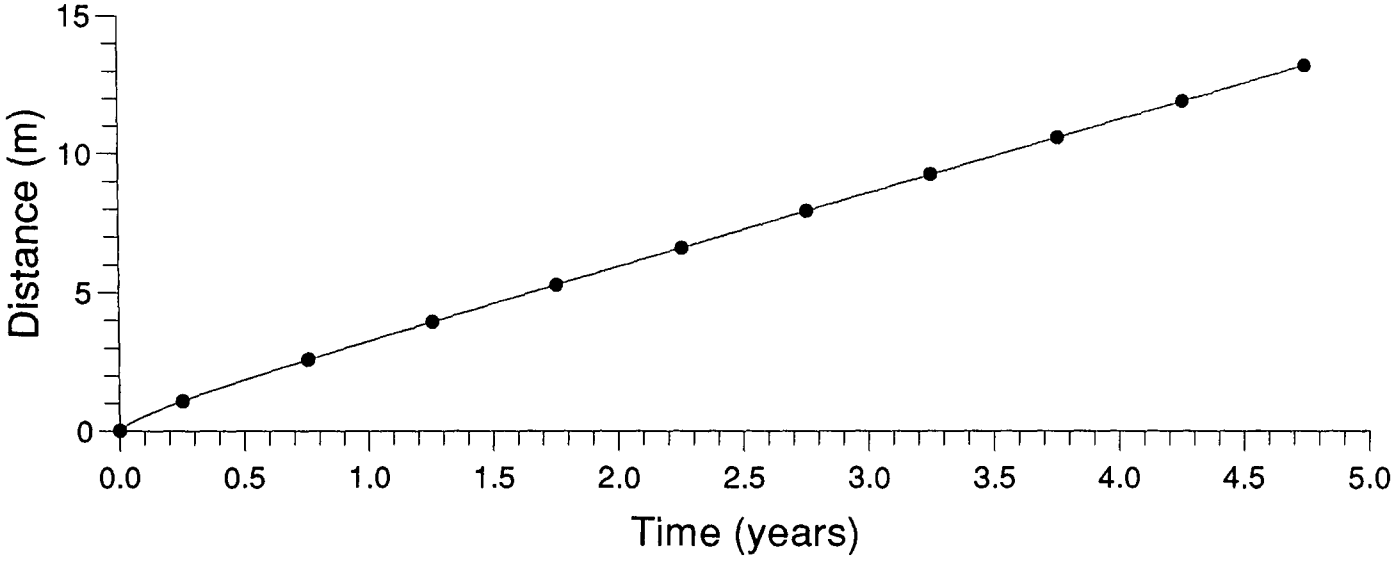

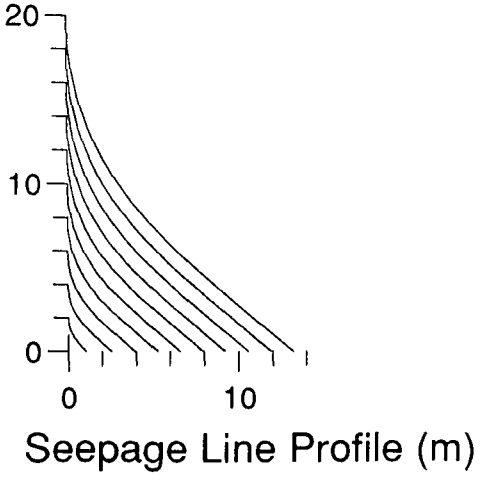

Advance of Seepage Line through an Idealized Tailings Dam

With permeability/porosity of $5 \times 10^{-8} ms^{-1}$ and tailings lagoon rise of 4m per year

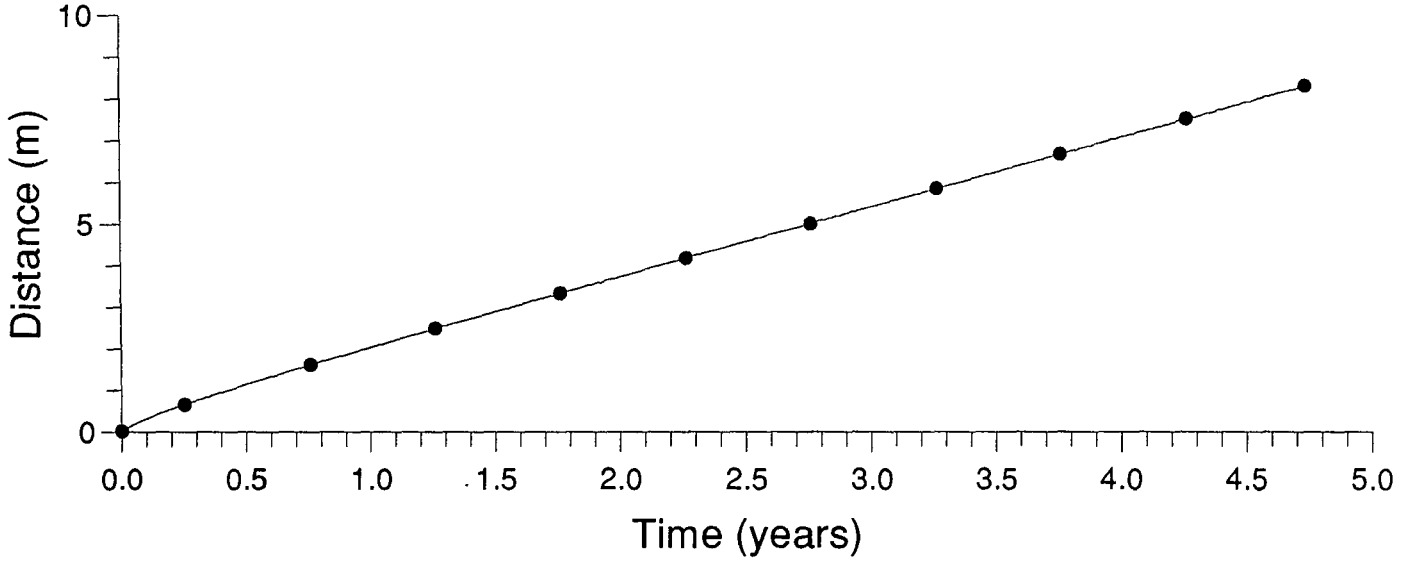

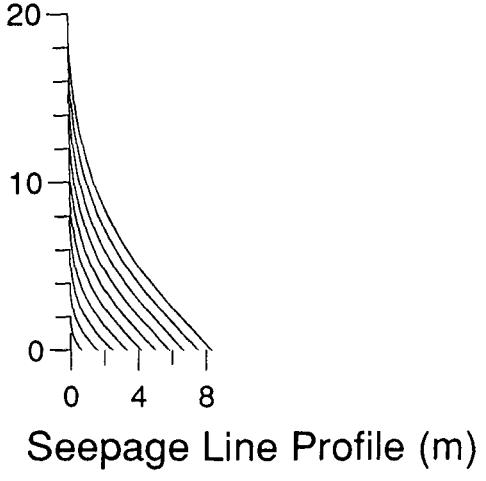

Advance of Seepage Line through an Idealized Tailings Dam

With permeability/porosity of $10^{-8}ms^{-1}$ and tailings lagoon rise of 4m per year